ALBERTIANA

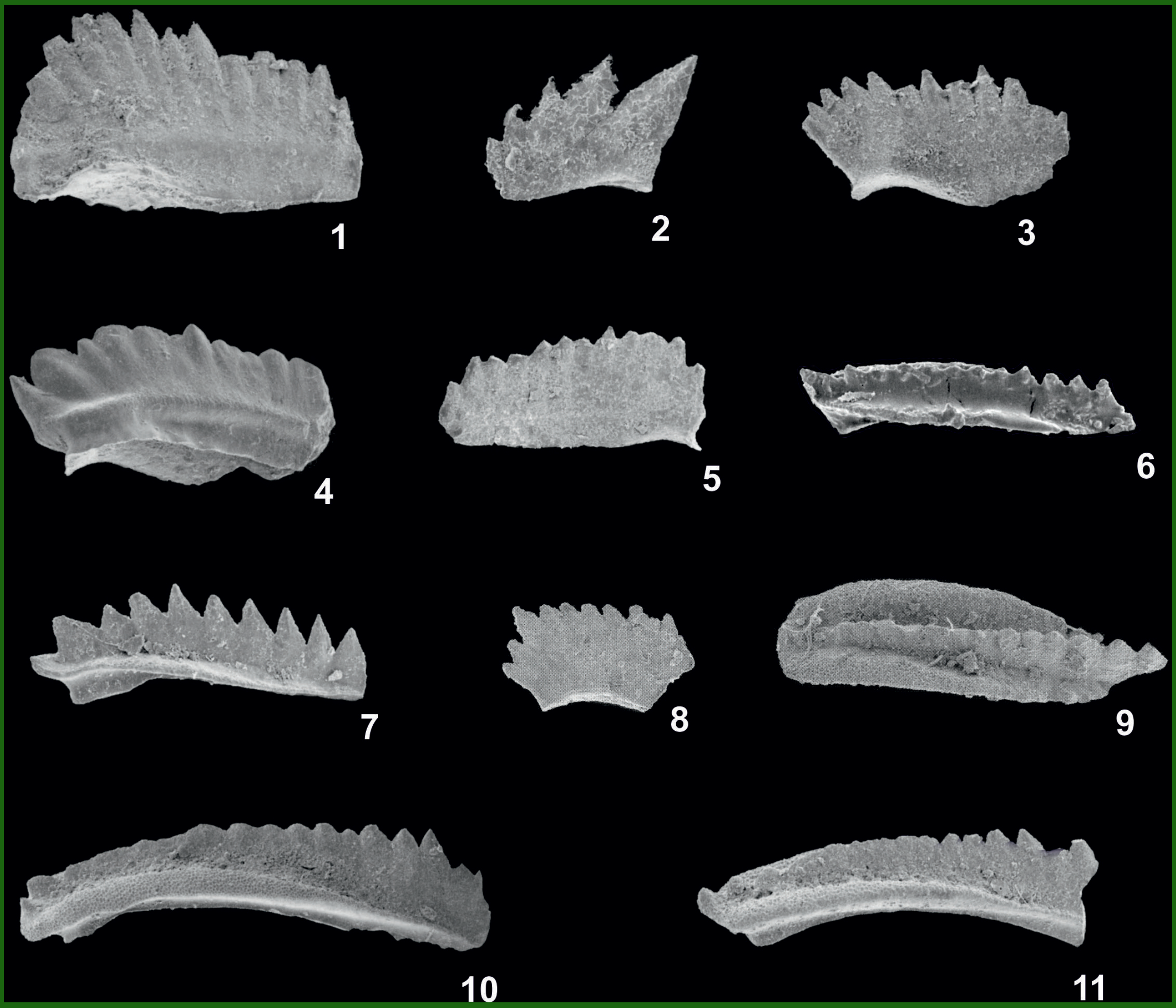

45

December 2019

ISSN 0619-4324

ALBERTIANA 44 • DECEMBER 2019

CONTENTS

Albertiana is the international journal of Triassic research. The primary aim of *Albertiana* is to promote the interdisciplinary collaboration and understanding among members of the I.U.G.S. Subcommission on Triassic Stratigraphy. *Albertiana* serves as the primary venue for the dissemination of orignal research on Triassic System. *Albertiana* also serves as a newsletter for the announcement of general information and as a platform for discussion of developments in the field of Triassic stratigraphy. *Albertiana* thus encourages the publication of contributions in which information is presented relevant to current interdisciplinary Triassic research and at provides a forum for short, relevant articles including. original research articles, reports on research and works in progress, reports on conferences, news items and conference announcements, *Albertiana* Forum: letters, comment and reply, and literature reviews. *Albertiana* is published bianually by SUNY Cortland's Paleontological Laboratory for the Subcommission on Triassic Stratigraphy. *Albertiana* is available as PDF at http://paleo.cortland.edu/Albertiana/

Cover Image: *Choristoceras marshi*, from Fraas (1895 Der Petrefaktensammler. - Leitfaden zum Sammeln und Bestimmen der Versteinerungen Deutschlands; K.G. Lutz' Verlag; Stuttgart).

Research Article

NEWS FROM THE PERMIAN-TRIASSIC GURYUL RAVINE SECTION (KASHMIR, INDIA): A FAULT CAUSING BIOSTRATIGRAPHIC CORRELATION PROBLEMS AND REMARKS ON THE DIENERIAN CONODONT UAZS

Leopold Krystyn[1], Micha Horacek[2]*, Rainer Brandner[3] and Ghulam M. Bhat[4]

[1] *Institute of Palaeontology, Vienna University, Althanstrasse 14, 1090 Vienna, Austria, Email: leopold.krystyn@univie.ac.at*
[2] *Institute of Lithospheric Research, Vienna University, Althanstrasse 14, 1090 Vienna, Austria Email: micha.horacek@josephinum.at*
[3] *Institute of Geology and Palaeontology, Innrain 52, 6020 Innsbruck, Austria, Email: rainer.brandner@uibk.ac.at*
[4] *Institute of Energy Research and Training, Bhadarwah Campus, University of Jammu, India, Email: bhatgm@jugaa.com.*
**corresponding author*

Abstract – Guryul Ravine (Kashmir, India) is unique in that it is the only ammonoid bearing expanded and complete Permian-Triassic boundary section along the entire southern Tethys margin. As such it may be important to note that during a field campaign in 2017 we identified a fault within the Griesbachian part of the section. Although it can be detected in aerial photographs (if searched for) it is quite difficult to be seen in the field. As this structure has not been described in previous publications we assume that it has been overlooked and thus might account for some problems in stratigraphic correlation between previous studies. Also, in a recently published study about Guryul Ravine, we identified some errors that we want to bring to attention

INTRODUCTION

The classic Guryul Ravine section in Kashmir/India has been studied for palaeontology since 1907 and 1909 by Hayden and Middlemiss, respectively. Teichert (1970) was the first to report a mixed Permo-Triassic fauna from there and a Japanese-Indian research group carried out an extensive palaeontological study (Nakazawa et al., 1970, 1975; Nakazawa and Kapoor 1981; Matsuda 1981, 1982, 1983, 1984). More recently, Algeo et al. (2007), Korte et al. (2010), Horacek et al. (2014) and Brookfield & Sun (2015) investigated the section. Baud et al. (2014) published a field guide containing a compilation of published and also new data.

Lately, following their high-resolution sampling, Brosse et al. (2017) reassessed and revised the conodont biochronology and presented a carbon isotope curve of the fifteen lowermost stratigraphical meters of the Khunamuh Formation at Guryul Ravine section, which they correlate with Member E in Nakazawa et al. (1975) above the sandstone layers of the topmost Zewan Formation (Member D of Nakazawa et al., 1975). This interval includes both the Permian-Triassic and the Griesbachian-Dienerian (lower-upper Induan) boundaries. Brosse et al. (2017) confirm the first occurrence of *Hindeodus parvus*, the index for the base of the Triassic (Yin et al., 2001), in the middle of sub-member E2 (Unit 56 of Matsuda, 1981) in bed GUR09 and characterize 11 Unitary Association Zones based on the conodont record from China and from Guryul Ravine. Brosse et al. (2017) identify the Griesbachian-Dienerian boundary (GDB) within the interval between UAZ8 and UAZ9, which corresponds in the Guryul Ravine section to the space between their bed numbers GUR310 and GUR311. Brosse et al. (2017) define the GDB by using as marker the first occurrence of *Sweetospathodus kummeli*, corresponding to the replacement of segminiplanate (here *Clarkina* and *Neoclarkina*)

Published online: February 21, 2019

Krystyn, L., Horacek, M., Brandner, R., and Bhat, G.M. 2019. News from the Permian-Triassic Guryul Ravine section (Kashmir, India): a fault causing biostratigraphic correlation problems and remarks on the Dienerian conodont UAZs *Albertiana*, vol. 45, 1–4.

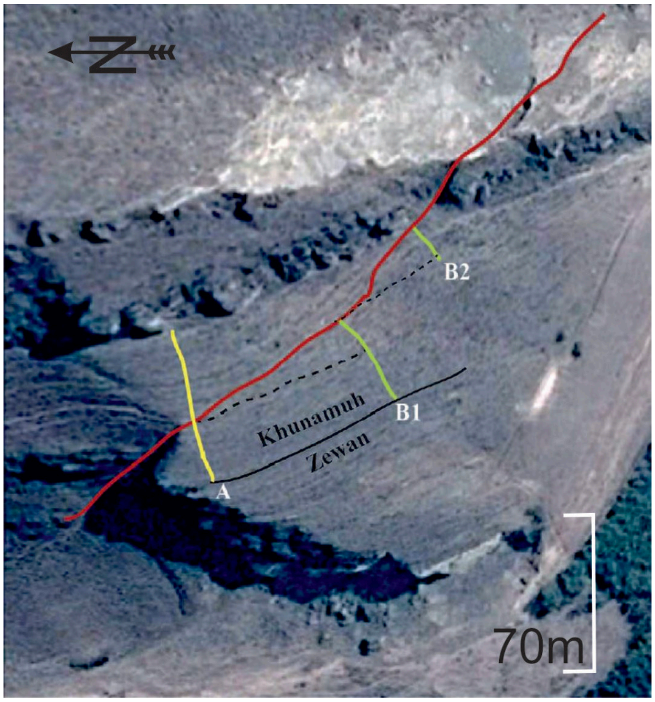

Figure 1–Aerial view of the Guryul Ravine section with indication of the fault and location of measured sections (base image from Google Earth). Red line indicates the trace of the fault, yellow line refers to the trace of the section of Brosse et al. (2017), green line indicates our section (unpublished) and probably also the Nakazawa et al. (1975) section, according to the almost perfect lithological match up to the base of F member. Black line is the boundary between the Zewan and Khunamuh Formations. Dashed lines indicate strike of beds below the fault.

by segminate (*Sweetospathodus* and *Neospathodus*) conodonts. Brosse et al. (2017, p.359) note that "this faunal turnover was possibly linked to a climate change at the Griesbachian-Dienerian transition, from a cool and dry to a hot and humid climate" and "This transition could be the trigger of the migration of neogondolellids towards high latitudes and of the radiation of neospathodids during the Dienerian." However, Brosse et al. (2017) state that a bed-by-bed correlation of their results with the log by Nakazawa et al. (1975) could not be achieved.

MATERIAL AND METHODS

After having visited the Guryul Ravine section several times in recent years we observed a high-angle fault with omission of beds at the study locality of Brosse et al. (2017) in the upper Griesbachian (Figs. 1 and 2). This fault results in a missing interval of approximately 5.5–6.0 metres (which is the upper part of the E3 member of Nakazawa et al., 1975) – nearly 40% of the Griesbachian in their section (Fig. 3) between beds 308 and 310 of Brosse et al. (2017). We believe that this unidentified fault, as a consequence, resulted in the problem to achieve a bed-by-bed correlation with Nakazawa et al. (1975) and Nakazawa and Kapoor (1981) respectively, as Brosse et al. (2017) note. When adding the missing part, a bed-by-bed sections correlation between these authors can be done (Fig. 3).

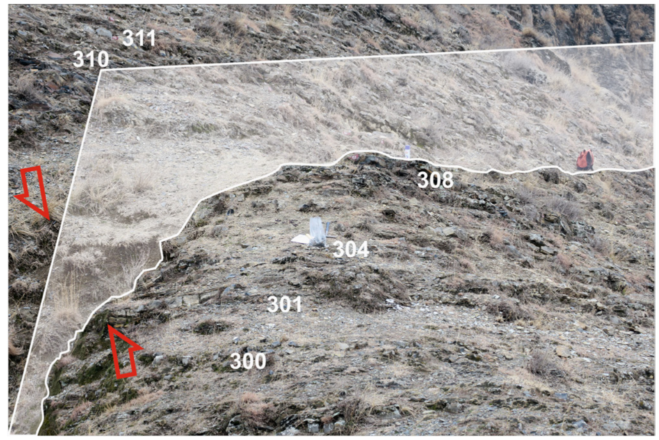

Figure 2 – Photograph of a part of the section investigated by Brosse et al. (2017). Note the bed numbers marked on the rocks in the field with the fault and its movement direction indicated.

Consequently, also the isotope curve presented by Brosse et al. (2017) has a gap that needs to be closed.

Furthermore, when comparing the section figure in Baud et al. (2014, fig. 23), which contains identical sample numbers, it is obvious that it does not fit to the figure published subsequently in Brosse et al. (2017). When comparing these two profiles of the same section (Baud et al., 2014; Brosse et al., 2017) we observe distinctive variations, e.g., a significant difference in distance between samples GUR299 and GUR300 with ca. 1m in Baud et al. (2014) and ca. 5m in Brosse et al. (2017). As this discrepancy occurs in the footwall of the fault in the section it cannot account for it. Furthermore, we could not identify such a variation in thickness between the two beds along strike over 100m distance. An explanation for these differences is required to rule out the possibility of merging samples from different parts of the section or combining disparate data (e.g., conodonts and isotopes) from only apparently identical sample numbers – however coming from different levels within the section.

RESULTS

Amending the stratigraphic log for the missing interval enables us to do a bed-by-bed correlation of Nakazawa et al. (2015) data with the detailed conodont record in Brosse et al. (2017) as noted above. Therefore, we can link the macro-fossil and sedimentological dataset of Nakazawa et al. (1975) to the conodont data set by Brosse et al. (2017). By combining the two data sets, we can correlate *Otoceras woodwardi* with *Hindeodus parvus*, *Ophiceras tibeticum* with *Clarkina krystyni* and note a good agreement in the finding of *Clarkina carinata* and *Hindeodus typicalis*. We have to stress, however, that the correlation is based entirely on the published data and the conodont stratigraphy will be again significantly revised by our ongoing study.

Brosse et al. (2017, fig. 18) report conodont Unitary Assemblage Zones (UAZ) with some very strange UAZs, i.e. UAZ10 and UAZ11 where *Sweetospathodus kummeli*, having an exceptionally long duration, is co-occurring with *Neogondolella chaohuensis*, *Eurygnathodus costatus* and *Neospathodus eowaageni*.

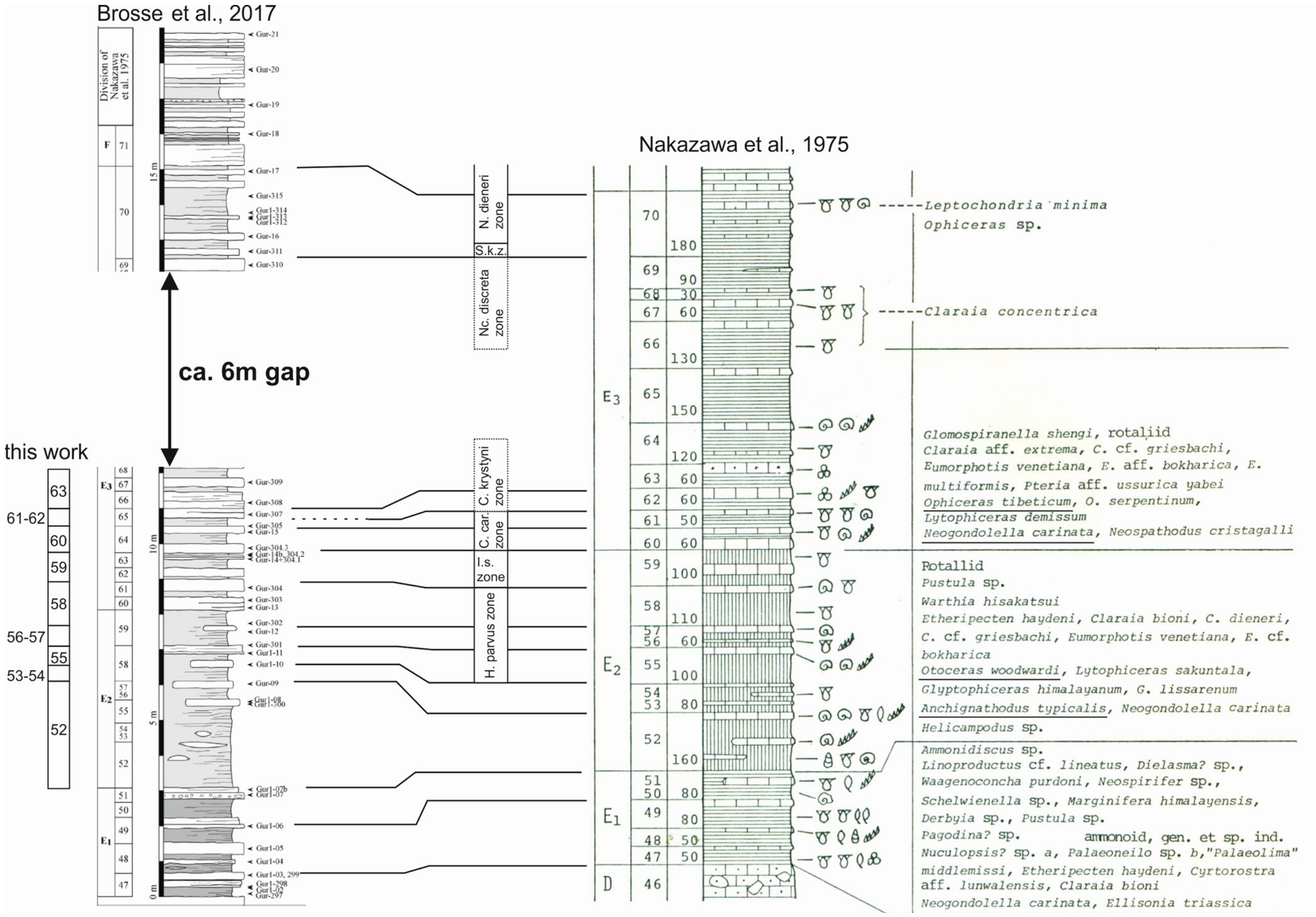

Figure 3 – Side-by-side sections data comparison between Nakazawa et al. (1975) and Brosse et al. (2017, modified), with a bed-by-bed correlation, position of the gap, and conodont zones after data of Brosse et al. (2017); fossils mentioned in text are underlined. H.= *Hindeodus*, I.s.= *Isarcicella staeschei*, C. car.= *Clarkina carinata*, C.= *Clarkina*, Nc.= *Neoclarkina*, S.k.z.= *Sweetospathodus kummeli* zone, N.= *Neospathodus*. Note, *Anchignathodus* is an old synonym for *Hindeodus*. Bed-by-bed correlation between Nakazawa et al. (1975) and Brosse et al. (2017) was achieved by lateral tracing of the individual beds between the two section lines in the field.

We are not aware of any section where these co-occurrences exist. To our experience so far and from published literature (Orchard, 2007; Chen et al., 2015; Zhang et al., 2007), *S. kummeli* only occurs over a very short interval and in association of just a few species (e.g., *Ns. dieneri*, *Nc. discreta*, *C. carinata*, *C. planata*, *C. taylorae*, *C. tulongensis*). This co-occurrence of further species in Brosse et al. (2017, fig. 18) probably points towards a confusion of species, admixture of samples, a condensed interval or something similar – to our current knowledge - or an error. On the other hand, according to Zhang et al. (2007), *S. kummeli* co-occurs with *Ns. cristagalli* and, therefore the range of *Ns. cristagalli* has to be revised in Brosse et al. (2017, fig. 18) too and in consequence also the UAZs. As we think that there are several problems and inconsistencies concerning the UAZ 9–11, we think that there is need for correction.

DISCUSSION AND CONCLUSIONS

The high-angle fault with omission of beds identified by us in the field 2017 now enables a bed-by-bed correlation of the Brosse et al. (2017) data with the results of Nakazawa et al. (1975). The correlation of the data sets produced by Nakazawa et al. (1975) and Brosse et al. (2017) allows the combination of micro- and macro-fossils identified hithero in the Guryul Ravine section. Our correlation confirms the co-existence of *Otoceras woodwardi* with *Hindeodus parvus* and *Ophiceras tibeticum* with *C. krystyni*. The correlation also shows a good agreement in the *Clarkina (Neogondolella) carinata* ranges (except that the lowermost mentioned occurrence in Member E1 by Nakazawa et al. (1975) has to be omitted). However, the reader needs to keep in mind that another revision of the conodont data will be shortly published by the authors.

ACKNOWLEDGEMENTS

This research was partially funded by the Austrian Academy of Science within the International Geological Correlation Program. A grant of the ÖAD (Österreichischer Austauschdienst), project No. IN 03/2013 to M. Horacek is thankfully acknowledged. We thank A. Baud for the constructive review and especially for significant improvement of Fig. 1. This publication is a contribution to IGCP projects 572 and 630.

REFERENCES

Algeo, T.J., Hannigan, R., Rowe, H., Brookfield, M., Baud, A., Krystyn, L. & Ellwood, B.B. 2007. Sequencing events across the Permian–Triassic boundary, Guryul Ravine (Kashmir, India). Palaeogeography, Palaeoclimatology, Palaeoecology, 252(1–2): 328–346.

Baud, A. & Bhat, G. 2014. The Permian-Triassic transition in the Kashmir Valley - IGCP 630 Field Guide Book. IGCP 630 First Annual Field Workshop in North India, (17-22 November, 2014, Srinagar, India), published by the IERT (Institute of Energy Research & Training), Jammu University, India. 36 pages.

Brookfield, M.E. & Sun, Y. 2015. Preliminare report on new conodont records from the Permian-Triassic boundary section at Guryul Ravine, Kashmir, India. Permophiles 61: 24–25.

Brosse, M., Baud, A., Bhat, G.M., Bucher, H., Leu, M., Vennemann, T. & Goudemand, N. 2017. Conodont-based Griesbachian biochronology of the Guryul Ravine section (basal Triassic, Kashmir, India). Geobios, 50: 359–387.

Chen, Y., Jiang, H., Lai, X., Yan, C., Richoz, S., Liu, X. & Wang, L. 2015. Early Triassic conodonts of Jiarong, Nanpanjiang Basin, southern Guizhou Province, South China. Journal of Asian Earth Sciences 105: 104–121.

Hayden, H.H. 1907. The stratigraphical position of the *Gangamopteris* beds of Kashmir. Records of the Geological Survey of India, 36: 23–39.

Horacek, M., Krystyn, L., Brandner, R. & Parcha, S. 2014. The Early Triassic in the Guryul Ravine (Kashmir/India). Pangeo Austria, Graz, 14–19 Sept., 2014.

Korte, C., Pande, P., Kalia, P., Kozur, H.W., Joachimski, M.M. & Oberhänsli, H. 2010. Massive volcanism at the Permian-Triassic boundary and its impact on the isotopic composition of the ocean and atmosphere. Journal of Asian Earth Sciences, 37: 293- 311.

Matsuda, T. 1981. Early Triassic Conodonts from Kashmir, India part 1: *Hindeodus* and *Isarcicella*. Journal of Geosciences, Osaka City University. 24: 75–108.

Matsuda, T. 1982. Early Triassic Conodonts from Kashmir, India part 2: *Neospathodus* 1. Journal of Geosciences, Osaka City University, 25: 87–102.

Matsuda, T. 1983. Early Triassic Conodonts from Kashmir, India part 3: *Neospathodus* 2. Journal of Geosciences, Osaka City University, 26: 87–110.

Matsuda, T. 1984. Early Triassic Conodonts from Kashmir, India part 4: *Gondolella* and *Platyvillosus*. Journal of Geosciences, Osaka City University, 27: 119–141.

Middlemiss, C.S. 1909. Gondwanas and related marine sedimentary systems of Kashmir. Records of the Geological Survey of India. 37: 286–327.

Nakazawa, K., Kapoor, H.M., Ishii, K.I., Bando, Y., Maegoya, T., Shimizu, D., Nogami, Y., Tokuoka, T. & Nohda, S. 1970. Preliminary report on the Permo-Trias of Kashmir. Memoirs of the Faculty of Science, Kyoto University Series of Geology and Mineralogy, 37: 163–172.

Nakazawa, K., Kapoor, H.M., Ishii, K.I., Bando, Y., Okimura, Y. & Tokuoka, T. 1975. The upper Permian and the lower Triassic in Kashmir, India. Memoirs of the Faculty of Science, Kyoto University Series of Geology and Mineralogy, 42: 1–160.

Nakazawa, K. & Kapoor, H.M. 1981. The upper Permian and Lower Triassic faunas of Kashmir. Memoir of the Geological Survey of India, Palaeontologia Indica 46, 1–204.

Orchard, M.J. 2007. Conodont diversity and evolution through the latest Permian and Early Triassic upheavals. Palaeogeography, Palaeoclimatology, Palaeoecology 252, 93–117.

Teichert, C., Kummel, B. & Kapoor, H.M. 1970. Mixed Permian-Triassic fauna, Guryul Ravine, Kashmir. Science, 167: 174–175.

Yin, H., Zhang, K., Tong, J., Yang, Z. & Wu, S. 2001. The global stratotype section and point (GSSP) of the Permian-Triassic boundary. Episodes, 24: 102–114.

Zhang, K., Tong, J., Shi, G.R., Lai, X., Yu, J., He, W., Peng, Y. & Jin, Y. 2007. Early Triassic conodont–palynological biostratigraphy of the Meishan D Section in Changxing, Zhejiang Province, South China. Palaeogeography, Palaeoclimatology, Palaeoecology, 252: 4–23.

TRIASSIC LITERATURE – 2016

Geoffrey Warrington

Honorary Visiting Fellow, School of Geography, Geology and the Environment, University of Leicester, LE1 7RH, UK

Email: gwarrington@btinternet.com

This compilation is based on the contents of over 500 serial titles and other publications. It is a continuation of the New Triassic Literature contributions that appeared in Albertiana up to December 2017 (44: 33–48), and includes items dated 2016, together with some pre-2016 titles that were not included in earlier compilations.

Abbassi, N., Ghavidel-Syooki, M., Yousefi, M. & Navidi Izad, N. 2016. Cruziana ichnofacies from Nayband Formation (Late Triassic) in the Parvadeh section, southwest Tabas, east Central Iran. Iranian Journal of Geology, 10(38): 1-15.

Abdolmalekai, J. & Tavakoli, V. 2016. Anachronistic facies in the early Triassic successions of the Persian Gulf and its palaeoenvironmental reconstruction. Palaeogeography, Palaeoclimatology, Palaeoecology, 446: 213-224.

Abdullin, F., Solé, J., Solari, L., Shchepetilnikova, V., Meneses-Rocha, J.J., Pavlinova, N. & Rodriguez-Trejo, A. 2016. Single grain apatite geochemistry of Permian-Triassic granitoids and Mesozoic and Eocene sandstones from Chiapas, southeast Mexico: implications for sediment provenance. International Geology Review, 58(9): 1132-1157.

Adatte, T., Planke, S., Svensen, H. & Kürschner, W.M. 2016. Preface: Impact, volcanism, global changes, and mass extinction. Palaeogeography, Palaeoclimatology, Palaeoecology, 441: 1-3.

Ajirlu, M.S., Moazzen, M. & Hajialioghli, R. 2016. Tectonic evolution of the Zagros Orogen in the realm of the Neotethys between the Central Iran and Arabian plates: an ophiolite perspective. Central European Geology, 19(1-4): 1-27.

Alfaro, E.M., Santos, A. & Ferrer, J.B.D. 2016. First evidence of rooting lycopsids preserved as imprints and trace fossils from the Silves Sandstone (Upper Triassic, eastern Algarve, South Portugal). Spanish Journal of Palaeontology, 31(1): 131-144.

Al Hseinat, M., Hübscher, C., Lang, J., Lüdmann, T., Ott, I. & Polom, U. 2016. Triassic to recent tectonic evolution of a crestal collapse graben above a salt-cored anticline in the Glückstadt Graben/North German Basin. Tectonophysics, 680: 50-66.

Al-Sheikhly, S.S., Al-Bazi, N.T.Sh. & Oboh-Ikuenobe, F.E. 2016. The Permian-Triassic boundary in the Kurdistan region of northern Iraq. Journal of Environment and Earth Science, 6(1): 39-51.

Al-Suwaidi, A.H., Steuber, T. & Suarez, M.B. 2016. The Triassic-Jurassic boundary event from an equatorial carbonate platform (Ghalilah Formation, United Arab Emirates). Journal of the Geological Society, London, 173(6): 949-953.

Alves, T.M. 2016. Polygonal mounds in the Barents Sea reveal sustained organic productivity towards the *P-T* boundary. Terra Nova, 28(1): 50-59.

Anderson, T., Kristofferson, M. & Elburg, M.A. 2016. How far can we trust provenance and crustal evolution information from detrital zircons? A South African case study. Gondwana Research, 34: 129-148.

Anell, I., Faleide, J.-I. & Braathen, A. 2016. Regional tectono-sedimentary development of the highs and basins of the northwestern Barents Shelf. Norwegian Journal of Geology, 96(1): 27-41.

Anell, I., Lecomte, I., Braathen, A. & Buckley, S.J. 2016. Synthetic seismic illumination of small-scale growth faults, paralic deposits and low-angle clinoforms: a case study of the Triassic successions on Edgeøya, NW Barents Shelf. Marine and Petroleum Geology, 77: 625-639.

Anfinson, O.A., Embry, A.F. & Stockli, D.F. 2016. Geochronologic constraints on the Permian-Triassic northern source region of the Sverdrup Basin, Canadian Arctic Islands. Tectonophysics, 691(A): 206-219.

Antczak, M. 2016. Late Triassic aetosaur (Archosauria) from Krasiejów (SW Poland): new species or an example of individual variation? Geological Journal, 51(5): 770-788.

Antić, M., Peytcheva, I. and 7 others. 2016. Pre-Alpine evolution of a segment of the north-Gondwanan margin: geochronological and geochemical evidence from the central Serbo-Macedonian Massif. Gondwana Research, 36: 523-544.

Antipin, V., Gerel, O., Perepelov, A., Odgerel, D. & Zolboo, T. 2016. Late Paleozoic and Early Mesozoic rare-metal granites in Central Mongolia and Baikal region: review of geochemistry,

Published online: May 17, 2019

Warrington, G. 2019. Triassic Literature – 2016. *Albertiana*, vol. 45, 5–38.

possible magma sources and related mineralization. Journal of GEOsciences, 61(1): 105-125.

Antonov, A.Yu. & Travin, A.V. 2016. On the problem of the scale and composition of Paleozoic and Mesozoic granitoid magmatism in the Khilok-Vitim fold belt of central Transbaikalia. Russian Journal of Pacific Geology, 10(2): 105-122.

Arboit, F., Collins, A.S., Morley, C.K., Jourdan, F., King, R., Foden, J. & Amrouch, K. 2016. Geochronological and geochemical studies of mafic and intermediate dykes from the Khao Khwang Fold-Thrust Belt: implications for petrogenesis and tectonic evolution. Gondwana Research, 36: 124-141.

Arboit, F., Collins, A.S., Morley, C.K., King, R. & Amrouch, K. 2016. Detrital zircon analysis of the southwest Indochina terrane, central Thailand: unravelling the Indosinian orogeny. Geological Society of America Bulletin, 128(5-6): 1024-1043.

Argyriou, T., Clauss, M., Maxwell, E.E., Furrer, H. & Sánchez-Villagra, M.R. 2016. Exceptional preservation reveals gastrointestinal anatomy and evolution in early actinopterygian fishes. Nature Scientific Reports, 6(18758), doi:10.1038/srep18758. (10pp).

Arkhangelsky, M.S., Zverkov, N.G., Zakharov, Yu.D. & Borisov, I.V. 2016. On the first reliable find of the genus *Tholodus* (Reptilia: Ichthyopterygia) in the Asian peripheral area of the Panthalassic Ocean. Paleontological Journal, 50(1): 78-86.

Armitage, P.J., Worden, R.H., Faulkner, D.R., Butcher, A.R. & Espie, A.A. 2016. Permeability of the Mercia Mudstone: suitability as a caprock to carbon capture and storage sites. Geofluids, 16(1): 26-42.

Arsairai, B., Wannakomol, A., Qinglai Feng & Chonglakmani, C. 2016. Paleoproductivity and paleoredox condition of the Huai Hin Lat Formation in northeastern Thailand. Journal of Earth Science, 27(3): 350-364.

Ascarrunz, E., Rage, J.-C., Legreneur, P. & Laurin, M. 2016. *Triadobatrachus massinoti*, the earliest known lissamphibian (Vertebrata: Tetrapoda) re-examined by μCT scan, and the evolution of trunk length in batrachians. Contributions to Zoology, 85(2): 201-234.

Ashchepkov, I.V., Kuligin, S.S., Vladykin, N.V., Downes, H., Vavilov, M.A., Nigmatulina, E.N., Babushkina, S.A., Tychkov, N.S. & Khmelnikova, O.S. 2016. Comparison of mantle lithosphere beneath early Triassic kimberlite fields in Siberian craton reconstructed from deep-seated xenocrysts. Geoscience Frontiers, 7(4): 639-662.

Avigad, D., Abbo, A. & Gerdes, A. 2016. Origin of the Eastern Mediterranean: Neotethys rifting along a cryptic Cadomian suture with Afro-Arabia. Geological Society of America Bulletin, 128(7-8): 1286-1296.

Bachan, A. & Payne, J.L. 2016. Modelling the impact of pulsed CAMP volcanism on $p CO_2$ and $\delta^{13}C$ across the Triassic-Jurassic transition. Geological Magazine, 153 (Special Issue 2): 252-270.

Bachmann, G.H. & Jiang Da-Yong. 2016. 13th International Field Workshop on the Triassic, Xingyi/Guizhou, southwestern China, August 1-5, 2016. Permophiles, 63: 46-50.

Baczko, M.B von & Ezcurra, M.D. 2016. Taxonomy of the archosaur *Ornithosuchus*: reassessing *Ornithosuchus woodwardi* Newton, 1894 and *Dasygnathoides longidens* (Huxley 1877). Earth and Environmental Science Transactions of the Royal Society of Edinburgh, 106(3): 199-205.

Baioumy, H. & Ulfa, Y. 2016. Facies analysis of the Semanggol Formation, south Kedah, Malaysia: a possible Permian-Triassic boundary section. Arabian Journal of Geosciences, 9(8): DOI 10.1007/s12517-016-2573-9 (16pp).

Balaky, S.M., Swrdashy, A.M. & Mamaseni, W.J. 2016. Permian-Triassic lithostratigraphic study in the Northern Thrust Zone (Ora), Iraqi Kurdistan region. Arabian Journal of Geosciences, 9(5): DOI 10.1007/s12517-016-2352-7 (21pp).

Barash, M.S. 2016. Changes in environmental conditions as the cause of the marine biota Great Mass Extinction at the Triassic-Jurassic boundary. Doklady Earth Sciences, 466(2): 119-122.

Barbolini, N., Bamford, M.K. & Tolan, S. 2016. Permo-Triassic palynology and palaeobotany of Zambia: a review. Palaeontologia Africana, 50: 18-30.

Barboni, R., Dutra, T.L. & Faccini, U.F. 2016. *Xylopteris* (Frenguelli) Stipacinic & Bonetti in the Middle-Upper Triassic (Santa Maria Formation) of Brazil. Ameghiniana, 53(5): 599-622.

Barbosa, É.N., Córdoba, V.C. & do Carmo Sousa, D. 2016. Stratigraphic evolution of the Upper Carboniferous-Lower Triassic sequence, Parnaíba Basin, Brazil. Brazilian Journal of Geology, 46(2): 181-198.

Barbosa-Gudiño, J.R., Torres-Hernández, J.R. & Villasuso-Martínez, R. 2016. Revisión estratigráfica y estructura de la Sierra Plomosa, Chihuahua. Revista Mexicana de Ciencias Geológicas, 33(2): 221-238.

Baresel, B., Bucher, H., Brosse, M., Bagherpour, B. & Schaltegger, U. 2016. High precision dating of mass extinction events: a combined zircon geochronology, apatite tephrochronology, and Bayesian age modelling approach of the Permian-Triassic boundary extinction. Geophysical Research Abstracts, 18, EGU2016-15085.

Basilone, L., Frixa, A., Trincianati, E. & Valenti, V. 2016. Permian-Cenozoic deep-water carbonate rocks of the Southern Tethyan Domain. The case of Central Sicily. Italian Journal of Geoscience, 135(2): 171-198.

Basilone, L., Sulli, A. & Morticelli, M.G. 2016. The relationships between soft-sediment deformation structures and synsedimentary extensional tectonics in Upper Triassic deep-water carbonate succession (southern Tethyan rifted continental margin – central Sicily). Sedimentary Geology, 344: 310-322.

Baucon, A. & De Carvalho, C.N. 2016. Stars of the aftermath: *Asteriacites* beds from the Lower Triassic of the Carnic Alps (Werfen Formation, Sauris di Sopra), Italy. Palaios, 31(4): 161-176.

Baud, A., Plasencia, P., Hirsch, F. & Richoz, S. 2016. Revised middle Triassic stratigraphy of the Swiss Prealps based on conodonts and correlation to the Briançonnais (Western Alps). Swiss Journal of Geosciences, 109(3): 365-377.

Bauer, M., Tóth, T.M., Raucsik, B. & Garaguly, I. 2016. Petrology and paleokarst features of the Gomba hydrocarbon reservoir (central Hungary). Central European Geology, 19(1-4): 28-59.

Bayetgoll, A. 2016. A sedimentological and ichnological analysis of wave-dominated open marine and river-dominated delta deposit from the Nayband formation (Upper Triassic) in Tabas block, central Iran. Geosciences, 25(99): 47-61. (Geological Survey of Iran: ISSN 1023-7429)

Bazhenov, M.L., Kozlovsky, A.M., Yarmolyuk, V.V., Fedorova, N.M. & Meert, J.G. 2016. Late Paleozoic paleomagnetism of South Mongolia: exploring relationships between Siberia, Mongolia and North China. Gondwana Research, 40: 124-141.

Beardmore, S.R. & Furrer, H. 2016. Preservation of Pachypleurosauridae (Reptilia; Sauropterygia) from the Middle Triassic of Monte San Giorgio, Switzerland. Neues Jahrbuch für Geologie und Paläontologie – Abhandlungen, 280(2): 221-240.

Beardmore, S.R. & Furrer, H. 2016. Taphonomic analysis of *Saurichthys* from two stratigraphic horizons in the Middle Triassic of Monte San Giorgio, Switzerland. Swiss Journal of Geosciences, 109(1): 1-16.

Beltrán-Triviño, A. & Winkler, W. 2016. Triassic magmatism on the transition from Variscan to Alpine cycles: evidence from U-Pb, Hf, and geochemistry of detrital minerals. Swiss Journal of Geosciences, 109(3): 309-328.

Ben Lasmar, R., Guellala, R., Zouhri, L., Sarsar Naouali, B., Garrach, M. & Inoubli, M.H. 2016. Hydrological study of the Triassic series in the Jeffara-Dahar region (southern part of Tunisia): contribution of well logs data and seismic reflection. Estudios Geológicos, 72(1): DOI 10.3989/egeol.43114.373 (19pp).

Benoit, J., Abdala, F., Manger, P.R. & Rubidge, B.S. 2016. The sixth sense in mammalian forerunners: variability of the parietal foramen and the evolution of the pineal eye in South African Permo-Triassic eutheriodont therapsids. Acta Palaeontolgica Polonica, 61(4): 777-789.

Benoit, J., Manger, P.R. & Rubidge, B.S. 2016. Palaeoneurological clues to the evolution of defining mammalian soft tissue traits. Nature Scientific Reports, 6(25604), doi:10.1038/srep25604. (10pp).

Benoit, J., Manger, P.R., Fernandez, V. & Rubidge, B.S. 2016. Cranial bosses of *Choerosaurus dejageri* (Therapsida, Therocephalia): earliest evidence of cranial display structures in eutheriodonts. PLoS ONE, 11(8): e0161457.doi:10.1371/journal.pone.0161457.

Benton, M. 2016. Evolutionary recovery after mass extinctions. Proceedings of the Open University Geological Society, 2: 1-8.

Benton, M.J. 2016. Palaeontology: dinosaurs, boneheads and recovery from extinction. Current Biology, 26(19): R887-889; dx.doi.org/10.1016/j.cub.2016.07.029.

Benton, M.J. 2016. The Triassic. Current Biology, 26(23): R1214-1218; dx.doi.org/10.1016/j.cub.2016.10.060.

Berra, F., Carminati, E., Jadoul, F. & Binda, M. 2016. Does compaction-induced subsidence control accommodation space at the top of prograding carbonate platforms? Constraints on the numerical modelling of the Triassic Esino Limestone (Southern Alps, Italy). Marine and Petroleum Geology, 78: 621-635.

Berra, F., Lanfranchi, A., Smart, P.L., Whitaker, F.F. & Ronchi, P. 2016. Forward modelling of carbonate platforms: sedimentological and diagenetic constraints from an application to a flat-topped greenhouse platform (Triassic, Southern Alps, Italy). Marine and Petroleum Geology, 78: 636-655.

Bercovici, A. & Vajda, V. 2016. Terrestrial Permian – Triassic boundary sections in South China. Global and Planetary Change, 143: 31-33.

Biakov, A.S., Zakharov, Yu.D. and 9 others. 2016. New data on the structure and age of the terminal Permian strata in the South Verkhoyansk region (*northeastern Asia*). Russian Geology and Geophysics, 57(2): 282-293.

Bin Liu, Chiang-Qian Ma, Yu-Heng Guo, Fu-Hao Xiong, Pan Guo & Xin Zhang. 2016. Petrogenesis and tectonic implications of Triassic mafic complexes with MORB/OIB affinities from the western Garzê-Litang ophiolitic mélange, central Tibetan Plateau. Lithos, 260: 253-267.

Bin Wang, Jian-Bo Zhou, Wilde, S.A., Xing-Zhou Zhang & Shou-Mai Ren. 2016. The timing of final closure of the Changchun-Yanji suture zone: constraints from detrital zircon U-Pb dating of the Triassic Dajianggang Formation, NE China. Lithos, 261: 216-231.

Bitner, M.A. & Emig, C.C. 2016. On the type species of *Lingularia*, and description of *Eolingularia* n. gen. Carnets de Geologie, 16(22): 543-555.

Blumenberg, M., Heunisch, C., Lückge, A., Scheeder, G. & Wiese, F. 2016. Photic zone euxinia in the central Rhaetian Sea prior to the Triassic-Jurassic boundary. Palaeogeography, Palaeoclimatology, Palaeoecology, 461: 55-64.

Boos, A.D.S., Kammerer, C.F., Schultz, C.L., Soares, M.B. & Ilha, A.L.R. 2016. A new dicynodont (Therapsida: Anomodontia) from the Permian of southern Brazil and its implications for bidentalian origins. PLoS ONE, 11(5): e0155000. doi:10.1371/journal.pone.0155000.

Bordy, E.M. & Krummeck, W.D. 2016. Enigmatic continental burrows from the Early Triassic transition of the Katberg and Burgersdorp formations in the Main Karoo Basin, South Africa. Palaios, 31(8): 389-403.

Borruel-Abadía, V., Barrenechea, J.F., Galán-Abellán, A.B., Alonso-Azcárate, J., De la Hora, R., Luque, F.J. & López-Gómez, J. 2016. Quantifying aluminium phosphate-sulphate minerals as markers of acidic conditions during the Permian-Triassic transition in the Iberian ranges, E Spain. Chemical Geology, 429: 10-20.

Botha-Brink, J., Codron, D., Huttenlocker, A.K., Angielczyk, K.D. & Ruta, M. 2016. Breeding young as a survival strategy during Earth's greatest mass extinction. Nature Scientific Reports, 6(24053), doi:10.1038/srep24053. (9pp).

Bragin, N., Dronov, A. & Raimbekov, Y. 2016. Middle Triassic rediolarians from the southeastern Pamirs (Republic of Tajikistan). Revue de Micropaléontologie, 59(4): 297-310.

Brand, U., Blamey, N. and 7 others. 2016. Methane hydrate: killer cause of Earth's greatest mass extinction. Palaeoworld, 25(4): 496-507.

Brandner, R., Gruber, A., Morelli, C. & Mair, V. 2016. Pulses of Neotethys-rifting in the Permomesozoic of the Dolomites. Geo.Alp, 13: 7-70.

Brański, P. & Mikulski, S.Z. 2016. Rare earth elements distribution in fine-grained deposits from the uppermost Triassic and Lower Jurassic of the Polish Basin: provenance and weathering of source area. Geological Quarterly, 60(2): 441-450.

Bröcker, M., Huyskens, M. & Berndt, J. 2016. U-Pb dating of detrital zircons from Andros, Greece: constraints for the time of sediment accumulation in the northern part of the Cycladic blueschist belt. Geological Journal, 51(3): 354-367.

Brogi, A., Liotta, D., Ruggieri, G., Capezzuoli, E., Meccheri, M. & Dini, A. 2016. An overview of the characteristics of geothermal carbonate reservoirs in southern Tuscany. Italian Journal of Geoscience, 135(1): 17-29.

Brom, K.R., Niedźwiedzki, R., Brachaniec, T., Ferré, B. & Salamon, M.A. 2016. Environmental control on shell size of the Middle Triassic bivalve *Plagiostoma*. Carnets de Geologie, 16(10): 297-305.

Brosse, M., Bucher, H. & Goudemand, N. 2016. Quantitative biochronology of the Permian-Triassic boundary in South China based on conodont unitary associations. Earth-Science Reviews, 155: 153-171.

Brusatte, S.L. 2016. Evolution: when dinosaurs bested their early rivals. Current Biology, 26(22): R1189-1191; dx.doi.org/10.1016/j.cub.2016.09.048.

Butler, R.J., Ezcurra, M.D., Montefeltro, F.C., Samathi, A. & Sobral, G. 2016. A new species of basal rhynchosaur (Diapsida: Archosauromorpha) from the early Middle Triassic of South Africa and the early evolution of Rhynchosauria. (Correction of article in volume 174(3): 571-588). Zoological Journal of the Linnean Society, 177(2): 1030.

Button, D.J., Barrett, P.M. & Rayfield, E.J. 2016. Comparative cranial myology and biomechanics of *Plateosaurus* and *Camarasaurus* and evolution of the suropod feeding apparatus. Palaeontology, 59(6): 887-913.

Cabreira, S.F., Kellner, A.W.A. and 11 others. 2016. A unique Late Triassic dinosauromorph assemblage reveals dinosaur ancestral anatomy and diet. Current Biology, 26(22): 3090-3095; dx.doi.org/10.1016/j.cub.2016.09.040.

Canile, F.M., Babinski, M. & Rocha-Campos, A.C. 2016. Evolution of the Carboniferous-Early Cretaceous units of Paraná Basin from provenance studies based on U-Pb, Hf and O isotopes from detrital zircons. Gondwana Research, 40: 142-169.

Cardello, G.L., Almqvist, B.S.G., Hirt, A.M. & Mancktelow, N.S. 2016. Determining the time of formation of the Rawil Depression in the Helvetic Alps by palaeomagnetic and structural methods. Geological Society, London, Special Publications, 425: 145-168.

Cariglino, B., Zavattieri, A.M., Gutiérrez, P.M. & Balarino, M.L. 2016. The paleobotanical record of the Triassic Cerro de las Cabras Formation at its type locality, Potrerillos, Mendoza (Uspallata Group): an historical account and first record of fossil flora. Ameghiniana, 53(2): 184-205.

Carpentier, C., Hadouth, S., Bouaziz, S., Lathuilière, B. & Rubino, J.-L. 2016. Basin geodynamics and sequence stratigraphy of Upper Triassic to Lower Jurassic deposits of southern Tunisia. Journal of African Earth Sciences, 117: 358-388.

Casacci, M., Bertinelli, A., Algeo, T.J. & Rigo, M. 2016. Carbonate-to-biosilica transition at the Norian-Rhaetian boundary controlled by rift-related subsidence in the western Tethyan Lagonegra Basin (southern Italy). Palaeogeography, Palaeoclimatology, Palaeoecology, 456: 21-36.

Cascales-Miñana, B., Diez, J.B., Gerrienne, P. & Cleal, C.J. 2016. A palaeobotanical perspective on the great end-Permian biotic crisis. Historical Biology, 28(8): 1066-1074.

Castiello, M., Renesto, S. & Bennett, S.C. 2016. The role of the forelimb in prey capture in the Late Triassic reptile *Megalancosaurus* (Diapsida, Drepanosauromorpha). Historical Biology, 28(8): 1090-1100.

Castro de Machuca, B. & López, M.G. 2016. Petrological review of the Baldecitos Formation (Triassic), western Sierras Pampeanas, Province of San Juan. Acta Geológica Lilloana, 26(1): 75-82.

Cattell, A. 2016. Redcliffe Sandstone revisited (Abstract). Geoscience in South-West England, 14(1): 85.

Césari, S.N. & Colombi, C. 2016. Palynology of the Late Triassic Ischigualasto Formation, Argentina: paleoecological and paleogeographic implications. Palaeogeography, Palaeoclimatology, Palaeoecology, 449: 365-384.

Changhwan Oh, Park, T.-Y.S., Junsun Woo, Bomfleur, B., Phillipe, M., Decombeix, A.-L., Kim, Y.-H.G. & Jonh Ik Lee. 2016. Triassic *Kykloxylon* wood (Umkomasiaceae, Gymnospermopsida) from Skinner Ridge, northern Victoria Land, East Antarctica. Review of Palaeobotany and Palynology, 233: 104-114.

Chao Wang, Liang Liu, Korhonen, F., Wen-Qiang Yang, Yu-Ting Cao, Shi-Ping Hu, Xiao-Hiu Zhu & Wen-Tian Liang. 2016. Origins of early Mesozoic granitoids and their enclaves from West Kunlun, NW China: implications for evolving magmatism related to closure of the Paleo-Tethys ocean. International Journal of Earth Sciences, 105(3): 941-964.

Chao Wang, Lin Ding, Li-yun Zhang, Kapp, P., Pullen, A. & Ya-hui Yue. 2016. Petrogenesis of Middle-Late Triassic volcanic rocks from the Gangdese belt, southern Lhasa terrane: implications for early subduction of Neo-Tethyan oceanic lithosphere. Lithos, 262: 320-333.

Chatalov, A., Stefanov, Y. & Ivanova, D. 2016. New data on the stratigraphy and sedimentology of the Triassic carbonate rocks in the Belotintsi strip, northwestern Bulgaria. Review of the Bulgarian Geological Society, 77(1): 27-49.

Chatzaras, V., Dörr, V., Gerdes, A., Krahl, J., Xypolias, P. & Zulauf, G. 2016. Tracking the Late Paleozoic to Early Mesozoic margin of northern Gondwana in the Hellenides: paleotectonic constraints from U-Pb detrital zircon ages. International Journal of Earth Sciences, 105(7): 1881-1899.

Chen Bo, Wang Zitian, Kang Li, Zhang Shuncun & Shi Ji'an. 2016. Diagenesis and pore evolution of Triassic Baikouquan Formation in Mabei region, Junggar Basin. Journal of Jilin University (Earth Science Edition), 46(1): 23-35.

Chen Chongyang, Gao Youfeng, Wu Haibo, Qu Xuejiao, Liu Zhiwen, Bai Xuefeng & Wang Pujun. 2016. Zircon U-Pb chronology of volcanic rocks in the Hailaer Basin, NE China and its geological implications. Earth Science – Journal of

China University of Geosciences, 2016(8): 1259-1274.

Chen Dongxia, Pang Xiongqi, Yang Keming, Zhu Weiping & Yan Qingxia. 2016. Genetic mechanism and formation of superimposed continuous tight sandstone reservoir in deep Xujiahe Formation in western Sichuan Depression. Journal of Jilin University (Earth Science edition), 2016(6): 1611-1623.

Chen Gong, Pei Xianzhi and 9 others. 2016. Zircon U-Pb geochronology, geochemical characteristics and geological significance of Chaohuolutaolegai granodiorite in Balong area, East Kunlun Mountains. Geological Bulletin of China, 35(12): 1990-2005.

Chen Jianzhou, He Lingxiong, Liu Libo, An Shengting & Shen Juan. 2016. An analysis of reservoir conditions and geochemical characteristics of the Triassic shale gas in Qilian region, Qinghai Province. Geological Bulletin of China, 35(1): 273-281.

Chen Wu, An Yin, Zuza, A.V., Jinyu Zhang, Wencan Liu & Lin Ding. 2016. Pre-Cenozoic geologic history of the central and northern Tibetan Plateau and the role of Wilson cycles in constructing the Tethyan orogenic system. Lithosphere, 8(3): 254-292.

Cheng Ji, Da-yong Jiang, Motani, R., Rieppel, O., Wei-cheng Hao & Zuo-yu Sun. 2016. Phylogeny of the Ichthyopterygia incorporating recent discoveries from South China. Journal of Vertebrate Paleontology, 36(1): e1025956 (18 pp.). DOI: 10.1080/02724634.2015.1025956.

Cheng Jun, Shi Weigang, Zhai Jie, Li Haibo & Liu Jianghua. 2016. Depositional setting and provenance analysis of Triassic nappe in the south of Bailing County, Tibet. Geological Bulletin of China, 35(9): 1472-1478.

Cheng Yen-nien, Wu Xiao-chun, Sato, T. & Shan His-yin. 2016. *Dawazisaurus brevis*, a new eosauropterygian from the Middle Triassic of Yunnan, China. Acta Geologica Sinica, 90(2): 401-424.

Chenyi Tu, Zhong-Qiang Chen & Harper, D.A.T. 2016. Permian-Triassic evolution of the Bivalvia: extinction-recovery patterns linked to ecological and taxonomic selectivity. Palaeogeography, Palaeoclimatology, Palaeoecology, 459: 53-62.

Chenyi Tu, Zhong-Qiang Chen, Retallack, G.J., Yuangeng Huang & Yuheng Fang. 2016. Proliferation of MISS-related microbial mats following the end-Permian mass extinction in terrestrial ecosystems: evidence from the Lower Triassic of the Yiyang area, Henan Province, North China. Sedimentary Geology, 333: 50-69.

Chong-jin Pang, Zheng-xiang Li, Yi-gang Xu, Shu-nv Wen & Krapež, B. 2016. Climatic and tectonic controls on Late Triassic to Middle Jurassic sedimentation in northeastern Guangdong Province, South China. Tectonophysics, 677-678: 68-87.

Chorowicz, J. 2016. Genesis of the Pieniny Klippen Belt in the Carpathians: possible effects of a major paleotransform fault in the Neo-Tethyan domain. Comptes Rendus Geoscience, 348(1): 15-22.

Chun Li, Xiao-chun Wu, Li-jun Zhao, Nesbitt, S.J., Stocker, M.R. & Li-ting Wang, 2016. A new armored archosauriform (Diapsida: Archosauromorpha) from the marine Middle Triassic of China, with implications for the diverse life styles of archosauriforms prior to the diversification of Archosauria. The Science of Nature, 103(11-12), article 95: DOI 10:1007/s00114-016-1418-4.

Ciarapica, G., Passeri, L., Bonetto, F. & Dal Piaz, G.V. 2016. Facies and Late Triassic fossils in the Roisan zone, Austroalpine Dent Blanche and Mt Mary-Cervino nappe system, NW Alps. Swiss Journal of Geosciences, 109(1): 69-81.

Cirrincione, R., Fiannacca, P., Lustrino, M., Romano, V., Tranchina, A. & Villa, I.M. 2016. Enriched asthenosphere melting beneath the nascent North African margin: trace element and Nd isotope evidence of middle-late Triassic alkali basalts from central Sicily (Italy). International Journal of Earth Sciences, 105(2): 595-609.

Clarke, J.T., Lloyd, G.T. & Friedman, M. 2016. Little evidence for enhanced phenotypic evolution in early teleosts relative to their living fossil sister group. Proceedings of the National Academy of Sciences of the United States of America, 113(41): 11531-11536.

Clarkson, M.O., Wood, R.A., Poulton, S.W., Richoz, S., Newton, R.J., Kasemann, S.A., Bowyer, F. & Krystyn, L. 2016. Dynamic anoxic ferruginous conditions during the end-Permian mass extinction and recovery. Nature Communications, 7, Article 12236. DOI: 10.1038/ncomms12236. (9pp).

Clemmensen, L.B., Milàn, J., Adolfssen, J.S., Estrup, E.J., Frobøse, N., Klein, N., Mateus, O. & Wings, O. 2016. The vertebrate-bearing Late Triassic Fleming Fjord Formation of central East Greenland revisited: stratigraphy, palaeoclimate and new palaeontological data. Geological Society, London, Special Publications, 434: 31-47.

Coleman, G. 2016. Dissecting the rise of the archosaurs. The Palaeontological Association Newsletter, 92: 96-99.

Condamine, F.L., Clapham, M.E. & Kergoat, G.J. 2016. Global patterns of insect diversification: towards a reconciliation of fossil and molecular evidence? Nature Scientific Reports, 6(19208), doi:10.1038/srep19208. (13pp).

Cong He, Liming Ji, Yuandong Wu, Ao Su & Mingzhen Zhang. 2016. Characteristics of hydrothermal sedimentation process in the Yanchang Formation, south Ordos Basin, China: evidence from element geochemistry. Sedimentary Geology, 344: 33-41.

Cooper, D.J.W., Toland, C., Ali, M.Y. & Green, O. 2016. Evolution of the Arabian continental margin of the northern Dibba Zone, eastern United Arab Emirates and Oman. Journal of Asian Earth Sciences, 129: 254-275.

Coram, R.A. & Radley, J.D. 2016. Devon's desert 'worms'. Geology Today, 32(2): 65-69.

Coturel, E.P., Morel, E.M. & Ganuza, D. 2016. Lycopodiopsids and equisetopsids from the Triassic of Quebrada de los Fósiles Formation, San Rafael Basin, Argentina. Geobios, 49(3): 167-176.

Csicsek, L.Á. & Fodor, L. 2016. Imbrication of Middle Triassic rocks near Öskü (Bakony Hills, western Hungary). Földtani Közlöny, 146(4): 355-370.

Cui Luo & Reitner, J. 2016. 'Stromatolites' built by sponges and microbes – a new type of Phanerozoic bioconstruction. Lethaia, 49(4): 555-570.

Danto, M., Witzmann, F. & Fröbisch, N.B. 2016. Vertebral development in Paleozoic and Mesozoic tetrapods revealed by paleohistological data. PLoS ONE, 11(4): e0152586. doi:10.1371/journal.pone.0152586.

Daoliang Chu, Jianxin Yu, Jinnan Tong, Benton, M.J., Haijun Song, Yunfei Huang, Ting Song & Li Tian. 2016. Biostratigraphic correlation and mass extinction during the Permian-Triassic transition in terrestrial-marine siliciclastic settings of South China. Global and Planetary Change, 146: 67-88.

Dash, B., Boldbaatar, E., Zorigtkhuu, O-E. & An Yin. 2016. Geochronology, geochemistry and tectonic implications of Late Triassic granites in the Mongolian Altai Mountains. Journal of Asian Earth Sciences, 117: 225-241.

Davis, K.E., Hill, J., Astrop, T.I. & Wills, M.W. 2016. Global cooling as a driver of diversification in a major marine clade. Nature Communications, 7, Article 13003. DOI: 10.1038/ncomms13003. (8pp).

Dawit, E.L. 2016. Paleoclimatic records of Late Triassic paleosols from Central Ethiopia. Palaeogeography, Palaeoecology, Palaeoclimatology, 449: 127-140.

Da-Yong Jiang, Motani, R. and 9 others. 2016. A large aberrant stem ichthyosauriform indicating early rise and demise of ichthyosauromorphs in the wake of the end-Permian extinction. Nature Scientific Reports, 6(26232), doi:10.1038/srep26232. (9pp).

De Baets, K., Hoffmann, R., Sessa, J.A. & Klug, C. 2016. Ammonoids. Palaeontology Online, 6, article 2, 1-15.

De Miguel Chaves, C., Garcia-Gil, S., Ortega, F., Sanz, J.L. & Pérez-Garcia, A. 2016. First Triassic tetrapod (Sauropterygia, Nothosauridae) from Castilla y Léon: evidence of an unknown taxon for the Spanish record. Journal of Iberian Geology, 42(1): 29-38.

De-Xin Kong, Ji-Feng Xu & Jian-Lin Chen. 2016. Oxygen isotope and trace element geochemistry of zircons from porphyry copper system: implications for Late Triassic metallogenesis within the Yidun Terrane, southeastern Tibetan Plateau. Chemical Geology, 441: 148-161.

Dean, C.D., Mannion, P.D. & Butler, R.J. 2016. Preservational bias controls the fossil record of pterosaurs. Palaeontology, 59(2): 225-247.

Debuysschere, M. 2016. A reappraisal of *Theroteinus* (Haramyida, Mammaliaformes) from the Upper Triassic of Saint-Nicholas-de-Port (France). PeerJ 4: e2592 https://doi.org/10.7717/peerj.2592.

Del Rey, A., Deckart, K., Arriagada, C. & Martinez, F. 2016. Resolving the paradigm of the late Paleozoic-Triassic Chilean magmatism: isotopic approach. Gondwana Research, 37: 172-181.

Deliang Liu, Rendeng Shi, Lin Ding, Qishuai Huang, Xiaoran Zhang, Yahui Yue & Liyun Zhang. 2016. Zircon U-Pb age and Hf isotopic compositions of Mesozoic granitoids in southern Qiangtang, Tibet: implications for the subduction of the Bangong-Nujiang Tethyan ocean. Gondwana Research, 41: 157-172.

Deng Wenbing, Pei Xianzhi and 9 others. 2016. LA-ICP-MS zircon U-Pb dating of the Chahantaolegai syenogranites in Xiangride area of East Kunlun and its geological significance. Geological Bulletin of China, 35(5): 687-699.

Didenko, A.N., Yong-fei Li, Peskov, Yu.A., Shou-liang Sun, Karetnikov, A.S. & Yong-heng Zhou. 2016. Closure of the Solonker basin: paleomagnetism of the Linxi and Xingfuzhilu formations (Inner Mongolia, China). Russian Journal of Pacific Geology, 10(5): 317-336.

Diedrich, C.G. 2016. *Chirotherium* trackways and feeding traces on seismic-influenced carbonate intertidals of the Middle Triassic of Central Europe: global food chain reactions onto horseshoe crab reproduction mud flat beaches of the Germanic Basin. Carbonates and Evaporites, 31(2): 187-211.

Dittrich, D. 2016. Kugelfelsen und Röhrenhöhlen als besondere Phänomene des Pfälzer Buntsandsteins. Mainzer geowissenschaftliche Mitteilungen, 44: 73-148.

Di-Ying Huang, Bechly, G. and 15 others. 2016. New fossil insect order Permopsocida elucidates major radiation and evolution of suction feeding in hemimetabolous insects (Hexapoda: Acercaria). Nature Scientific Reports, 6(23004), doi:10.1038/srep23004. (9pp).

Donskaya, T.V., Gladkochub, D.P., Mazukabzov, A.M., Wang, T., Guo, L., Rodionov, N.V. & Demonterova, E.I. 2016. Mesozoic granitoids in the structure of the Bezymyannyi metamorphic-core complex (*western Transbaikalia*). Russian Geology and Geophysics, 57(11): 1591-1605.

Dou Wenchao, Liu Luofu, Wu Kangjun & Xu Zhengjian. 2016. Pore structure characteristics and its effect on permeability by mercury injection measurement: an example from Triassic Chang-7 reservoir, southwest Ordos Basin. Geological Review, 62(2): 502-512.

Drymala, S.M. & Zanno, L.E. 2016. Osteology of *Carnufex carolinensis* (Archosauria: Pseudosuchia) from the Pekin Formation of North Carolina and its implications for early crocodylomorph evolution. PLoS ONE, 11(6): e0157528. doi:10.1371/journal.pone.0157528.

Du Fangpeng, Wang Jianqiang, Niu Junqiang, Tan Furong, Yang Chuang & Yan Mingming. 2016. Characteristics and its significance of soft sedimentary deformations of the Upper Triassic Bagong Formation in southeastern Qiangtang Block. Journal of Jilin University (Earth Science edition), 2016(3): 661-670.

Du Zhili, Tian Ya, Liu Hongjun, Wang Fengqin, Du Xiaodi, Yuan Yuan & Tong Lihua. 2016. Shale gas resource potential evaluation of Chang 9 Member, Fm Yanchang in South Ordos Basin. Journal of Jilin University (Earth Science edition), 2016(2): 358-367.

Duan Yaoyao, Li Yalin & Duan Zhiming. 2016. The discovery of the Early Triassic gabbro rocks of the Duolong accretionary complexes in southern Qiangtang terrane of Tibet and its geological significance. Geological Bulletin of China, 35(6): 887-893.

Dynowski, J.F., Nebelsick, J.H., Klein, A. & Roth-Nebelsick, A, 2016. Computational fluid dynamics analysis of the fossil crinoid *Encrinus liliiformis* (Echinodermata: Crinoidea). PLoS ONE, 11(5): e0156408. doi:10.1371/journal.pone.0156408.

Dzik, J. & Sulej, T. 2016. A late Early Triassic long-necked reptile with a bony pectoral shield and gracile appendages.

Acta Palaeontologica Polonica, 61(4): 805-823.

Ebbestad, J.O.R. 2016. Carl Wiman and the foundation of Mesozoic vertebrate palaeontology in Sweden. Geological Society, London, Special Publications, 434: 15-29.

Egbobawaye, E.I., 2016. Whole-rock geochemistry and mineralogy of Triassic Montney Formation, northeastern British Columbia, Western Canada Sedimentary Basin. International Journal of Geosciences, 7(12): 91-114.

Ehiro, M. 2016. Additional Early Triassic (late Olenekian) ammonoids from the Osawa Formation at Yamaya, Motoyoshi area, South Kitakami Belt, northeast Japan. Paleontological Research, 20(1): 1-6.

Ehiro, M., Sasaki, O. & Kano, H. 2016. Ammonoid fauna of the Upper Olenekian Osawa Formation in the Utatsu area, South Kitakami Belt, northeastern Japan. Paleontological Research, 20(2): 90-104.

Eltom, H.A., Abdullatif, O.M., Babalola, L.O., Bashari, M.A., Yassin, M., Osman, M.S. & Abdulraziq, A.M. 2016. Geochemical characterization of the Permian-Triassic transition at outcrop, central Saudi Arabia. Journal of Petroleum Geology, 39(1): 95-113.

Enayati-Bidgoli, A.H. & Rahimpour-Bonab, H. 2016. A geological based reservoir zonation scheme in a sequence stratigraphic framework: a case study from the Permo-Triassic gas reservoirs, offshore Iran. Marine and Petroleum Geology, 73: 36-58.

Engelmann de Oliveira, C.H., Jelinek, A.R., Chemale, F. Jr. & Bernet, M. 2016. Evidence of post-Gondwana breakup in Southern Brazilian Shield: insights from apatite and zircon fission track thermochronology. Tectonophysics, 666: 173-187.

Ezcurra, M.D. 2016. The phylogenetic relationships of basal archosauromorphs, with an emphasis on the systematics of proterosuchian archosauriforms. PeerJ 4: e1778 https://doi.org/10.7717/peerj.1778.

Fan Mengmeng, Li Wenhou & Bu Jun. 2016. Rare earth element characteristics of sediment samples of Triassic maximum flooding period in Longdong area of Ordos Basin and their provenance significance. Geological Bulletin of China, 35(1): 390-397.

Fan Mengmeng, Li Wenhou & Yuan Zhen. 2016. Diagenesis and its influence on porosity of Chang 6 reservoir in southeast Ordos Basin. Geological Bulletin of China, 35(2): 448-453.

Fan Song, Hu Li, Renfu Shao, Aimin Shi, Xiaoshuan Bai, Xiaorong Sheng, Heiss, E. & Wanzhi Cai. 2016. Rearrangement of mitochondrial tRNA genes in flat bugs (Hemiptera: Aradidae). Nature Scientific Reports, 6(25725), doi:10.1038/srep25725. (9pp).

Fang Xiang, Yuwan Wang, Qin Feng, Deyan Zhang & Junxing Zhao. 2016. Further research on chlorite rims in sandstones: evidence from the Triassic Yanchang Formation in the Ordos basin, China. Arabian Journal of Geosciences, 9(7): DOI 10.1007/s12517-016-2518-3 (11pp).

Fangyang Hu, Shuwen Liu, Wanyi Zhang, Zhengbin Deng & Xu Chen. 2016. A westward propagating slab tear model for Late Triassic Qinling orogenic belt geodynamic evolution: insights from the petrogenesis of the Caoping and Shahewan intrusions, central China. Lithos, 262: 486-506.

Farshid, E., Hamdi, B., Hairapetian, V. & Aghanabati, S.A. 2016. Conodont biostratigraphy of the Permian-Triassic boundary in the Baghuk mountain section northwest of Abadeh. Geosciences, 25(99): 285-294. (Geological Survey of Iran: ISSN 1023-7429).

Faure, M., Wei Lin, Yang Chu & Lepvrier, C. 2016. Triassic tectonics of the southern margin of the South China Block. Comptes Rendus Geoscience, 348(1): 5-14.

Faure, M., Wei Lin, Yang Chu & Lepvrier, C. 2016. Triassic tectonics of the Ailaoshan Belt (SW China): Early Triassic collision between the South China and Indochina blocks, and Middle Triassic intracontinental shearing. Tectonophysics, 683: 27-42.

Fei Wang, Huile Feng and 7 others. 2016. Relief history and denudation evolution of the northern Tibetan margin: constraints from $^{40}Ar/^{39}Ar$ and (U-Th)/He dating and implications for far-field effect of rising plateau. Tectonophysics, 675: 196-208.

Fengyang Xiong, Zhenxue Jiang and 8 others. 2016. The role of the residual bitumen in the gas storage capacity of mature lacustrine shale: a case study of the Triassic Yanchang shale, Ordos Basin, China. Marine and Petroleum Geology, 69: 205-215.

Ferriere, J., Baumgartner, P.O. & Chanier, F. 2016. The Maliac Ocean: the origin of the Tethyan Hellenic ophiolites. International Journal of Earth Sciences, 105(7): 1941-1963.

Firi, K.F., Sremac, J. & Vlahović, I. 2016. First evidence of Permian-Triassic shallow-marine transitional deposits in northern Croatia: Samoborsko Gorje Hills. Swiss Journal of Geosciences, 109(3): 401-413.

Fleming, E.J., Flowerdew, M.J., Smyth, H.R., Scott, R.A., Morton, A.C., Omma, J.E., Frei, D. & Whitehouse, M.J. 2016. Provenance of Triassic sandstones on the southwest Barents Shelf and the implication for sediment dispersal patterns in northwest Pangaea. Marine and Petroleum Geology, 78: 516-535.

Fong, R.K.M., LeBlanc, A.R.H. & Reisz, R.R. 2016. Dental history of *Coelophysis bauri* and the evolution of early dinosaurian periodontal tissues (Abstract). Vertebrate Anatomy Morphology Palaeontology, 2: 32.

Foote, M., Ritterbush, K.A. & Miller, A.I. 2016. Geographic ranges of genera and their constituent species: structure, evolutionary dynamics, and extinction resistance. Paleobiology, 42(2): 269-288.

Fortuny, J., Marcé-Nigué, J., Steyer, J.-S., De Esteban-Trivigno, S., Mujal, E. & Gil, L. 2016. Comparative 3D analyses and palaeoecology of giant early amphibians (Temnospondyli: Stereospondyli). Nature Scientific Reports, 6(30387), doi:10.1038/srep30387. (10pp).

Foster, W.J. 2016. The evolution of modern reef ecosystems. The Palaeontological Association Newsletter, 93: 57-59.

Foth, C., Ezcurra, M.D., Sookias, R.B., Brusatte, S.L. & Butler, R.J. 2016. Unappreciated diversification of stem archosaurs during the Middle Triassic predated the dominance of dinosaurs. BMC Evolutionary Biology, 16:188. DOI 10.1186/s12862-016-0761-6. (10pp).

Foth, C., Hedrick, B.P. & Ezcurra, M.D. 2016. Cranial ontogenetic variation in early saurischians and the role of heterochrony in the diversification of predatory dinosaurs. PeerJ 4: e1589 https://doi.org/10.7717/peerj.1589.

Francheschi, M., Preto, N., Maragon, A., Gattolin, G. & Meda, M. 2016. High precipitation rate in a Middle Triassic carbonate platform: implications on the relationship between seawater saturation state and carbonate production. Earth and Planetary Science Letters, 444: 215-224.

Frankovic, A., Eguiluz, L. & Martínez-Torres, L.M. 2016. Geodynamic evolution of the Salinas de Añana diapir in the Basque-Cantabrian Basin, western Pyrenees. Journal of Structural Geology, 83: 13-27.

Fraser, N.C. 2016. Palaeontology: a hook to the past. Current Biology, 26(20): R922-R925; dx.doi.org/10.1016/j.cub.2016.07.053.

Freudenberger, W. 2016. Der Obere Buntsandstein in Kernbohrungen im südöstlichen Rhönvorland. Geologica Bavarica, 114: 59-90.

Freudenberger, W., Friedlein, V. & Schulze, M. 2016. Die Forschungsbohrung Neuenbuch 1 bei Stadtprozelten/Unterfranken. Geologica Bavarica, 114: 9-40.

Friedlein, V. 2016. Kleinzyklengliedeung und Formationgrenzen der Forschungsbohrung Neuenbuch 1. Geologica Bavarica, 114: 41-58.

Fuhao Xiong, Changqian Ma, Hong'an Jiang & Hang Zhang. 2016. Geochronology and petrogenesis of Triassic high-K calc-alkaline granodiorites in the East Kunlun orogen, West China: juvenile lower crust melting during post-collisional extension. Journal of Earth Science, 27(3): 474-490.

Fu-Jun Ma, Qiu-Jun Wang, Jun-Ling Dong, Hao-Fei Wang, Zi-Xi Wang, Feng-Tai Zhang & Bai-Nian Sun. 2016. A new plant assemblage from the Middle Triassic volcanic tuffs of Pingchuan, Gansu, northwestern China and its paleoenvironmental significance. Paläontologische Zeitschrift, 90(2): 349-376.

Fujisaki, W., Sawaki, Y., Yamamoto. S., Sato, T., Nishizawa, M., Windley, B.F. & Maruyama, S. 2016. Tracking the redox history and nitrogen cycle in the pelagic Panthalassic deep ocean in the Middle Triassic to Early Jurassic: insights from redox-sensitive elements and nitrogen isotopes. Palaeogeography, Palaeoclimatology, Palaeoecology, 449: 397-420.

Fulong Cai, Lin Ding, Laskowski, A.K., Kapp, P., Houqi Wang, Qiang Xu & Liyun Zhang. 2016. Late Triassic paleogeographic reconstruction along the Neo-Tethyan Ocean margins, southern Tibet. Earth and Planetary Science Letters, 435: 105-114.

Fulong Cai, Lin Ding, Wei Yao, Laskowski, A.K., Qiang Xu, Ji'en Zhang & Kyaing Sein. 2016. Provenance and tectonic evolution of Lower Paleozoic-Upper Mesozoic strata from Sibumasu terrane, Myanmar. Gondwana Research, 41: 325-336.

Gacesa, R., Dunlap, W.C., Barlow, D.J., Laskowski, R.A. & Long, P.F. 2016. Rising levels of atmospheric oxygen and evolution of Nrf2. Nature Scientific Reports, 6(27740), doi:10.1038/srep27740. (5pp).

Gaetani, M. 2016. Brachiopods from the type section of the Bithynian Substage (Anisian, Middle Triassic, northwestern Turkey). Revista Italiana di Paleontologia e Stratigrafia, 122(2): 61-76.

Gale, L., Skaberne, D., Peybernes, C., Martini, R., Čar, J. & Rožič, B. 2016. Carnian reefal blocks in the Slovenian Basin, eastern Southern Alps. Facies, 62(4): DOI 10.1007/s10347-016-0474-8. (15pp).

Gao ZhiYong, Zhou ChuanMin, Feng JiaRui, Wu Hao & Li Wen. 2016. Relationship between the Tianshan Mountains Uplift and depositional environment evolution of the basins in Mesozoic-Cenozoic. Acta Sedimentologica Sinica, 34(3): 415-435.

Garbelli, C., Angiolini, L., Brand, U., Shu-zhong Shen, Jadoul, F., Posenato, R., Azmy, K. & Chang-qun Cao. 2016. Neotethys seawater chemistry and temperature at the dawn of the end Permian mass extinction. Gondwana Research, 35: 272-285.

Gardiner, N.J., Searle, M.P., Morley, C.K., Whitehouse, M.P., Spencer, C.J. & Robb, L.J. 2016. The closure of Palaeo-Tethys in eastern Myanmar and northern Thailand: new insights from zircon U-Pb and Hf isotope data. Gondwana Research, 39: 401-422.

Gardner, J.D. 2016. The fossil record of tadpoles. Fossil Imprint, 72(1-2): 17-44.

Garner, J.D. & Rage, J.-C. 2016. The fossil record of lissamphibians from Africa, Madagascar, and the Arabian Plate. Palaeodiversity and Palaeoenvironments, 96(1): 169-220.

Gastaldo, R.A. & Neveling, J. 2016. Comment on: "Anatomy of a mass extinction: sedimentological and taphonomic evidence for drought-induced die-offs at the Permo-Triassic boundary in the main Karoo Basin, South Africa" by R.M.H. Smith and J. Botha-Brink, Palaeogeography, Palaeoclimatology, Palaeoecology 396:99-118. Palaeogeography, Palaeoclimatology, Palaeoecology, 447: 88-91.

Gawlick, H.-J., Goričan, Š., Missoni, S., Dumitrica, P., Lein, R., Frisch, W. & Hoxha, L. 2016. Middle and Upper Triassic radiolarite components from the Kcira-Dushi-Komani ophiolite mélange and their provenance (Mirdita Zone, Albania). Revue de Micropaléontologie, 59(4): 359-380.

Gawlick, H.-J., Missoni, S. & Suzuki, H. 2016. Triassic radiolarite and carbonate components from a Jurassic ophiolitic mélange (Dinaridic Ophiolite Belt). Swiss Journal of Geosciences, 109(3): 473-494.

Geluk, M.C. & Röhling, H.-G. 2016. A tectono-stratigraphic model for the depositional history and basin development of the Permian-Early Triassic at the southern margin of the Southern Permian Basin (The Netherlands and adjacent parts of Belgium and Germany). Zeitschrift der Deutschen Gesellschaft für Geowissenschaften, 167(2-3): 149-166.

Ghosh, N., Basu, A.R., Bhargava, O.N., Shukla, U.K., Ghatak, A., Garzione, C.N. & Ahluwalia, A.D. 2016. Catastrophic environmental transition at the Permian-Triassic Neo-Tethyan margin of Gondwanaland: geochemical, isotopic and sedimentological evidence in the Spiti Valley, India. Gondwana Research, 34: 324-345.

Ghosh, P., Vasiliev, M.V. and 7 others. 2016. Tracking the migration of the Indian continent using the carbonate clumped isotope technique on Phanerozoic soil carbonates. Nature Scientific Reports, 6(22187), doi:10.1038/srep22187. (7pp).

Gianechini, F.A., Cordorniú, L., Arcucci, A.B., Elias, G.C. & Rivarola, D. 2016. Archosauriform remains from the Late Triassic of San Luis province, Argentina, Quebrada del Barro Formation, Marayes–El Carrizal Basin. Journal of South American Earth Sciences, 66: 110-124.

Gierlowski-Kordesch, E.H., Falcon-Lang, H.J. & Cassle, C.F. 2016. Reply to comment on the paper of Gierlowski-Kordesch and Cassle "The 'Spirorbis' problem revisited: Sedimentology and biology of microconchids in marine-nonmarine transitions" [Earth-Science Reviews, 148 (2015): 209-227]. Earth-Science Reviews, 152: 201-204.

Giesler, D., Gehrels, G., Pecha, M., White, C., Yokelson, I. & McClelland, W.C. 2016. U-Pb and Hf isotopic analysis of detrital zircons from the Taku terrane, southeast Alaska. Canadian Journal of Earth Sciences, 53(10): 979-992.

Glen, R.A., Belousova, E. & Griffin, W.L. 2016. Different styles of modern and ancient non-collisional orogens and implications for crustal growth: a Gondwanaland perspective. Canadian Journal of Earth Sciences, 53(11): 1372-1415.

Glorie, S. & De Grave, J. 2016. Exhuming the Meso-Cenozoic Kyrgyz Tianshan and Siberian Altai-Sayan: a review based on low-temperature thermochronology. Geoscience Frontiers, 7(2): 155-170.

Golding, M.L., Mortensen, J.K., Ferri, F., Zonneveld, J.-P. & Orchard, M.J. 2016. Determining the provenance of Triassic sedimentary rocks in northeastern British Columbia and western Alberta using detrital zircon geochronology, with implications for regional tectonics. Canadian Journal of Earth Sciences, 53(2): 140-155.

Golding, M.L. & Orchard, M.J. 2016. New species of the conodont *Neogondolella* from the Anisian (Middle Triassic) of northeastern British Columbia, Canada, and their importance for regional correlation. Journal of Paleontology, 90(6): 1197-1211.

González, S.N., Greco, G.A., González, P.D., Sato, A.M., Lambías, E.J. & Varela, R. 2016. Geochemistry of a Triassic dyke swarm in the North Patagonian Massif, Argentina. Implications for a postorogenic event of the Permian Gondwanide orogeny. Journal of South American Earth Sciences, 70: 69-82.

Grasby, S.E., Beauchamp, B., Bond, D.P.G., Wignall, P.B. & Sanei, H. 2016. Mercury anomalies associated with three extinction events (Capitanian Crisis, Latest Permian Extinction and the Smithian/Spathian Extinction) in NW Pangea. Geological Magazine, 153(Special Issue 2): 285-297.

Grasby, S.E., Beauchamp, B. & Knies, J. 2016. Early Triassic productivity crises delayed recovery from the world's worst mass extinction. Geology, 44(9): 779-782.

Gregori, D.A., Saini-Eidukat, B., Benedini, L., Strazzere, L., Barros, M. & Kostadinoff, J. 2016. The Gondwana Orogeny in Northern Patagonian Massif: evidences from the Caita Có granite, La Seña and Pangaré mylonites, Argentina. Geoscience Frontiers, 7(4): 621-638.

Griffin, C.T. & Nesbitt, S.J. 2016. The femoral ontogeny and long bone histology of the Middle Triassic (?Late Anisian) dinosauriform *Asilisaurus kongwe* and implications for the growth of early dinosaurs. Journal of Vertebrate Paleontology, 36(3): e1111224 (22 pp.). DOI: 10.1080/02724634.2016.1111224.

Griffin, C.T. & Nesbitt, S.J. 2016. Anomalously high variation in postnatal development is ancestral for dinosaurs but lost in birds. Proceedings of the National Academy of Sciences of the United States of America, 113(51): 14757-14762.

Gruntmeyer, K., Konietzko-Meier, D. & Bodzioch, A. 2016. Cranial bone histology of *Metoposaurus krasiejowensis* (Amphibia, Temnospondyli) from the Late Triassic of Poland. PeerJ 4: e2685 https://doi.org/10.7717/peerj.2685. (25pp).

Guang-hui Xu & Li-jun Zhao. 2016. A Middle Triassic stem-neopterygian fish from China shows remarkable secondary sexual characteristics. Chinese Science Bulletin, 61(4): 338-344.

Guang-Hui Xu & Xin-Ying Ma. 2016. A Middle Triassic stem-neopterygian fish from China sheds new light on the peltopleuriform phylogeny and internal fertilization. Chinese Science Bulletin, 61(22): 1766-1774.

Guangdi Liu, Zhelong Chen, Xulong Wang, Gang Gao, Baoli Xiang, Jiangling Ren & Wanyan Ma. 2016. Migration and accumulation of crude oils from Permian lacustrine source rocks to Triassic reservoirs in the Mahu depression of Junggar Basin, NW China: constraints from pyrrolitic nitrogen compounds and fluid inclusion analysis. Organic Geochemistry, 101: 82-98.

Guex, J. 2016. Retrograde Evolution During Major Extinction Crises. SpringerBriefs in Evolutionary Biology, xv+77pp. DOI: 10.1007/978-3-319-27917-6.

Guex, J., Galster, F. & Hammer, Ø. 2016. Calibrating Biochronological Zones with Geochronology. In: Guex, J., Galster, F. & Hammer, Ø. (eds). Discrete Biochronological Time Scales. Switzerland: Springer International Publishing, 87-100.

Guex, J., Pilet, S., Müntener, O., Bartolini, A., Spangenberg, J., Schoene, B., Sell, B. & Schaltegger, U. 2016. Thermal erosion of cratonic lithosphere as a potential trigger for mass-extinction. Nature Scientific Reports, 6(23168), doi:10.1038/srep23168. (9pp).

Guido, A., Mastandrea, A., Stefani, M. & Russo, F. 2016. Role of autochthonous versus detrital micrite in depositional geometries of Middle Triassic platform carbonate systems. Geological Society of America Bulletin, 128(5-6): 989-999.

Guillaume, B., Pochat, S., Monteaux, J., Husson, L. & Choblet, G. 2016. Can eustatic charts go beyond first order? Insights from the Permian-Triassic. Lithosphere, 8(5): 505-518.

Guoshan Li, Yongbiao Wang, Shi, G.R., Wei Liao & Lixue Yu. 2016. Fluctuations of redox conditions across the Permian-Triassic boundary – new evidence from the GSSP section in Meishan of South China. Palaeogeography, Palaeoecology, Palaeoclimatology, 448: 48-58.

Hagdorn, H. 2016. From benthic to pseudoplanktonic life: morphological remodeling of the Triassic crinoid

Traumatocrinus and the Jurassic *Seirocrinus* during habitat change. Paläontologische Zeitschrift, 90(2): 225-241.

Haijin Xu, Junfeng Zhang, Yongfeng Wang & Wenlong Liu. 2016. Late Triassic alkaline complex in the Sulu UHP terrane: implications for post-collisional magmatism and subsequent fractional crystallization. Gondwana Research, 35: 390-410.

Haijun Song, Jinnan Tong, Wignall, P.B., Mao Luo, Li Tian, Huyue Song, Yunfei Huang & Daoliang Chu. 2016. Early Triassic disaster and opportunistic foraminifers in South China. Geological Magazine, 153(Special Issue 2): 298-315.

Hall, M.R., Rigby, S.P., Dim, P., Bateman, K., Mackintosh, S.J. & Rochelle, C.A. 2016. Post-CO_2 injection alteration of the pore network and intrinsic permeability tensor for a Permo-Triassic sandstone. Geofluids, 16(2): 249-263.

Halpin, J.A., Hai Thanh Tran, Chun-kit Lai, Meffre, S., Crawford, A.J. & Khin Zaw. 2016. U-Pb zircon geochronology and geochemistry from NE Vietnam: a 'tectonically disputed' territory between the Indochina and South China blocks. Gondwana Research, 34: 254-273.

Han Liu, Bao-di Wang, Long Ma, Rui Gao, Li Chen, Xiao-bo Li & Li-quan Wang. 2016. Late Triassic syn-exhumation magmatism in central Qiangtang: evidence from the Sangehu adakitic rocks. Journal of Asian Earth Sciences, 132: 9-24.

Hansen, B.B., Milàn, J., Clemmensen, L.B., Adolfssen, J.S., Estrup, E.J., Klein, N., Mateus, O. & Wings, O. 2016. Coprolites from the Late Triassic Kap Stewart Formation, Jameson Land, East Greenland: morphology, classification and prey inclusions. Geological Society, London, Special Publications, 434: 49-69.

Hansma, J., Tohver, E., Schrank, C., Jourdan, F. & Adams, D. 2016. The timing of the Cape Orogeny: new $^{40}Ar/^{39}Ar$ age constraints on deformation and cooling of the Cape Fold Belt, South Africa. Gondwana Research, 32: 122-137.

Hao Qiang, Lin Liangbiao, Yu Yu, Gao Jian & Qian Lijun. 2016. Research on provenance and characteristics of sandstone composition of Xujiahe Formation in southern Sichuan. Northwestern Geology, 48(4)2016: 110-120.

Hao Songli, Li Zhaoyu & Li Wenhou. 2016. Sedimentary characteristics of turbidite of Chang 7 member in southwestern Ordos Basin. Geological Bulletin of China, 35(2): 424-432.

Hao Wu, Cai Li, Jingwen Chen & Chaoming Xie. 2016. Late Triassic tectonic framework and evolution of central Qiangtang, Tibet, SW China. Lithosphere, 8(2): 141-149.

Hao Yang, Wen-chun Ge, Qian Yu, Zheng Ji, Xi-wen Liu, Tan-long Zhang & De-xin Tian. 2016. Zircon U-Pb-Hf isotopes, bulk-rock geochemistry and petrogenesis of Middle to Late Triassic I-type granitoids in the Xing'an Block, northeast China: implications for early Mesozoic tectonic evolution of the central Great Xing'an Range. Journal of Asian Earth Sciences, 119: 30-48.

Harper, C.J., Taylor, T.N., Krings, M. & Taylor, E.L. 2016. Structurally preserved fungi from Antarctica: diversity and interactions in late Palaeozoic and Mesozoic polar forest ecosystems. Antarctic Sciences, 28(3): 153-173.

Haßlwanter, S. & Simon, T. 2016. Porenzemente, Senkung und Hebung von Kalksteinen des Marbach-Ooliths, Oberer Muschelkalk. Jahreshefte der gesellschaft für Naturkunde in Württemburg, 172: 109-127.

He Bizhu & Zheng Menglin. 2016. Structural characteristics and formation dynamics: a review of the main sedimentary basins in the continent of China. Acta Geologica Sinica, 90(4): 1156-1194.

He Zhang, Ri-Sheng Ye, Bing-Xiang Liu, Yan Wang, Yuan-Shuo Zhang, Siebel, W. & Fukun Chen. 2016. Partial melting of the South Qinling orogenic crust, China: evidence from Triassic migmatites and diorites of the Foping dome. Lithos, 260: 44-57.

Henares, S., Arribas, J., Cultrone, G. & Viseras, C. 2016. Muddy and dolomitic rip-up clasts in Triassic fluvial sandstones: origin and impact on potential reservoir properties (Argana Basin, Morocco). Sedimentary Geology, 339: 218-233.

Henares, S., Caracciolo, L., Viseras, C., Fernández, J. & Yeste, L.M. 2016. Diagenetic constraints on heterogeneous reservoir quality assessment: a Triassic outcrop analog of meandering fluvial reservoirs. AAPG Bulletin, 100(9): 1377-1398.

Hendrickx, C., Abdala, F. & Choiniere, J. 2016. Postcanine microstructure in *Cricodon metabolus*, a Middle Triassic gomphodont cynodont from south-eastern Africa. Palaeontology, 59(6): 851-861.

Hendrickx, C. & Carrano, M.T. 2016. Erratum on "An overview of non-avian theropod discoveries and classification". PalArch's Journal of Vertebrate Palaeontology, 13(2): 1-7.

Hennig, J., Hall, R. & Armstrong, R.A. 2016. U-Pb zircon geochronology of rocks from west Central Sulawesi, Indonesia: extension-related metamorphism and magmatism during the early stages of mountain building. Gondwana Research, 32: 41-63.

Herbst, R. & Crisafulli, A. 2016. *Buckya austroamericana* nov. gen. et sp. (Bennettitales) from the Upper Triassic Laguna Colorado Formation (El Tranquilo Group), Santa Cruz province, Argentina. Serie Correlación Geológica, 32(1-2): 85-100.

Hess, H., Etter, W. & Hagdorn, H. 2016. Roveacrinida (Crinoidea) from Late Triassic (early Carnian) black shales of Southwest China. Swiss Journal of Palaeontology, 135(2): 249-274.

Heunisch, C. & Röhling, H.-G. 2016. Early Triassic phytoplankton episodes in the Lower and Middle Buntsandstein of the Central European Basin. Zeitschrift der Deutschen Gesellschaft für Geowissenschaften, 167(2-3): 227-248.

Hinsken, T., Bröcker, M., Berndt, J. & Gärtner, C. 2016. Maximum sedimentation ages and provenance of metasedimentary rocks from Tinos Island, Cycladic blueschist belt, Greece. International Journal of Earth Sciences, 105(7): 1923-1940.

Hips, K., Haas, J. & Győri, O. 2016. Hydrothermal dolomitization of basinal deposits controlled by a synsedimentary fault system in Triassic extensional setting, Hungary. International Journal of Earth Sciences, 105(4): 1215-1231.

Hochuli, P.A. 2016. Interpretation of "fungal spikes" in Permian-Triassic boundary sections. Global and Planetary Change, 144: 48-50.

Hochuli, P.A., Sanson-Barrera, A., Schneebeli-Hermann, E. & Bucher, H. 2016. Severest crisis overlooked – worst disruption of terrestrial environments postdates Permian-Triassic mass extinction. Nature Scientific Reports, 6(28372), doi:10.1038/srep28372. (7pp).

Holmer, L.E., Popov, L.E., Klishevich. I. & Pour, M.G. 2016. Reassessment of the Early Triassic lingulid brachiopod '*Lingula*' *borealis* Bittner, 1899 and related problems of lingulid taxonomy. GFF, 138(4): 519-525.

Hong-Fu Zhang, Dong-Ya Zou, Santosh, M. & Bin Zhu, 2016. Phanerozoic orogeny triggers reactivation and exhumation in the northern part of the Archean-Paleoproterozoic North China Craton. Lithos, 261: 46-54.

Hounslow, M.W. 2016. Geomagnetic reversal rates following Palaeozoic superchrons have a fast restart mechanism. Nature Communications, 7, article 12507. DOI: 10.1038/ncomms12507. (13pp).

Hu Nie, Xin Wan, He Zhang, Jian-Feng He, Zhen-Hui Hou, Siebel, W. & Fukun Chen. 2016. Ordovician and Triassic mafic dykes in the Wudang terrane: evidence for opening and closure of the South Qinling ocean basin, central China. Lithos, 266-267: 1-15.

Hua Yang, Xiaobing Niu, Liming Xu, Shengbin Feng, Yuan You, Xiaowei Liang, Fang Wang & Dandan Zhang. 2016. Exploration potential of shale oil in Chang7 Member, Upper Triassic Yanchang Formation, Ordos Basin, NW China. Petroleum Exploration and Development, 43(4): 560-569.

Hui Zhang, Chang-qun Cao and 7 others. 2016. The terrestrial end-Permian mass extinction in South China. Palaeogeography, Palaeoecology, Palaeoclimatology, 448: 108-124.

Hu-Ting Wu, Wei-Hong He, Yang Zhang, Ting-Lu Yang, Yi-Fan Xiao, Bing Chen & Weldon, E.A. 2016. Palaeobiogeographic distribution patterns and processes of *Neochonetes* and *Fusichonetes* (Brachiopoda) in the late Palaeozoic and earliest Mesozoic. Palaeoworld, 25(4): 508-518.

Hunt, A.P. & Lucas, S.G. 2016. The case for archetypal vertebrate ichnofacies. Ichnos, 23(3-4): 237-247.

Huttenlocker, A.K. & Sidor, C.A. 2016. The first karenitid (Therapsida, Therocephalia) from the Upper Permian of Gondwana and the biogeography of Permo-Triassic therocephalians. Journal of Vertebrate Paleontology, 36(4): e1111897 (12 pp.). DOI: 10.1080/02724634.2016.1111897.

Hyžný, M., Haug, C. & Haug, J.T. 2016. *Mesoprosopon triasinum* from the Triassic of Australia revisited: the oldest eumalacostracan larva known to date and its significance for interpreting fossil cycloids. Gondwana Research, 37: 86-97.

Ibarra, Y., Corsetti, F.A., Greene, S.E. & Bottjer, D.J. 2016. A microbial carbonate response in synchrony with the end-Triassic mass extinction across the SW UK. Nature Scientific Reports, 6(19808), doi:10.1038/srep19808. (8pp).

Isaa, A., Ghaderi, A., Ashouri, A.R. & Korn, D. 2016. Late Permian and Early Triassic conodonts of the Zal section in the northwest of Iran. Journal of Stratigraphy and Sedimentary Researches, 32(3): 55-74.

Ito, T., Xin Qian & Qinglai Feng. 2016. Geochemistry of Triassic siliceous rocks of the Muyinhe Formation in the Changning-Menglian belt of southwest China. Journal of Earth Science, 27(3): 403-411.

Izokh, A.E., Medvedev, Ya.A., Fedoseev, G.S., Polyakov, G.V., Nikolaeva, I.V. & Palesskii, S.V. 2016. Distribution of PGE in Permo-Triassic basalts of the Siberian Large Igneous Province. Russian Geology and Geophysics, 57(5): 809-821.

Jackson, C.A.-L. & Lewis, M.M. 2016. Structural style and evolution of a salt-influenced rift basin margin: the impact of variations in salt composition and the role of polyphase extension. Basin Research, 28(1): 81-102.

Jamil, A., Ghani, A.A., Khin Zaw, Osman, S. & Long Xiang Quek. 2016. Origin and tectonic implications of the ~200 Ma, collision-related Jerai pluton of the Western Granite Belt, Peninsular Malaysia. Journal of Asian Earth Sciences, 127: 32-46.

Japsen, P., Green, P.F., Bonow, J.M. & Erlstöm, M. 2016. Episodic burial and exhumation of the southern Baltic Shield: epeirogenic uplifts during and after break-up of Pangaea. Gondwana Research, 35: 357-377.

Jattiot, R., Bucher, H., Brayard, A., Monnet, C., Jenks, J.F. & Hautmann, M. 2016. Revision of the genus *Anasibirites* Mojsisovics (Ammonoidea): an iconic and cosmopolitan taxon of the late Smithian (Early Triassic) extinction. Papers in Palaeontology, 2(1): 155-188.

Jerram, D.A., Svensen, H.H., Planke, S., Polozov, A.G. & Torsvik, T.H. 2016. The onset of flood volcanism in the north-western part of the Siberian Traps: explosive volcanism versus effusive lava flows. Palaeogeography, Palaeoclimatology, Palaeoecology, 441: 38-50.

Jian-gang Wang, Fu-yuan Wu, Garzanti, E., Xiumian Hu, Wei-qiang Ji, Zhi-chao Liu & Xiao-chi Liu. 2016. Upper Triassic turbidites of the northern Tethyan Himalaya (Langjiexue Group): the terminal of a sediment-routing system sourced in the Gondwanide Orogen. Gondwana Research, 34: 84-98.

Jian-Jun Fan, Cai Li, Chao-Ming Xie & Yi-Ming Liu. 2016. Depositional environment and provenance of the upper Permian-Lower Triassic Tianquanshan Formation, northern Tibet: implications for the Palaeozoic evolution of the southern Qiangtang, Lhasa, and Himalayan terranes in the Tibetan Plateau. International Geology Review, 58(2): 228-245.

Jie Tang, Wen-liang Xu, Feng Wang, Shuo Zhao & Wei Wang. 2016. Early Mesozoic southward subduction history of the Mongol-Okhotsk oceanic plate: evidence from geochronology and geochemistry of Early Mesozoic intrusive rocks in the Erguna Massif, NE China. Gondwana Research, 31: 218-240.

Jin-Cheng Xie, Di-Cheng Zhu, Guochen Dong, Zhi-Dan Zhao, Qing Wang & Xuanxue Mo. 2016. Linking the Tengchong Terrane in SW Yunnan with the Lhasa Terrane in southern Tibet through magmatic correlation. Gondwana Research, 39: 217-229.

Jingeng Sha, Yaqiong Wang, Yanhong Pan, Xiaogang Yao, Xin Rao, Huawei Cai & Xiaolin Zhang. 2016. Temporal and spatial distribution patterns of the marine-brackish-water bivalve *Waagenoperna* in China and its implications for climate and palaeogeography through the Triassic–Jurassic transition. Palaeogeography, Palaeoclimatology, Palaeoecology, 464: 43-50.

Jing-yu Wu, Su-ting Ding, Qi-jia Li, Bai-nian Sun & Yong-dong Wang. 2016. Reconstructing paleoatmospheric CO_2 levels based on fossil Ginkgoites from the Upper Triassic and Middle Jurassic of northwest China. Paläontologische Zeitschrift, 90(2): 377-387.

Jones, M.T., Jerram, D.A., Svensen, H.H. & Grove, C. 2016. The effects of large igneous provinces on the global carbon and sulphur cycles. Palaeogeography, Palaeoclimatology, Palaeoecology, 441: 4-21.

Jordan, N. & Clements, D. 2016. Field Meeting Report: Nottingham; following the GA Building Stones Conference. Magazine of the Geologists' Association, 15(3): 17-20.

Jordan, P. 2016. Reorganisation of the Triassic stratigraphic nomenclature of northern Switzerland: overview and the new Dinkelberg, Kaiseraugst and Zeglingen formations. Swiss Journal of Geosciences, 109(2): 241-255.

Jordan, P., Pietsch, J.S., Bläsi, H., Furrer, H., Kündig, N., Looser, N. & Wetzel, A. 2016. The middle to late Triassic Bänkerjoch and Klettgau formations of northern Switzerland. Swiss Journal of Geosciences, 109(2): 257-284.

Jun Chen, Shu-zhong Shen and 12 others. 2016. High-resolution SIMS oxygen isotope analysis on conodont apatite from South China and implications for the end-Permian mass extinction. Palaeogeography, Palaeoecology, Palaeoclimatology, 448: 26-38.

Jun Liu. 2016. *Yuanansuchus maopingchangensis* sp. nov., the second capitosauroid temnospondyl from the Middle Triassic Badong Formation of Yuanan, Hubei, China. PeerJ 4: e1903 https://doi.org/10.7717/peerj.1903.

Jun Shen, Qinglai Feng, Algeo, T.J., Chao Li, Planavsky, N.J., Lian Zho & Mingliang Zhang. 2016. Two pulses of oceanic environmental disturbance during the Permian-Triassic boundary crisis. Earth and Planetary Science Letters, 443: 139-152.

Kainian Huang & Opdyke, N.D. 2016. Paleomagnetism of the Upper Triassic rocks from south of the Ailaoshan Suture and the timing of the amalgamation between the South China and the Indochina Blocks. Journal of Asian Earth Sciences, 119: 118-127.

Kamata, Y., Ueno, K., Miyahigashi, A., Hara, H., Hisada, K., Charoentitirat, T. & Charusiri, P. 2016. Geological significance of the discovery of Middle Triassic (Ladinian) radiolarians from the Hong Hoi Formation of the Lampang Group, Sukhothai Zone, northern Thailand. Revue de Micropaléontologie, 59(4): 347-358.

Kammann, J., Hübscher, C., Boldreel, L.O. & Nielsen, L. 2016. High resolution shear-wave seismics across the Carlsberg Fault zone south of Copenhagen – implications for linking Mesozoic and late Pleistocene structures. Tectonophysics, 682: 56-64.

Kammerer, C.F., Butler, R.J., Bandyopadhyay, S. & Stocker, M.R. 2016. Relationships of the Indian phytosaur *Parasuchus hislopi* Lydekker, 1885. Papers in Palaeontology, 2(1): 1-23.

Kano, Y., Brenzinger, B., Nützel, A., Wilson, N.G. & Schrödl, M. 2016. Ringiculid bubble snails recovered as the sister group to sea slugs (Nudipleura). Nature Scientific Reports, 6(30908), doi:10.1038/srep30908. (11pp).

Karádi, V., Pelikán, P. & Haas, J. 2016. Conodont biostratigraphy of Upper Triassic dolomites of the Buda Hills (Transdanubian Range, Hungary). Földtani Közlöny, 146(4): 371-386.

Kati, M., Magganas, A., Zambetakis-Lekkas, A. & Logotheti, V. 2016. Late Triassic carbonate breccias and boulders from the Sub-Pelagonian Platform in Attica, Greece: constraints on the platform evolution. Neues Jahrbuch für Geologie und Paläontologie – Abhandlungen, 282(3): 291-303.

Kaya, A. 2016. Tectono-stratigraphic reconstruction of the Keban metamorphites based on new fossil findings, Eastern Turkey. Journal of African Earth Sciences, 124: 245-257.

Ke Li, Jolivet, M., Zhicheng Zhang, Jianfeng Li & Wenhao Tang. 2016. Long-term exhumation history of the Inner Mongolian Plateau constrained by apatite fission track analysis. Tectonophysics, 666: 121-133.

Ke Yan & Zeng Yong. 2016. Global brachiopod diversity analysis from Changhsingian (late Permian) to Late Triassic. Acta Palaeontologica Sinica, 55(4): 439-450.

Kear, B.P., Lindgren, J., Hurum, J.H., Milàn, J. & Vajda, V. 2016. An introduction to the Mesozoic biotas of Scandinavia and its Arctic territories. Geological Society, London, Special Publications, 434: 1-14.

Kear, B.P., Poropat, S.F. & Bazzi, M. 2016. Late Triassic capitosaurian remains from Svalbard and the palaeobiogeographical context of Scandinavian Arctic temnospondyls. Geological Society, London, Special Publications, 434: 113-126.

Kelley, N.P., Motani, R., Embree, P. & Orchard, M.J. 2016. A new Lower Triassic ichthyopterygian assemblage from Fossil Hill, Nevada. PeerJ 4: e1626 https://doi.org/10.7717/peerj.1626.

Keppie, F. 2016. How subduction broke up Pangaea with implications for the supercontinent cycle. Geological Society, London, Special Publications, 424: 265-288.

Keppie, J.D., Dostal, J. & Shellnutt, J.G. 2016. Old and juvenile source of Paleozoic and Mesozoic basaltic magmas in the Acatlán and Ayú complexes, southern Mexico: Nd isotopic constraints. Tectonophysics, 681: 376-384.

Kershaw, S., Collin, P.-Y. & Crasquin, S. 2016. Comment on Lehrmann et al. new sections and observations from the Nanpanjiang Basin, South China. Palaios, 31(3): 111-117.

Kershaw, S. & Li Guo. 2016. Beef and cone-in-cone calcite fibrous cements associated with the end-Permian and end-Triassic mass extinctions: reassessment of processes of formation. Journal of Palaeogeography, 5(1): 28-42.

Khan, A.A. & Shuib, M.L. 2016. A review of the Bentong-Raub Suture vis-à-vis new insight of the tectonic evolution of Malay Peninsula, South East Asia. Acta Geologica Sinica, 90(5): 1865-1886.

Kiliç, A.M. 2016. A new pelagic conodont taxon of the Central Pontides (Turkey). Turkish Journal of Earth Sciences, 25(5): 456-466.

Kiliç, A.-M., Plasencia, P., Ishida, K., Guex, J. & Hirsch, F. 2016. Proteromorphosis of *Neospathodus* (Conodonta) during the Permian-Triassic crisis and recovery. Revue de Micropaléontologie, 59(1): 33-39.

Kirichkova, A.I. & Esenina, A.V. 2016. Middle Triassic pteridosperms (Pinophyta) of the Timan-Pechora Basin, Stratigraphy and Geological Correlation, 24(2): 105-117.

Kiss, G.B., Molnar, F. & Palinkaš, L. 2016. Hydrothermal processes related to Triassic and Jurassic submarine basaltic complexes in northeastern Hungary and in the Dinarides and Hellenides. Geologia Croatica, 69(1): 39-64.

Kiss, G.B., Oláh, E., Zaccarini, F. & Szakáll, S. 2016. Neotethyan rift-related ore occurrences: study of an accretionary mélange complex (Darnó Unit, NE Hungary). Geologica Carpathica, 67(1): 105-115.

Klausen, T.G., Ryseth, A., Helland-Hansen, W. & Gjelberg, H.K. 2016. Progradational and backstepping shoreface deposits in the Ladinian to Early Norian Snadd Formation of the Barents Sea. Sedimentology, 63(4): 893-916.

Klein, H., Milàn, J. and 7 others. 2016. Archosaur footrpints (cf. *Brachychirotherium*) with unusual morphology from the Upper Triassic Fleming Fjord Formation (Norian-Rhaetian) of East Greenland. Geological Society, London, Special Publications, 434: 71-85.

Klein, H., Wizevich, M.C., Thüring, B., Marty, D., Thüring, S., Falkingham, P. & Meyer, C.A. 2016. Triassic chirotheriid footprints from the Swiss Alps: ichnotaxonomy and depositional environment (Cantons Wallis & Glarus). Swiss Journal of Palaeontology, 135(2): 295-314.

Klein, N. & Griebeler, E.M. 2016. Bone histology, microanatomy, and growth of the nothosauroid *Simosaurus gaillardoti* (Sauropterygia) from the Upper Muschelkalk of southern Germany/BadenWürttemberg. Comptes Rendus Paleovol, 15(1-2): 142-162.

Klein, N., Sander, P.M., Krahl, A., Scheyer, T.M. & Houssaye, A. 2016. Diverse aquatic adaptations in *Nothosaurus* spp. (Sauropterygia) – inferences from humeral histology and microanatomy. PLoS ONE, 11(7): e0158448. doi:10.1371/journal.pone.0158448.

Klein, N., Voeten, D.F.A.E., Haarhuis, A. & Bleeker, M. 2016. The earliest record of the genus *Lariosaurus* from the early Middle Anisian (Middle Triassic) of the Germanic Basin. Journal of Vertebrate Paleontology, 36(4): e1163712 (9 pp.). DOI: 10.1080/02724634.2016.1163712.

Klompmaker, A.A., Nützel, A. & Kaim, A. 2016. Drill hole convergence and a quantitative analysis of drill holes in mollusks and brachiopods from the Triassic of Italy and Poland. Palaeogeography, Palaeoclimatology, Palaeoecology, 457: 342-359.

Knaust, D. & Neumann, C. 2016. *Asteriacites* von Schlotheim, 1820 – the oldest valid ichnogenus name – and other asterozoan-produced fossils. Earth-Science Reviews, 157: 111-120.

Knaust, D., Uchman, A. & Hagdorn, H. 2016. The probable isopod burrow *Sinusichnus seilacheri* isp. n. from the Middle Triassic of Germany: an example of behavioural convergance. Ichnos, 23(1-2): 138-146.

Knoll, A.H. & Follows, M.J. 2016. A bottom-up perspective on ecosystem change in Mesozoic oceans. Proceedings of the Royal Society of London, B.283(1841). 20161755; DOI: 10.1098/rspb.2016. 1755.

Kogan, I. & Romano, C. 2016. Redescription of *Saurichthys madagascariensis* Piveteau, 1945 (Actinopterygii, Early Triassic), with implications for the early saurichthyid morphotype. Journal of Vertebrate Paleontology, 36(4): e1151886 (21 pp.). DOI: 10.1080/02724634.2016.1151886.

Kogan, I. & Romano, C. 2016. A new postcranium of *Saurichthys* from the Early Triassic of Spitsbergen. Paläontologie, Stratigraphie, Fazies, 23: 205-221. [Freiberger Forschungshefte, C 550].

Komatsu, T., Takashima, R. and 7 others. 2016. Carbon isotopic excursions and detailed ammonoid and conodont biostratigraphies around Smithian-Spathian boundary in the Bac Thuy Formation, Vietnam. Palaeogeography, Palaeoclimatology, Palaeoecology, 454: 65-74.

Kondla, D., Sanei, H., Clarkson, C.R., Ardakani, O.H., Xibo Wang & Chunqing Jiang. 2016. Effects of organic and mineral matter on reservoir quality in a Middle Triassic mudstone in the Canadian Arctic. International Journal of Coal Geology, 153: 112-126.

Kong-Yang Zhu, Zheng-Xiang Li, Xi-Sheng Xu, Wilde, S.A. & Han-Lin Chen. 2016. Early Mesozoic ferroan (A-type) and magnesian granitoids in eastern South China: tracing the influence of flat-slab subduction at the western Pacific margin. Lithos, 240-243: 371-381.

Konotio, I., Lagnaoui, A., Chellai, E.H., Fabuel-Perez, I. & Redfern, J. 2016. Reconnaissance des caractères sédimentaires et ichnofaciès des grès triasiques de Tighadwine, Haut-Atlas de Marrackech-Maroc. Boletin Geológico y Minero, 127(2-3): 361-374.

Kozłowska, M., Barski, M., Mieszkowski, R. & Antoszewska, K. 2016. A new Triassic-Jurassic section in the southern part of the Holy Cross Mts. (Poland) - implications for palaeogeography. Geological Quarterly, 60(2): 365-384.

Kozu, S., Apsorn Sardsud, Doungrutai Saesaengseerung, Chedchan Pothichaiya, Agematsu, S. & Sashida, K. 2016. An overview of dinosaur footprints from the Khorat Group, northeastern Thailand, and characteristics of the dinosaur ichnofauna. Fossils – The Palaeontological Society of Japan, 100: 109-123.

Krainer, K. & Meyer, M. 2016. Innsbruck's geology in a nutshell: from the Hafelekar to the Hötting Breccia. Geo.Alp, 13: 215-228.

Krapovikas, V., Mángano, M.G., Buatois, L.A. & Marsicano, C.A. 2016. Integrated ichnofacies models for deserts: recurrent patterns and megatrends. Earth-Science Reviews, 157: 61-85.

Kubo, T. & Kubo, M.O. 2016. Nonplantigrade foot posture: a constraint on dinosaur body size. PLoS ONE, 11(1): e0145716. doi:10.1371/journal.pone.0145716. (14pp).

Kustatscher, E., Bernardi, M., Petti, F.M., Avanzini, M. & Tomasoni, R. 2016. Late Paleozoic and Mesozoic terrestrial environments in the Dolomites and surrounding areas. Geo. Alp, 13: 71-116.

Labandeira, C.C., Kustatscher, E. & Wappler, T. 2016. Floral assemblages and patterns of insect herbivory during the Permian to Triassic of northeastern Italy. PLoS ONE, 11(11): e0165205. Doi:10.1371/journal.pone.0165205. (49pp).

Lacerda, M.B., Mastrantonio, B.M., Fortier, D.C. & Schultz, C.L. 2016. New insights on *Prestosuchus chiniquensis* Huene, 1942 (Psurosuchia, Loricata) based on new specimens from the "Tree Sanga" outcrop, Chiniquá Region, Rio Grande do Sul, Brazil. PeerJ 4: e1622 https://doi.org/10.7717/peerj.1622. (47pp).

Lagnaoui, A., Klein, H., Saber, H., Fekkak, A., Belahmira, A. & Schneider, J.W. 2016. New discoveries of archosaur and other footprints from the Timezgadiouine Formation (Irohalene Member, Upper Triassic) of the Argana Basin, western High Atlas, Morocco – ichnotaxonomic implications. Palaeogeography, Palaeoclimatology, Palaeoecology, 453: 1-9.

Lakin, R.J., Duffin, C.J., Hildebrandt, C. & Benton, M.J. 2016. The Rhaetian vertebrates of Chipping Sodbury, South Gloucestershire, UK, a comparative study. Proceedings of the Geologists' Association, 127(1): 40-52.

Lamsdell, J.C. 2016. Horseshoe crab phylogeny and independent colonizations of fresh water: ecological invasion as a driver for morphological innovation. Palaeontology, 59(2): 181-194.

Lara, M.B. & Bo Wang. 2016. New hemipteran insects (Eoscarterellidae, Scytinopteridae, and Protosyllidiidae) from the Upper Triassic Potrerillos Formation of Mendoza, Argentina. Paläontologische Zeitschrift, 90(1): 49-61.

Lau, K.V., Maher, K. and 8 others. 2016. Marine anoxia and delayed Earth system recovery after the end-Permian extinction. PNAS, 113(9): 2360-2365.

Lautenschlager, S., Brassey, C.A., Button, D.J. & Barrett, P.M. 2016. Decoupled form and function in disparate herbivorous dinosaur clades. Nature Scientific Reports, 6(26495), doi:10.1038/srep26495. (10pp).

Lautenschlager, S. & Butler, R.J. 2016. Neural and endocranial anatomy of Triassic phytosaurian reptiles and convergence with fossil and modern crocodylians. PeerJ 4: e2251 https://doi.org/10.7717/peerj.2251. (20pp).

Le Yao, Aretz, M., Jitao Chen, Webb, G.E. & Xiangdong Wang. 2016. Global microbial carbonate proliferation after the end-Devonian mass extinction: mainly controlled by demise of skeletal bioconstructors. Nature Scientific Reports, 6(39694), doi:10.1038/srep39694. (9pp).

LeBlanc, A.R.H., Reisz, R.R., Brink, K.S. & Abdala, F. 2016. Heterochrony and the evolution of mammalian tooth attachment (Abstract). Vertebrate Anatomy Morphology Palaeontology, 2: 37-38.

Lecuona, A., Ezcurra, M.D. & Irmis, R.B. 2016. Revision of the early crocodylomorph *Trialestes romeri* (Archosauria, Suchia) from the lower Upper Triassic Ischigualasto Formation of Argentina: one of the oldest-known crocodylomorphs. Papers in Palaeontology, 2(4): 585-622.

Ledneva, G.V., Peaseb, V.L. & Bazylevc, B.A. 2016. Late Triassic siliceous-volcano-terrigenous deposits of the Chukchi Peninsula: composition of igneous rocks, U-Pb age of zircons, and geodynamic interpretations. Russian Geology and Geophysics, 57(8): 1119-1134.

Lehrmann, D.J., Bentz, J.M. and 15 others. 2016. Reply: Permian-Triassic microbialite and dissolution surface environmental controls on the genesis of marine microbialites and dissolution surface associated with the end-Permian mass extinction: new sections and observations from the Nanpanjiang Basin, South China. Palaios, 31(3): 118-121.

Lei Gong, Lianbo Zeng, Zhiyong Gao, Rukai Zhu & Benjian Zhang. 2016, Reservoir characterization and origin of tight gas sandstones in the Upper Triassic Xujiahe formation, western Sichuan Basin, China. Journal of Petroleum Exploration and Production Technology, 6(3): 319-329.

Lei Liang, Jinnan Tong, Haijun Song, Ting Song, Li Tian, Huyue Song & Haiou Qiu. 2016. Lower-Middle Triassic conodont biostratigraphy of the Mingtang section, Nanpanjiang Basin, South China. Palaeogeography, Palaeoclimatology, Palaeoecology, 459: 381-393.

Lei Xiang, Schoepfer, S.D., Hua Zhang, Dong-xun Yuan, Chang-qun Cao, Quan-feng Zheng, Henderson, C.M. & Shu-zhong Shen. 2016. Oceanic redox evolution across the end-Permian mass extinction at Shangsi, South China. Palaeogeography, Palaeoecology, Palaeoclimatology, 448: 59-71.

Legendre, L.J., Guénard, G., Botha-Brink, J. & Cubo, J. 2016. Palaeohistological evidence for ancestral high metabolic rate in archosaurs. Systematic Biology, 65(6): 989-996.

Leleu, S., Hartley, A.J., van Oosterhout, C., Kennan, L., Ruckwied, K. & Geres, K. 2016. Structural, stratigraphic and sedimentological characterisation of a wide rift system: the Triassic rift system of the Central Atlantic Domain. Earth-Science Reviews, 158: 89-124.

Lerch, B., Karlsen, D.A., Matapour, Z., Seland, R. & Backer-Owe, K. 2016. Organic geochemistry of Barents Sea petroleum: thermal maturity and alteration and mixing processes in oils and condensates. Journal of Petroleum Geology, 39(2): 125-147.

Lessner, E.J., Stocker, M.R., Smith, N.D., Turner, A.H., Irmis, R.B. & Nesbitt. S.J. 2016. A new rauisuchid (Archosauria: Pseudosuchia) from the Upper Triassic (Norian) of New Mexico increases the diversity and temporal range of the clade. PeerJ 4: e2336 https://doi.org/10.7717/peerj.2336. (28pp).

Li Chun, Rieppel, O., Cheng Long & Fraser, N.C. 2016. The earliest herbivorous marine reptile and its remarkable jaw apparatus. Science Advances, 2(5). DOI: 10.1126/sciadv.1501659. (4pp).

Li HongWei, Li Fei, Hu Guang, Tan XiuCheng & Li Ming. 2016. A review of studies on global changes of sea level across the Permian Triassic boundary. Acta Sedimentologica Sinica, 34(6): 1077-1091.

Li Huan, Xi Xiaoshuang, Sun Huashan, Kong Hua, Wu Qianhong, Wu Chengming & Gabo-Ratio, J.A.S. 2016. Geochemistry of the Batang Group in the Zhaokalong area, Yushu, Qinghai: implications for the Late Triassic tectonism in the northern Sanjiang region, China. Acta Geologica Sinica, 90(2): 704-721.

Li Junjian, Tang Wenlong and 8 others. 2016. Re-Os isotopic dating of molybdenites from the Bilugangan porphyry Mo deposit in Abag Banner, Inner Mongolia, and its geological significance. Geological Bulletin of China, 35(4): 519-523.

Li Qiu-peng, Wan You-li, Jiang Qi, Ding Xiao-qi, Liu Xi-xiang, Ren Qi-hao, Gao Shan & Chen Jun. 2016. Diagenesis and favourable diagenetic facies zones of the Chang-6 oil reservoirs in the Binxian-Changwu region, Ordos Basin. Sedimentary Geology and Tethyan Geology, 36(2016:4): 21-29.

Li Rong, Hu ZhongGui, Zhang Hang, Hu MingYi, Chan Xuan, Zhu YiXin & Liu Fei. 2016. Depositional pattern and reservoir distribution of Changxing Formation intra-platform reef and shoal in Wolonghe-Yangduxi zone of eastern Sichuan Basin. Acta Sedimentologica Sinica, 34(5): 973-982.

Li Xianghui, Wang Chengshan, Liu Shugen, Ran Bo, Xu Wenli & Zhou Yong. 2016. Chronology of the volcanic rock intercalations within the flysch of the Songpan-Ganzi folded belt and its geological significance. Geological Bulletin of China, 35(6): 879-886.

Li Ya, Yao Jian-xin, Wang Si-en & Pang Qi-qing. 2016. Middle-Late Triassic terrestrial strata and establishment of stages in the Ordos Basin. Acta Geoscientica Sinica, 2016(3): 267-276.

Li Zhiguang, Sun Zuoyu, Jiang Dayong & Ji Chang. 2016. LA-ICP-MS zircon U-Pb age of the fossil layer of Triassic Xingyi fauna from Xingyi, Guizhou, and its significance. Geological Review, 62(3): 779-790.

Li Zhucang, Li Yongjun, Qi Jianhong, Zhang Haifeng, Yang Zhiyong, Liu Zhibing & Zhou Ye. 2016. Geochemical characteristics and tectonic significance of the volcanic rocks from the Lower Triassic Huari Formation in west Qinling. Northwestern Geology, 48(1)2016: 26-33.

Liang Qiu, Dan-ping Yan, Shaung-li Tang, Qin Wang, Wen-xin Yang, Xiangli Tang & Jibin Wang. 2016. Mesozoic geology of southwestern China: Indosinian foreland overthrusting and subsequent deformation. Journal of Asian Earth Sciences, 122: 91-105.

Limarino, C.O., Ciccioli, P.L., Krapovickas, V. & Beneditto, L.D. 2016. Estratigrafía de las sucesiones Mesozoicas, Paleógenas y Neógenas de las quebradas Santo Domingo y El Peñón (Precordillera septentrional Riojana). Revista de la Asociación Geológica Argentina, 73(3): 301-318.

Liming Ji, Cong He, Mingzhen Zhang, Yuandong Wu & Xiangbo Li. 2016. Bicyclic alkanes in source rocks of the Triassic Yanchang Formation in the Ordos Basin and their inconsistency in oil-source correlation. Marine and Petroleum Geology, 72: 359-373.

Lindström, S. 2016. Palynofloral patterns of terrestrial ecosystem change during the end-Triassic event – a review. Geological Magazine, 153(Special Issue 2): 223-251. (Erratum: 355).

Lindström, S., Irmis, R.B., Whiteside, J.H., Smith, N.D., Nesbitt, S.J. & Turner, A.H. 2016. Palynology of the upper Chinle Formation in northern New Mexico, U.S.A.: implications for biostratigraphy and terrestrial ecosystem change during the Late Triassic (Norian-Rhaetian). Review of Palaeobotany and Palynology, 225: 106-131.

Linol, B., de Wit, M.J., Barton, E., de Wit, M(Mike), J.C. & Guillocheau, F. 2016. U-Pb detrital zircon dates and source provenance analysis of Phanerozoic sequences of the Congo Basin, central Gondwana. Gondwana Research, 29(1): 208-219.

Li-Qin Li & Yong-Dong Wang. 2016. Late Triassic palynofloras in the Sichuan Basin, South China: synthesis and perspective. Palaeoworld, 25(2): 212-238.

Liqin Li, Yongdong Wang, Zhaosheng Liu, Ning Zhou & Yan Wang. 2016. Late Triassic palaeoclimate and palaeoecosystem variations inferred by palynological record in the northeastern Sichuan Basin, China. Paläontologische Zeitschrift, 90(2): 327-348.

Liu Dongliang, Li Haibing, Sun Zhiming, Pei Junling, Wang Huan, Pan Jiawei & Wang Meng. 2016. The major magmatic events in the Qimantag Mountain of Tibetan Plateau since Paleozoic and its implications. Geological Bulletin of China, 35(12): 2014-2026.

Liu Jian-feng, Li Jin-yi, Sun Li-xin, Yin Dong-fang & Zheng Pei-xi. 2016. Zircon U-Pb dating of the Jiujingzi ophiolite in Bairin Left Banner, Inner Mongolia: constraints on the formation and evolution of the Xar Moron River suture zone. Geology in China, 43(6) 2016: 1947-1962.

Liu Jinheng, Hu Peiyuan, Li Cai, Xie Chaoming, Fan Jianjun & Yu Yunpeng. 2016. The establishment and significance of the Upper Permian-Lower Triassic Tianquanshan Formation in central Qiangtang, northern Tibet: the constraint on the tectonic evolution of Lungmu Co-Shuanghu-Lancang River area. Geological Bulletin of China, 35(5): 667-673.

Liu Jinlong, Sun Fengyue, Zhang Yajing, Ma Fang, Liu Fengxu & Zeng Le. 2016. Zircon U-Pb geochronology, geochemistry and Hf isotopes of Nankouqian granitic intrusion in Qingyuan region, Liaoning Province. Earth Science – Journal of China University of Geosciences, 2016(1): 55-66.

Liu Mingjie, Liu Zhen, Wang Peng & Pan Gaofeng. 2016. Diagenesis of the Triassic Yanchang Formation tight sandstone reservoir in the Xifeng-Ansai area of Ordos Basin and its porosity evolution. Acta Geologica Sinica, 90(3): 956-970.

Long, J.A., Large, R.R. and 7 others. 2016. Severe selenium depletion in the Phanerozoic oceans as a factor in three global mass extinction events. Gondwana Research, 36: 209-218.

López-Arbarello, A., Bürgin. T., Furrer, H. & Stockar, R. 2016. New holostean fishes (Actinopterygii: Neopterygii) from the Middle Triassic of the Monte San Giorgio (Canton Ticino, Switzerland). PeerJ 4: e2234 https://dx.doi.org/10.7717/peerj.2234. (61pp).

Lozovsky, V.R., Balabanov, Yu.P., Karasev, E.V., Novikov, I.V., Ponomarenko, A.G. & Yaroshenko, O.P. 2016. The terminal Permian in European Russia: Vyaznikovian Horizon, Nedubrovo Member, and Permian-Triassic boundary. Stratigraphy and Geological Correlation, 24(4): 364-380.

Lucas, S.G., Rinehart, L.F., Heckert, A.B., Hunt, A.P. & Spielmann, J.A. 2016. Rotten Hill: a Late Triassic bonebed in the Texas Panhandle, USA. New Mexico Museum of Natural History and Science, Bulletin 72: 97pp.

Ma Long, Liu Han, Wu Cheng-shu, Li Zhong-xiong, Li Yong, Wei Hong-wei & Deng Qi. 2016. The age and geological significance of the Shanzixingshan volcanic rocks in Shuanghu of Northern Tibet. Journal of Stratigraphy, 40(4): 389-395.

Ma Yao, Li Wenhou, Liu Zhe, Huang Haiyu, Yang Bo & Xu Xing. 2016. Characteristics of microscopic pore structure in the low permeability sandstone reservoir: a case study of Chang 9 of Yanchang Formation in Zhijing-Ansai area of Ordos Basin. Geological Bulletin of China, 35(2): 398-405.

Ma Zhonghao, Chen Qingshi, Shi Zhongwang, Wang Cheng, Du Wugang & Zhao Changying. 2016. Geochemistry of oil shale from Chang 7 reservoir of Yanchang Formation in south Ordos Basin and its geological significance. Geological Bulletin of China, 35(9): 1550-1558.

Malaza, N., Ken Liu & Baojin Zhao. 2016. Subsidence analysis and burial history of the Late Carboniferous to Early Jurassic Soutpansberg Basin. Limpopo Province, South Africa. Acta Geologica Sinica, 90(6): 2000-2007.

Malyshev, S.V., Khudoley, A.K., Prokopiev, A.V., Ershova, V.B., Kazakova, G.G. & Terentyeva, L.B. 2016. Source rocks of Carboniferous-Cretaceous terrigenous sediments of the northeastern Siberian Platform: results of Sm-Nd isotope-geochemical studies. Russian Geology and Geophysics, 57(3): 421-433.

Mao Luo, George, A.D. & Zhong-Qiang Chen. 2016. Sedimentology and ichnology of two Lower Triassic sections in South China: implications for the biotic recovery following the end-Permian mass extinction. Global and Planetary Change, 144: 198-212.

Mao Luo, Zhong-Qiang Chen, Shi, G.R., Yuheng Fang, Haijun Song, Zhihai Jia, Yuangeng Huang & Hao Yang, 2016. Upper Lower Triassic stromatolite from Anhui, South China: geobiologic features and paleoenvironmental implications. Palaeogeography, Palaeoclimatology, Palaeoecology, 451: 40-54.

Maodu Yan, Dawen Zhang, Xiaomin Fang, Haidong Ren, Weilin Zhang, Jinbo Zan, Chunhui Song & Tao Zhang, 2016. Paleomagnetic data bearing on the Mesozoic deformation of the Qiangtang Block: implications for the evolution of the Paleo- and Meso-Tethys. Gondwana Research, 39: 292-316.

Marcelino, V.R. & Verbruggen, H. 2016. Multi-marker metabarcoding of coral skeletons reveals a rich microbiome and diverse evolutionary origins of endolithic algae. Nature Scientific Reports, 6(31508), doi:10.1038/srep31508. (9pp).

Marinova, I. & Damyanov, Z. 2016. Plate tectonic aspects of the Triassic carbonate-hosted stratiform-stratabound base-metal deposits in the Western Balkan, NW Bulgaria. Geologia Croatica, 69(1): 65-73.

Marsicano, C.A., Irmis, R.B., Mancuso, A.C., Mundil, R. & Chemale, F. 2016. The precise temporal calibration of dinosaur origins. PNAS, 113(3): 509-513.

Martinelli, A.G., Soares, M.B. & Schoch, R.R. 2016. Owenettids and procolophonids from the lower Keuper shed new light on the diversity of parareptiles in the German Middle Triassic. Journal of Paleontology, 90(1): 92-101.

Martinelli, A.G., Soares, M.B. & Schwanke, C. 2016. Two new cynodonts (Therapsida) from the middle-early Late Triassic of Brazil and comments on South American Probainognathians. PLoS ONE, 11(10): e0162945. doi:10.1371/journal.pone.0162945. (43pp).

Martínez, R.N., Apaldetti, C., Correa, G.A. & Abelín, D. 2016. A Norian lagerpetid dinosauromorph from the Quebrada del Barro Formation, northwestern Argentina. Ameghiniana, 53(1): 1-13.

Matthews, K.J., Maloney, K.T., Zahirovic, S., Williams, S.E., Seton, M. & Müller, R.D. 2016. Global plate boundary evolution and kinematics since the late Paleozoic. Global and Planetary Change, 146: 226-250.

Matysik, M. 2016. Facies types and depositional environments of a morphologically diverse carbonate platform: a case study from the Muschelkalk (Middle Triassic) of Upper Silesia, southern Poland. Annales Societatis Geologorum Poloniae, 86(2): 119-164.

Matysik, M. & Surmik, D. 2016. Depositional conditions of vertebrate remains within the Lower Muschelkalk (Anisian) peritidal carbonates of the "Stare Gliny" quarry near Olkusz (Kraków-Silesia region, southern Poland). Przegląd Geologiczny, 64(7): 495-503.

Maxwell, E.E., Diependaal, H., Winkelhorst, H., Goris, G. & Klein, N. 2016. A new species of *Saurichthys* (Actinopterygii: Saurichthyidae) from the Middle Triassic of Winterswijk, The Netherlands. Neues Jahrbuch für Geologie und Paläontologie – Abhandlungen, 280(2): 119-134.

McElwain, J.C., Montañez, J.D., White, J.P. & Yiotis, C. 2016. Was atmospheric CO_2 capped at 1000 ppm over the past 300 million years? Palaeogeography, Palaeoclimatology, Palaeoecology, 441: 653-658.

McLoughlin, S. & Strullu-Derrien, C. 2016. Biota and palaeoenvironment of a high middle-latitude Late Triassic peat-forming ecosystem from Hopen, Svalbard archipelago. Geological Society, London, Special Publications, 434: 87-112.

McPhee, B.W. & Choiniere, J.N. 2016. A hyper-robust sauropod dinosaur ilium from the Upper Triassic-Lower Jurassic Elliot Formation of South Africa: implications for the functional diversity of basal Sauropodomorpha. Journal of African Earth Sciences, 123: 177-184).

Mears, E.M., Rossi, V. and 9 others. 2016. The Rhaetian (Late Triassic) vertebrates of Hampstead Farm Quarry, Gloucestershire, UK. Proceedings of the Geologists' Association, 127(4): 478-505.

Meier, T., Soomro, R.A., Viereck, L., Lebedev, S., Behrmann, J.H., Weidle, C., Cristiano, L. & Hanemann, R. 2016. Mesozoic and Cenozoic evolution of the Central European lithosphere. Tectonophysics, 692(A): 58-73.

Meijia Song, Liangshu Shu & Santosh, M. 2016. Early Mesozoic granites in the Nanling Belt, South China: implications for intracontinental tectonics associated with stress regime transformation. Tectonophysics, 676: 148-169.

Meng Duan, Yaoling Niu, Juanjuan Kong, Pu Sun, Yan Hu, Yu Zhang, Shuo Chen & Jiyong Li. 2016. Zircon U-Pb geochronology, Sr-Nd-Hf isotopic composition and geological significance of the Late Triassic Baijiazhuang and Lvjing granitic plutons in West Qinling Orogen. Lithos, 260: 443-456.

Meng Hao, Zhong Da-kang, Li Zhuo-pei, Liu Yun-long, Zhao Jing & Yang Yue-dong. 2016. Sequence stratigraphy and sedimentary facies of the Fifth Member of the Upper Triassic Xujiahe Formation of the middle part of the West Sichuan Depression, South China. Journal of Stratigraphy, 40(3): 278-289.

Mette, W., Thibault, N., Krystyn, L., Korte, C., Clémence, M.-E., Ruhl, M., Rizzi, M. & Ullmann, C.V., 2016. Rhaetian (Late Triassic) biotic and carbon isotope events and intraplatform basin development in the Northern Calcareous Alps, Tyrol, Austria. Geo.Alp, 13: 233-256.

Midoun, M. & Seddiki, A. 2016. The mafic, ultramafic and metamorphic xenoliths in Triassic evaporite complexes, north-west Algeria, Boletin Geológico y Minero, 127(2-3): 333-344.

Midwinter, D., Hadlari, T., Davis, W.J., Dewing. K. & Arnott, R.W.C. 2016. Dual provenance signatures of the Triassic northern Laurentian margin from detrital-zircon U-Pb and Hf-isotope analysis of the Triassic-Jurassic strata in the Sverdrup Basin. Lithosphere, 8(6): 668-683.

Miklavc, P., Celarc, B. & Šmuc, A. 2016. Anisian Strelovec Formation in the Robanov kot, Savinja Alps (northern Slovenia). Geologija, 59(1): 23-34.

Milidragovich, D., Chapman, J.B., Bichlmaier, S., Canil, D. & Zagorevski, A. 2016. H_2O-driven generation of picritic melts in the Middle to Late Triassic Stuhini arc of the Stikine terrane, British Columbia, Canada. Earth and Planetary Science Letters, 454: 65-77.

Mills, B.J.W., Belcher, C.M., Lenton, T.M. & Newton, R.J. 2016. A modelling case for high atmospheric oxygen concentrations during the Mesozoic and Cenozoic. Geology, 44(12): 1023-1026.

Milner, A.C. & Barrett, P.M. 2016. Smith Woodward's contributions on fossil tetrapods. Geological Society, London, Special Publications, 430: 289-309.

Min Zeng, Xiang Zhang, Hui Cao, Ettensohn, F.R., Wenbin Cheng & Xinghai Lang. 2016. Late Triassic initial subduction of the Bangong-Nujiang Ocean beneath Qiangtang revealed: stratigraphic and geochronological evidence from Gaize, Tibet. Basin Research, 28(1): 147-157.

MingGuo Zhai, YanBin Zhang and 7 others. 2016. Renewed profile of the Mesozoic magmatism in Korean Peninsula: regional correlation and broader implication for cratonic destruction in the North China Craton. SCIENCE CHINA Earth Sciences, 59(12): 2355-2388.

Mingli Wan., Weiming Zhou, Peng Tang, Lujun Liu & Jun Wang. 2016. *Xenoxylon junggarensis* sp. nov., a new gymnospermous fossil wood from the Norian (Triassic) Huangshanjie Formation in northwestern China, and its palaeoclimatic implications. Palaeogeography, Palaeoclimatology, Palaeoecology, 441: 679-687.

Mingshuai Zhu, Fochin Zhang, Laicheng Miao, Bataar, M., Anaad, C., Shunhu Yang & Xingbo Li. 2016. Geochronology and geochemistry of the Triassic bimodal volcanic rocks and coeval A-type granites of the Olzit area, Middle Mongolia: implications for the tectonic evolution of Mongol–Okhotsk Ocean. Journal of Asian Earth Sciences, 122: 41-57.

Mingsong Li, Chunju Huang, Hinnov, L., Ogg, J., Zhong-qiang Chen & Yang Zhang. 2016. Obliquity-forced climate during the Early Triassic hothouse in China. Geology, 44(8): 623-626.

Mingsong Li, Ogg, J., Yang Zhang, Chunju Huang, Hinnov, L., Zhong-Qiang Chen & Zhuoyan Zou. 2016. Astronomical tuning of the end-Permian extinction and the Early Triassic Epoch of South China and Germany. Earth and Planetary Science Letters, 441: 10-25.

Mogucheva, N.K. 2016. Flora from the Induan stage (Lower Triassic) of Middle Siberia. Stratigraphy and Geological Correlation, 24(3): 252-266.

Mohamed, K.R., Joeharry, N.A.M., Leman, M.S. & Ali, C.A. 2016. The Gua Musang Group: a newly proposed stratigraphic unit for the Permo-Triassic sequence of Northern Central Belt, Peninsular Malaysia. Bulletin of the Geological Society of Malaysia, 62: 131-142.

Mohammedyasin, S.M., Lippard, S.J., Omosanya, K.O., Johansen, S.E. & Harishidayat, D. 2016. Deep-seated faults and hydrocarbon leakage in the Snøhvit Gas Field, Hammerfest Basin, southwestern Barents Sea. Marine and Petroleum Geology, 77: 160-178.

Mondal, S. & Harries, P.J. 2016. Phanerozoic trends in ecospace utilization: the bivalve perspective. Earth-Science Reviews, 152: 106-118.

Mondal, S. & Harries, P.J. 2016. The effect of taxonomic corrections on Phanerozoic generic richness trends in marine bivalves with a discussion on the clade's overall history. Paleobiology, 42(1): 157-171.

Monti, M. & Franzese, J.R. 2016. Tectonostratigraphic analysis of the Puesto Viejo Group (San Rafael, Argentina): evolution of a Triassic continental rift. Latin American Journal of Sedimentology and Basin Analysis, 23(1): 1-33.

Morton, A., Knox, R. & Frei, D. 2016. Heavy mineral and zircon age constraints on provenance of the Sherwood Sandstone Group (Triassic) in the eastern Wessex Basin, UK. Proceedings of the Geologists' Association, 127(4): 514-526.

Moss, D.K., Ivany, L.C., Judd, E.J., Cummings, P.W., Bearden, C.E., Woo-Jun Kim, Artruc, E.G. & Driscoll, J.R. 2016. Lifespan, growth rate and body size across latitude in marine Bivalvia, with implications for Phanerozoic evolution. Proceedings of the Royal Society of London, B. 283(1836). 20161364; DOI: 10.1098/rspb.2016. 1364. (7pp).

Mouro, L.D., Zatoń, M., Fernandes, A.C.S. & Waichel, B.L. 2016. Laval cases of caddisfly (Insecta: Trichoptera) affinity in Early Permian marine environments of Gondwana. Nature Scientific Reports, 6(19215), doi:10.1038/srep19215. (7pp).

Moustafa, M.S.H., Pope, M.C., Grossman, E.L. & Mriheel, I.Y. 2016. Carbon and oxygen isotope variations of the Middle–Late Triassic Al Aziziyah Formation, northwest Libya. Journal of African Earth Sciences, 118: 149-162.

Mueller, S., Hounslow, M.W. & Kürschner, W.M. 2016. Integrated stratigraphy and palaeoclimate history of the Carnian Pluvial Event in the Boreal Realm: new data from the Upper Triassic Kapp Toscana Group in central Spitsbergen (Norway). Journal of the Geological Society, London, 173(1): 186-202.

Mueller, S., Krystyn, L. & Kürschner, W.M. 2016. Climate variability during the Carnian Pluvial Phase – a quantitative palynological study of the Carnian sedimentary succession at Lunz am See, Northern Calcareous Alps, Austria. Palaeogeography, Palaeoclimatology, Palaeoecology, 441: 198-211.

Mujal, E., Gretter, N. and 11 others. 2016. Constraining the Permian-Triassic transition in continental environments: stratigraphic and paleontological record from the Catalan Pyrenees (NE Iberian Peninsula). Palaeogeography, Palaeoclimatology, Palaeoecology, 445: 18-37.

Mujal, E., Gretter, N. and 11 others. 2016. Insights into the Permian/Triassic transition in Western Tethys: new stratigraphic and paleontological data from the Catalan Pyrenees (NE Iberian Peninsula). Permophiles, 63: 21-27.

Müller, R.D., Seton, M. and 10 others. 2016. Ocean basin evolution and global-scale plate reorganization events since Pangea breakup. Annual Review of Earth and Planetary

Sciences, 44: 107-138.
Müller, R.T., Langer, M.C., Furtado Cabreira, S. & Dias-da-Silva, S. 2016. The femoral anatomy of *Pampadromaeus barberenai* based on a new specimen from the Upper Triassic of Brazil. Historical Biology, 28(5): 656-665.
Murillo, W.A., Veith-Hillebrand, A., Horsfield, B. & Wilkes, H. 2016. Petroleum source, maturity and mixing in the southwestern Barents Sea: new insights from geochemical and isotope data. Marine and Petroleum Geology, 70: 119-143.
Mustoe, G. & Acosta, M. 2016. Origin of petrified wood color. Geosciences, 6(2); doi:10.3390/geosciences6020025 (24pp.).
Naeser, C.W., Naeser, N.D., Newell, W.L., Southworth, S., Edwards, L.E. & Weems, R.E. 2016. Erosional and depositional history of the Atlantic Passive Margin as recorded in detrital zircon fission-track ages and lithic detritus in Atlantic coastal plain sediments. American Journal of Science, 316(2): 110-168.
Nagy, J. 2016. A sequence stratigraphic model of benthic foraminiferal facies trends with Triassic and Jurassic examples. Marine Micropaleontology, 122: 99-114.
Nak Kyu Kim & Sung Hi Choi. 2016. Petrogenesis of Late Triassic ultramafic rocks from the Andong Ultramafic Complex, South Korea. Lithos, 264: 28-40.
Natal'in, B.A., Sunal, G., Gün, E., Bo Wang & Yang Zhiqing. 2016. Precambrian to Early Cretaceous rocks of the Strandja Massif (northwestern Turkey): evolution of a long-lasting magmatic arc. Canadian Journal of Earth Sciences, 53(11): 1312-1335.
Ndiaye, M., Ngom, P.M., Gorin, G., Villeneuve, M., Sartori, M. & Medou, J. 2016. A new interpretation of the deep-part of Senegal-Mauritanian Basin in the Diourbel-Thies area by integrating seismic, magnetic, gravimetric and borehole data: implication for petroleum exploration. African Journal of Earth Sciences, 121: 330-341.
Nemčok, M., Rybár, S., Ekkertová, P., Kotulová, J., Hermeston, S.A. & Jones, D. 2016. Transform-margin model of hydrocarbon migration: the Guyana-Suriname case study. Geological Society, London, Special Publications, 431: 199-217.
Nemčok, M., Rybár, S. and 11 others. 2016. Development history of the southern terminus of the Central Atlantic; Guyana-Suriname case study. Geological Society, London, Special Publications, 431: 145-178.
Newell, A.J. & Shariatipour, S.M. 2016. Linking outcrop analogue with flow simulation to reduce uncertainty in sub-surface carbon capture and storage: an example from the Sherwood Sandstone Group of the Wessex Basin, UK. Geological Society, London, Special Publications, 436: 231-246.
Niedźwiedzki, G., Badjek, P., Owocki, K. & Kear, B.P. 2016. An early Triassic polar predator ecosystem revealed by vertebrate coprolites from the Bulgo Sandstone (Sydney Basin) of southeastern Australia. Palaeogeography, Palaeoclimatology, Palaeoecology, 464: 5-15.
Niedźwiedzki, G., Badjek, P., Qvarnström, M., Sulej, T., Sennikov, A.G. & Golubev, V.K. 2016. Reduction of vertebrate coprolite diversity associated with the end-Permian extinction event in Vyazniki region, European Russia. Palaeogeography, Palaeoclimatology, Palaeoecology, 449: 77-90.
Niedźwiedzki, G., Sennikov, A. & Brusatte, S.L. 2016. The osteology and systematic position of *Dongusuchus efremovi* Sennikov, 1988 from the Anisian (Middle Triassic) of Russia. Historical Biology, 28(4): 550-570.
Ning Tian, Yongdong Wang, Phillipe, M, Liqin Li, Xiaoping Xie & Zikun Jiang. 2016. New record of fossil wood *Xenoxylon* from the Late Triassic in the Sichuan Basin, southern China and its paleoclimatic implications. Palaeogeography, Palaeoclimatology, Palaeoecology, 464: 65-75.
Niu Haiping, Li Yongjun, Liu Yunhua, Du Yuliang, Hu Xiaolong & Zhao Renfu. 2016. "Open-Close" evolution and Triassic Tethyan-type sedimentation in Qinling orogenic belt. Northwestern Geology, 48(3)2016: 1-12.
Nordt, L., Tubbs, J. & Dworkin, S. 2016. Stable carbon isotope record of terrestrial organic materials for the last 450 Ma yr. Earth-Science Reviews, 159: 103-117.
Novikov, I.V. 2016. New temnospondyl amphibians from the basal Triassic of the Obshchii Syrt Highland, eastern Europe. Paleontological Journal, 50(3): 297-310.
Nu Guangzhi, Tao Wei, Liang Wentian, Li Yang & Ran Yazhou. 2016. Magnetic mineralogy and fabric reliability constraints of Late Triassic Yanzhiba pluton in South Qinling Mountain. Geological Bulletin of China, 35(9): 1522-1528.
Ogg, J.G., Ogg, G.M. & Gradstein, F.M. 2016. A Concise Geologic Time Scale 2016. Elsevier, 234pp.
Oghenekome, M.E., Chatterjee, T.K., Hammond, N.Q. & van Bever Donker, J.M. 2016. Provenance study from petrography of the late Permian – Early Triassic sandstones of the Balfour Formation Karoo Supergroup, South Africa. Journal of African Earth Sciences, 114: 125-132.
Oh, C., Park, T.-Y.S., Woo, J., Bomfleur, B., Phillipe, M., Decombeix, A.-L., Kim, Y.-H.G. & Lee, J.I. 2016. Triassic *Kykloxylon* wood (Umkomasiaceae, Gymnospermopsida) from Skinner Ridge, northern Victoria Land, East Antarctica. Review of Palaeobotany and Palynology, 233: 104-114.
Olierook, H.K.H. & Timms, N.E. 2016. Quantifying multiple Permian-Recent exhumation events during the break-up of eastern Gondwana: sonic transit time analysis of the central and southern Perth Basin. Basin Research, 28(6): 796-826.
Oliva-Urcia, B., Casas, A.M., Moussaid, B., Villalaín, J.J., El Ouardi, H., Sato, R., Torres-López, S. & Román-Berdiel, T. 2016. Tectonic fabrics vs mineralogical artefacts in AMS analysis: a case study of the Western Morocco extensional Triassic basins. Journal of Geodynamics, 94-95: 13-33.
Olivarius, M. & Nielsen, L.H. 2016. Triassic paleogeography of the greater eastern Norwegian-Danish Basin: constraints from provenance analysis of the Skagerrak Formation. Marine and Petroleum Geology, 69: 168-182.
Olivier, N., Brayard, A., Vennin, E., Escarguel, G., Fara, E., Bylund, K.G., Jenks, J.F. & Caravaca, G. 2016. Evolution of depositional settings in the Torrey area during the Smithian (Early Triassic, Utah, USA) and their significance for the biotic recovery. Geological Journal, 51(4): 600-626.
O'Meara, R.N. & Asher, R.J. 2016. The evolution of growth patterns in mammalian versus nonmammalian cynodonts.

Paleobiology, 42(3): 439-464.

Omarini, R.H., Gasparon, M., De Min, A. & Comin-Chiaramont, P. 2016. An overview of the Mesozoic-Cenozoic magmatism and tectonics in Eastern Paraguay and central Andes (Western Gondwana): implications for the composition of mantle sources. Journal of South American Earth Sciences, 72: 302-314.

Onoue, T., Sato, H., Yamashita, D., Ikehara, M., Yasukawa, K., Fujinaga, K., Kato, Y. & Matsuoka, A. 2016. Bolide impact triggered the Late Triassic extinction event in equatorial Panthalassa. Nature Scientific Reports, 6(29609), doi:10.1038/srep29609. (8pp).

Onoue, T., Zonneveld, J.-P., Orchard, M.J., Yamashita, M., Yamashita, K., Sato, H. & Kusaka, S. 2016. Paleoenvironmental changes across the Carnian/Norian boundary in the Black Bear Ridge section, British Columbia, Canada. Palaeogeography, Palaeoclimatology, Palaeoecology, 441: 721-733.

Ortega-Flores, B., Solari, L.A. & de Jesús Escalona-Alcázar, F. 2016. The Mesozoic successions of western Sierra de Zacatecas, Central Mexico: provenance and tectonic implications. Geological Magazine, 53(4): 696-717.

Paes Neto, V.D., Parkinson, A.H., Pretto, F.A., Soares, M.B., Schwanke, C., Schultz, C.L. & Kellner, A.W. 2016. Oldest evidence of osteophagic behaviour by insects from the Triassic of Brazil. Palaeogeography, Palaeoclimatology, Palaeoecology, 453: 30-41.

Pan Lei, Shen Ji-shan & Hao Jing-yu. 2016. Provenance types and controlling factors of the 4th member of the Xujiahe Formation in the Yuanba-Tongnanba area, northeastern Sichuan. Sedimentary Geology and Tethyan Geology, 36(2016:1): 104-108.

Pángaro, F., Ramos, V.A. & Pazos, P.J. 2016. The Hesperides basin: a continental-scale Upper Palaeozoic to Triassic basin in southern Gondwana. Basin Research, 28(5): 685-711.

Paris, G., Donnadieu, Y., Beaumont, V., Fluteau, F. & Goddéris, Y. 2016. Geochemical consequences of intense pulse-like degassing during the onset of the Central Atlantic Magmatic Province. Palaeogeography, Palaeoclimatology, Palaeoecology, 441: 74-82.

Parker, W.G. 2016. Revised phylogenetic analysis of the Aetosauria (Archosauria: Pseudosuchia); assessing the effects of incongruent morphological character sets. PeerJ 4: e1583 https://doi.org/10.7717/peerj.1583.

Parker, W.G. 2016. Osteology of the Late Triassic aetosaur *Scutarx deltatylus* (Archosauria: Pseudosuchia). PeerJ 4: e2411 https://doi.org/10.7717/peerj.2411.

Parveen, S. & Bhowmik, N. 2016. *Nidpuria falcatum* sp. nov. and associated vegetative shoots from the Triassic of Nidpur, Madhya Pradesh, India. Review of Palaeobotany and Palynology, 224(2): 169-180.

Paterson, N.W., Mangerud, G., Cetean, C.G., Mørk, A., Lord, G.S., Klausen, T.G. & Mørkved, P.T. 2016. A multidisciplinary biofacies characterisation of the Late Triassic (late Carnian-Rhaetian) Kapp Toscana Group on Hopen, Arctic Norway. Palaeogeography, Palaeoclimatology, Palaeoecology, 464: 16-42.

Patruno, S. & Reid, W. 2016. New plays on the Greater East Shetland Platform (UKCS Quadrants 3, 8-9, 14-16) – part 1: regional setting and a working petroleum system. First Break, 34(12): 33-43.

Pattemore, G.A. 2016. The structure of umkomasiacean fructifications from the Triassic of Queensland. Acta Palaeobotanica, 56(1): 17-40.

Pattemore, G.A. 2016. Megaflora of the Australian Triassic-Jurassic: a taxonomic revision. Acta Palaeobotanica, 56(2): 121-182.

Pavanatto, A.E.B., Müller, R.T., Stock Da-Rosa, A.A. & Dias-da-Silva, S. 2016. New information on the postcranial skeleton of *Massetognathus ochagaviae* Barberena, 1981 (Eucynodontia, Traversodontidae), from the Middle Triassic of southern Brazil. Historical Biology, 28(7): 978-989.

Payne, J.L., Bush, A.M., Chang, E.T., Heim, N.A., Knope, M.L. & Pruss, S.B. 2016. Extinction intensity, selectivity and their combined macroevolutionary influence in the fossil record. Biology Letters, 12(9): 20160202. DOI: 10. 1098/rsbl.2016.0202. (5pp).

Peng ChengMing, Wang Gang, Chen YuanLin, Li ZhengYou, Xue LingWen, Yang Hui, Lu YingHui & Hou Yun. 2016. Triassic paleocurrent study in the middle-northern part of the Nanpanjiang deep basin. Acta Sedimentologica Sinica, 34(6): 1120-1132.

Peng Guo, Wen-Liang Xu, Jie-Jiang Yu, Feng Wang, Jie Tang & Yu Li. 2016. Geochronology and geochemistry of Late Triassic bimodal igneous rocks at the eastern margin of the Songnen-Zhangguangcai Range massif, northeast China: petrogenesis and tectonic implications. International Geology Review, 58(2): 196-215.

Peng Zhijun, Wu Pandeng, Liu Songbai & Zhang Peng. 2016. An analysis of sediments characteristics of Early-Middle Triassic Longwuhe Formation of Guomaying area in Guinan County, Qinghai Province. Geological Bulletin of China, 35(9): 1506-1511.

Pereira, M.F., Gama, C., Chichorro, M., Silva, J.B., Gutiérrez-Alonso, G., Hofmann, M., Linnemann, U. & Gärtner, A. 2016. Evidence for multi-cycle sedimentation and provenance constraints from detrital zircon U-Pb ages: Triassic strata of the Lusitanian basin, western Iberia. Tectonophysics, 681: 318-331.

Pereira, Z., Fernandes, P., Lopes, G., Marques, J. & Vasconcelos, L. 2016. The Permian-Triassic transition in the Moatize-Minjova Basin, Karoo Supergroup, Mozambique: a palynological perspective. Review of Palaeobotany and Palynology, 226: 1-19.

Perotti, C., Chiariotti, L., Bresciani, I., Cattaneo, L. & Toscani, G. 2016. Evolution and timing of salt diapirism in the Iranian sector of the Persian Gulf. Tectonophysics, 679: 180-198.

Petsios, E. & Bottjer, D.J. 2016. Quantitative analysis of the ecological dominance of benthic disaster taxa in the aftermath of the end-Permian mass extinction. Paleobiology, 42(3): 380-393.

Peterffy, O., Calner, M. & Vajda, V. 2016. Early Jurassic microbial mats–a potential response to reduced biotic activity in the aftermath of the end-Triassic mass extinction event. Palaeogeography, Palaeoclimatology, Palaeoecology, 464:

76-85.

Peybernes, C., Chablais, J., Onoue, T., Escarguel, G. & Martini, R. 2016. Paleoecology, biogeography, and evolution of reef ecosystems in the Panthalassa Ocean during the Late Triassic: insights from reef limestone of the Sambosan Accretionary Complex, Shikoku, Japan. Palaeogeography, Palaeoclimatology, Palaeoecology, 457: 31-51.

Peybernes, C., Chablais, J., Onoue, T. & Martini, R. 2016. Mid-oceanic shallow-water carbonates of the Panthalassa domain: new microfacies data from the Sambosan Accretionary Complex, Shikoku Island, Japan. Facies, 62(4): DOI 10.1007/s10347-016-0475-7. (27pp).

Peyravi, M., Rahimpour-Bonab, H., Nader, F.H. & Kamali, M.R. 2016. Chemo-stratigraphy as a tool for sequence stratigraphy of the Early Triassic Kangan Formation, north of the Persian Gulf. Carbonates and Evaporites, 31(2): 163-178.

Peyre de Fabrègues, C. & Allain, R. 2016. New material and revision of *Melanorosaurus thabanensis*, a basal sauropodomorph from the Upper Triassic of Lesotho. PeerJ 4: e1639 https://doi.org/10.7717/peerj.1639.

Pieroni, V. 2016. Turriculate gastropods (Coelostylinidae) from the Esino limestone outcrop (Ladinian, Lombardy) of the Stoppani Collection housed at the Museo Civico di Storia Naturale, Milan (Italy). Natural History Sciences, 3(2): 41-49.

Pietsch, C., Petsios, E. & Bottjer, J. 2016. Sudden and extreme hypothermals, low-oxygen, and sediment influx drove community phase shifts following the end-Permian mass extinction. Palaeogeography, Palaeoclimatology, Palaeoecology, 451: 183-196.

Pietsch, J.S., Wetzel, A. & Jordan, P. 2016. A new lithostratigraphic scheme for the Schinznach Formation (upper part of the Muschelkalk Group of northern Switzerland). Swiss Journal of Geosciences, 109(2): 285-307.

Pillai, S.S.K., Meena, K.L., Tewari, R. & Joshi, R. 2016. Early Triassic palynomorphs from Kuraloi Block, Belphar area, Ib-River coalfield, Mahanadi basin, Odisha. Journal of the Geological Society of India, 88(6): 693-704.

Pinheiro, F.L. 2016. A fragmentary dinosaur femur and the presence of Neotheropoda in the Upper Triassic of Brazil. Revista Brasileira de Paleontologia, 19(2): 211-216.

Pinheiro, F.L., França, M.A.G., Lacerda, M.B., Butler, R.J. & Schultz, C.L. 2016. An exceptional fossil skull from South America and the origins of the archosauriform radiation. Nature Scientific Reports, 6(22817), doi:10.1038/srep22817. (7pp).

Plasencia, P., Márquez-Aliaga, A., Pérez-Valera, J.A., Baud, A., Sudar, M., Kiliç, A.-M. & Hirsch, F. 2016. Comments on: A review of the evolution, biostratigraphy, provincialism and diversity of Middle and early Late Triassic conodonts. Papers in Palaeontology, 2(3): 451-456.

Pole, M., Yongdong Wang, Bugdaeva, E.V., Chong Dong, Ning Tian, Liqin Li & Ning Zhou. 2016. The rise and demise of *Podozamites* in east Asia–an extinct conifer life style. Palaeogeography, Palaeoclimatology, Palaeoecology, 464: 97-109.

Polozov, A.G., Svensen, H.H., Planke, S., Grishina, S.N., Fristad, K.E. & Jerram, D.A. 2016. The basalt pipes of the Tunguska Basin (Siberia, Russia): high temperature processes and volatile degassing into the end-Permian atmosphere. Palaeogeography, Palaeoclimatology, Palaeoecology, 441: 51-64.

Polufuntikova, L.I. & Fridovsky, V.Yu. 2016. Lithological features, reconstruction of redox setting, and composition of the provenances of the Upper Triassic Kular-Nera shale belt. Russian Journal of Pacific Geology, 10(3): 218-229.

Ponomarenko, A.G. 2016. Insects during the time around the Permian-Triassic crisis. Paleontological Journal, 50(2): 174-186.

Ponomarenko, A.G. 2016. New beetles (Insecta: Coleoptera) from the Lower Triassic of European Russia. Paleontological Journal, 50(3): 286-292.

Posenato, R. 2016. Systematics of lingulide brachiopods from the end-Permian mass extinction interval. Revista Italiana di Paleontologia e Stratigrafia, 122(2): 85-108.

Pott, C. 2016. *Westerheimia pramelreuthensis* from the Carnian (Upper Triassic) of Lunz, Austria: more evidence for a unitegmic seed coat in early Bennettitales. International Journal of Plant Sciences, 17(9): 771-791.

Pott, C., Schmeißner, S., Dütsch, G. & Van Konijnenburg-van-Cittert, J.H.A. 2016. Bennettitales in the Rhaetian flora of Wüstenwelsberg, Bavaria, Germany. Review of Palaeobotany and Palynology, 232: 98-118.

Pott, C., van der Burgh, J. & van Konijnenburg-van-Cittert, J.H.A. 2016. New ginkgophytes from the Upper Triassic-Lower Cretaceous of Spitsbergen and Edgeøya (Svalbard, Arctic Norway): the history of Ginkgoales on Svalbard. International Journal of Plant Sciences, 17(2): 175-197.

Powell, J.H., Stephenson, M.H., Nicora, A., Rettori, R., Borlenghi, L.M. & Perri, M.C. 2016. The Permian-Triassic boundary, Dead Sea, Jordan: transitional alluvial to marine depositional sequences and biostratigraphy. Rivista Italiana di Paleontologia e Stratigrafia, 122(3): 23-40.

Pretto, F.A., Veiga, F.H., Langer, M.C. & Schultz, C.L. 2016. A juvenile sauropodomorph tibia from the 'Botucaraí Hill', Late Triassic of southern Brazil. Revista Brasileira de Paleontologia, 19(3): 407-414.

Previtera, E., Mancuso, A.C., de la Fuente, M.S. & Sánchez, E.S. 2016. Diagenetic analysis of tetrapod from the Upper Triassic, Puesto Viejo Group, Argentina. Andean Geology, 43(2): 197-214.

Pritchard, A.C., Turner, A.H., Irmis, R.B., Nesbitt, S.J. & Smith, N.D. 2016. Extreme modification of the tetrapod forelimb in a Triassic diapsid reptile. Current Biology, 26(20): 2779-2786; dx.doi.org/10.1016/j.cub.2016.07.084.

Qianhong Wu, Jingya Cao, Hua Kong, Yongjun Shao, Huan Li, Xiaoshuang Xi & Xuantong Deng. 2016. Petrogenesis and tectonic setting of the early Mesozoic Xitian granitic pluton in the middle Qin-Hang Belt, South China: constraints from zircon U-Pb ages and bulk-rock trace element and Sr-Nd-Pb isotopic compositions. Journal of Asian Earth Sciences, 128: 130-148.

Qinghai Xu, Wanzhong Shi, Xiangyang Xie, Manger, W., McGuire, P., Xiaoming Zhang, Ren Wang & Zhuang Wu. 2016. Deep-lacustrine sandy debrites and turbidites in the lower Triassic Yanchang Formation, southeast Ordos Basin, central China: facies distribution and reservoir quality. Marine and Petroleum Geology, 77: 1095-1107.

Qiu Xincheng, Tong Jinnan, Tian Li, Chu Daoliang, Song Ting & Li Dongdong. 2016. The biostratigraphic correlation of the Permian-Triassic boundary in Jinzhong section, Weining, Guizhou, South China. Earth Science – Journal of China University of Geosciences, 2016(10): 1709-1722.

Quan-Feng Zheng, Chang-Qun Cao, Yue Wang, Hua Zhang & Yi Ding. 2016. Microbialite concretions in a dolostone crust at the Permian-Triassic boundary of the Xishan section in Jiangsu Province, South China. Palaeoworld, 25(2): 188-198.

Qvarnström, M., Niedźwiedzki, G. & Žigaitė, Ž. 2016. Vertebrate coprolites (fossil faeces): an underexplored *Konservat-Lagerstätte*. Earth-Science Reviews, 162: 44-57.

Radley, J.D. & Coram, R.A. 2016. The Chester Formation (Early Triassic, southern Britain): sedimentary response to extreme greenhouse climate? Proceedings of the Geologists' Association, 127(5): 552-557.

Rahimi, A., Adabi, M.H., Aghanabati, A., Majidifard, M.R. & Jamali, A.M. 2016. Dolomitization mechanism based on petrography and geochemistry in the Shotori Formation (Middle Triassic), central Iran. Open Journal of Geology, 6(9): 1149-1168.

Ran Ye, Wang GuiWen, Lai Jin, Zhou ZhengLong, Cui YuFeng, Dai QuanQi, Chen Jing & Wang ShuChen. 2016. Quantitative characterization of diagenetic facies of tight sandstone oil reservoir by using logging crossplot: a case study on Chang 7 tight sandstone oil reservoir in Huachi area, Ordos Basin. Acta Sedimentologica Sinica, 34(4): 694-706.

Ran Ye, Wang Gui-wen, Zhou Zheng-long, Lai Jin, Dai Quan-qi, Chen Jing, Fan Xu-qiang & Wang Shu-chen. 2016. Identification of lithology and lithofacies type and its application to Chang 7 tight oil in Heshui area, Ordos Basin. Geology in China, 43(4): 1331-1340.

Reichow, M.K., Saunders, A.D., Scott, R.A., Millar, I.L., Barfod, D., Pringle, M.S., Rogers, N.W. & Hammond, S. 2016. Petrogenesis and timing of mafic magmatism, South Taimyr, Arctic Siberia: a northerly continuation of the Siberian Traps? Lithos, 248-251: 382-401.

Reinhold, K. & Hammer, J. 2016. Steinsalzlager in den salinaren Formationen Deutschlands. Zeitschrift der Deutschen Gesellschaft für Geowissenschaften, 167: 167-190.

Ren Dazhong, Sun Wei, Huang Hai, Liu Dongke, QXuefeng & Lei Qihong. 2016. Formation mechanism of Chang 6 tight sandstone reservoir in Jiyuan oilfield, Ordos Basin. Earth Science – Journal of China University of Geosciences, 2016(10): 1735-1744.

Ren Haidong, Wang Tao, Zhang Lei, Wang Xiaoxia, Huang He, Feng Chengyou, Teschner, C. & Song Peng. 2016. Ages, sources and tectonic settings of the Triassic igneous rocks in the easternmost segment of the East Kunlun Orogen, central China. Acta Geologica Sinica, 90(2): 641-668.

Renchao Yang, van Loon, A.J., Wei Yin, Aiping Fan & Zuozhen Han. 2016. Soft-sediment deformation structures in cores from lacustrine slurry deposits of the Late Triassic Yanchang Fm. (central China). Geologos, 22(3): 201-211.

Rey, K., Amiot, R. and 12 others. 2016. Global climate perturbations during the Permian-Triassic mass extinctions recorded by continental tetrapods from South Africa. Gondwana Research, 37: 384-396.

Rigaud, S., Vachard, D., Schlagintweit, F. & Martini, R. 2016. New lineage of Triassic aragonitic foraminifera and reassessment of the class Nodosariata. Journal of Systematic Palaeontology, 14(11): 919-938.

Rigo, M., Bertinelli, A. and 10 others. 2016. The Pignola-Abriola section (southern Apennines, Italy): a new GSSP candidate for the base of the Rhaetian Stage. Lethaia, 49(3): 287-306.

Rinehart, L.F. & Lucas, S.G. 2016. *Eocyclotosaurus appetolatus*, a Middle Triassic amphibian: osteology, life history, and paleobiology. New Mexico Museum of Natural History and Science, Bulletin 70: 118pp.

Robertson, A.H.F., Parlak, O., Yildirim, N., Dumitrica, P. & Tasli, K. 2016. Late Triassic rifting and Jurassic-Cretaceous passive margin development of the southern Neotethys: evidence from the Adiyaman area, SE Turkey. International Journal of Earth Sciences, 105(1): 167-201.

Romano, C., Koot, M.B., Kogan, I., Brayard, A., Minikh, A.V., Brinkmann, W., Bucher, H. & Kriwet, J. 2016. Permian-Triassic Osteichthyes (bony fishes): diversity dynamics and body size evolution. Biological Reviews, 91(1): 106-147.

Romano, C., Ware, D., Brühwiler, T., Bucher, H. & Brinkmann, W. 2016. Marine Early Triassic Osteichthyes from Spiti, Indian Himalayas. Swiss Journal of Palaeontology, 135(2): 275-294.

Romero-Sarmiento, M.-F., Euzen, T., Rohais, S., Chunqing Jiang & Littke, R. 2016. Artificial thermal maturation of source rocks at different thermal maturity levels: application to the Triassic Montney and Doig formations in the Western Canada Sedimentary Basin. Organic Geochemistry, 97: 148-162.

Ruffell, A., Simms, M.J. & Wignall, P.B. 2016. The Carnian Humid Episode of the Late Triassic – a review. Geological Magazine, 153(Special Issue 2): 271-284.

Saberzadeh, B., Rashidi, K. & Vahidinia, M. 2016. Upper Triassic foraminifera from Howz-e Khan member of Nayband Formation in central Iran (south of Naybandan). Geosciences, 25(98): 283-301. (Geological Survey of Iran: ISSN 1023-7429)

Sack, P.J., Berry, R.F., Gemmell, J.B., Meffre, S. & West, A. 2016. U-Pb zircon geochronology from the Alexander terrane, southeast Alaska: implications for the Greens Creek massive sulphide deposit. Canadian Journal of Earth Sciences, 53(12): 1458-1475.

Sadovnikov, G.N. 2016. Evolution of the biome of the Middle Siberian Trappean Plateau. Paleontological Journal, 50(5): 518-532.

Sagar, M.W., Palin, J.M., Tulloch, A.J. & Heath, L.A. 2016. The geology, geochronology and affiliation of the Glenroy Complex and adjacent plutonic rocks, southeast Nelson. New Zealand Journal of Geology and Geophysics, 59(1): 213-235.

Saito, R., Kaiho, K. and 7 others. 2016. Secular changes in environmental stresses and eukaryotes during the Early Triassic to the early Middle Triassic. Palaeogeography, Palaeoclimatology, Palaeoecology, 451: 35-45.

Salah, I., Jemail, M., Karoui-Yaakoub, N., Sdiri, A., Ayed, N.

& Boughdiri, M. 2016. Properties of Debadid evaporates (northern Tunisia) for potential use in industrial fields. Open Journal of Geology, 6(12): 1525-1538.

Sánchez-Beristain, F. & Reitner, J. 2016. Palaeoecology of new fossil associations from the Cipit boulders, St. Cassian Formation (Ladinian–Carnian, Middle–Upper Triassic; Dolomites, NE Italy). Paläontologische Zeitschrift, 90(2): 243-269.

Sánchez-Moya, Y., Herrero, M.J. & Sopeña, A. 2016. Strontium isotopes and sedimentology of a marine Triassic succession (upper Ladinian) of the westernmost Tethys, Spain. Journal of Iberian Geology, 42(2): 171-186.

Sang-Bong Yi, Chang Whan Oh, Seung-Yeol Lee, Seon-Gyu Choi, Taesung Kim & Keewook Yi. 2016. Triassic mafic and intermediate magmatism associated with continental collision between the North and South China cratons in the Korean Peninsula. Lithos, 246-247: 149-164.

Sanz de Galdeano, C. & Ruiz Cruz, M.D. 2016. Late Palaeozoic to Triassic formations unconformably deposited over the Ronda peridotites (Betic Cordilleras): evidence for their Variscan time of emplacement. Estudios Geológicos, 72(1): DOI 10.3989/egeol.42046.368 (24pp).

Sapin, F., Davaux, M., Dall'asta, M., Lahmi, M., Baudot, G. & Ringenbach, J.-C. 2016. Post-rift subsidence of the French Guiana hyper-oblique margin: from rift-inherited subsidence to Amazon deposition effect. Geological Society, London, Special Publications, 431: 125-144.

Sarigül, V. 2016. New basal dinosauromorph records from the Dockum Group of Texas, USA. Palaeontologia Electronica, 19.2.21A: 1-16.

Sato, H., Shirai, N., Ebihara, M., Onoue, T. & Kiyokawa, S. 2016. Sedimentary PGE signatures in the Late Triassic ejecta deposits from Japan: implications for the identification of impactor. Palaeogeography, Palaeoclimatology, Palaeoecology, 442: 36-47.

Saunders, A.D. 2016. Two LIPS and two Earth-system crises: the impact of the North Atlantic Igneous Province and the Siberian Traps on the Earth-surface carbon cycle. Geological Magazine, 153(Special Issue 2): 201-222.

Sawaki, Y., Yibing Li, Asanuma, H., Sakata, S., Suzuki, K., Hirata, T. & Windley, B.F. 2016. New chronological constraints on Neoarchean gneisses, Proterozoic cover sediments, and Triassic granite, Jixian, China. Palaeogeography, Palaeoclimatology, Palaeoecology, 459: 182-197.

Schaal, E.K., Clapham, M.E., Rego, B.L., Wang, S.C. & Payne, J.L. 2016. Comparative size evolution of marine clades from the Late Permian through Middle Triassic. Paleobiology, 42(1): 127-142.

Schmidt, A., Skeffington, R.A. and 10 others. 2016. Selective environmental stress from sulphur emitted by continental flood basalt eruptions. Nature Geoscience, 9(1): 77-82.

Schneider, J.W. & Scholze, F. 2016. A new Late Pennsylvanian to Early Triassic conchostracan biostratigraphy. Permophiles, 63: 37-43.

Schobben, M., Ullman, C.V. and 7 others. 2016. Discerning primary versus diagenetic signals in carbonate carbon and oxygen isotope records: an example from the Permian-Triassic boundary of Iran. Chemical Geology, 422: 94-107.

Schoch, R.R. & Desojo, J.B. 2016. Cranial anatomy of the aetosaur *Paratypothorax andressorum* Long & Ballew, 1985, from the Upper Triassic of Germany and its bearing on aetosaur phylogeny. Neues Jahrbuch für Geologie und Paläontologie – Abhandlungen, 279(1): 73-95.

Schoch, R.R. & Seegis, D. 2016. A Middle Triassic palaeontological gold mine: the vertebrate deposits of Vellberg (Germany). Palaeogeography, Palaeoclimatology, Palaeoecology, 459: 249-267.

Schoepfer, S.D., Algeo, T.D., Ward, P.D., Williford, K.H. & Haggart, J.H. 2016. Testing the limits in a greenhouse ocean: did low nitrogen availability limit marine productivity during the end-Triassic mass extinction? Earth and Planetary Science Letters, 451: 138-148.

Scholze, F., Schneider, J.W. & Werneburg, R. 2016. Conchostracans in continental deposits of the Zechstein-Buntsandstein transition in central Germany: taxonomy and biostratigraphic implications for the position of the Permian-Triassic boundary within the Zechstein Group. Palaeogeography, Palaeoclimatology, Palaeoecology, 449: 174-193.

Schultz, C.L., Langer, M.C. & Montefeltro, F.C. 2016. A new rhynchosaur from south Brazil (Santa Maria Formation) and rhynchosaur diversity patterns across the Middle-Late Triassic boundary. Paläontologische Zeitschrift, 90(3): 593-609. (Erratum, ibid. 643).

Schultz, S.K., Furlong, C.M. & Zonneveld, J.-P. 2016. The co-occurrence of *Trypanites* and *Glossofungites* substrate-controlled trace-fossil assemblages in a Triassic mixed siliciclastic-carbonate depositional system: Baldonnel Formation, Williston Lake, B.C., Canada. Journal of Sedimentary Research, 86(8): 894-913.

Schweigert, G., Fuchs, D. & Salomon, H.M. 2016. First record of a xiphoteuthidid coleoid (Cephalopoda: Aulacoceratida) from the Germanic Triassic (Erfurt Formation, Ladinian). Paläontologische Zeitschrift, 90(4): 765-769.

Schweitzer, C.E., Feldmann, R.M. and 8 others. 2016. Morphology, systematics, and paleoecology of *Tridactylastacus* (Crustacea, Decapoda, Glypheidae, Litogastridae). Journal of Paleontology, 90(6): 1100-1111.

Sciscio, L. & Bordy, E.M. 2016. Palaeoclimatic conditions in the Late Triassic–Early Jurassic of southern Africa: a geochemical assessment of the Elliot Formation. Journal of African Earth Sciences, 119: 102-119.

Scriven, S. 2016. Fossils of the Jurassic Coast. Lulworth: The Jurassic Coast Trust: 219pp.

Şengör, A.M.C. 2016. The structural evolution of the Albula Pass region, Graubünden, eastern Switzerland: the origin of the various vergences in the structure of the Alps. Canadian Journal of Earth Sciences, 53(11): 1279-1311.

Senowbari-Daryan, B. 2016. Upper Triassic miliolids of "*Cucurbita* group": aspects of the systematic classification. Jahrbuch der Geologischen Bundesanstalt Wien, 156(1-4): 187-215.

Senowbari-Daryan, B. & Link, M. 2016. Hypercalcified inozoan sponges from the Norian reef carbonates of Turkey. Revue de

Paléobiologie, 35(1): 279-339.

Sevastjanova, I., Hall, R., Rittner, M., Saw Mu Tha Lay Paw, Tin Tin Naing, Alderton, D.H. & Comfort, G. 2016. Myanmar and Asia united, Australia left behind long ago. Gondwana Research, 32: 24-40.

Servais, T., Martin, R.E. & Nützel, A. 2016. The impact of the 'terrestrialisation process' in the late Palaeozoic: pCO_2, pO_2, and the 'phytoplankton blackout'. Review of Palaeobotany and Palynology, 224(2): 26-37.

Shan Li, Sunlin Chung, Wilde, S.A., Tao Wang & Wenjiao Xiao. 2016. How Central Asian orogeny evolves: new insights from end-Permian to Middle Triassic magmatic record along the Solonker Suture Zone. Acta Geologica Sinica, 90(5): 1907-1908.

Shan Li, Sun-Lin Chung, Wilde, S.A., Tao Wang, Wen-Jiao Xiao & Qia-Qian Guo. 2016. Linking magmatism with collision in an accretionary orogen. Nature Scientific Reports, 6(25751), doi:10.1038/srep25751. (12pp).

Shan Liang, Zhang Dongming, Pang Yingchun, Liu Jiajun, Zhang Wanyi, Zhao Xinmin & Zhang Zhongping. 2016. Late Triassic magmatic activity in the Daqiao gold deposit of West Qinling belt: zircon U-Pb chronology and Lu-Hf isotope evidence. Geological Bulletin of China, 35(12): 2045-2057.

Shan Xiang, Zou ZhiWen, Meng XiangChao, Tang Yong, Guo HuaJun, Chen NengGui & Xu Yang. 2016. Provenance analysis of Triassic Baikouquan Formation in the area around Mahu Depression, Junggar Basin. Acta Sedimentologica Sinica, 34(5): 930-939.

Sheng-Sheng Chen, Ren-Deng Shi, Guo-Ding Yi & Hai-Bo Zou. 2016. Middle Triassic volcanic rocks in the Northern Qiangtang (Central Tibet): geochronology, petrogenesis, and tectonic implications. Tectonophysics, 666: 90-102.

Sheng-Sheng Chen, Ren-Deng Shi and 7 others. 2016. Middle Triassic ultrapotassic rhyolites from the Tanggula Pass, southern Qiangtang, China: a previously unrecognized stage of silicic magmatism. Lithos, 264: 258-276.

Shi Weigang, Zhang Wenfeng, Cheng Jun & Zhai Jie. 2016. Geochemistry, isotopic chronology and tectonic significance of diorite in the south of Bailing County, Tibet. Geological Bulletin of China, 35(9): 1463-1471.

Shi Yujiang, Li Wenhou, Wang Changsheng, Zhang Xiaoli, Zhang Shaohua & Song Ping. 2016. Turbidite fan and its controlling effects on hydrocarbon accumulation in the Chang 7 Member of Triassic Yanchang Formation in Ordos Basin. Geological Bulletin of China, 35(2): 406-414.

Shifeng Wang, Yasi Mo, Chao Wang & Peisheng Ye. 2016. Paleotethyan evolution of the Indochina Block as deduced from granites in northern Laos. Gondwana Geology, 38: 183-196.

Shigeta, Y. & Kumagae, T. 2016. Spathian (late Olenekian, Early Triassic) ammonoids from the Artyon area, South Primorye, Russian Far East and implications for the timing of the recovery of the oceanic environment. Paleontological Research, 20(1): 48-60.

Skrzycki, P. 2016. The westernmost occurrence of Gnathorhiza in the Triassic, with a discussion of the stratigraphic and palaeogeographic distribution of the genus. Fossil Record, 19(1): 17-29.

Slater, T.S., Duffin, C.J., Hildebrandt, C., Davies, T.G. & Benton, M.J. 2016. Microvertebrates from multiple bone beds in the Rhaetian of the M4–M5 motorway junction, South Gloucestershire, U.K. Proceedings of the Geologists' Association, 127(4): 464-477.

Smirčić, D., Lugović, B., Aljinović, D., Hrvatović, H., Kolar-Jurkovšek, T., Jurkovšek, B. & Gajšak, F. 2016. Middle Triassic autoclastic deposits from southwestern Bosnia and Herzegovina. Rudarsk-Geološko-Nafti Zbornik, 31(2). DOI: 10.17794/rgn.2016.2.1. (12pp).

Sobolev, P., Franke, D. and 7 others. 2016. Reconnaissance study of organic geochemistry and petrology of Paleozoic-Cenozoic potential hydrocarbon source rocks from the New Siberian Islands, Arctic Russia. Marine and Petroleum Geology, 78: 30-47.

Song Haijun & Tong Jinnan, 2016. Mass extinction and survival during the Permian-Triassic crisis. Earth Science – Journal of China University of Geosciences, 2016(6): 901-918.

Song Ping, Li Wenhou, Lu Jincai, Gu Duanyang, Qin Caihong & Li Zhaoyu. 2016. A study of tight reservoir diagenesis in the Chang 7 Member of Triassic Yanchang Formation, Jiyuan-Longdong area, Ordos Basin. Geological Bulletin of China, 35(2): 415-423.

Song Weimin, Tao Nan and 12 others. 2016. Geochronology and geochemistry of the Aolansandui pluton in Horqin Right Wing Middle Banner of Inner Mongolia. Geological Bulletin of China, 35(6): 932-942.

Song Zhongbao, Zhang Yulian and 10 others. 2016. LA-ICP-MS zircon U-Pb age of the Yemaquan granodiorite in the Qimantag area, Qinghai Province and its geological implications. Geological Bulletin of China, 35(12): 2006-2013.

Songqi Pan, Horsfield, B., Caineng Zou & Zhi Yang. 2016. Upper Permian Junggar and Upper Triassic Ordos lacustrine source rocks in northwest and central China: organic geochemistry, petroleum potential and predicted organofacies. International Journal of Coal Geology, 158: 90-106.

Songtao Wu, Caineng Zou and 7 others. 2016. Characteristics and origin of tight oil accumulations in the Upper Triassic Yanchang Formation of the Ordos Basin, north-central China. Acta Geologica Sinica, 90(5): 1821-1837.

Sorokin, A.A., Kotov, A.B., Kudryashov, N.M. & Kovach, V.P. 2016. Early Mesozoic granitoid and rhyolitic magmatism of the Bureya Terrane of the Central Asian Orogenic Belt: age and geodynamic setting. Lithos, 261: 181-194.

Sowiżdżał, A. & Kaczmarczyk, M. 2016. Analysis of thermal parameters of Triassic, Permian and Carboniferous sedimentary rocks in central Poland. Geological Journal, 51(1): 65-76.

Specht, S. 2016. Die Forschungsbohrung Stadtlauringen 1 in Unterfranken. Geologica Bavarica, 114: 91-118.

Spector, A., Epstein, S.A. & Schieck, D. 2016. Geophysical evidence for Mesozoic syn-rift salt diapirism in Southeast Bahamas. Carbonates and Evaporites, 31(2): 109-114.

Spencer, C.J., Harris, R.A. & Major, J.R. 2016. Provenance of Permian-Triassic Gondwana sequence units accreted to the Banda Arc in the Timor region: constraints from zircon U-Pb and Hf isotopes. Gondwana Geology, 38: 28-39.

Spikings, R., Reitsma, M.J., Boekhout, F., Mišković, A., Ulianov, A., Chiaradia, M., Gerdes, A. & Schaltegger, U. 2016. Characterisation of Triassic rifting in Peru and implications for the early disassembly of western Pangaea. Gondwana Research, 35: 124-143.

Stanienda, K.J. 2016. Carbonate phases rich in magnesium in the Triassic limestones of the eastern part of the Germanic Basin. Carbonates and Evaporites, 31(4): 387-405.

Staples, R.D., Gibson, H.D., Colpron, M. & Ryan, J.J. 2016. An orogenic wedge model for diachronous deformation, metamorphism, and exhumation in the hinterland of the northern Canadian Cordillera. Lithosphere, 8(2): 165-184.

Stewart, S.A., Reid, C.T., Hooker, N.P. & Kharouf, O.W. 2016. Mesozoic siliciclastic reservoirs and petroleum system in the Rub' Al-Khali basin, Saudi Arabia. AAPG Bulletin, 100(5): 819-841.

Stricker, S., Jones, S.J. & Grant, N.T. 2016. Importance of vertical effective stress for reservoir quality in the Skagerrak Formation, Central Graben, North Sea. Marine and Petroleum Geology, 78: 895-909.

Stricker, S., Jones, S.J., Sathar, S., Bowen, L. & Oxtoby, N. 2016. Exceptional reservoir quality in HPHT reservoir settings: examples from the Skagerrak Formation of the Heron Cluster, North Sea, UK. Marine and Petroleum Geology, 77: 198-215.

Strickson, E., Prieto-Márquez, A., Benton, M.J. & Stubbs, T.L. 2016. Dynamics of dental evolution in ornithopod dinosaurs. Nature Scientific Reports, 6(28904), doi:10.1038/srep28904. (11pp).

Stocker, M.R., Nesbitt, S.J., Criswell, K.E., Parker, W.G., Witmer, L.M., Rowe, T.B., Ridgely, R. & Brown, M.A. 2016. A dome-headed stem archosaur exemplifies convergence among dinosaurs and their distant relatives. Current Biology, 26(19): 2674-2680; dx.doi.org/10.1016/j.cub.2016.07.066.

Stubbs, T.L. & Benton, M.J. 2016. Ecomorphological diversification of Mesozoic marine reptiles: the roles of ecological opportunity and extinction. Paleobiology, 42(4): 547-573.

Sun, Y.-D., Tintori, A., Lombardo, C. & Jiang, D.-Y. 2016. New miniature neopterygians from the Middle Triassic of Yunnan Province, South China. Neues Jahrbuch für Geologie und Paläontologie – Abhandlungen, 282(2): 135-156.

Sun, Y.D., Wignall, P.B. and 7 others. 2016. Climate warming, euxinia and carbon isotope perturbations during the Carnian (Triassic) Crisis in South China. Earth and Planetary Science Letters, 444: 88-100.

Surmik, D. 2016. *Hemilopas mentzeli*, an enigmatic marine reptile from the Middle Triassic of Poland revisited. Neues Jahrbuch für Geologie und Paläontologie – Abhandlungen, 282(2): 209-223.

Surmik, D., Boczarowski, A., Balin, K., Dulski, M., Szade, J., Kremer, B. & Pawlicki, R. 2016. Spectroscopic studies on organic matter from Triassic reptile bones, Upper Silesia, Poland. PLoS ONE, 11(3): e0151143. doi:10.1371/journal.pone.0151143.

Svetlitskaya, T.V. & Nevolko, P.A. 2016. Late Permian-Early Triassic traps of the Kuznetsk Basin, Russia: geochemistry and petrogenesis in respect to an extension of the Siberian Large Igneous Province. Gondwana Research, 39: 57-76.

Szczygielski, T. & Sulej, T. 2016. Revision of the Triassic European turtles *Proterochersis* and *Murrhardtia* (Reptilia, Testudinata, Proterochersidae), with the description of new taxa from Poland and Germany. Zoological Journal of the Linnean Society, 177(2): 395-427.

Tackett, L.S. 2016. Late Triassic durophagy and the origin of the Mesozoic marine revolution. Palaios, 31(4): 122-124.

Tackett, L.S. & Bottjer, D.J. 2016. Paleoecological succession of Norian (Late Triassic) benthic fauna in eastern Panthalassa (Luning and Gabbs formations, west-central Nevada). Palaios, 31(4): 190-202.

Talamali, S., Chaouchi, R. & Benayad, S. 2016. Sedimentological evolution of the Lower Series formation in the southern area of the Hassi R'Mel field, Saharan Platform, Algeria. Arabian Journal of Geosciences, 9(6): DOI 10.1007/s12517-016-2506-7 (16pp)

Tamura, T., Tsunekawa, N., Nemoto, M., Inagaki, K., Hirano, T. & Sato, F. 2016. Molecular evolution of gas cavity in [NeFeSe] hydrogenases resurrected *in silico*. Nature Scientific Reports, 6(19742), doi:10.1038/srep19742. (10pp).

Tan Cong, Yu Bingsong, Ruan Zhuang, Liu Ce, Zhu Xi, Xie Haochen & Luo Zhong. 2016. High-resolution sequence stratigraphy division of Yanchang Formation in southwestern Ordos Basin. Journal of Jilin University (Earth Science edition), 2016(2): 336-347.

Tan Mei, Zhao Bing, Zhou Bingyang & Zhang Xiaoshi. 2016. Geochemical characteristics and genesis of T/P clay and event clay in Da-fang area, Guizhou Province. Geological Bulletin of China, 35(6): 979-988.

Tanner, L.H., Kyte, F.T., Richoz, S. & Krystyn, L. 2016. Distribution of iridium and associated geochemistry across the Triassic-Jurassic boundary in sections at Kuhjoch and Kendlbach, Northern Calcareous Alps, Austria. Palaeogeography, Palaeoecology, Palaeoclimatology, 449: 13-26.

Tanner, L.H. & Lucas, S.G. 2016. Stratigraphic distribution and significance of a 15 million-year record of fusain in the Upper Triassic Chinle Group, southwestern USA. Palaeogeography, Palaeoecology, Palaeoclimatology, 461: 261-271.

Tao Wang, Shaoqun Dong, Shenghe Wu, Huaimin Xu & Pengfei Hou. 2016. Numerical simulation of hydrocarbon migration in tight reservoir based on Artificial Ant Colony Algorithm: a case of the Chang 8_1 reservoir of the Triassic Yanchang Formation in the Huaqing area, Ordos Basin, China. Marine and Petroleum Geology, 78: 17-29.

Tao Wu, Long Xiao & Changqian Ma. 2016. U-Pb geochronology of detrital and inherited zircons in the Yidun arc belt, eastern Tibet Plateau and its tectonic implications. Journal of Earth Science, 27(3): 461-473.

Tao Wu, Long Xiao, Wilde, S.A., Chang-Qian Ma, Zi-Long Li, Yi Sun & Qiong-Yao Zhan. 2016. Zircon U-Pb age and Sr-Nd-Hf isotope geochemistry of the Ganluogou dioritic complex in the northern Triassic Yidun arc belt, eastern Tibetan Plateau: implications for the closure of the Garzê-Litang Ocean. Lithos, 248-251: 94-108.

Tavakoli, V. 2016. Ocean chemistry revealed by mineralogical and geochemical evidence at the Permian-Triassic Mass Extinction, offshore the Persian Gulf, Iran. Acta Geologica Sinica, 90(5): 1852-1864.

Taylor, P.D. 2016. Competition between encrusters on marine hard substrates and its fossil record. Palaeontology, 59(4): 481-497.

Tekin, U.K., Bedi, Y., Okuyucu, C., Göncüoglu, M.C. & Sayit, K. 2016. Radiolarian biochronology of upper Anisian to upper Ladinian (Middle Triassic) blocks and tectonic slices of volcano-sedimentary successions in the Mersin Mélange, southern Turkey: new insights for the evolution of Neotethys. Journal of African Earth Sciences, 124: 409-426.

Tennant, P. 2016. Mesozoic crocodyliforms. Palaeontology Online, 6, article 6, 1-15.

Teofilo, G., Festa, V., Sabato, L., Spalluto, L. & Tropeano, M. 2016. 3D modelling of the Tremiti salt diapir in the Gorgano offshore (Adriatic Sea, southern Italy): constraints on the Tremiti Structure development. Italian Journal of Geoscience, 135(3): 474-485.

Tetiker, S., Yalçin, H. & Bozkaya, Ö. 2016. Diagenesis/metamorphism history of Lower Triassic Çığlı Group rocks in Uludere-Uzungeçit (Şurnak) area (eastern part of the southeast Anatolian autochthone). Türkiye jeoloji bülteni / Geological Bulletin of Turkey, 59(3): 323-340.

Thibodeau, A.M., Ritterbuch, K. and 7 others. 2016. Mercury anomalies and the timing of biotic recovery following the end-Triassic mass extinction. Nature Communications, 7, Article 11147. DOI: 10.1038/ncomms11147. (8pp).

Thomazo, C., Vennin, E. and 10 others. 2016. A diagenetic control on the Early Triassic Smithian-Spathian carbon isotopic excursions recorded in the marine settings of the Thaynes Group (Utah, USA). Geobiology, 14(3): 220-236.

Thuy, B. & Stöhr, S. 2016. A new morphological phylogeny of the Ophiuroidea (Echinodermata) accords with molecular evidence and renders microfossils accessible for cladistics. PLoS ONE, 11(5): e0156140. doi:10.1371/journal.pone.0156140.

Tinglu Yang, Weihong He, Kexin Zhang, Shunbao Wu, Yang Zhang, Mingliang Yue, Huiting Wu & Yifan Xiao. 2016. Palaeoecological insights into the Changhsingian-Induan (latest Permian-earliest Triassic) bivalve fauna at Dongpan, southern Guangxi, South China. Alcheringa, 40(1): 98-117.

Tintori, A., Lombardo, C. & Kustatscher, E. 2016. The Pelsonian (Anisian, Middle Triassic) fish assemblage from the Monte Prà della Vacca/Kühwiesenkopf (Braies Dolomites, Italy). Neues Jahrbuch für Geologie und Paläontologie – Abhandlungen, 282(2): 181-200.

Tobia, F.H. & Aqrawi, A.M. 2016. Geochemistry of rare earth elements in carbonate rocks of the Mirga Mir Formation (Lower Triassic), Kurdistan region, Iraq. Arabian Journal of Geosciences, 9(4): DOI 10.1007/s12517-015-2148-1 (13pp).

Tobia, F.H. & Shangola, S.S. 2016. Mineralogy, geochemistry and depositional environment of the Beduh Shale (Lower Triassic), Northern Thrust Zone, Iraq. Turkish Journal of Earth Sciences, 25(4): 367-391.

Tomimatsu, Y., Onoue, T. & Nozaki, T. 2016. Stratigraphy and radiolarian ages of stratifrom manganese deposits from the Chichibu Belt in the Saiki area, eastern Oita Prefecture, Japan. Journal of the Geological Society of Japan, 122(6): 267-273.

Tongbin Shao, Nanfei Cheng & Maoshuang Song. 2016. Provenance and tectonic-paleogeographic evolution: constraints from detrital zircon U-Pb ages of Late Triassic-Early Jurassic deposits in the northern Sichuan Basin, central China. Journal of Asian Earth Sciences, 127: 12-31.

Tongtherm, K., Nabhitabhata, J., Srisuk, P., Nutadhira, T. & Tonnayopas, D. 2016. New records of nautiloids and ammonoid cephalopod fossils from peninsular Thailand. Swiss Journal of Palaeontology, 135(1): 153-168.

Toro, J., Miller, E.L., Prokopiev, A.V., Xiaojing Zhang & Veselovskiy, R. 2016. Mesozoic orogens of the Arctic from Novaya Zemlya to Alaska. Journal of the Geological Society, London, 173(6): 989-1006.

Torshizian, H.A. 2016. A study of the tectonic origin and the source of the clastic sediments of the Miankuhi formation in the Tarik Dareh region (Torbat Jam, NE Iran). Iranian Journal of Earth Science, 8(1): 45-51.

Trammer, J. 2016. Genus-level versus species-level extinction rates. Acta Geologica Polonica, 66(3): 261-265.

Trotteyn, M.J. & Paulina-Carabajal, A. 2016. Braincase and neuroanatomy of *Pseudochampsa ischigualastensis* and *Tropidosuchus romeri* (Archosauriformes, Proterochampsia). Ameghiniana, 53(5): 527-542.

Tvedt, A.B.M., Rotevatn, A. & Jackson, C.A.-L. 2016. Supra-salt normal fault growth during the rise and fall of a diapir: perspectives from 3D seismic reflection data, Norwegian North Sea. Journal of Structural Geology, 91: 1-26.

Twidale, C.R. 2016. Enigmatic mesozoic paleoforms revisited: the Australian experience. Earth-Science Reviews, 155: 82-92.

Uchman, A., Hanken, N.-M., Nielsen, J.K., Grundvåg, S.-A. & Piasecki, S. 2016. Depositional environment, ichnological features and oxygenation of Permian to earliest Triassic marine sediments in central Spitsbergen, Svalbard. Polar Research, 35: http//dx.doi.org/10.3402/polar.v35.24782, (21pp.).

Ullah, M., Ullah, S., Mussawar, U., Jan, I.U., Khan, M.A.A. & Khan, M.K. 2016. Transgressive-regressive (T-R) sequence analysis of the Early Triassic section of the Potwar Basin Pakistan. Journal of Himalayan Earth Sciences, Special Volume, 2016: 56.

Ullmann, C.V., Campbell, H.J., Frei, R. & Korte, C. 2016. Oxygen and carbon isotope and Sr/Ca signatures of high-latitude Permian to Jurassic calcite fossils from New Zealand and New Caledonia. Gondwana Geology, 38: 60-73.

Urlichs, M. 2016. Phyletic relationships among *Allocerantites* species from the upper Erfurt Formation of Thuringia (Late Ladinian, Germany) and from the Early Ladinian of Recoaro (Italy) and Toulon (France). Neues Jahrbuch für Geologie und Paläontologie – Abhandlungen, 282(1): 27-35.

Ustaömer, T., Ustaömer, P.A., Robertson, A.H.F. & Geerdes, A. 2016. Implications of U-Pb and Lu-Hf isotopic analysis of detrital zircons for the depositional age, provenance and tectonic setting of the Permian-Triassic Palaeotethyan Karakaya Complex, NW Turkey. International Journal of Earth Sciences, 105(1): 7-38.

Vaez-Javadi, F. 2016. Plant fossil remains from the Kalariz formation in the East Yurt mine, Azadshahr and its correlation with other florizones in Iran and the world. Geosciences, 25(99): 95-111. (Geological Survey of Iran: ISSN 1023-7429)

Van de Schootbrugge, B. & Wignall, P.B. 2016. A tale of two extinctions: converging end-Permian and end-Triassic scenarios. Geological Magazine, 153(Special Issue 2): 332-354.

Van der Lelij, R., Spikings, R., Ulianov, A., Chiaradia, M. & Mora, A. 2016. Palaeozoic to Early Jurassic history of the northwestern corner of Gondwana, and implications for the evolution of the Iapetus, Rheic and Pacific oceans. Gondwana Research, 31: 271-294.

Van Konijnenburg-van Cittert, J.H.A., Kustatscher, E., Pott, C., Schmeissner, S., Dütsch, G. & Krings, M. 2016. New data on *Selaginellites coburgensis* from the Rhaetian of Wüstenwelsberg (Upper Franconia, Germany). Neues Jahrbuch für Geologie und Paläontologie – Abhandlungen, 280(2): 177-181.

Van Kranendonk, M.J. & Kirkland, C.L. 2016. Conditioned duality of the Earth system: geochemical tracing of the supercontinent cycle through Earth history. Earth-Science Reviews, 160: 171-187.

Vavrek, M.J. 2016. The fragmentation of Pangaea and Mesozoic terrestrial vertebrate diversity. Biology Letters, 12(9): 20160492. DOI: 10. 1098/rsbl.2016.0528.

Vea, I.M. & Grimaldi, D.A. 2016. Putting scales into evolutionary time: the divergence of major scale insect lineages (Hemiptera) predates the radiation of modern angiosperm hosts. Nature Scientific Reports, 6(23487), doi:10.1038/srep23487. (11pp).

Vegas, M., Vázquez, J.T., Olaiz, A.J. & Medialdea, T. 2016. Tectonic model for the latest Triassic-Early Jurassic extensional event in and around the Iberian Peninsula. Geogaceta, 60: 23-26.

Velikoslavinskii, S.D., Kotov, A.B. and 9 others. 2016. Mesozoic age of the Gilyui metamorphic complex in the junction zone of the Selenga-Stanovoi and Dzhugdzhur-Stanovoi superterranes, Central Asian Fold Belt. Doklady Earth Sciences, 468(2): 561-565.

Verrière, A., Brockelhurst, N. & Fröbisch, J. 2016. Assessing the completeness of the fossil record: comparison of different methods applied to parareptilian tetrapods (Vertebrata: Sauropsida). Paleobiology, 42(4): 680-695.

Viega de Oliviera, T. & Schultz, C.L. 2016. Functional morphology and biomechanics of the cynodont *Trucidocynodon riograndensis* from the Triassic of southern Brazil: pectoral girdle and forelimb. Acta Palaeontologia Polonica, 61(2): 377-386.

Voinova, I.P. 2016. Volcanic rocks of the Khabarovsk accretionary complex, southern Far East Russia. Russian Journal of Pacific Geology, 10(3): 230-238.

Von Baczko, M.B. & Desojo, J.B. 2016. Cranial anatomy and palaeoneurology of the archosaur *Riojasuchus tenuisceps* from the Los Colorados Formation, La Rioja, Argentina. PLoS ONE, 11(2): e0148575. doi:10.1371/journal.pone.0148575.

Wang GuangWei, Li PingPing, Hao Fang, Zou HuaTao & Yu XinYa. 2016. Distribution and origin of the Third Member of the Feixianguan Formation in the Jiannan area: comprehensive analysis from three-dimensional seismic, petrography, and geochemistry. Acta Sedimentologica Sinica, 34(1): 168-180.

Wang, L., Wignall, P.B., Yongbiao Wang, Haishui Jiang, Yadong Sun, Guoshan Li, Jinling Yuan & Xulong Lai. 2016. Depositional conditions and revised age of the Permo-Triassic microbialites at Gaohua section, Cili County (Hunan Province, South China). Palaeogeography, Palaeoclimatology, Palaeoecology, 443: 156-166.

Wang Lei, Long Wenguo, Zhou Dai, Xu Wangchun & Jin Xinbiao. 2016. Late Triassic zircon U-Pb ages and Sr-Nd-Hf isotopes of Darongshan granites in southeastern Guangxi and their geological implications. Geological Bulletin of China, 35(8): 1291-1303.

Wang Yue, Wang Xunlian & Wang Ye. 2016. Discussion on age of "Sailiyakedaban Group" in southern Yencheng, South Xinjiang, NW China. Earth Science – Journal of China University of Geosciences, 2016(7): 1099-1109.

Wanlu Fu, Da-yong Jiang, Montañez, I.P., Meyers, S.R., Motani. R. & Tintori, A. 2016. Eccentricity and obliquity paced carbon cycling in the Early Triassic and implications for post-extinction ecosystem recovery. Nature Scientific Reports, 6(27793), doi:10.1038/srep27793. (7pp).

Warrington, G. 2016. British Triassic palaeontology: literature supplement 38. Mercian Geologist, 19(1): 63.

Webb, M. & White, L.T. 2016. Age and nature of Triassic magmatism in the Netoni Intrusive Complex, West Papua, Indonesia. Journal of Asian Earth Sciences, 132: 58-74.

Weems, R.E., Tanner, L.H. & Lucas, S.G. 2016. Synthesis and revision of the lithostratigraphic groups and formations in the Upper Permian – Lower Jurassic Newark Supergroup of eastern North America. Stratigraphy, 13(2): 111-153.

Wei Xiaolin, Zeng Xiaoping, Gan Chenpin, Zhang Dexin & Yu Xiaoliang. 2016. Geochemistry and geological significance of intermediate-acid intrusive rocks in Chaganganuo area, east Kunlun. Northwestern Geology, 48(2)2016: 1-10.

Weibel, R., Lindström, S., Pedersen, G.K., Johansson, L., Dybkjær, K., Whitehouse, M.J., Boyce, A.J. & Leng, M.J. 2016. Groundwater table fluctuations recorded in zonation of microbial siderites from end-Triassic strata. Sedimentary Geology, 342: 47-65.

Weihong He, Shi, G.R. and 7 others. 2016. Patterns of brachiopod faunal and body-size changes across the Permian-Triassic boundary: evidence from the Daoduishan section in Meishan area, South China. Palaeogeography, Palaeoecology, Palaeoclimatology, 448: 72-84.

Weihong Zhu, Shenghe Wu, Zhijun Yin, Tao Han, Yiming Wu, Wenjie Feng, Ya'nan Luo & Cen Cao. 2016. Braided river delta outcrop architecture: a case study of Triassic Huangshanjie Formation in Kuche depression, Tarim Basin, NW China. Petroleum Exploration and Development, 43(3): 528-536.

Weiwei Yang, Guangdi Liu & Yuan Feng. 2016. Geochemical significance of 17 *a*(H)-diahopane and its application in oil-source correlation of the Yanchang formation in Longdong area, Ordos basin, China. Marine and Petroleum Geology, 71: 238-249.

Wenlei Song, Cheng Xu, Smith, M.P., Kynicky, J., Huang, K., Chunwan Wei, Li Zhou & Qihai Shu. 2016. Origin of unusual HREE-Mo-rich carbonatites in the Qinling orogen, China. Nature Scientific Reports, 6(37377), doi:10.1038/srep37377. (10pp).

Wenlong Ding, Peng Dai, Dingwei Zhu, Yeqian Zhang, Jianhua He, Ang Li & Ruyue Wang. 2016. Fractures in continental shale reservoirs: a case study of the Upper Triassic strata in the SE Ordos Basin, Central China. Geological Magazine, 153(4): 663-680.

WenShan Chen, Yi-chang Huang, Chang-hao Liu, Han-ting Feng, Sun-lin Chung & Yuan-hsi Lee. 2016. U-Pb zircon geochronology constraints on the ages of the Tananao Schist Belt and timing of orogenic events in Taiwan: implications for a new tectonic evolution of the South China Block during the Mesozoic. Tectonophysics, 686: 68-81.

Wenya Lyu, Lianbo Zeng, Zhongqun Liu, Guoping Liu & Kewei Zu. 2016. Fracture response of conventional logs in tight-oil sandstone: a case study of the Upper Triassic Yanchang Formation in southwest Ordos Basin, China. AAPG Bulletin, 100(9): 1399-1417.

Wenzheng Zhang, Hua Yang, Xinyu Xia, Liqin Xie & Guwei Xie. 2016. Triassic chrysophyte cyst fossils discovered in the Ordos Basin, China. Geology, 44(12): 1031-1034.

Werning, S. & Nesbitt, S.J. 2016. Bone histology and growth in *Stenaulorhynchus stockleyi* (Archosauromorpha: Rhynchosauria) from the Middle Triassic of the Ruhuhu Basin of Tanzania. Comptes Rendus Paleovol, 15(1-2): 163-175.

Whiteside, D.I., Duffin, C.J., Gill, P.G., Marshall, J.E.A. & Benton, M.J. 2016. The Late Triassic and Early Jurassic fissure faunas from Bristol and South Wales: stratigraphy and setting. Palaeontologia Polonica, 67: 257-287.

Wignall, P.B. & Van de Schootbrugge, B. 2016. Middle Phanerozoic mass extinctions and a tribute to the work of Professor Tony Hallam. Geological Magazine, 153(Special Issue 2): 195-200.

Wignall, P.B., Bond, D.P.G., Yadong Sun, Grasby, S.E., Beauchamp, B., Joachimski, M.M. & Blomeier, D.P.G. 2016. Ultra shallow-marine anoxia in an Early Triassic shallow-marine clastic ramp (Spitsbergen) and the suppression of benthic radiation. Geological Magazine, 153(Special Issue 2): 316-331.

Winguth, A.M.E., 2016. Changes in productivity and oxygenation during the Permian-Triassic transition. Geology, 44(9): 783-784.

Witzmann, F., Sachs, S, & Nyhuis, C.J. 2016. A new species of *Cyclotosaurus* (Stereospondyli: Capitosauria) from the Late Triassic of Bielefeld, NW Germany, and the intrarelationships of the genus. Fossil Record, 19(2): 83-100.

Wojewoda, J., Rauch, M. & Kowalski, A. 2016. Synsedimentary seismotectonic features in Triassic and Cretaceous sediments in the Intrasudetic Basin (U Devěti křížů locality) – regional implications. Geological Quarterly, 60(2): 355-364.

Wolfe, J.M., Daley, A.C., Legg, D.A. & Edgecombe, G.D. 2016. Fossil calibrations for the arthropod Tree of Life. Earth-Science Reviews, 160: 43-110.

Worden, R.H., Benshatwan, M.S., Potts, G.J. & Elgarmadi, S.M. 2016. Basin-scale fluid movement patterns revealed by veins: Wessex Basin, UK. Geofluids, 16(1): 149-174.

Wu Cai-lai, Lei Min, Wu Di & Li Tian-xiao. 2016. Zircon SHRIMP dating and genesis of granites in Wulan area of northern Qaidam. Acta Geoscientica Sinica, 37(4): 493-516.

Xianbing Xu, Shuai Tang & Shoufa Lin, 2016. Detrital provenance of Early Mesozoic basins in the Jiangnan domain, South China: paleogeographic and geodynamic implications. Tectonophysics, 675: 141-158.

Xiangbo Li, Zhanlong Yang, Jing Wang, Huaqing Liu, Qinlin Chen, Rong Wanyan, Jianbo Liao & Zhiyong Li. 2016. Mud-coated intraclasts: a criterion for recognizing sandy mass-transport deposits – deep-lacustrine massive sandstone of the Upper Triassic Yanchang Formation, Ordos Basin, Central China. Journal of Asian Earth Sciences, 129: 98-116.

Xianghui Li, Mattern, F., Chaokai Zhang, Qinggao Zeng & Guozheng Mao. 2016. Multiple sources of the Upper Triassic flysch in the eastern Himalaya Orogen, Tibet, China: implications for palaeogeography and palaeotectonic evolution. Tectonophysics, 666: 12-22.

Xiangyang Xie. 2016. Provenance and sediment dispersal of the Triassic Yanchang Formation, southwest Ordos Basin, China. Sedimentary Geology, 335: 1-16

Xiaojing Zhang, Pease, V., Skogseid, J. & Wohlgemuth-Ueberwasser, C. 2016. Reconstruction of tectonic events on the northern Eurasia margin of the Arctic, from U-Pb detrital zircon provenance investigations of late Paleozoic to Mesozoic sandstones in the southern Taimyr Peninsula. Geological Society of America Bulletin, 128(1-2): 29-46.

Xiaomin Fang, Chunhui Song and 8 others. 2016. Mesozoic litho- and magneto-stratigraphic evidence from the central Tibetan Plateau for megamonsoon evolution and potential evaporites. Gondwana Research, 37: 110-129.

Xiao Xiong, Laimin Zhu and 9 others. 2016. Geology and geochemistry of the Triassic Wenquan Mo deposit and Mo-mineralized granite in the Western Qinling Orogen, China. Gondwana Research, 30 (Special Issue): 159-178.

Xiao-chun Wu, Li-jun Zhao, Sato, T., Sheng-xiao Gu & Xing-sheng Jin. 2016. A new specimen of *Hupehsuchus nanchangensis* Young, 1972 (Diapsida, Hupehsuchia) from the Triassic of Hubei, China. Historical Biology, 28(1-2): 43-52.

Xiao-Fei Qiu, Hong-Mei Yang, Xiao-Ming Zhao, Shan-Song Lu, Nian-Wen Wu. Li-Guo Zhang & Chun-Hong Zhang. 2016. Early Triassic gneissoid granites in the Gaozhou area (Yunkai Massif), South China: implications for the amalgamation of the Indochina and South China blocks. The Journal of Geology, 124(3): 395-409.

Xiaowan Xing, Yuejun Wang & Yuzhi Zhang. 2016. Detrital zircon U-Pb geochronology and Lu-Hf isotopic compositions of the Wuliangshan metasediment rocks in SW Yunnan (China) and its provenance implications. Journal of Earth Science, 27(3): 412-424.

Xin Qian, Qinglai Feng, Yuejun Wang, Wenqiang Yang, Chonglakmani, C. & Monjai, D. 2016. Petrochemistry and tectonic setting of the Middle Triassic arc-like volcanic rocks in the Sayabouli area, NW Laos. Journal of Earth Science, 27(3): 365-377.

Xin Qian, Yuejun Wang, Qinglai Feng, Jian-Wei Zi, Yuzhi

Zhang & Chonglakmani, C. 2016. Petrogenesis and tectonic implication of the Late Triassic post-collisional volcanic rocks in Chiang Khong, NW Thailand. Lithos, 248-251: 418-431.

Xinyu He, Jionghui Wang, Changming Wang, Carranza, E.J.M., Liang Chen & Bin Wu. 2016. Petrogenesis, zircon U-Pb age, and geochemistry of the A-type Moguo syenite, western Henan Province: implications for the Mesozoic tectono-magmatic evolution of the Qinling Orogen. Journal of Earth System Science, 125(3): 585-603.

Xiugen Fu, Jian Wang, Fuwen Tan, Ming Chen, Zhongxiong Li, Yuhong Zeng & Xinglei Feng. 2016. New insights about petroleum geology and exploration of Qiangtang Basin, northern Tibet, China: a model for low-degree exploration. Marine and Petroleum Geology, 77: 323-340.

Xiu-Mei Lu, WeiWei Zhang & Xing-Yue Liu. 2016. New long-proboscid lacewings of the mid-Cretaceous provide insights into ancient plant-pollinator interactions. Nature Scientific Reports, 6(25382), doi:10.1038/srep25382. (12pp).

Xiyao Li, Jianping Zheng, Sanzhong Li, Bo Liu, Lu Xiang, Yongming Wang & Xin Liu. 2016. Late Triassic orogenic collapse and Palaeo-Pacific slab roll-back beneath central South China: constraints from mafic granulite xenoliths and structural features. Geological Journal, 51(Supplement S1): 123-136.

Ya-Sheng Wu, Gong-Liang Yu, Hong-Xia Jiang, Li-Jing Liu & Rui Zhao. 2016. Role and lifestyle of calcified cyanobacteria (*Stanieria*) in Permian-Triassic boundary microbialites. Palaeogeography, Palaeoecology, Palaeoclimatology, 448: 39-47.

Yabumoto, Y. & Brito, P.M. 2016. A new Triassic coelacanth, *Whiteia oishii* (Sarcopterygii, Actinistia) from West Timor, Indonesia. Paleontological Research, 20(3): 233-246.

Yalçin, H., Bozkaya, Ö. & Takçi, M. 2016. Diagenetic history of rock units of Bozkir Unit controlled by Triassic rifting, Bozkir-Konya. Bulletin of the Mineral Research and Exploration, 153: 63-90.

Yamashita, D., Yasuda, C., Ishibashi, T., Martini, R. & Onoue, T. 2016. Stratigraphy and conodont and ammonoid ages of Upper Triassic Nakijin Formation in Hedomisaki area, Okinawa-jima, Japan. Journal of the Geological Society of Japan, 122(9): 477-493.

Yan Hu, Yaoling Niu, Jiyong Li, Lei Ye, Juanjuan Kong, Shuo Chen, Yu Zhang & Guorui Zhang. 2016. Petrogenesis and tectonic significance of the late Triassic mafic dikes and felsic volcanic rocks in the East Kunlun Orogenic Belt, northern Tibet Plateau. Lithos, 245: 205-222.

Yan Ke, Shu-zhong Shen, Shi, G.R., Jun-xuan Fan, Hua Zhang, Li Qiao & Yong Zeng. 2016. Global brachiopod palaeobiogeographical evolution from Changhsingian (Late Permian) to Rhaetian (Late Triassic). Palaeogeography, Palaeoecology, Palaeoclimatology, 448: 4-25.

Yanan Zhou, Xin Cheng and 10 others. 2016. Paleomagnetic study on the Triassic rocks from the Lhasa Terrane, Tibet, and its paleogeographic implications. Journal of Asian Earth Sciences, 121: 108-119.

Yang Changqing, Yang Yanqiu, Li Gang, Yang Chuansheng & Yang Jinyu. 2016. The Mesozoic basin-mountain coupling process of the southern East China Sea Shelf Basin and its adjacent land area. Acta Geologica Sinica, 90(3): 1051-1052.

Yang Fu, Chang Gang, Li Shuheng, Lei Panpan & Tian Tao. 2016. Diagenesis and porosity evolution of Chang 8 oil reservoir group in Qingcheng-Heshui area. Northwestern Geology, 48(4)2016: 207-218.

Yang Hua, Fu Qiang, Qi YaLin, Zhou XinPing, Gong Ning & Huang ShaoXiong. 2016. The paleontology phase zones and its geological significance on the Late Triassic Yanchang Stage palaeo-lacustrine Ordos Basin. Acta Sedimentologica Sinica, 34(4): 688-693.

Yang Jun-quan, Liu Yong-shun, Zhang Su-rong, Yang Yong-heng, Zhang Feng & Rong He. 2016. Two Triassic magmatic activities in Binbalechagan area of Dong Ujimqin Banner, Inner Mongolia: geochronologic record, petrogenesis and tectonic setting. Geology in China, 43(6) 2016: 1913-1931.

Yang Lirong, Song Haijun, Tong Jinnan, Chu Daoliang, Liang Lei, Wu Kui & Tian Li. 2016. The extinction pattern of foraminifers during the Permian-Triassic crisis at the Maochang section, Ziyun, Guizhou Province, South China. Acta Micropalaeontologica Sinica, 33(3): 229-250.

Yang Zhang, Shi, G.R. and 8 others. 2016. Significant pre-mass extinction animal body-size changes: evidence from the Permian-Triassic boundary brachiopod faunas of South China. Palaeogeography, Palaeoecology, Palaeoclimatology, 448: 85-95.

Yangli Yu, Xin Wang, Gang Rao & Renfu Wang. 2016. Mesozoic reactivated transpressional structures and multi-stage tectonic deformation along the Hong-Che fault zone in the northwestern Junggar Basin, NW China. Tectonophysics, 679: 156-168.

Yanlong Chen, Kolar-Jurkovšek, T., Jurkovšek, B., Aljinović, D. & Richoz, S. 2016. Early Triassic conodonts and carbon isotope record of the Idrija-Žiri area, Slovenia. Palaeogeography, Palaeoclimatology, Palaeoecology, 444: 84-100.

Yanlong Chen, Krystyn, L., Orchard, M.J., Xu-Long Lai & Richoz, S. 2016. A review of the evolution, biostratigraphy, provincialism and diversity of Middle and early Late Triassic conodonts. Papers in Palaeontology, 2(2): 235-263.

Yanlong Chen, Krystyn, L., Orchard, M.J., Xu-Long Lai & Richoz, S. 2016. Reply to comments on: A review of the evolution, biostratigraphy, provincialism and diversity of Middle and early Late Triassic conodonts. Papers in Palaeontology, 2(3): 457-461.

Yanlong Chen, Neubauer, T.A., Krystyn, L. & Richoz, S. 2016. Allometry in Anisian (Middle Triassic) segminiplanate conodonts and its implications for conodont taxonomy. Palaeontology, 59(5): 725-741.

Yan-hui Wang, Engel, M.S. and 7 others. 2016. Fossil record of stem groups employed in evaluating the chronogram of insects (Arthropoda: Hexapoda). Nature Scientific Reports, 6(38939), doi:10.1038/srep38939. (12pp).

Yan-wan Wu, Cai Li, Meng-jing Xu, Sheng-qing Xiong, Zheng-guo Fan, Chao-ming Xie & Ming Wang. 2016. Petrology and geochemistry of metabasalts from the Taoxinghu ophiolite, central Qiangtang, northern Tibet: evidence for a continental back-arc basin system. Austrian Journal of Earth Sciences,

109(2): 166-177.
Yao Jianxin, Bo Jingfang and 11 others. 2016. Status of stratigraphy research in China. Acta Geologica Sinica, 90(4): 1069-1081.
Ye Xiaozhou, Sun Zhiming, Li Haibing, Cao Yong, Zhang Lei, Wang Leizhen & Zhao Yue. 2016. New paleomagnetic result of Early Triassic rocks from the Longmenshan belt and its tectonic implications. Geological Bulletin of China, 35(6): 971-978.
Ying-Hui Lu, Zi-Fu Zhao & Yong-Fei Zheng. 2016. Geochemical constraints on the source nature and melting conditions of Triassic granites from South Qinling in central China. Lithos, 264: 141-157.
Yong Li, Shuwen Dong, Yueqiao Zhang, Jianhua Li, Jinbao Su & Baofu Han. 2016. Episodic Mesozoic constructional events of central South China: constraints from lines of evidence of superimposed folds, fault kinematic analysis, and magma geochronology. International Geology Review, 58(9): 1076-1107.
Yong Zhou, Youliang Ji and 7 others. 2016. Controls on reservoir heterogeneity of tight sand oil reservoirs in Upper Triassic Yanchang Formation in Longdong area, southwest Ordos Basin, China: implications for reservoir quality prediction and oil accumulation. Marine and Petroleum Geology, 78: 110-135.
Yu GuanMei & Shi Guo. 2016. Trace fossils and their palaeoenvironmental significance of the Early Triassic Anshun Formation in Huaxi area, Guiyang. Acta Sedimentologica Sinica, 34(4): 615-625.
Yu Zhang, Yangyang Chen, Qichao Zhang & Xianghong Meng. 2016. Tectonic sequences of Triassic strata in the southern Ordos Basin, China. Stratigraphy, 13(3): 205-219.
Yu Zhang, Yaoling Niu, Yan Hu, Jinju Liu, Lei Ye, Juanjuan Kong & Meng Duan. 2016. The syncollisional granitoid magmatism and continental crust growth in the West Kunlun Orogen, China – evidence from geochronology and geochemistry of the Arkarz pluton. Lithos, 245: 191-204.
Yuanku Meng, Zhiqin Xu, Santosh, M., Xuxuan Ma, Xijie Chen, Guolin Guo & Fei Liu. 2016. Late Triassic crustal growth in southern Tibet: evidence from the Gangdese magmatic belt. Gondwana Research, 37: 449-464.
Yue Shaofei, Wang Hua, Yan Detian, Huang Chuanyan, Chang Dayu, Li Xiaopeng & Zhang Jing. 2016. The sedimentary characteristics and evolution law of Triassic, Luoyi District. Earth Science – Journal of China University of Geosciences, 2016(10): 1683-1695.
Yuejun Wang, Huiying He, Cawood, P.A., Srithai, B., Qinglai Feng, Weiming Fan, Yuzhi Zhang & Xin Qian. 2016. Geochronological, elemental and Sr-Nd-Hf-O isotopic constraints on the petrogenesis of the Triassic post-collisional granitic rocks in NW Thailand and its Paleotethyan implications. Lithos, 266-267: 264-286.
Yu-Xia Zhang, Zhi-Wu Li, Li-Dong Zhu, Ki-Jun Zhang, Wen-Guang Yang & Xin Jin. 2016. Newly discovered eclogites from the Bangong Meso-Tethyan suture zone (Gaize, central Tibet, western China): mineralogy, geochemistry, geochronology, and tectonic implications. International Geology Review, 58(5): 547-587.
Yunpeng Dong, Zhao Yang and 8 others. 2016. Mesozoic intracontinental orogeny in the Qinling Mountains, central China. Gondwana Research, 30 (Special Issue): 144-158.
Yuruo Shi, Anderson, J.L., Linlin Li, Jing Ding, Cui Liu, Wei Zhang & Chonghui Shen. 2016. Zircon ages and Hf isotopic compositions of Permian and Triassic A-type granites from central Inner Mongolia and their significance for late Palaeozoic and early Mesozoic evolution of the Central Asian Orogenic Belt. International Geology Review, 58(8): 967-982.
Yuruo Shi, Anderson, J.L., Zhonghai Wu, Zhenyu Wang, Linlin Li & Jing Ding. 2016. Age and origin of early Paleozoic and Mesozoic granitoids in Western Yunnan Province, China: geochemistry, SHRIMP zircon ages, and Hf-in-zircon isotopic compositions. The Journal of Geology, 124(5): 617-630.
Zadeh, M.K., Mondol, N.H. & Jahren, J. 2016. Compaction and rock properties of Mesozoic and Cenozoic mudstones and shales, northern North Sea. Marine and Petroleum Geology, 76: 344-361.
Zakharov, Y.D. & Smyshlyaeva, O.P. 2016. New middle Olenekian (early Triassic) ammonoids of South Primorye. Paleontological Journal, 50(3): 229-238.
Zanchi, A., Zanchetta, S., Balini, M. & Ghassemi, M.R. 2016. Oblique convergence during the Cimmerian collision: evidence from the Triassic Aghdarband Basin, NE Iran. Gondwana Geology, 38: 149-170.
Zatoń, M., Niedźwiedski, G., Blom, H. & Kear, B.P. 2016. Boreal earliest Triassic biotas elucidate globally depauperate hard substrate communities after the end-Permian mass extinction. Nature Scientific Reports, 6(36345), doi:10.1038/srep36345. (10pp).
Zatoń, M., Wilson, MA. & Vinn, O. 2016. Comment on the paper of Gierlowski-Kordesch and Cassle "The '*Spirorbis*' problem revisited: Sedimentology and biology of microconchids in marine-nonmarine transitions" [Earth-Science Reviews, 148 (2015): 209-227]. Earth-Science Reviews, 152: 198-200.
Zhanfeng Qiao, Janson, X., Anjiang Shen, Jianfeng Zheng, Hongliu Zeng & Xiaofang Wang. 2016. Lithofacies, architecture and reservoir heterogeneity of tidal-dominated platform marginal oolitic shoal: an analogue of oolitic reservoirs of Lower Triassic Feixianguan Formation, Sichuan Basin, SW China. Marine and Petroleum Geology, 76: 290-309.
Zhang Ji-dong, Fan Yong-gui and 7 others. 2016. Middle-Late Triassic radiolarian fossils from the Zhongba region, Xizang and their geological implications. Sedimentary Geology and Tethyan Geology, 36(2016:4): 1-6.
Zhang Jing, Shao Jun, Zhou Yongheng, Bao Qingzhong & Wang Hongbo. 2016. Geochemical characteristics of rocks and U-Pb, Re-Os age of the Badaguan Cu-Mo deposit in Chen Barag Banner, Inner Mongolia. Geological Bulletin of China, 35(8): 1388-1399.
Zhang Qian, Sun Wei, Ming HongXia, Wang Qian & Zhang LongLong. 2016. Micro-pore structure of diagenetic facies of Chang-6_3 reservoir and distribution of high quality reservoir in Banqiao-Heshui area. Acta Sedimentologica Sinica, 34(2):

336-345.

Zhang San, Yang Bo, Li Tingyan, Wang Huiling, Zhang Zhenhong & Wang Lingli. 2016. Sedimentary facies and evolution of Chang 9 oil formation in Yanchang Formation, Zhijing-Ansai area, Ordos Basin. Geological Bulletin of China, 35(10): 1964-1970.

Zhang Shun-li, Song Xiu-zhang, Lu Zheng-xiang, Yang Xiang & Qing Yuan-hua. 2016. Reservoir characteristics and controlling factors in the 4th member of the Xujiahe Formation in the Xinchang structural zone. Sedimentary Geology and Tethyan Geology, 36(2016:1): 98-103.

Zhang Wei, Zhou Hanwen, Zhu Yunhai, Mao Wulin, Tong Xin, Ma Zhanqing & Cao Yongliang. 2016. The evolution of Triassic granites associated with mineralization within East Kunlun Orogenic Belt: evidence from the petrology, geochemistry and zircon U-Pb geochronology of the Mohexiala pluton. Earth Science – Journal of China University of Geosciences, 2016(8): 1334-1348.

Zhang Wenhui, Wang Cuizhi, Li Xiaomin & Liu Wenyuan. 2016. Zircon SIMS U-Pb age, Hf and O isotopes of mafic dikes, southwest Fujian Province. Advances in Earth Science (Journal of Xidian University), 31(3): 320-334.

Zhang Xiangyun, Wang Genhou, Zhao Jun, Cui Xiaofeng, Bai Xiang & Nie Xiaoyong. 2016. Geochemical characteristics, formation age and tectonic environment of the Mankeyidingsayi rocks in the Wuxilike area of Altay. Geological Bulletin of China, 35(8): 1376-1387.

Zhang Xiao-qing, Zhang Guo-quan and 7 others. 2016. Wildfire event at the Triassic-Jurassic boundary: approaches, progress, and perspective. Acta Palaeontologica Sinica, 55(3): 331-345.

Zhang Yingli, Wang Zongqi, Wang Gang, Li Qian & Lin Jianfei. 2016. Chromian spinel, zircon age constraints on the provenance of Early Triassic Feixianguan Formation sandstones from Huize area, upper Yangtze region. Geological Review, 62(1): 54-72.

Zhang Yu-ying, Jiang Da-yong, He Zhi-liang, Gao Bo, Liu Zhong-bao & Nie Hai-kuan. 2016. Microfacies and palaeoenvironment analysis of the middle-upper member of the Nanlinghu Formation (Lower Triassic), Chaohu, Anhui Province. Journal of Stratigraphy, 40(3): 290-296.

Zhang Zhenhong, Zhu Jing, Yu Fang, Li Cheng, Wang Lingli & Li Wenhou. 2016. Reservoir characteristics of thick sandstone and micro-anisotropy of delta front micro-facies: a case study of Chang 6 reservoir in Wucangbu area. Geological Bulletin of China, 35(2): 440-447.

Zhao Zelin, Li Junjian and 7 others. 2016. TIMS zircon U-Pb isotopic dating of Salazha Mountain granites from the northern margin of Alxa, Inner Mongolia, and its tectonic implications. Geological Bulletin of China, 35(4): 599-604.

Zhe Cao, Guangdi Liu, Hongbin Zhan, Chaozheng Li, Yuan You, Chengyu Yang & Hang Jiang. 2016, Pore structure characterization of Chang-7 tight sandstone using MICP combined with N_2GA techniques and its geological control factors. Nature Scientific Reports, 6(36919), doi:10.1038/srep36919. (13pp).

Zhelong Chen, Guangdi Liu, Xulong Wang, Gang Gao, Baoli Xiang, Jiangling Ren, Wanyun Ma & Qiong Zhang. 2016. Origin and mixing of crude oils in Triassic reservoirs of Mahu slope area in Junggar Basin, NW China: implication for control on oil distribution in basin having multiple source rocks. Marine and Petroleum Geology, 78: 373-389.

Zheng Wei, Qi Yongan, Zhang Zhonghui & Xing Zhifeng. 2016. Characteristic and geological significance of microbially induced sedimentary structures (MISS) in terrestrial P-T boundary in Xingyang, western He'nan Province. Advances in Earth Science, 2016(7): 737-750.

Zhengbin Deng, Shuwen Liu, Wanyi Hu & Qiugen Li. 2016. Petrogenesis of the Guangtoushan granitoid suite, central China: implications for Early Mesozoic geodynamic evolution of the Qinling Orogenic Belt. Gondwana Research, 30 (Special Issue): 112-131.

Zhen-Ju Zhou, Shi-Dong Mao, Yan-Jing Chun & Santosh, M. 2016. U-Pb ages and Lu-Hf isotopes of detrital zircons from the southern Qinling Orogen: implications for Precambrian to Phanerozoic tectonics in central China. Gondwana Research, 35: 323-337.

Zhenglong Zhou, Guiwen Wang, Ye Ran, Jin Lai, Yufeng Cui & Xianling Zhao. 2016. A logging identification method of tight oil reservoir lithology and lithofacies: a case from Chang7 Member of Triassic Yanchang Formation in Heshui area, Ordos Basin, NW China. Petroleum Exploration and Development, 43(1): 65-73.

ZhenHua Xue, QingHua Shang, WenYing Jiang, QingChen Wang & ShuangJian Li. 2016. Emplacement age and tectonic implications of the brecciated limestone at the edge of the Longmenshan klippe. Science China Earth Sciences, 59(3): 590-600.

Zhenyu Li, Lin Ding, Lippert, P.C., Peiping Song, Yahui Yue & van Hinsbergen, D.J.J. 2016. Paleomagnetic constraints on the Mesozoic drift of the Lhasa terrane (Tibet) from Gondwana to Eurasia. Geology, 44(9): 727-730.

Zhi-Guang Li, Da-Yong Jiang, Rieppel, O., Motani, R., Tintori, A., Zuo-Yu Sun & Cheng Ji. 2016. A new species of *Xinpusaurus* (Reptilia, Thallatosauria) from the Ladinian (Middle Triassic) of Xingyi, Guizhou, southwestern China. Journal of Vertebrate Paleontology, 36(6): e1218340 (7pp).

Zhiwei Liao, Wenxuan Hu, Jian Cao, Xiaolin Wang, Suping Yao & Ye Wan. 2016. Permian-Triassic boundary (PTB) in the Lower Yangtze region, southeastern China: a new discovery of deep-water archive based on organic carbon isotopic and U-Pb geochronological studies. Palaeogeography, Palaeoclimatology, Palaeoecology, 451: 124-139.

Zhiwei Liao, Wenxuan Hu, Jian Cao, Xiaolin Wang, Suping Yao, Haiguang Wu & Ye Wan. 2016. Heterogeneous volcanism across the Permian-Triassic boundary in South China and implications for the latest Permian mass extinction: new evidence from volcanic ash layers in the Lower Yangtze region. Journal of Asian Earth Sciences, 127: 197-210.

Zhiyong Zhang, Wenbin Zhu, Dewen Zheng, Bhai Zheng & Wei Yang, 2016. Apatite fission track thermochronology in the Kukuketage and Aksu areas, NW China: implication for tectonic evolution of the northern Tarim. Geoscience Frontiers, 7(2): 171-180.

Zhong Yuan, Liu Hong, Tan XiuCheng, Lian ChengBo, Liao

JiJia, Liu MingJie, Hu Guang & Cao Jian. 2016. Using high resolution sequence stratigraphy to study the framework of sand-rich strata and predict the sweet spots of reservoir: taking Xujiahe Formation in Hechuan area, Sichuan Basin as example. Acta Sedimentologica Sinica, 34(4): 758-774.

Zhonghua Tian, Wenjiao Xiao, Zhiyong Zhang & Xu Lin. 2016. Fission-track constraints on superposed folding in the Beishan orogenic belt, southernmost Altaids. Geoscience Frontiers, 7(2): 181-196.

Zhongyi Zhang, Shijia Chen and 7 others. 2016. Tight oil accumulation mechanisms of Triassic Yanchang Formation Chang 7 Member, Ordos Basin, China. Petroleum Exploration and Development, 43(4): 644-654.

Zhou Xiang, He Sheng, Chen Zhaoyuo, Liu Ping & Wang Furong. 2016. Characteristics and controlling factors of source rocks in Yanchang Formation sequence framework, Ordos Basin. Earth Science – Journal of China University of Geosciences, 2016(6): 1055-1066.

Zhou Zhi-cheng, Luo Hui and 8 others. 2016. The sharp change between the ecosystems of two organic deposits across the Permian-Triassic boundary in the Yudongzi section, Jiangyou, Sichuan, South China. Acta Palaeontologica Sinica, 55(1): 70-86.

Zhu Guo-ren, Guan Jun-lei, Wang Guo-zhi, Zheng Lai-lin, Long Teng, Lu Xu-yang & Xu Peng. 2016. The granites from the Huangcaoling region, Luchun, Yunnan: SHRIMP zircon U-Pb chronology and geological implications. Sedimentary Geology and Tethyan Geology, 36(2016:4): 77-84.

Zhu Min, Chan Hanlin, Zhou Jing & Yang Shufeng. 2016. Provenance of Early Triassic in Yanyuan Basin, Upper Yangtze and its implication for the tectonic evolution. Earth Science – Journal of China University of Geosciences, 2016(8): 1309-1321.

Zimmermann, S. & Hall, R. 2016. Provenance of Triassic and Jurassic sandstones in the Banda Arc: petrography, heavy minerals and zircon geochronology. Gondwana Research, 37: 1-19.

Zonneveld, J.-P., Furlong, C.M. & Sanders, S.C. 2016. Triassic echinoids (Echinodermata) from the Aksala Formation, north Lake Laberge, Yukon Territory, Canada. Papers in Palaeontology, 2(1): 87-100.

Zulauf, G., Dörr, W., Krahl, J., Lahaye, Y., Chatzaras, V. & Xypolias, P. 2016. U-Pb zircon and biostratigraphic data of high-pressure/low-temperature metamorphic rocks of the Talea Ori: tracking the Paleotethys suture in central Crete, Greece. International Journal of Earth Sciences, 105(7): 1901-1922.

Zuoyu Sun, Dayong Jiang, Cheng Ji & Weicheng Hao. 2016. Integrated biochronology for Triassic marine vertebrate faunas of Guozhou Province, South China. Journal of Asian Earth Sciences, 118: 101-110.

Additional pre-2016 titles:

Adabi, M.H., Ghavidel-Syooki, M. & Aryafar. 2015. The study of the Late Anisian deposits in Kal-e Angur and Kal-e Ghalak sections, in the Aghdarband tectonic window (NE of Iran). Iranian Journal of Geology, 33(9): 15pp.

Bai Yun-shan, Duan Qi-fa, Niu Zhi-jun, Tang Chao-yang & Zhao Xiao-ming. 2014. Geochemical characteristics and its tectonic significance of Upper Triassic Batang group volcano rocks in Zhahe area, Zhiduo County, southern Qinghai Province. Journal of Geology and Mineral Resources of South China, 2014(4): 319-327.

Bechis, F., Cristallini, E.O., Giambiagi, L.B., Yagupsky, D.L., Guzmán, G. & García, V.H. 2014. Transtensional tectonics induced by oblique reactivation of previous lithospheric anisotropies during the Late Triassic to Early Jurassic rifting in the Neuquén Basin: insights from analog models. Journal of Geodynamics, 79: 1-17.

Blendinger, W., Bertini, A., Lohmeier, S. & Meißner, E. 2013. Dolomite in Triassic Dolomite. Claustaler Geowissenschaften, 9.

Burgess, S.D. & Bowring, S.A. 2015. High-precision geochronology confirms voluminous magmatism before, during, and after Earth's most severe extinction. Science Advances, 1(7). DOI: 10.1126/sciadv.1500470. (14pp).

Deng Baozhu, Yu Lixue, Wang Yongbiao, Li Guoshan & Meng Yafei. 2015. Evolution of marine conditions and sedimentation during the Permian-Triassic transition in Chibi of Hubei Province. Earth Science – Journal of China University of Geosciences, 2015(2): 317-326.

Deutschman, A., Meschede, M. & Obst, K. 2013. Distribution of Triassic rocks at the north-eastern margin of the North German Basin – first insights of re-processed 2D reflection profiles in the southern Baltic Sea. Schriftenreihe der Deutschen Gesellschaft für Geowissenschaften, 82: 37.

Diao Fan, Ween Zhi-gang, Zou Hua-you & Li Na. 2013. Sedimentary characteristics of shallow-water deltas in Chang 8 oil-bearing interval in eastern Gansu, Ordos Basin. Earth Science – Journal of China University of Geosciences, 38(6): 1289-1298.

Feng Wenjie, Wu Shenghe, Xia Qinyu, Li Junfei & Wu Shunwei. 2015. Micro-facies modelling of alluvial fan reservoir based on geological vector information: a case study on the Lower Triassic Karamay Formation, Yizhong area, Karamay oilfield, NW China. Geological Bulletin of China Universities, 18(3): 449-460.

Ferreiro Mählmann, R., Wolf, M., Bernoulli, D., Petschick, R., Meister, P., Mullis, J., Giger, M. & Krumm, H. 2015. Traces of burial-induced Permo-Triassic and Jurassic heating discriminated from the Cretaceous Upper-Austroalpine orogenetic diagenetic-metamorphic pattern by organic matter studies and maturity modelling, Mittelbünden, Switzerland. Schriftenreihe der Deutschen Gesellschaft für Geowissenschaften, 87: 51-52.

Gancarz, M. 2015. A characterisation of the geothermal potential of the Muschelkalk deposits' location, with the prospective of its utilization in balneology and recreation (southern Poland). Geology, Geophysics & Environment, 41(4): 333-342.

Gao Wenping, Hong Han-lie, and 7 others. 2013. Fine structure and their genetic significance of clay minerals from the Permian-Triassic boundary, Huaxi area, Guizhou Province. Earth Science – Journal of China University of Geosciences, 38(6): 1253-1262.

Ghori, K.A.R. 2013. Petroleum geochemistry and petroleum systems modelling of the Canning Basin, Western Australia. Geological Survey of Western Australia, Report 124, 33pp.

Haghighat, N. & Mansuri. P. 2015. Litho-biostratigraphy of Permian and Lower Triassic deposits in the Sibestan section (northwest of Tehran). Geosciences, 24(95): 45-54. (Geological Survey of Iran: ISSN 1023-7429).

Hajian Barzi, M., Aleali, M., Jahani, D. & Falah Kheyrkhah, M. 2015. Microfacies, sedimentary environment, sequence stratigraphy and strontiun dating of the Dashtak Formation in the Persian Gulf, Fars and Izeh regions. Geosciences, 24(95): 185-198. (Geological Survey of Iran: ISSN 1023-7429).

Hámor-Vidó, M. & Hufnagel, H. 2015. Organic petrological assessment of the facies evolution of the Norian-Rhaetian carbonate-rich environment of Rezi-1 well samples, western Hungary. Schriftenreihe der Deutschen Gesellschaft für Geowissenschaften, 87: 89.

Hao Tian-qi, Ji Cheng, Sun Zuo-yu, Jiang Da-yong & Tintori, A. 2015. Conodonts in coprolites from the Early Triassic of Chaohu, Anhui. Journal of Stratigraphy, 39(2): 188-196.

He Weihong, Zhang Kexin and 9 others. 2015. End-Permian faunas from Yangtze Basin and its marginal region: implications for palaeogeographical and tectonic environments. Earth Science – Journal of China University of Geosciences, 2015(2): 275-289.

He Xiao-Liang. 2014. Geochemical characteristics and tectonic environment of Late Triassic intrusive rocks along Badaoban area, Dulan County, Qinghai Province. Journal of Geology and Mineral Resources of South China, 2014(3): 218-231.

Henstra, G.A., Rotevatn, A., Gawthorpe, R.L. & Ravnås, R. 2015. Evolution of a major segmented fault during multiphase rifting: the origin of plan-view zigzag geometry. Journal of Structural Geology, 74: 45-63.

Hermsen, E., Taylor, T.N., Taylor, E.L. & Stevenson, D.W. 2007. Cycads from the Triassic of Antarctica: permineralized cycad leaves. International Journal of Plant Sciences, 168(7): 1099-1112.

Hu Bin, Lu Xu-hui & Song Hui-bo. 2015. Lower Triassic ichnofossils and sedimentary environments in the Dengfeng area, western Henan Province. Journal of Stratigraphy, 39(4): 454-465.

Huang Yunfei, Tong Jinnan, Xiang Ye, Xiao Chuantao, Song Haijun, Tian Li, Song Ting & Chu Daoliang. 2015. The extinction and delayed recovery of bivalves during the Permian-Triassic crisis. Earth Science – Journal of China University of Geosciences, 2015(2): 334-345.

Ji Cheng. 2014. The stratigraphic distribution, migration and phylogeny of the Triassic sauropterygians. Journal of Stratigraphy, 38(2): 195-199.

Ji Liu-xiang, Luo Wei, Liu Feng & Ouyang Shu. 2015. Triassic sporopollen and acritarchs from northern Qilian Mountain (Qinghai) and their stratigraphical significance. Journal of Stratigraphy, 39(4): 367-379.

Kalantarzadeh, Z., Adabi, M.H. & Rahimpour Bohab, H. 2015. Study of original carbonate mineralogy of the Nayband Formation using geochemical evidences in Darbidkhoon, Tarz, Gitry and Kuhbanan stratigraphic sections, SE of Iran. Geosciences, 24(94): 203-216. (Geological Survey of Iran: ISSN 1023-7429).

Lei Min, Wu Cailai, Wu Xiuping, Gao Yuanhong, Wu Suoping, Chen Qilong & Qin Haipeng. 2011. Zircon SHRIMP U-Pb datings of granite and its enclave from Xinyuan pluton, southern Qinling mountains, and their geological significances. Geological Review, 57(6): 889-899.

Li Jianghai, Zhou Xiaobei, Li Weibo, Wang Honghao, Liu Zhonglan, Zhang Huatian & Abitkazy, T. 2015. Preliminary reconstruction of tectonic paleogeography of Tarim Basin and its adjacent areas from Cambrian to Triassic, NW China. Geological Review, 61(6): 1225-1234.

Li Rong, Hu Zhonggui, Hu Mingyi, Meng Lingtao, Liu Dongxi, Liao Yisha & Pu Junwei. 2015. Reservoir characteristics and main control factors of the Feixianguan Formation in the Qilixia-Yunanchang area, southeastern Sichuan Basin. Geological Bulletin of China Universities, 18(4): 642-652.

Li Yun, Han Xu, Niu Zhi-zhong, Li Jing, He Jian & Qiao Yu-lan. 2014. Geology characteristics of Chang-7 reservoir of Yanchang Formation in Xiasiwan oil field. Northwestern Geology, 47(1)2014: 249-254.

Li Yun-dong & Liu Xiao-yu. 2014. Geochemistry and tectonic setting of Late Triassic volcanic rocks in Reshui area, Qinghai. Northwestern Geology, 47(3)2014: 14-25.

Li Zhao-yu, Li Wen-hou, Liu Xiao-yu & Ma Kai. 2014. Characteristics of Chang 6 reservoir of the Huaqing area in the Ordos Basin. Northwestern Geology, 47(3)2014: 101-109.

Liu Fen, Zhu Xiaomin, Li Yang, Xu Liming, Zhu Shifa & Xue Mengge. 2015. Characteristics of the Late Triassic deep-water slope break belt in southwestern Ordos Basin and its control on sandbodies. Geological Bulletin of China Universities, 18(4): 674-684.

Looy, C.V., Collinson, M.E., Van Konijnenburg-Van Cittert, J.H.A., Visscher, H. & Brain, A.P.R. 2005. The ultrastructure and botanical affinity of end-Permian spore tetrads. International Journal of Plant Sciences, 166(5): 875-887.

Mahbobipour, H. & Bashari, A.R. 2014. Study of petrography and petrophysics of Permian-Triassic carbonate sediments in Qatar – south Fars Arch. Iranian Journal of Petroleum Geology, 3(7): 34-49.

Mannani, M. & Yazdi, S. 2015. Palaeoecology of Late Triassic deposits, in Dizlu section north of Isfahan, central Iran based on scleractinian corals. Geosciences, 24(95): 281-290. (Geological Survey of Iran: ISSN 1023-7429).

Martínez, N., Laura Tobares, M., Giaccardi, A., Aguilera, D., Roquet, M.B. & Giambiagi, L. 2012. Gondwanic pyroclastic deposits in the southern Sierra de Varela, San Luis Province: petrography and geochemistry. Serie Correlación Geológica, 28(1): 23-32.

Masaoke, Y. & Suzuki, S. 2015. Facies analysis of the Jito Formation (Upper Triassic Nariwa Group) in Jito area, Kawakami, Okayama Pref., SW Japan. Okayama University Earth Science Reports, 22(1): 31-39.

Meier, S., Bauer, J.F. & Philipp, S.L. 2015. Fault zone characteristics, fracture systems and permeability implications of Middle Triassic Muschelkalk in southwest Germany. Journal

of Structural Geology, 70: 170-189.
Minzoni, M., Lehrmann, D.J. and 11 others. 2014. Triassic Tank: platform margin and slope architecture in space and time, Nanpanjiang Basin, South China. SEPM Special Publications, 105: 84-113.
Monibi, S., Khodaei, N. & Zamani Pozveh, Z. 2013. Lithostratigraphy and biostratigraphy of the Upper Dalan and Lower Kangan units in Persian Gulf with special emphasis on the Permo-Triassic boundary. Iranian Journal of Petroleum Geology, 3(4): 52-71.
Murphy, P.J. & Moseley, M. 2015. Sediment-filled cavities in the Morecambe Bay karst (UK): examples from the Warton and Silverdale area. Cave and Karst Science, 42(3): 144-147.
Obermaier, M., Ritzmann, N. & Aigner, T. 2015. Multi-level stratigraphic heterogeneities in a Triassic shoal grainstone. Oman mountains, Sultanate of Oman: layer-cake or shingles? GeoArabia, 20(2): 115-142.
Parra-Garcia, M., Sanchez, G., Dentith, M.C. & George, A.D. 2014. Regional structural and stratigraphic study of the Canning Basin, Western Australia. Geological Survey of Western Australia, Report 140, 215pp.
Photiades, A., Pomoni-Papaioannou, F.A. & Kostopoulou, V. 2010. Correlation of Late Triassic and Early Jurassic Lofer-type carbonates from the Peloponnesus Peninsula, Greece. Bulletin of the Geological Society of Greece, 43(2): 726-736.
Rashidi, K. & Saberzadeh, B. 2015. The Upper Triassic sphinctozoan sponges of the Howz-e-khan Member of the Nayband Formation, southwest of Naybandan, east central Iran. Geosciences, 24(94): 173-182. (Geological Survey of Iran: ISSN 1023-7429).
Schmieder, M., Schwarz, W.H., Trieloff, M., Tohver, E., Buchner, E., Hopp, J. & Osinski, G.R. 2015. New ^{40}Ar/^{39}Ar dating of the Clearwater Lake impact structures (Québec, Canada) – not the binary asteroid impact it seems? Geochimica et Cosmochimica Acta, 148: 304-324.
Schoch, R.R. & Sues, H.-D. 2015. A Middle Triassic stem-turtle and the evolution of the turtle body plan. Nature, 523: 584-587.
Seidel, E., Meschede, M. & Obst, K. 2013. Distribution of Triassic sediments in the Baltic Sea east of Ruegen Island based on reprocessed Petrobaltic seismic data. Schriftenreihe der Deutschen Gesellschaft für Geowissenschaften, 82: 99.
Sha Shao-li, Liu Xue-long, Zhao Chang-juan & Zhang Na. 2013. The subdivision and correlation of the Triassic strata in northwest Yunnan. Journal of Stratigraphy, 37(3): 343-348.
Sheikholeslami, M.R. 2015. The effects of Mid-Cimmerian event in north east of Iran. Geosciences, 24(94): pp? (Geological Survey of Iran: ISSN 1023-7429).
Tabibi, S.N., Asilian Mahabadi, H., Movahed, B. & Haji Hosseinloo, H. 2012. Reservoir evaluation of the Kangan Formation based on petrophysical and petrographic studies in one of Persian Gulf fields. Iranian Journal of Petroleum Geology, 3(3): 136-154.
Tian Yang, Xie Guogang, Wang Lingzhan, Tu Bing, Zhao Xiaoming & Zeng Bufo. 2015. Provenance and tectonic settings of Triassic Xujiahe Formation in Qiyueshan area, southwest Hubei: evidences from petrology, geochemistry and zircon U-Pb ages of clastic rocks. Earth Science – Journal of China University of Geosciences, 2015(12): 2021-2036.
Tohver, E., Lana, C. and 9 others. 2012. Geochronological constraints on the age of a Permo-Triassic impact event: U-Pb and ^{40}Ar/^{39}Ar results from the 40 km Araguainha structure in central Brazil. Geochimica et Cosmochimica Acta, 86: 214-227.
Tong Jinnan & Yin Hongfu. 2015. Triassic chronostratigraphy and Chinese stages. Earth Science – Journal of China University of Geosciences, 2015(2): 289-197.
Wang Jian-xin, Kang Kong-yue & Hou Ming-cai. 2014. Sedimentary facies and provenance analysis of Upper Triassic Goulushankecuo Formation in Tuotuohe area of Qinghai Province. Northwestern Geology, 47(4)2014: 123-130.
Whidden, K.J., Dumoulin, J.A., Whalen, M.T., Hutton, E., Moore, T.E. & Gaswirth, S.B. 2014. Distal facies variability within the Upper Triassic part of the Otuk Formation in northern Alaska. SEPM Special Publications, 105: 384-405.
Wilson, P., Elliott, G.M., Gawthorpe, R.L., Jackson, C.A.-L., Michelsen, L. & Sharp, I.R. 2015. Lateral variation in structural style along an evaporite-influenced rift fault system in the Halten Terrace, Norway: influence of basement structure and evaporite facies. Journal of Structural Geology, 79: 110-123.
Wolf, M., Kaufmann, D., Bebiolka, A.-C., Weitkamp, A. & Jähne, F. 2013. From Data to Model: a workflow for 3D facies-modelling using the example of the Buntsandstein in the central German North Sea sector. Schriftenreihe der Deutschen Gesellschaft für Geowissenschaften, 82: 115.
Wolf, M., Steuer, S., Röhling, H.-G., Rebscher, D. & Jähne-Klingberg, F. 2015. Lithofacies distribution in the Central European Basin: a 3D model of the Buntsandstein facies in the central German North Sea. Zeitschrift der Deutschen Gesellschaft für Geowissenschaften, 166(4): 341-359.
Wu Songtao, Zou Caineng, Zhu Rukai, Yuan Xuanjun, Yao Jingli, Yang Zhi, Sun Liang & Bai Bin. 2015. Reservoir quality characterization of Upper Triassic Chang 7 shale in Ordos Basin. Earth Science – Journal of China University of Geosciences, 2015(11): 1810-1823.
Xiong Lin-fang, Liu Chi-yang, Wang Jian-qiang & Zhang Dong-dong. 2015. Depositional sequence of the Triassic Yanchang Formation in the Ordos Basin. Journal of Stratigraphy, 39(3): 345-350.
Yin Chao, Hao Wei-cheng, Ji Cheng, Jiang Da-yong & Sun Zuo-yu. 2014. The Panxian and Luoping faunas: implications for the Triassic recovery from end-Permian mass extinction. Journal of Stratigraphy, 38(3): 328-335.
Yu Cong, Yao Hua-Zhou, Zhao Xiao-Ming & Yang Zhen-Qiang. 2015. Carbonate microfacies in strata near the Permian-Triassic boundary and the volcanic activity evidence in the early Triassic of Lichuan area, western Hubei Province. Journal of Geology and Mineral Resources of South China, 2015(2): 115-124.
Zhang Chengfeng, L(U) Hongbo, Xia Bangdong & Fang Zhong. 2011. Markov Chain simulation on the rhythmic sequences of Middle Triassic flysch in Nanpanjiang Basin, SW China. Geological Review, 57(5): 632-640.

Zhang Lijun, Zhao Zhao & Gong Yiming. 2015. Trace fossils as a proxy of the Big 5 biotic and environmental events in the Phanerozoic. Earth Science – Journal of China University of Geosciences, 2015(2): 381-396.

Zhang Xi, Sun Wei, Ren Dazhong, Qu Xuefeng & Lei Qihong. 2015. The feature of ultra low permeability reservoir and the types of the microscopic pore structure – taken Chang-6 oil-bearing formation in Jiyuan oilfield of Ordos Basin as an example. Geological Review, 61(5): 1192-1198.

Zheng Zhongwen, Liu Jianchao & Li Rongxi. 2015. Controls on oil accumulation in sandstone beds with low permeability by micro-structure: example from the western area of Fengfuchuan oilfield in northern Shaanxi. Northwestern Geology, 48(4)2015: 234-242.

Zheng Zhong-wen & Wu Yan-jun. 2014. Study on sedimentary and evolution characteristics of the Yanchang Formation in western exploratory area of Fengfuchuan oilfield in Ordos Basin. Northwestern Geology, 47(3)2014: 110-120.

Zhou Min, Fu Wan-lu, Zhang Chao, Ni Pei-gang & Ji Cheng. 2015. Geological significance of the fish-bearing concretions near the Smithian-Spathian boundary, Olenekian, Early Triassic. Journal of Stratigraphy, 39(4): 395-402.

Zhou Zuomin, Xia Caifu, Xu Qian & Gao Dafei. 2011. Geological and geochemical characteristics of Middle Triassic syenite-granite suite in Hainan Island and its geotectonic implications. Geological Review, 57(4): 515-531.

Zhu Xiaomin, Liu Fen, Zhu Shifa, Xu Liming, Niu Xiaobing & Liang Xiaowei. 2015. On the tectonic property of the provenance area of the Upper Triassic Yanchang Formation in Longdong area, Ordos Basin. Geological Bulletin of China Universities, 18(3): 416-425.

Zwenger, W. & Koszinski, A. 2009. Die lithostratigraphische gliederung des Unteren Muschelkalks von Rüdersdorf bei Berlin (Mittlere Trias, Anisian). Brandenburgische Geowissenschaftlichen Beitrage, 16(1/2): 29-53.

Research Article

A CANDIDATE GSSP FOR THE BASE OF THE ANISIAN FROM KÇIRA, ALBANIA

Giovanni Muttoni[1]*, Alda Nicora[1], Marco Balini[1], Miriam Katz[2], Morgan Schaller[2], Dennis V. Kent[3], Matteo Maron[1], Selam Meço[4], Roberto Rettori[5], Viktor Doda[6], and Shaquir Nazaj[4]

[1]*Dipartimento di Scienze della Terra 'Ardito Desio', via Mangiagalli 34, 20133 Milan, Italy.*
[2]*Department of Earth and Environmental Sciences, Rensselaer Polytechnic Institute, Troy, New York, 12180, USA.*
[3]*Earth and Planetary Sciences, Rutgers University, Piscataway, New Jersey, USA and Paleomagnetics Lab, Lamont-Doherty Earth Observatory, Palisades New York 10964, USA.*
[4]*Faculty of Geology and Mining, Tiranë, Albania.*
[5]*Dipartimento di Scienze della Terra, Piazza Università, 06100 Perugia, Italy.*
[6]*Albanian Geological Survey, Myslym Keta, Tiranë, Albania.*

*Corresponding author, *Email: giovanni.muttoni1@unimi.it*

Abstract– We present a summary of previously published Olenekian–Anisian boundary magnetostratigraphic and biostratigraphic results from the Kçira area of northern Albania. We focus on the stratigraphically complete Kçira-A section that represents a potential candidate Global Boundary Stratotype Section and Point (GSSP) for the base of the Anisian Stage of the Triassic System. The previously published conodont biostratigraphy from Kçira-A and ancillary sections located nearby has been updated using modern taxonomic criteria and correlated to the available ammonoid and benthic foraminifera biostratigraphy. Previously published magnetobiostratigraphic data reveal the occurrence at Kçira-A, and ancillary sections, of a well-defined magnetic polarity reversal pattern of primary origin that allows global correlations ensuring the exportability of biostratigraphic datums (e.g., the first occurrence of conodont *Chiosella timorensis*) falling close to the Kclr/Kc2n polarity transition. A suite of pilot samples has also been studied for bulk carbon and oxygen isotopes stratigraphy, yielding reasonable values that suggest good preservation of primary material. These data indicate that with additional studies, Kçira-A would represent an ideal base Anisian GSSP.

INTRODUCTION

Arthaber (1911) and Nopcsa (1929) first described an Early Triassic ammonoid fauna within a reddish nodular limestone succession from the Kçira area of northern Albania. In this area, Muttoni et al. (1996) reported a detailed magnetostratigraphic record of an Olenekian/Anisian boundary section termed Kçira-A that was correlated to the vertical distribution of key conodonts (figured by Meço, 2010 and reported also below), ammonoids, and benthic foraminifera species. Ancillary sections from the same nodular limestone unit were also studied for magneto-biostratigraphy (Kçira-B) and magnetostratigraphy (Kçira-C), and were correlated to the reference Kçira-A section. Ammonoids from Kçira-A and a further ancillary section (Kçira-G) were appraised by Germani (1997). A geologic map of the Kçira area (Muttoni et al., 1996) was recently augmented by additional biostratigraphic and tectonic observations and data (Gawlick et al., 2008, 2014, 2016), which complements geologic studies of Albania (Meço, 2000 and references therein). These studies reveal that the thicker and stratigraphically more complete Kçira-A section has excellent potential as a candidate Global Boundary Stratotype Section and Point (GSSP) for the base of the Anisian Stage of the Triassic System. In this paper, we summarize key magneto-biostratigraphy aspects of Kçira-A and ancillary sections,

Published online: August 2, 2019

Muttoni, G., Nicora, A., Balini, M., Katz, M., Schaller, M., Kent, D., Maron, M., Meço, S., Rettori, R., Doda, V., & Nazaj, S.. 2019. A candidate GSSP for the base of the Anisian from Kçira, Albania. *Albertiana*, vol. 45, 39–49.

describe new carbon and oxygen isotope results, and discuss future developments aimed at formally proposing Kçira-A as candidate Anisian GSSP.

GEOLOGY AND LITHOSTRATIGRAPHY

Kçira is located in northern Albania about 130 km (2.5 hours by car) north of Tirana. This area is characterized by a complex mélange of blocks, ranging in size from a few meters to some kilometers, comprised of Early to Late Triassic limestones, Triassic volcanics, and Triassic radiolarites, embedded in a thick Bathonian–Callovian (Jurassic) radiolaritic-ophiolitic unit (Fig. 1A) (Gawlick et al., 2008, 2014, 2016; Gaetani et al., 2015). The Kçira-A section crops out to the northwest of the new Kçira village (Fig. 1A, B, C), together with additional ancillary sections described in this study, that have been correlated by means of lithostratigraphy, magnetostratigraphy, and biostratigraphy (Fig. 2) as discussed below. These sections are part of an Olenekian–Anisian nodular limestone belt that probably formed as a single slab prior to being embedded into the Jurassic radiolaritic-ophiolitic unit. This tectonic mélange is part of the Kçira-Dushi-Komani radiolaritic flysch (ophiolitic Mélange) at the sole of the Mirdita Zone ophiolites (Gaetani et al., 2015; Gawlick et al., 2016 and references therein).

The Kçira-A (main) section is about 42 m thick, whereas the ancillary Kçira-B section, located a few meters away within the same outcrop, is about 4.5 m thick. On the basis of magnetostratigraphic correlation, projected layers of Kçira-B partially overlap with the basal portion of Kçira-A (Fig. 2). As reported in Muttoni et al. (1996), both sections are comprised of reddish to pale pink wackestones and mudstones arranged in cm thick nodular beds that are strongly amalgamated to form meter-scale composite layers. These limestones were termed the Han-Bulog Limestone by Muttoni et al. (1996), but red nodular limestones of the Bulog Formation in southwest Serbia are Anisian in age and developed on top of a drowned Middle Anisian (Pelsonian) shallow-water carbonate ramp (Sudar et al., 2013). Therefore, as proposed by Gawlick et al. (2014), the Olenekian–Anisian red nodular limestones of Kçira (rosenrot Knollenkalk of Nopcsa, 1929 equivalent to the Han-Bulog Limestone of Muttoni et al., 1996) should not be termed Bulog (or Hallstatt, or Han-Bulog) Limestone, at least in the Olenekian section. We

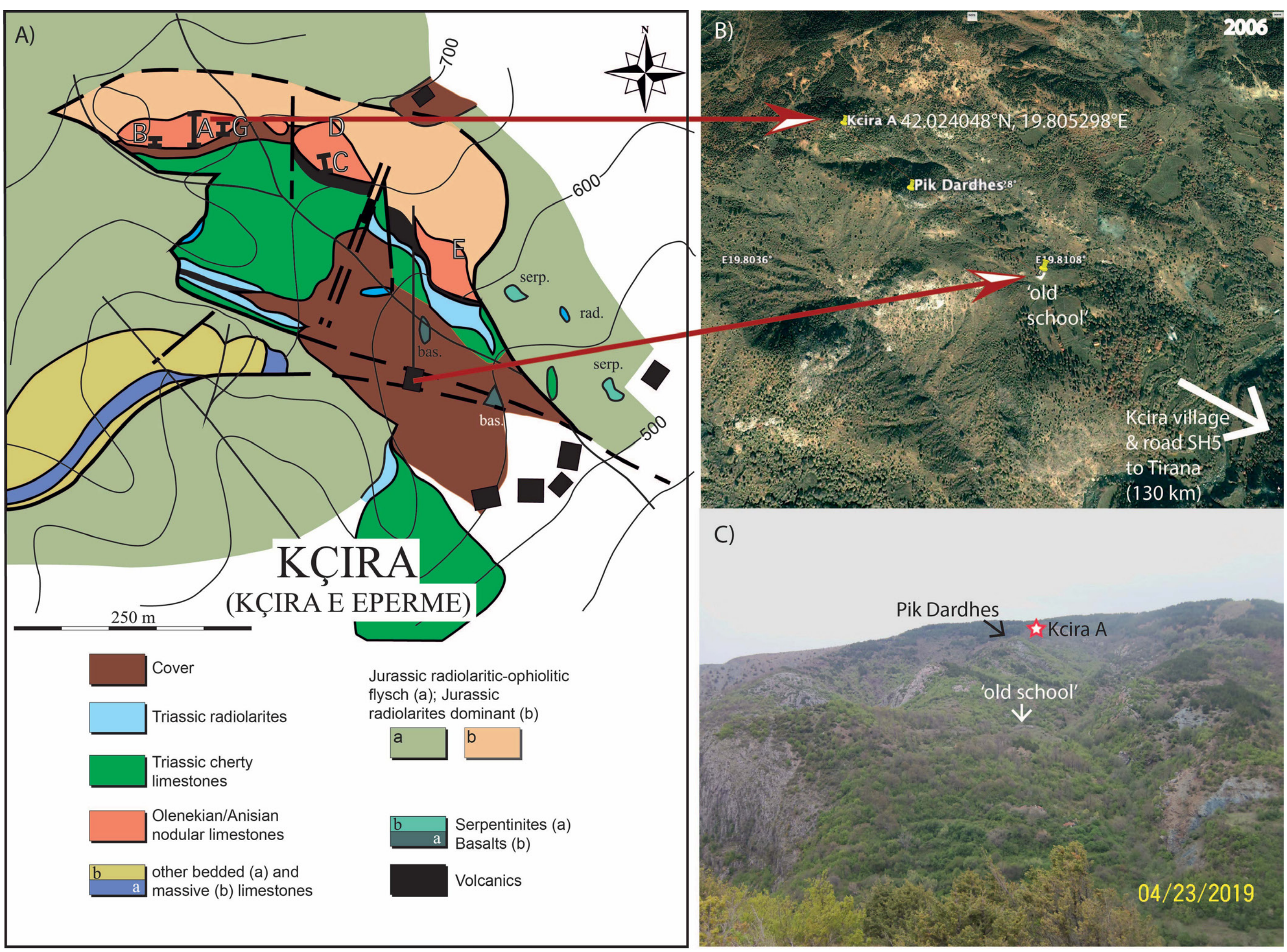

Figure 1 – *A*, Geological map of the Kçira area (modified after Muttoni et al., 1996 using data from Gawlick et al., 2014). 'A', 'B', 'C', 'G' are sections Kçira-A, Kçira-B, Kçira-C, and Kçira-G; 'D' and 'E' are additional sites of paleontological or lithological interest described in Muttoni et al. (1996). *B*, Aerial view and *C*, picture of the Kçira area with location of conspicuous points and the Kçira-A GSSP candidate.

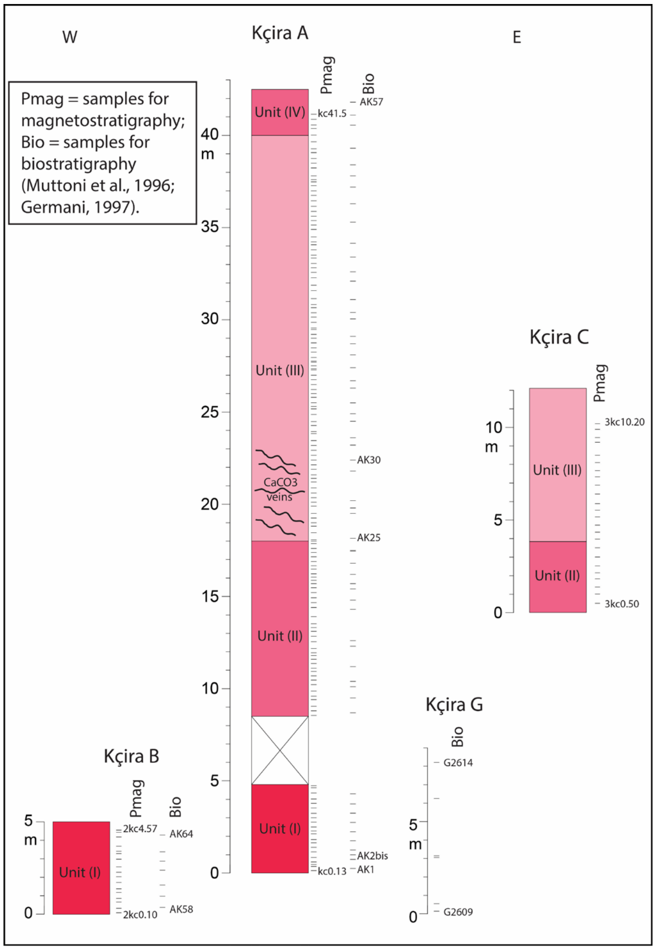

Figure 2 – Main lithological units of the correlated Kçira sections discussed in the text with position of paleomagnetic (Pmag) and biostratigraphic (Bio) samples after Muttoni et al. (1996) and Germani (1997).

provisionally and informally refer to these Olenekian–Anisian limestones as nodular limestones of Kçira.

The basal 4.8 m of nodular limestones at Kçira-A (as well as the entire Kçira-B) are reddish and clay-rich, with pervasive bedding-parallel stylolites (lithologic Unit I, Fig. 2). Above a cover extending up to meter level 8.5, amalgamated nodular limestones become pink (Unit II) and then pale pink (Unit III) (Fig. 2). A set of cm thick calcite veins cut the bedding between meter 18 and 23 at Kçira-A. The uppermost few meters of Kçira-A contain packstones, which are more pink, richer in bioclasts, and are more distinctly bedded (Unit IV, Fig. 2). The top of the Kçira nodular limestone is marked by small neptunian dikes sealed by a cm thick silicified crust of uncertain age, as observed at site D (Fig. 1A).

The Kçira-C section is 10.2 m thick and located about 100 m east of Kçira-A and Kçira-B (Fig. 1A). Although a detailed lithological description was not made for Kçira-C, an upsection decrease in red pigmentation to pink closely resembles that observed at Kçira-A (Fig. 2), which provides a first order means of lithological correlation (Muttoni et al., 1996). Kçira-G is located in between Kçira-A and Kçira-C (Fig. 1A), but no lithological description is provided (Germani, 1997). Based on projected layers, Kçira-G should correspond to the basal Kçira-A as well as the entire Kçira-B sections (Fig. 2).

Two sections were previously studied for magnetostratigraphy and biostratigraphy (Kçira-A and Kçira-B; Muttoni et al., 1996), Kçira-C only for magnetostratigraphy (Muttoni et al., 1996), and Kçira-G only for biostratigraphy (Germani, 1997). The Kçira-A and Kçira sections are most likely the localities described by Nopcsa (1929). Bedding attitude (azimuth of dip/dip) varies from 347°E/34° at Kçira-A to 12°E/45°E at Kçira-B and Kçira-C.

BIOSTRATIGRAPHY

Conodonts

Conodonts from Kçira-A and Kçira-B sections originally reported by Muttoni et al. (1996) have been revised in this study according to recent advances in conodont taxonomy. Some conodont species of Muttoni et al. (1996) were later illustrated by Meço (2010) and are reported in Figure 3. The conodont fauna from these sections is abundant and well preserved. The CAI (Color Alteration Index, Epstein et al., 1977) is 3, indicating that the host rock reached burial temperatures of 110°–200°C. The conodont main events are grouped as follows from the base to the top (Fig. 4; see also key species in Fig. 3):

1. The conodont association from lithologic Units I and II is represented by *Triassospathodus abruptus* Orchard, 1995, *T. triangularis* (Bender, 1970), *Spathicuspus spathi* (Sweet, 1970), *T. homeri* (Bender, 1970), *Gladigondolella carinata* Bender, 1970, *T. symmetricus* (Orchard, 1995), *T. brochus* (Orchard, 1995), *Neogondolella* sp., *N.* sp. A, *Triassospathodus* sp., and *Gladigondolella tethydis* (Huckreide, 1958). This fauna is mostly consistent with fauna 3 of Orchard (1995) and with the fauna described in the lower part of the Deşli Caira section (North Dobrugea, Romania) by Gradinaru et al. (2007) and Orchard et al. (2007a), as well as in the Lower Guandao section (Guizhou Province, China) by Orchard et al. (2007b). These faunas are altogether attributed to the late mid Spathian.

2. The appearance of *Chiosella gondolelloides* (Bender, 1970) (sample AK28, 20.2 m) is an easily recognized datum that predates the occurrence of *C. timorensis* (Nogami,1968; AK30, 22.4 m). This is in broad agreement with data from Chios (Gaetani et al., 1992; Muttoni et al., 1995), Deşli Caira (Gradinaru et al., 2007; Orchard et al., 2007a) and Lower and Upper Guandao (Orchard et al., 2007b). The appearance of *Chiosella timorensis* (=*Gondolella timorensis* in Gaetani et al., 1992; Muttoni et al., 1995) may be used to approximate the base of the Anisian (Gradinaru et al., 2006, 2007; Orchard et al., 2007a, 2007b) especially when ammonoids are absent. Orchard (1995), Gradinaru et al. (2007), Orchard et al. (2007a, 2007b) have well summarized and described the taxonomy of these species.

3. *Neogondolella regalis* Mosher, 1970 appears at 26.7 m (AK37) and is interpreted to span the late Aegean and mid Bithynian (Mosher, 1970; Gedik, 1975; Nicora, 1977; Kovacs & Kozur, 1980).

4. *Paragondolella bulgarica* Budurov and Stefanov (1975) appears at 28.7 m (AK40) and is a proxy for the base of the Bithynian substage. It ranges up to the boundary interval of the *Binodosus* and *Trinodosus* ammonoid Zones (Budurov & Stefanov, 1972, 1975; Gedik, 1975; Nicora, 1977; Kovacs & Kozur, 1980; Balini & Nicora, 1998; Farabegoli & Perri, 1998; Kovacs & Ralisch-Felgenhauer, 2005; Balini et al., 2019).

5. Nicoraella kokaeli (Tatge, 1956) appears at 35.3m (AK49) and approximates the base of the Pelsonian substage (Nicora, 1977; Kovacs & Kozur, 1980; Balini & Nicora, 1998; Farabegoli & Perri, 1998).

6. Paragondolella bifurcata bifurcata (Budurov and Stefanov, 1972) appears at 33.4 m (AK47) while *P. bifurcata hunbuloghi* Sudar and Budurov, 1979 appears at 35.3 m (AK49). These species are attributed to the Pelsonian substage (Budurov & Stefanov, 1972, 1975; Sudar & Budurov, 1979; Kovacs & Kozur, 1980; Balini & Nicora, 1998; Kovacs & Ralisch-Felgenhauer, 2005).

Based on the conodont fauna, the Kçira-A section covers the late mid Spathian to Pelsonian while Kçira-B section is restricted to the late mid Spathian.

Ammonoids

The lower part of the Kçira-A section (Unit I of Figs. 2–4) is rich in ammonoids. From this part of the section, Germani (1997) described a small fauna with high diversity that is middle Spathian (*Subcolumbites* Zone sensu Guex et al., 2010

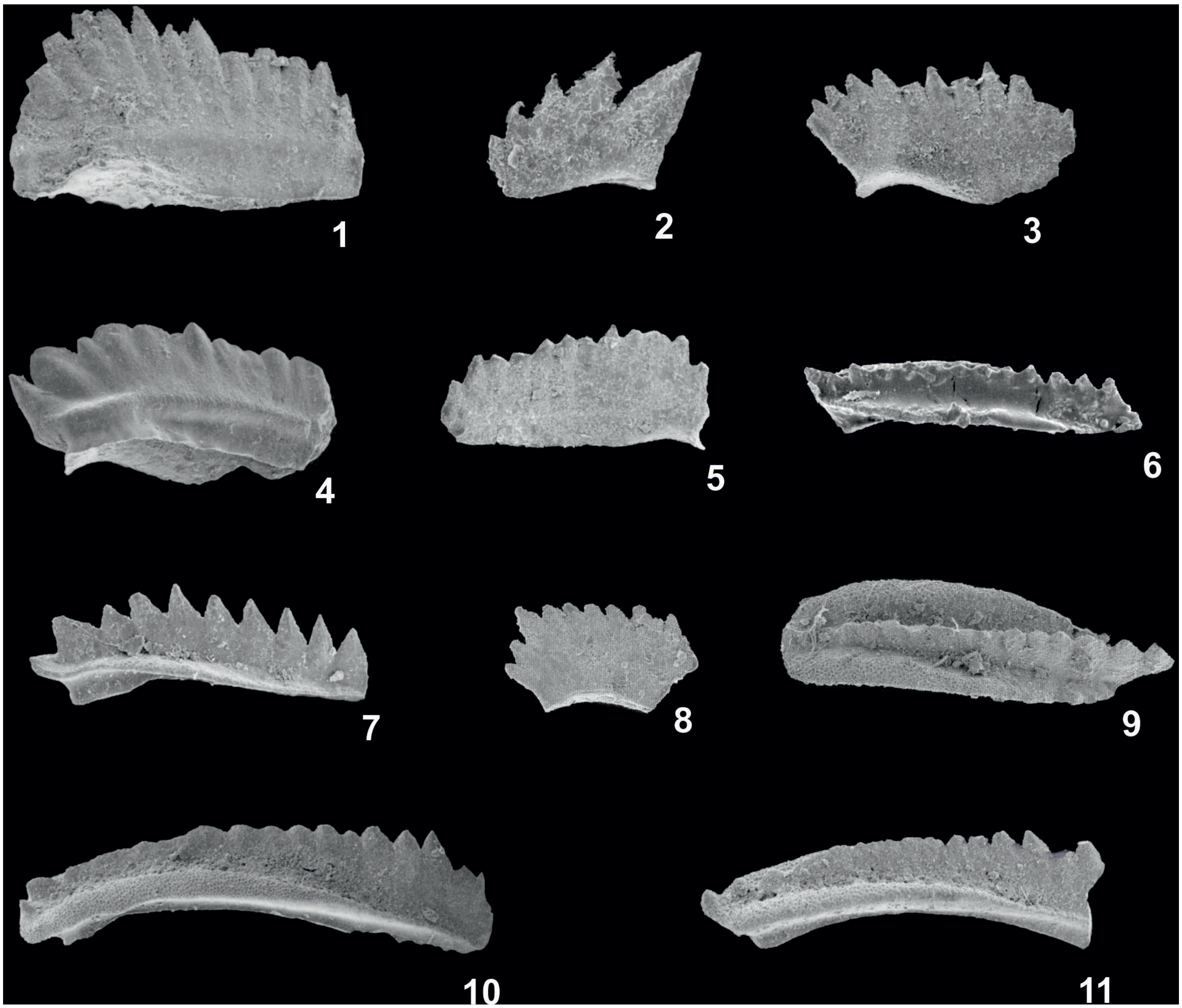

Figure 3 – Conodonts from Kçira-A and Kçira-B of Muttoni et al. (1996), figured in Meço (2010), and taxonomically updated in this study. (1) *Triassospathodus abruptus* Orchard, 1995, lateral view, Kçira-B, sample AK62, x 70. (2) *Spathicuspus spathi* (Sweet, 1970), lateral view, Kçira-A, sample AK13, x 120. (3) *Triassospathodus homeri* (Bender, 1970), lateral view, Kçira-A, sample AK8, x 80. (4) *Chiosella timorensis* (Bender, 1970), lateral view, Kçira-A, sample AK31, x 82. (5) *Chiosella gondolelloides* (Bender, 1970), lateral view, Kçira-A, sample AK35, x 90. (6) *Neogondolella regalis* Mosher, 1970, oblique-upper view, Kçira-A, sample AK37, x 100. (7) *Paragondolella bulgarica* (Budurov & Stefanov, 1972), juvenile stage, lateral view, Kçira-A, sample AK42, x 110. (8) *Nicoraella kokaeli* (Tatge, 1956), lateral view, Kçira-A, sample AK55, x 105. (9) *Paragondolella bifurcata hunbuloghi* (Sudar and Budurov,1979), oblique-upper view, Kçira-A, sample AK52, x 80. (10) *Paragondolella bifurcata bifurcata* (Budurov and Stefanov, 1972), lateral view, Kçira-A, sample AK48, x 80. (11) *Paragondolella bifurcata bifurcata* Budurov & Stefanov, 1972, lateral view, Kçira-A, sample AK48, x 80.

and Jenks et al., 2013). This fauna (Fig. 5) is dominated by *Subcolumbites* and *Albanites*, in addition to leiostraceans, and is almost equivalent to the fauna described from Kçira by Arthaber (1911). Ammonoid assemblages also indicate middle Spathian at Kçira-B and Kçira-G (Germani, 1997). Ammonoids also are reported from the middle and upper part of the Kçira-A section (Germani, 1997) in Units III and IV (Fig. 5), but they are long-ranging leiostracean that verify the presence of Anisian strata, but thus far a more refined age assignment is not possible.

Benthic Foraminifera

As outlined in Muttoni et al. (1996), benthic foraminifera are very scarce in the lower part of Kçira-A (Fig. 5). *Gaudryina*? n. sp. is discontinuously present from meter 14.3 (AK17) to 22.4 (AK30), where *Meandrospira dieneri*? appears. A more diversified and abundant fauna was recovered from meter 28.1 to 34.2 at Kçira-A (samples AK39 to AK48). This assemblage is characterized by *Ophtalmidium* aff. *O. abriolense*, *Arenovidalina chialingchiangensis, Pilammina densa*, *Meandrospira dinarica*, *Earlandia amplimuralis* and *E. gracilis*. An Anisian age not younger than Pelsonian is attributed to this assemblage. It is noteworthy that *P. densa* occurs in association with conodonts of Bithynian age.

PALEOMAGNETISM

Paleomagnetic properties

Samples for paleomagnetic analyses were collected with a portable water-cooled rock drill and oriented with a magnetic compass. Sections Kçira-A and Kçira-B were sampled at an average interval of 20–25 cm, while sampling at 40–50 cm was applied at Kçira-C (Fig. 6; Muttoni et al., 1996). Based on standard rock-magnetic experiments, Muttoni et al. (1996) concluded that nodular layers of the lower half of Kçira-A (Units I–II), as well as of Unit I of Kçira-B, were characterized by abundant hematite, contributing to the relatively high natural remanent magnetization (NRM) (Fig. 6A) and magnetic susceptibility, as well as the pervasive reddish-pink hues typical of this part of the succession. In contrast, pale-pink nodular layers above (Unit III) preserve a mineralogical association of less abundant magnetite coexisting with hematite, giving lower NRM and magnetic susceptibility, although the lowest values between meter 18 and 23 at Kçira-A are also associated with a dense network of calcite veins (Fig. 6A). The top of Unit III has a few samples with very high NRM intesities and univectorial component trajectories during thermal demagnetization that are interpreted as due to lightning-induced IRM (Isothermal remanent magnetization), whereas the uppermost few meters of the Kçira succession (Unit IV) are richer in resedimented carbonate layers that might have enhanced the concentration of detrital magnetite (see Muttoni et al., 1996 for details).

Upon application of thermal demagnetization, a characteristic (Ch) component with either northeast-and-down or southwest-and-up directions was resolved in 88% of the samples in the temperature range between about 400°C and either 520–575°C or 650–680°C (Fig. 7A). These Ch component directions display variable mean angular deviation (MAD; Fig. 6B) values depending on NRM intensities (Fig. 6A). They show dual polarity at all investigated sections (Fig. 7B), albeit the normal and reverse mean polarity directions depart from antipodality by up to 27°, perhaps due to contamination of the Ch magnetizations by an initial viscous component broadly aligned along the present-day field direction (Fig. 7A). The three mean directions from Kçira-A, Kçira-B, and Kçira-C (Fig. 7B) show some degree of convergence after correction for bedding tilt, the Fisher precision parameter k increasing by a factor of 3 with a full (100%) tilt correction, suggesting that the Ch magnetizations were acquired before deformation. However, the limited difference in bedding attitudes makes the fold test statistically inconclusive (see Muttoni et al., 1996 for details).

Magnetostratigraphy and correlations with sections from the literature

A virtual geomagnetic pole (VGP) was calculated for each sample Ch component direction after correction for bedding tilt. The latitude of the sample VGP with respect to the overall mean (north) paleomagnetic pole (i.e. VGP latitude) was used to delineate the magnetic polarity stratigraphy (Fig. 6C, D). At Kçira-A, the VGP latitudes define a sequence of polarity intervals extending from Kc1n.1n at the base to Kc3r at the top. Submagnetozone Kc1n.1r near the base of Kçira-A nicely correlates to the short reverse polarity interval at Kçira-B, lending credibility to this single sample-based reversal. Finally, the magnetic polarity stratigraphy at Kçira-C shows an excellent match with Kçira-A across multiple polarity reversals in the Kc1r interval (Fig. 6), which also contain several biostratigraphic events potentially useful to define the base of the Anisian.

According to the recent Triassic geomagnetic polarity scale of Maron et al. (2019), the magnetostratigraphic sequence of Kçira-A correlates reasonably well with the Lower and Upper Guandao (Lehrmann et al., 2015), Chios (Muttoni et al., 1995), and Desli Caira (Gradinaru et al., 2007) sections (see Figures 11 and 12 in Maron et al., 2019). According to this correlation scheme that incorporates U-Pb age data from Guandao (Lehrmann et al., 2015), Kçira-A should extend from approximately 248 to 244 Ma, and the level containing the appearance of *Chiosella timorensis* should have an interpolated age of ~247.3 Ma (Lehrmann et al., 2015; see also Maron et al., 2019).

CHEMOSTRATIGRAPHY

Carbon isotope stratigraphy provides additional means to correlate among marine sections, and under the right circumstances (and with the independent magnetostratigraphic constraints above) can allow correlation between terrestrial and marine sections (see review by Salzman & Thomas, 2012). The $\delta^{13}C_{carb}$ of bulk sedimentary carbonate can be an important tool to use in sections that lack sufficient biomagnetostratigraphy, especially in older time periods (e.g., Paleozoic, Cramer and

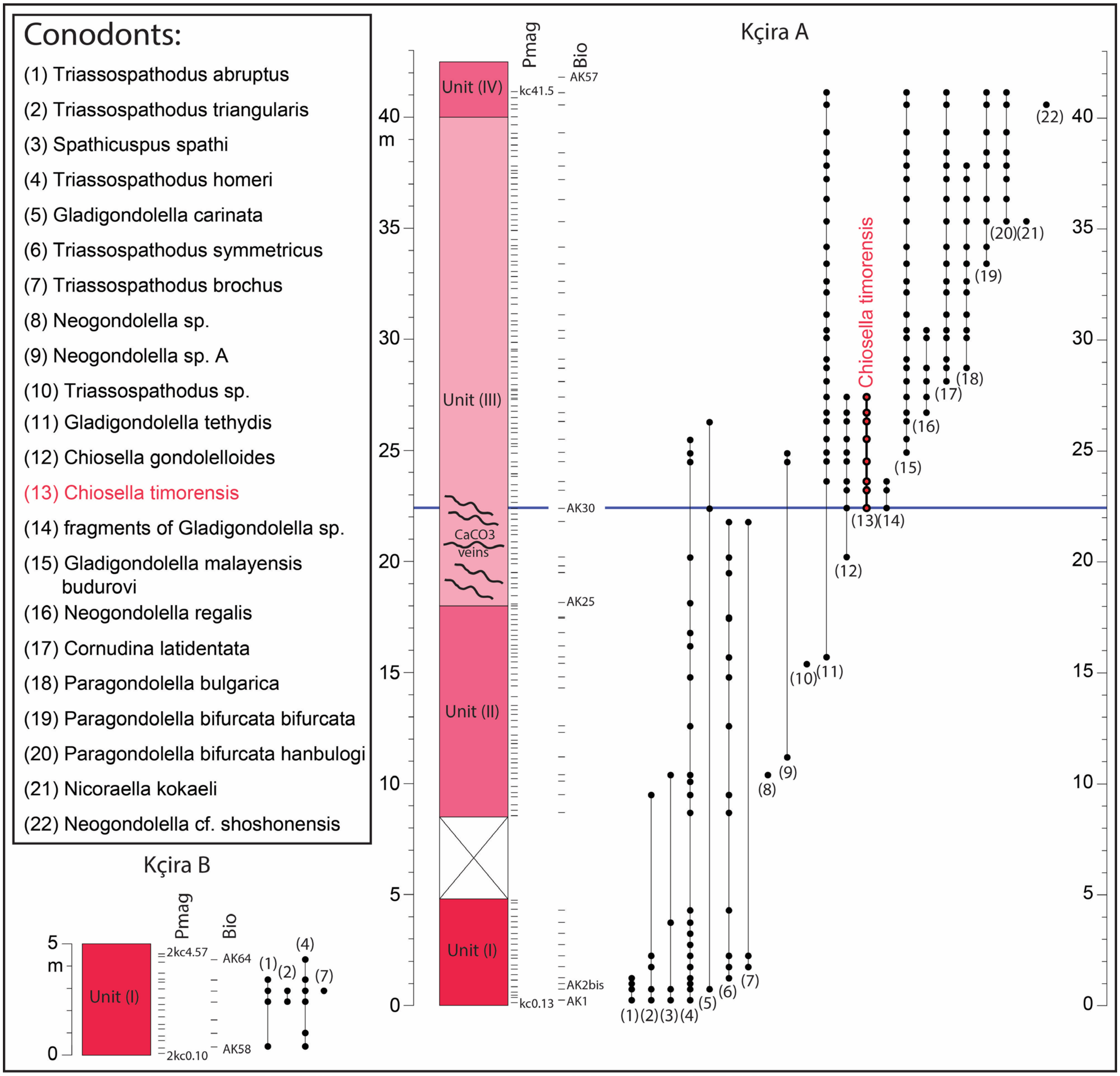

Figure 4 – Vertical distribution of conodonts from Kçira-A and Kçira-B after Muttoni et al. (1996) with taxonomic revision from this study (see also Fig. 3 for pictures of key conodonts).

Saltzmann, 2005; Middle–Late Triassic, Muttoni et al., 2014). The detailed biomagnetostratigraphic framework at Kçira will provide the necessary context to identify and constrain useful carbon isotopic events and trends associated with the base of the Anisian, which then can be used as a template for carbon isotope stratigraphy elsewhere. The Olenekian–Anisian boundary interval is known to contain carbon isotope excursions (e.g., Richoz et al., 2007) that, by virtue of their large amplitudes and global nature, represent useful markers for the base of the Anisian. Therefore, we will analyze carbon stable isotopes on bulk $CaCO_3$ from the Kçira section, and the attendant oxygen isotopes will be used as a metric of the degree of diagenetic alteration (in general, carbon isotopes of calcite are more resistant to diagenetic alteration than oxygen isotopes [Marshall, 1992]).

We conducted a pilot study of bulk carbonate stable isotopes ($\delta^{18}O$, $\delta^{13}C$) using rock samples that were prepared with a Buehler Isomet low speed saw to avoid veins. These selected samples were broken into millimeter fragments using a rock hammer, and then crushed for 15 to 20 minutes, or until completely powdered, at low speed in a Fritsch Ball Mill or an Across International HQ-NO4 Vertical Planetary Ball Mill. Between each crushing, the agate bowl (lid, rubber washer, and cup) was cleaned and rinsed thoroughly to remove any remaining powdered sample. Stable isotopes were measured on bulk sediment samples in the Stable

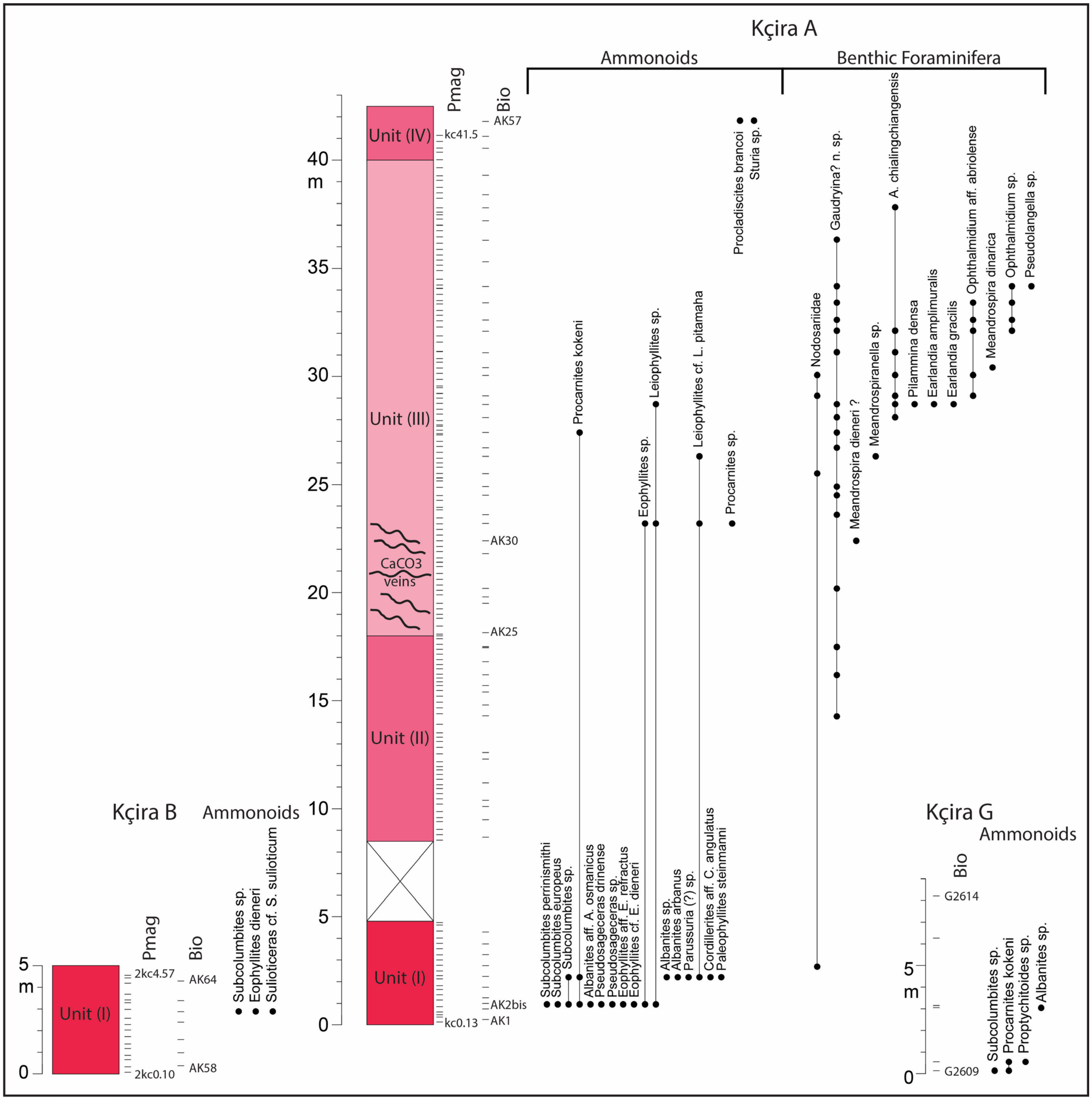

Figure 5 – Vertical distribution of ammonoids from Kçira-A, Kçira-B, and Kçira-G after Germani (1997), and of benthic foraminifera from Kçira-A after Muttoni et al. (1996).

Isotope Lab at Rutgers University using a multiprep peripheral device and analyzed on an Micromass Optima mass spectrometer. Samples were reacted in 100% phosphoric acid at 90°C for 13 min. Values are reported relative to V-PDB through the analysis of an internal standard calibrated with NBS-19 (1.95‰ for $\delta^{13}C$), as reported by Coplen (1995).

Our pilot study of bulk sedimentary $CaCO_3$ shows that Kçira-A samples yield reasonable values, and the $\delta^{18}O$ is consistent with an expected marine range (e.g., see Veizer and Prokoph, 2015), indicating good preservation of primary material (Fig. 8). In particular, the pilot bulk $\delta^{18}O$ is comparable to that of conodont bioapatite (Trotter et al. 2015) that show correlative temperature changes with pCO_2 in the Late Triassic (Knobbe and Schaller 2018). Because of the broadly similar diagenetic and tectonic histories of these sections, we can expect similar results for the Anisian. Relatively little sedimentary carbonate is produced in deep waters, and therefore bulk sediment/rock samples best characterize the average $\delta^{13}C$ of the total carbonate produced and preserved in the marine system (Shackleton, 1987).

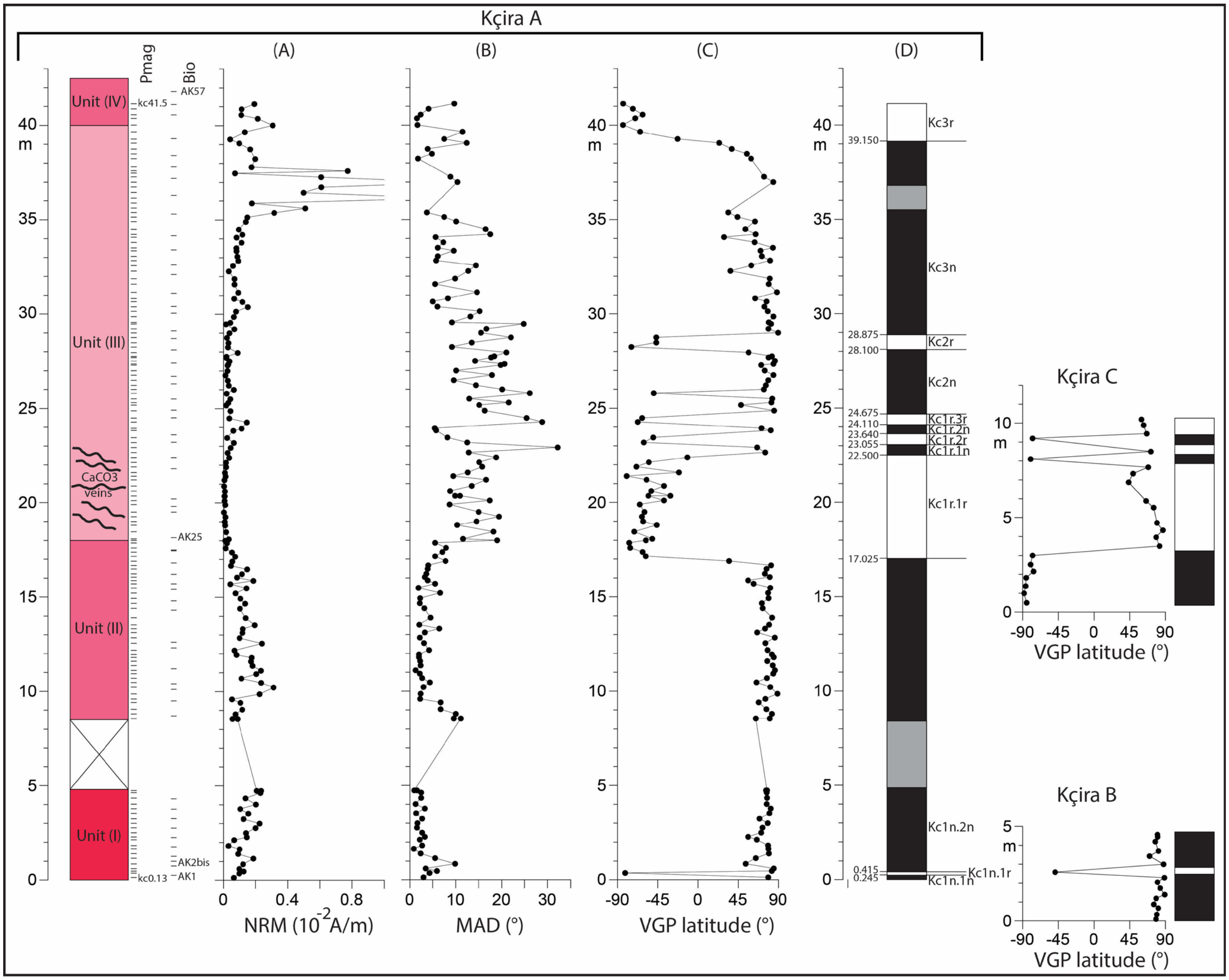

Figure 6 – Paleomagnetic properties of Kçira-A, Kçira-B, and Kçira-C samples. For Kçira-A. ***A***, Natural remanent magnetization (NRM). **B**, Mean angular deviation (MAD) of the characteristic Ch component. ***C***, Relative virtual geomagnetic pole (VGP) latitudes of the characteristic Ch component. ***D***, Magnetic polarity interpretation with filled (open) bars representing normal (reverse) polarity; single-sample polarity zones are shown by half bars. Also reported are the VGP latitudes and magnetic polarity zones of Kçira-B and Kçira-C (data from Muttoni et al., 1996).

DISCUSSION AND FUTURE DIRECTIONS

In virtue of its stratigraphic continuity, quality of magnetostratigraphic and biostratigraphic (especially conodonts) records, promising chemostratigraphic data, relatively simple accessibility (130 km by car from the capital city Tirana and near a village with accommodations and provisions), and logistics support provided by the Geological Survey of Albania, we consider Kçira-A a reliable GSSP to define the base of the Anisian. Potential events under scrutiny and critical discussion to define the base Anisian include at present both biostratigraphic and magnetostratigraphic datums (Fig. 8):

1. The FO of *Gladigondolella tethydis* at meter 15.70 (sample AK20).

2. The FO of *Chiosella timorensis* at meter 22.40 (sample AK30).

3. The last occurrence (LO) of *Gladigondolella carinata* at meter 26.30 (sample AK36), albeit this conodont has at present a very discuntinuous distribution at Kçira-A (Fig. 8).

4. The base of magnetozone Kc1r.1r at meter 17.025.

5. The base of magnetozone Kc1r.1n (= MT1n of Hounslow et al., 2007) at meter 22.50 close to the FO of *Chiosella timorensis* at meter 22.40.

6. The base of magnetozone Kc2n at meter 24.675.

Aside magnetostratigraphy that is already well-resolved (Muttoni et al., 1996), these and/or possibly other biostratigraphic events potentially useful to approximate the base of the Anisian would need to be re-assessed and better defined with additional sampling at Kçira-A to demonstrate their ability for global correlation. Dedicated sampling would also be needed to provide the section with a continuous $\delta^{13}C$ and $\delta^{18}O$ record coupled with microfacies analysis.

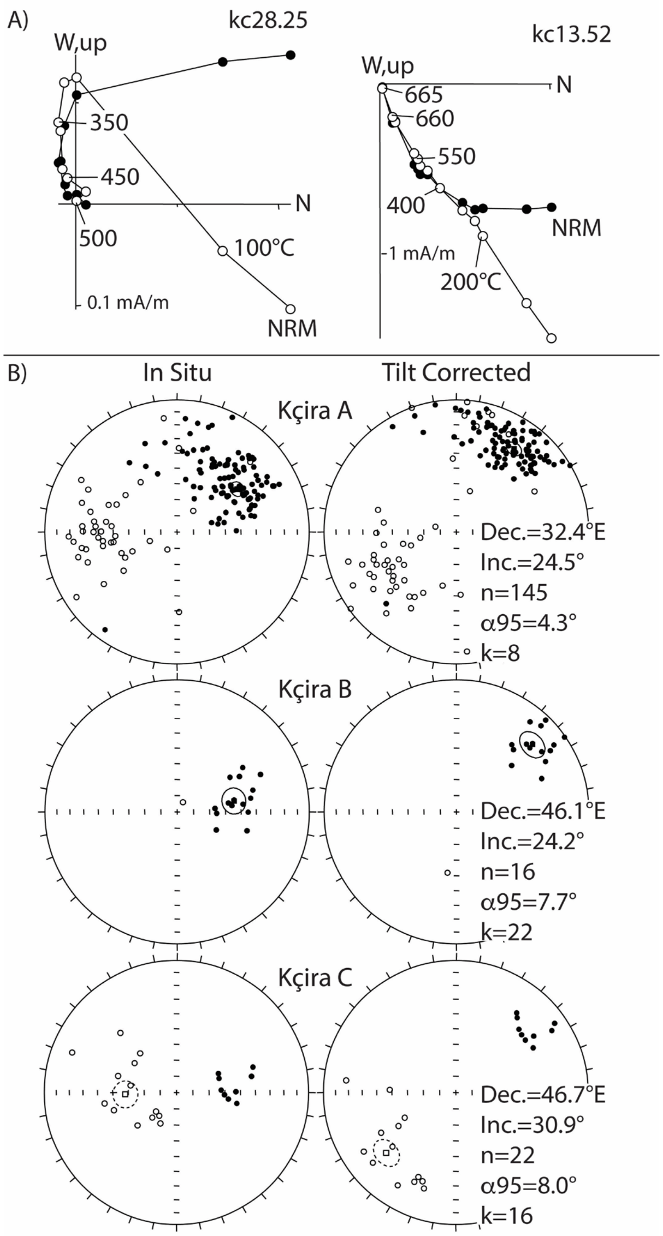

Figure 7 – Paleomagnetic properties of Kçira-A, Kçira-B, and Kçira-C samples. ***A***, Zijderveld thermal demagnetograms of representative samples from Kçira-A. Closed symbols are projections onto the horizontal plane and open symbols are projections onto the vertical plane in in situ coordinates and demagnetization temperatures are expressed in °C. ***B***, Equal-area projections before (in situ) and after bedding tilt correction of the characteristic Ch component directions from Kçira-A, Kçira-B, and Kçira-C, with associated site-mean directions calculated with standard Fisher statistics (data from Muttoni et al., 1996).

ACKNOWLEDGEMENTS

Mark Hounslow and Christopher McRoberts are thanked for comments on earlier versions of this manuscript. Digital listings of data can be made available upon request to the corresponding author.

REFERENCES

Arthaber, G. von 1911. Die Trias von Albanien. Beiträge zur Paläontologie Österreich-Ungarns, 24: 169–277.

Balini, M. & Nicora, A. 1998. Stop 3.3°: Conodonts from the Pelsonian-Illyrian Section of Dont (Zoldo Valley, Belluno). *In*, Perri M. C. & Spalletta C. (eds.), ECOS VII Southern Alps Field Trip Guidebook. Giornale di Geologia, Serie 3, 60: 260–267.

Budurov, K. & Stefanov, S. 1972. Plattform-Conodonten und ihre Zonen in der mittleren Trias Bulgariens. Mitteilungen der Gesellschaft der Geologie und Bergbaustudenten in Österreich, 21: 829–852.

Budurov, K. & Stefanov, S. 1975. Neue Daten uber die Conodonten-Chronologie der balkaniden mittleren Trias. Comptes Rendus de l'Académie Bulgare des Sciences, 28: 791–794.

Coplen, T. B. 1995. Discontinuance of SMOW and PDB. Nature, 375: 285.

Cramer, B. D., & Saltzman, M. R. 2005. Sequestration of ^{12}C in the deep ocean during the early Wenlock (Silurian) positive carbon isotope excursion. Palaeogeography, Palaeoceanography, Palaeoclimatology, 219: 333–349.

Epstein, A. G., Epstein, J. B., & Harris, L. D. 1977. Conodont color alteration: an index to organic metamorphism. U.S. Geological Survey, Professional Paper, 995, 36 pp.

Farabegoli, E. & Perri, M. C. 1998. Stop 3.3B: Middle Triassic conodonts at the Pelsonian/ Illyrian boundary of the Nosgieda section (Southern Alps, Italy). *In*, Perri M. C. & Spalletta C. (eds.), ECOS VII Southern Alps Field Trip Guidebook. Giornale di Geologia, Serie 3, 60: 268–274.

Gaetani, M., Jacobshagen, V., Nicora, A., Kauffmann, G., Tselepidis, V., Sestini, N. F., Mertmann, D. & Skourtsis-Coroneou, V. 1992. The Early-Middle Triassic boundary at Chios (Greece). Rivista Italiana di Paleontologia e Stratigrafia., 98: 181–204.

Gaetani, M., Meço, S., Rettori, R., Henderson, C. M. & Tulone, A. 2015. The Permian and Triassic in the Albanian Alps. Acta Geologica Polonica, 65(3): 271–295.

Gawlick, H.-J., Goričan, Š., Missoni, S., Dumitrica, P., Lein, R., Frisch, W. & Hoxha. L. 2016. Middle and Upper Triassic radiolarite components from the Kçira-Dushi-Komani ophiolitic mélange and their provenance (Mirdita Zone, Albania). Revue de Micropaléontologie, 59(4): 359–380.

Gawlick, H.-J., Frisch, W., Hoxha, L., Dumitrica, P., Krystyn, L., Lein, R., Missoni, S. & Schlagintweit, F. 2008. Mirdita Zone ophiolites and associated sediments in Albania reveal Neotethys Ocean origin. International Journal of Earth Sciences, 97(4): 865.

Gawlick, H., Lein, R., Missoni, S., Krystyn, L., Frisch, W. & Hoxha, L. 2014. The radiolaritic-argillaceous Kcira-Dushi-Komani sub-ophiolithic Hallstatt Mélange in the Mirdita Zone of Northern Albania. Buletini i Shkencave Gjeologjike, Spec. Issue, 4: 1–32.

Gedik, I. 1975. Die Conodonten der Trias auf der Kocaeli-Halbinsel (Türkey). Palaeontographica, 150: 99–160.

Germani, D. 1997. New data on ammonoids and biostratigraphy

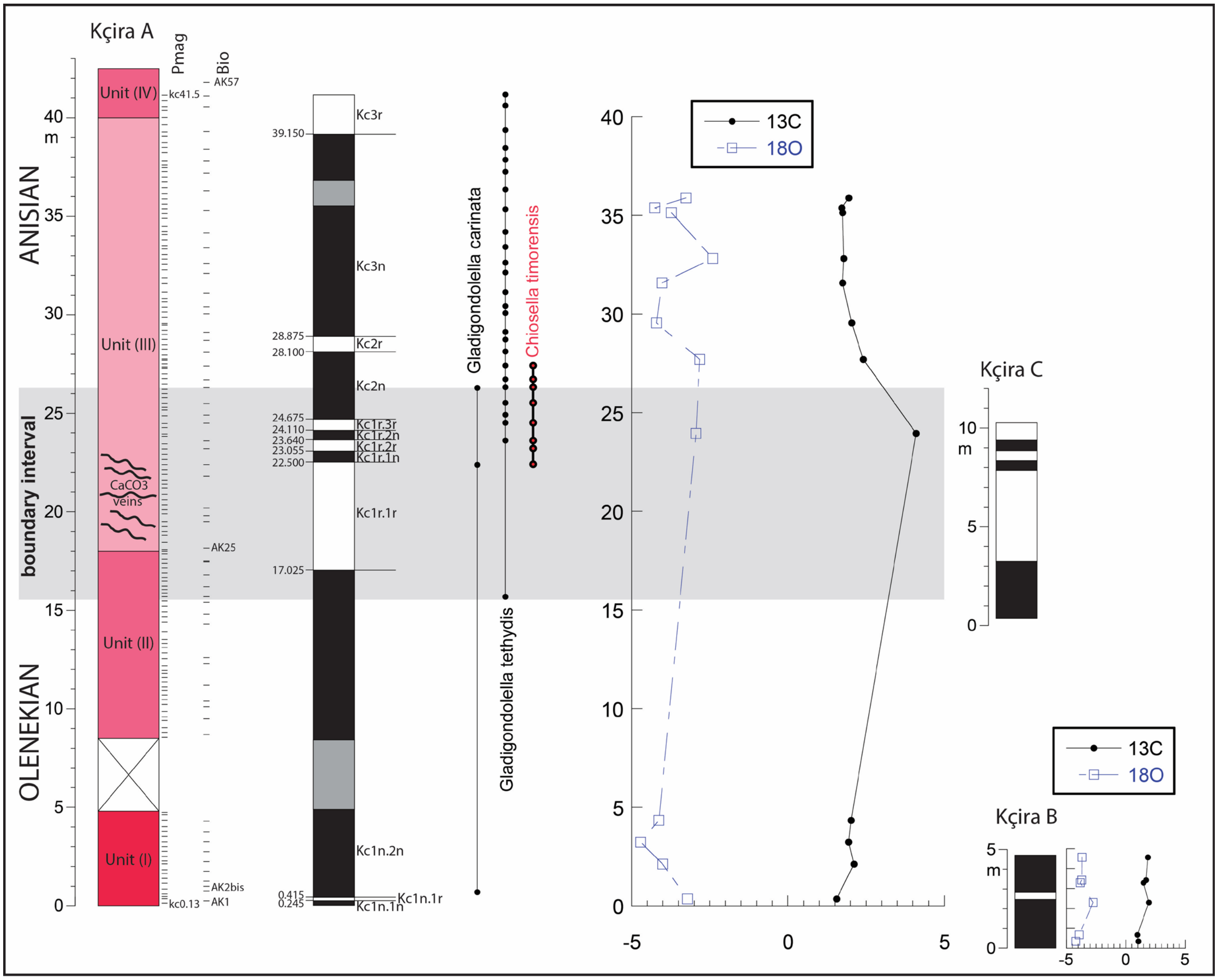

Figure 8 – Summary of magnetostratigraphic and key biostratigraphic events at Kçira-A across the Olenekian–Anisian boundary interval. Also shown are the magnetic stratigraphies of Kçira-B and Kçira-C, as well as the bulk C and O isotopes pilot data from Kçira-A and Kçira-B.

of the classical Spathian Kçira sections (Lower Triassic, Albania). Rivista Italiana di Paleontologia e Stratigrafia, 103(3): 267–292.

Grădinaru, E., Kozur, H., Nicora, A. & Orchard, M. J. 2006. The *Chiosella timorensis* lineage and correlation of the ammonoids and conodonts around the base of the Anisian in the GSSP candidate at Deşli Caira (North Dobrogea, Romania). Albertiana, 34: 34–38.

Grădinaru, E., Orchard, M. J., Nicora, A., Gallet, Y., Besse, J., Krystyn, L., Sobolev, E. S., Atudorei, V. & Ivanova, D. 2007. The Global Boundary Stratotype Section and Point (GSSP) for the base of the Anisian Stage: Deşli Caira Hill, North Dobrogea, Romania. Albertiana, 36: 54–71.

Guex, J., Hungerbühler, A., Jenks, J. F., O'Dogherty, L., Atudorei V., Taylor, D. G., Bucher, H. & Bartolini, A. 2010. Spathian (Lower Triassic) ammonoids from western USA (Idaho, California, Utah and Nevada). Mémoires de Géologie (Lausanne), 49: 1–211.

Hounslow, M.W., Szurlies, M., Muttoni, G. & Nawrocki, J. 2007. The magnetostratigraphy of the Olenekian-Anisian boundary and a proposal to define the base of the Anisian using a magnetozone datum. Albertiana 36: 72–77.

Jenks, J., Guex, J., Hungerbühler, A., Taylor, D. G. & Bucher, H. 2013. Ammonoid biostratigraphy of the early Spathian *Columbites parisianus* Zone (Early Triassic) at Bear Lake Hot Springs, Idaho. *In*, Tanner, L. H., Spielmann, J. A. & Lucas, S. G. (eds.), 2013, The Triassic System. New Mexico Museum of Natural History and Science Bulletin, 61: 268–283.

Knobbe, T. K., & Schaller, M. F. 2018. A tight coupling between atmospheric pCO_2 and sea-surface temperature in the Late Triassic. Geology, 46: 43–46.

Kovacs, S. & Kozur, H. 1980. Stratigraphische Reichweite der wichtigsten Conodonten (ohne Zahnreichen conodonten) der Mittel- und Obertrias. Geologisch-Paläontologische Mitteilungen Innsbruck, 10: 47–78.

Kovacs, S. & Ralisch-Felgenhauer, E. 2005. Middle anisian (Pelsonian) platform conodonts from the Triassic of the Mecsek Mts. (South Hungary) – Their taxonomy and stratigraphic significance. Acta Geologica Hungarica, 48: 69–105

Kozur, H., Mostler, H. & Krainer, K. 1998. *Sweetospathodus* n. gen. and *Triassospathodus* n. gen., Two important Lower Triassic Conodont Genera. Geologia Croatica, 51: 1–5.

Lehrmann, D. J., Stepchinski, L., Altiner, D., Orchard, M. J., Montgomery, P., Enos, P., Elwood, B. B., Bowring, S. A., Ramezani, J., Wang, H., Wei, J., Yu, M., Griffiths, J. D., Minzoni, M., Schaal, E. K., Li, X., Meyer, K. M. & Payne, J. L. 2015. An integrated biostratigraphy (conodonts and foraminifers) and chronostratigraphy (paleomagnetic reversals, magnetic susceptibility, elemental chemistry, carbon isotopes and geochronology) for the Permian-Upper Triassic strata of Guandao section, Nanpanjiang Basin, South China. Journal of Asian Earth Sciences, 108: 117–135.

Maron, M., Muttoni, G., Rigo, M., Gianolla, P. & Kent D. V. 2019. New magnetobiostratigraphic results from the Ladinian of the Dolomites and implications for the Triassic geomagnetic polarity timescale. Palaeogeography, Palaeoclimatology, Palaeoecology, 517, 52–73.

Marshall, J. D. 1992. Climatic and oceanographic isotopic signals from the carbonate rock record and their preservation. Geological Magazine, 129: 143–160.

Meço, S. 2010. Litho-biostratigraphy and the conodonts of Palaeozoic/Triassic deposits in Albania. Palaeontographica Abteilung, A: 131–197.

Meço, S. & Aliaj, S. 2000. Geology of Albania. Beiträge zur Regionalen Geologie der Erde, Gebrüder Borntraeger Verlagsbuchhandlung, 246 pp.

Mosher, L. C. 1970. New conodont species as Triassic fossil guide. Journal of Paleontology, 42: 947–954.

Muttoni, G., Kent, D. V., Meço, S., Nicora, A., Gaetani, M., Balini, M., Germani, D. & Rettori, R. 1996. Magneto-biostratigraphy of the Spathian to Anisian (Lower to Middle Triassic) Kçira Section, Albania. Geophysical Journal International, 127: 503–514.

Muttoni, G., Kent, D. V. & Gaetani, M. 1995. Magnetostratigraphy of a Lower-Middle Triassic boundary section from Chios (Greece). Physics of the Earth and Planetary Interiors, 92: 245–261.

Muttoni, G., Mazza, M., Mosher, D., Katz, M. E., Kent, D. V., Balini, M. 2014. A Middle– Late Triassic (Ladinian–Rhaetian) carbon and oxygen isotope record from the Tethyan Ocean. Palaeogeography, Palaeoclimatology, Palaeoecology, 399: 246–259.

Nicora, A. 1977. Lower Anisian platform-conodonts from the Tethys and Nevada: taxonomic and stratigraphic revision. Palaeontographica, 157: 88–107.

Nopcsa, F. 1929. Geologie und Geographie Nordalbaniens. Geologica Hungarica, Series Geologica, 3: 1–620.

Orchard, M. J. 1995. Taxonomy and correlation of Lower Triassic (Spathian) seminate conodonts from Oman and revision of some species of *Neospathodus*. Journal of Paleontology, 69: 110–122.

Orchard, M. J., Grădinaru, E. & Nicora, A. 2007a. A summary of the conodont succession around the Olenekian-Anisian boundary at Deşli Caira, North Dobrogea, Romania. *In*, Lucas, S. G. & Spielmann, J. A. (eds.), The Global Triassic. New Mexico Museum of Natural History and Science Bulletin, 41: 34–345.

Orchard, M. J., Lehrmann, D. J., Jiayong, W., Hongmei, W. & Taylor, H. 2007b. Conodonts from the Olenekian-Anisian boundary beds, Guandao, Guizhou Provice, China. *In*, Lucas, S. G. & Spielmann, J. A. (eds.), The Global Triassic. New Mexico Museum of Natural His¬tory and Science Bulletin, 41: 347–354.

Richoz, S., Krystyn, L., Horacek, M. & Spötl, C. 2007. Carbon isotope record of the Induan-Olenekian candidate GSSP Mud and comparison with other sections. Albertiana, 35: 35–40.

Saltzman, M. R. & Thomas, E. 2012. Carbon isotope stratigraphy. *In*, Gradstein, F. M., Ogg, J. G., Schmitz, M. & Ogg, G. (eds.), The Geologic Time Scale 2012: Boston, Massachusetts, Elsevier, p. 207–232.

Shackleton, N. J. 1987. Oxygen isotopes, ice volume and sea level. Quaternary Science Reviews, 6: 183–190.

Sudar, M. & Budurov, K. 1979. New conodonts from the Triassic in Yugoslavia and Bulgaria. Geologica Balcanica, 9: 47–52.

Sudar, M. N., Gawlick, H.-J., Lein, R., Missoni, S., Kovacs, S. & Jovanović, D. 2013. Depositional environment, age and facies of the Middle Triassic Bulog and Rid formations in the Inner Dinarides (Zlatibor Mountain, SW Serbia): evidence for the Anisian break-up of the Neotethys Ocean. Neues Jahrbuch für Geologie und Paläontologie-Abhandlungen, 269(3): 291–320.

Trotter, J. A., Williams, I. S., Nicora, A., Mazza, M. & Rigo, M. 2015. Long-term cycles of Triassic climate change: a new $\delta^{18}O$ record from conodont apatite. Earth and Planetary Science Letters, 415: 165–174.

Veizer, J. & Prokoph, A. 2015. Temperatures and oxygen isotopic composition of Phanerozoic oceans. Earth-Science Reviews, 146: 92–104.

Research Article

THE CARNIAN-NORIAN BOUNDARY GSSP CANDIDATE AT BLACK BEAR RIDGE, BRITISH COLUMBIA, CANADA: UPDATE, CORRELATION, AND CONODONT TAXONOMY

Michael J. Orchard

Geological Survey of Canada, 1500-605 Robson Street, Vancouver, B.C., V6B 5J3, Canada
Email: mike.orchard@canada.ca

Abstract – Re-assessment of conodonts from the Carnian-Norian boundary (CNB) at Black Bear Ridge (BBR), British Columbia and Pizzo Mondello (PM), Sicily improves correlation. Fossil endemism is less of a problem than are differing taxonomic approaches. Re-evaluation of literature suggests that most platform genera differentiated at BBR can also be recognized at PM. These are *Carnepigondolella*, *Ancyrogondolella*, ?*Kraussodontus*, *Metapolygnathus*, *Norigondolella*, *Parapetella*, *Primatella*, and *Quadralella*. Only *Acuminatella* at BBR is endemic, whereas use of *Hayashiella* and *Paragondolella* at PM is discounted. Hence, faunal turnovers PM-T1 and PM-T3 are not strongly endemic. Standardization of the conodont nomenclature facilitates improves correlation of the two GSSP candidates: top *Carnepigondolella samueli* Zone at BBR is equivalent to a position within the "*Epigondolella*" *vialovi* Zone at PM; the *Primatella primitia* Zone can be recognized in both sections; correlation of the *Metapolygnathus parvus* Subzone is strengthened by 14 new conodont identifications at PM, including relatives of the *Pr. gulloae* Zone index; the lower Norian succession of *Ancyrogondolella quadrata* succeeded by *An. triangularis*, well-known in western Canada, appears corrupted at PM.

The FAD of *Metapolygnathus parvus* alpha morphotype can be correlated between sections, as can the simultaneous demise of typical Carnian taxa. At BBR, the concurrent appearance of diminutive conodont species corresponds to geochemical excursions implying anoxia and a temperature maximum during the *Me. parvus* Subzone. Within 1 m above this datum, the FAD of other fossil proxies occur, including an array of conodonts, the bivalve *Halobia austriaca*, and the ammonoid *Pterosirenites* sp.. The *Me. parvus* Subzone corresponds to the uppermost part of the traditional Carnian ammonoid zone of *Klamathites macrolobatus*.

INTRODUCTION

This paper provides a summary of the conodont biostratigraphy and other salient features of the Carnian-Norian boundary (CNB) succession at Black Bear Ridge (BBR), British Columbia, Canada, a candidate for the Global Stratotype Section and Point (GSSP) for the stage boundary (Orchard, 2007b, c). It also presents a further rationale for the BBR conodont taxonomy presented earlier (Orchard, 2013, 2014) and, through that filter, re-assesses the conodont succession described from Pizzo Mondello (PM), Sicily, Italy (Mazza et al., 2011, 2012a, b, 2018; Mazza & Martinez-Perez, 2015; Rigo et al., 2018): similarities between the two successions are greater than previously recognized, but significant anomalies remain. Alternative horizons for CNB definition are considered.

A thorough description of the conodonts and their succession across the CNB at BBR was provided by Orchard (2014) following the earlier introduction of new genera (Orchard, 2013). The conodonts and ammonoids from the entire BBR succession on Williston Lake identify strata ranging from within the upper Carnian up to the Hettangian of the Lower Jurassic (Orchard et al., 2001a, b). The studied CNB interval represents the lowest ~90 m of the succession, starting within the upper Carnian Ludington Formation and extending into the Pardonet

Published online: Septermber 13, 2019

Orchard, M.J. 2019. The Carnian-Norian GSSP candidate at Black Bear Ridge, British Columbia, Canada: update, correlation and conodont taxonomy. *Albertiana*, vol. 45, 50–68.

Formation as high as the base of the lower Norian *Malayites dawsoni* (ammonoid) Zone.

The succession of Ludington and Pardonet formations formed under low energy conditions in a deep water, lower slope - basin paleoenvironment, as a distal ramp facies at the passive western margin of Pangaea (Zonneveld et al., 2010; Onoue et al., 2016). A rich pelagic fauna occurs in the Pardonet Formation and ammonoids occurring at multiple levels show that the studied section includes both the upper Carnian *Klamathites macrolobatus* Zone and the succeeding lower Norian *Stikinoceras kerri* Zone (see Tozer, 1994; McRoberts & Krystyn, 2011; Balini et al., 2012). Conodont faunas occur throughout the section, and are often abundant in the Pardonet Formation (Orchard, 2014, fig. 5). Pelagic bivalves are common and have been described by McRoberts (2011). Some ichthyoliths (Johns et al., 1997; Johns, in Orchard et al., 2001a, b) and brachiopods (Sandy, in Orchard et al., 2001a, b) have been described, as have several ichthyosaurians from nearby localities (Gowan 1995, 1996). Geochemical analyses across the boundary interval have been undertaken for $\delta^{13}C_{org}$ (Williford, 2007); for $^{87}Sr/^{86}Sr$, $\delta^{13}C_{carb}$, $\delta^{18}O_{carb}$, and the redox sensitive elements (V, Ni, and Cr) (Onoue et al., 2016); and for $\delta^{18}O_{PO4}$ in conodont apatite (Sun et al., 2019; in press). Magnetostratigraphic sampling failed to reveal a primary signal (Muttoni et al., 2001).

CONODONT DIVERSITY AND ENDEMISM

Different taxonomic approaches have been taken by conodont researchers in the Upper Triassic (Orchard, 2014; Mazza et al., 2012b, 2018). This has resulted in different morphological scope for several genera, variable diagnoses of species, and a resulting nomenclature that makes comparison of the primary candidate successions at Black Bear Ridge (BBR) and Pizzo Mondello (PM) in Sicily more challenging. Mazza et al. (2018, p. 82-3) noted that correlations between the two were problematic, citing differing paleolatitudes and paleoecologically induced endemism. The extent of this provincialism is examined here and found to be less than was previously thought.

Conodonts from all CNB successions are generally dominated by gondola-shaped platform elements of variable shape and oral ornament. These features have been weighted differently by authors. The taxonomy of the less common scaphate elements (Sweet, 1988), of *Neocavitella* and *Misikella*, and the coniform *Zieglericonus* is more straightforward, but these genera are rare or absent at BBR.

The generic classification of platform conodonts from BBR (Orchard, 1991a, 2013, 2014) focuses primarily on the configuration of anterior platform margins (see taxonomy). There is an increase in the amplitude of anterior platform nodes and denticles displayed by platform elements through the Upper Triassic. Platform shape, posterior ornament, relative blade-carina length, and pit position differentiate species within genera, with several of them showing similar evolutionary trends that involve concurrent platform reduction, blade lengthening, and anterior pit migration. Within the study interval, diminutive platform species evolve iteratively, near the top of the *C. samueli* Zone and particularly around the base of the *Me. parvus* Subzone within the *Pr. primitia* Zone.

In addition to eight platform genera described from the CNB interval at BBR (see below), about 150 lesser taxonomic entities (species, subspecies, morphotypes) have been differentiated (Orchard, 2014). This diversity underpins the precise placement of significant faunal horizons expressed as three zones and nine subzones, one of which (the *Me. parvus* Subzone) is further divided into three intervals (Orchard, 2104, figs. 3-6; Figure 1). At PM, about 45 conodont taxa representing 6 platform genera are described by Mazza et al. (2012, amended Rigo et al., 2018, Mazza et al., 2018) from the same CNB interval; they are: *Carnepigondolella*, *Epigondolella*, *Hayashiella*, *Metapolygnathus*, *Norigondolella*, and *Paragondolella*. For reasons described below, and based on published illustrations, these are re-interpreted as species of the genera *Carnepigondolella*, *Ancyrogondolella*, ?*Kraussodontus*, *Metapolygnathus*, *Norigondolella*, *Parapetella*, *Primatella*, and *Quadralella*. These are most of the genera described from BBR, although the numbers of species/morphotypes differentiated are far fewer at PM. Only the platform genus *Acuminatella* appears to be totally absent at PM and can reasonably be regarded as a North American endemic.

The comparatively high numbers of taxa differentiated at BBR compared with PM arises from contrasting taxonomic approaches, summarized as 'splitting' and 'lumping'. The former is adopted at BBR (Orchard, 2014) where a typological approach promulgates a richness of taxa that enables stratigraphic and geographic ranges of distinct morphospecies to be discovered, and a potential increase in points of correlation. This is particularly important because many species have previously been broadly interpreted by authors, as is evident in the PM literature. Standardization of the taxonomies used at BBR and PM is the key to optimize correlation of the two CNB successions.

KEY CONODONT DATUMS AT BBR & CORRELATION WITH PM

Significant stratigraphic horizons established at BBR are shown as zones and subzones in Figure 1, which also shows conodont abundance through the entire section and the ranges of genera. Figure 2 shows ranges of both conodonts and macrofossils across the narrower CNB interval. Lower and upper boundary boundaries for the *Pr. primitia* Zone mark significant faunal turnovers, with the disappearance and appearance of genera, each preceded by accelerated evolution and peak abundances (Orchard, 2014, fig. 5). Species of *Carnepigondolella* are also relatively small at the top of the *C. samueli* Zone (*C. spenceri* Subzone), prior to their extinction. A third turnover showing similar attributes occurs within the *Pr. primitia* Zone, where the *Me. parvus* Subzone shows a major reduction in typical Carnian taxa and element diminution in several lineages. The top of the *Me. parvus* Subzone is marked by the virtual disappearance of all Carnian platform genera other than *Primatella* and *Acuminatella*, which are later joined by common *Norigondolella*. Other than these three turnover events, boundaries between subzones of the *C. samueli* and succeeding *Pr. primitia* zones are defined by an

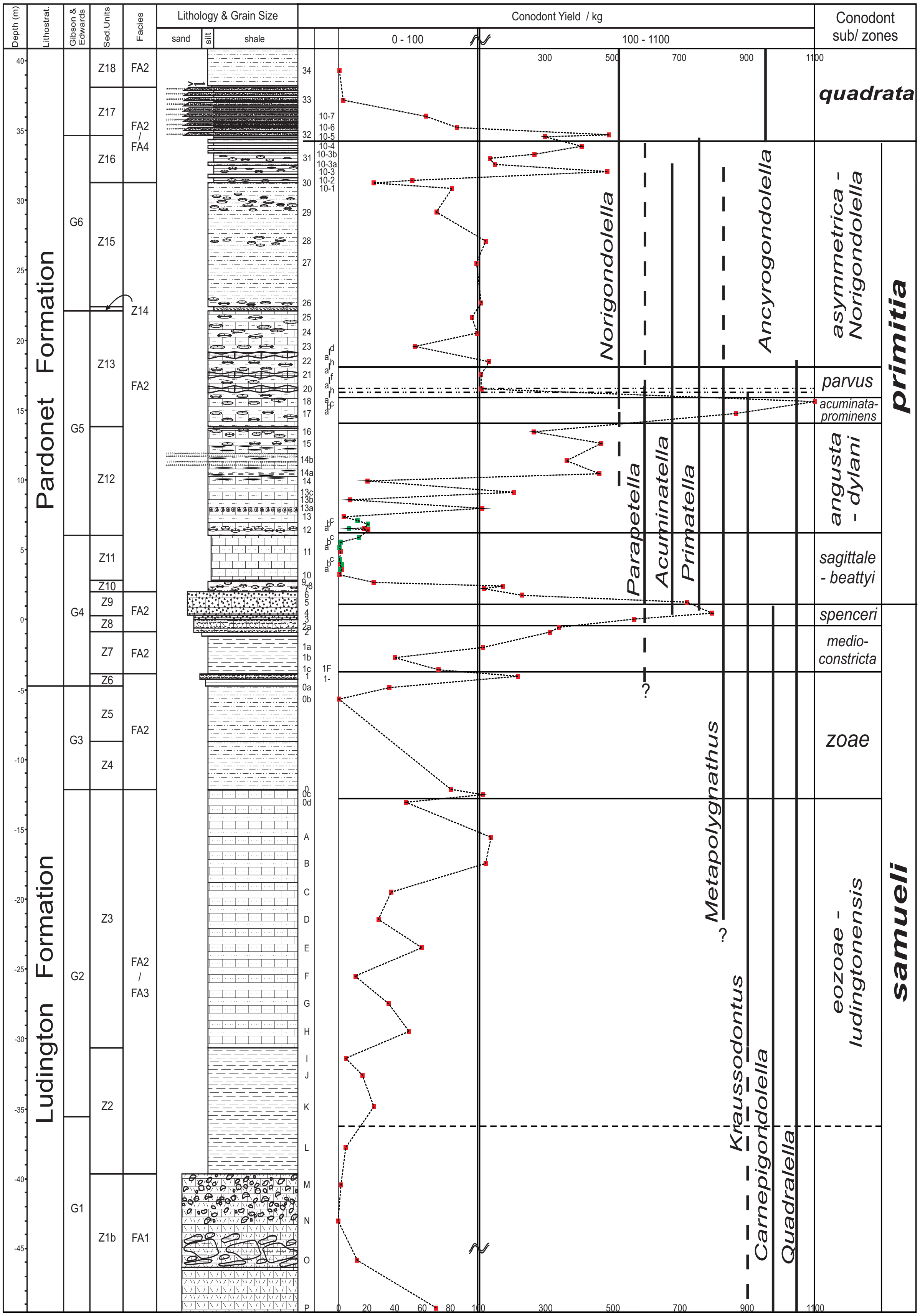

Figure 1 – Conodont zonation, conodont yield, and stratigraphic ranges of genera across the Carnian-Norian boundary interval at Black Bear Ridge. Columnar section on left adapted from Zonneveld et al. (2010), to which the reader is referred for a discussion of the sedimentary units on the left (modified from Orchard, 2014, fig. 5).

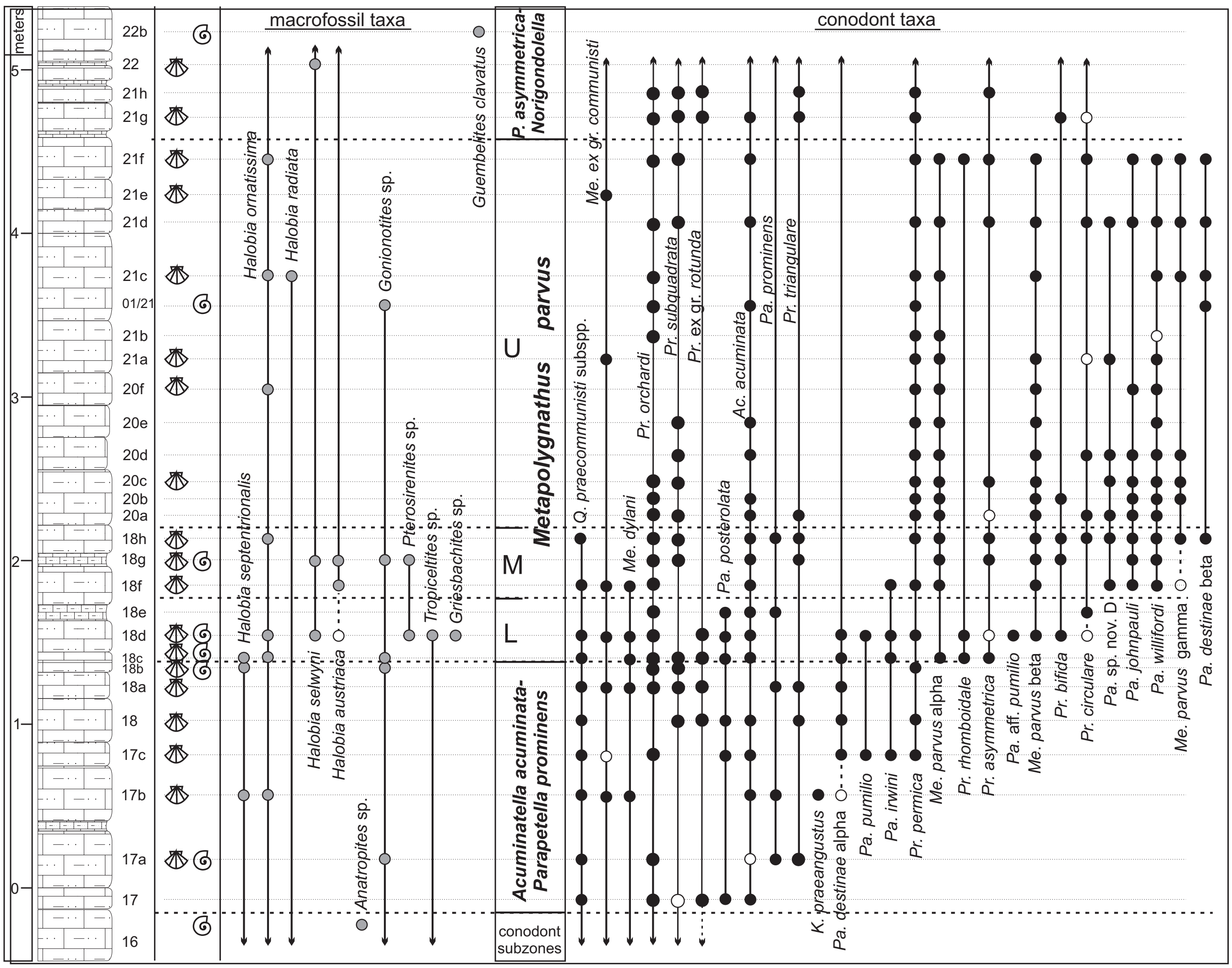

Figure 2 – The CNB boundary interval at Black Bear Ridge showing (from left) sample numbers, macrofossil (bivalve, ammonoid) occurrences (gray dots) and ranges, conodont subzones, and key conodont occurrences (black dots) and ranges for the ~5 m interval; clear dots mean uncertain occurrence. Conodont genera abbreviations are *Ac.= Acuminatella*, *K.= Kraussodontus*, *Me.= Metapolygnathus*, *Pa.= Parapetella*, *Pr.= Primatella*; *Q. = Quadralella*. (Modified from Orchard, 2014, fig. 28).

evolutionary succession of species (Orchard, 2014, figures 7-25).

At PM, three conodont faunal turnovers - termed T1, T2 and T3 – were identified by Mazza et al. (2010) and slightly revised by Rigo et al. (2018, fig. 6.4), who also introduced new Tethyan conodont zones. In terms of the latter, turnover T1 corresponds to the base of the "*Epigondolella*" *vialovi* Interval Zone at PM, and T2 and T3 correspond respectively to the base and top of their *Me. parvus* Zone (see also Mazza et al., 2018, fig. 5). This correlation differs from that proposed by Orchard (2014, fig. 5), who was misguided by the differing scope of genera and their apparent ranges in the two sections. The equivalence of BBR and PM zonation are considered here in the light of taxonomic revisions discussed in detail below.

The *Carnepigondolella* clade and the range of "*Epigondolella*"

Carnepigondolella is the common ornate platform conodont that occurs globally in the upper Carnian. In North America, its range is thought to lie largely or wholly within the *Tropites welleri* ammonoid Zone, although no direct association of the conodont and ammonoid zone is currently known. The genus disappears by end of the *C. samueli* Zone at BBR, which is believed to correspond to the beginning of the final ammonoid zone of the Carnian, the *K. macrolobatus* Zone. No such correlation has been suggested at PM, where the scope of *Carnepigondolella* has been very different. However, Mazza et al. (2018, p. 87-8, fig. 2; not correct in fig. 5) concluded that turnover T1 at PM corresponds to the top *C. samueli* Zone at BBR because of the disappearance of *Carnepigondolella* at that level has parallels with the reduction in *Carnepigondolella* at PM.

There are two problems with this correlation. First, at PM, *Carnepigondolella* species typical of the *C. samueli* Zone range upward into the "*E.*" *vialovi* Zone alongside "*Epigondolella*" species, which progressively replace the former genus according to Mazza et al. (2018). This correlation fails to take into account that the "*Epigondolella*" species like those identified by Mazza et al. (2012a; Rigo et al., 2018) in the "*E.*" *vialovi* Zone are included in *Carnepigondolella* by Orchard (2014). The *C. spenceri* Subzone at the top of the *C. samueli* Zone at BBR is marked by a rapid succession of *Carnepigondolella* species showing reduced platforms, lengthening blades, and anterior migration of the pit (Orchard, 2014, fig. 17, 18). The anterior denticles of these species are comparable to other *Carnepigondolella* species and they are viewed as advanced representatives of that genus rather than a separate genus, and certainly not *Epigondolella* sensu stricto, a genus that occurs first in middle Norian strata (Orchard, 2018).

The same evolutionary trends are common to both BBR and PM. They are manifest in the successive appearance of the alpha and beta morphotypes of *Carnepigondolella pseudodiebeli* sensu Orchard (2014) at BBR, and in the appearance of *C. spenceri* and allied forms. Morphotypes of *C. pseudodiebeli* at BBR are comparable at PM to *C. pseudodiebeli* and "*Epigondolella*" *vialovi* sensu Mazza & Martínez-Pérez (2015, pl. 2), and *C. spenceri* is comparable with "*Epigondolella*" *heinzi* (Rigo et al., 2018, p. 206). Hence, the upper part of the *C. samueli* Zone at BBR is equivalent to some part of the "*E.*" *vialovi* Zone, and its top is best drawn within the latter zone (Figure 3).

A second anomaly of the earlier proposed correlation of base "*E.*" *vialovi* Zone with top *C. samueli* Zone concerns the range of other genera. Many *Quadralella* species (called *Hayashiella* and *Paragondolella* by Mazza et al., 2018) disappear at that level at PM, whereas *Q. angulata*, *Q. carpathica*, *Q. oertlii,* and *Q. tuvalica*, as well as others newly described, range well above the *C. samueli* Zone at BBR. The explanation for this difference may lie in the ecological competition, as invoked for these taxa by Mazza et al. (2009), although the competition is not evident at BBR. It is also notable that other species such as *Q. kathleenae*, *Me. dylani* and *Me. praecommunisti* (*Quadralella* sensu Orchard), as well as other species formerly included in the latter species (*Parapetella clareae*, ?*Kraussodontus roberti*) occur within the *C. samueli* Zone

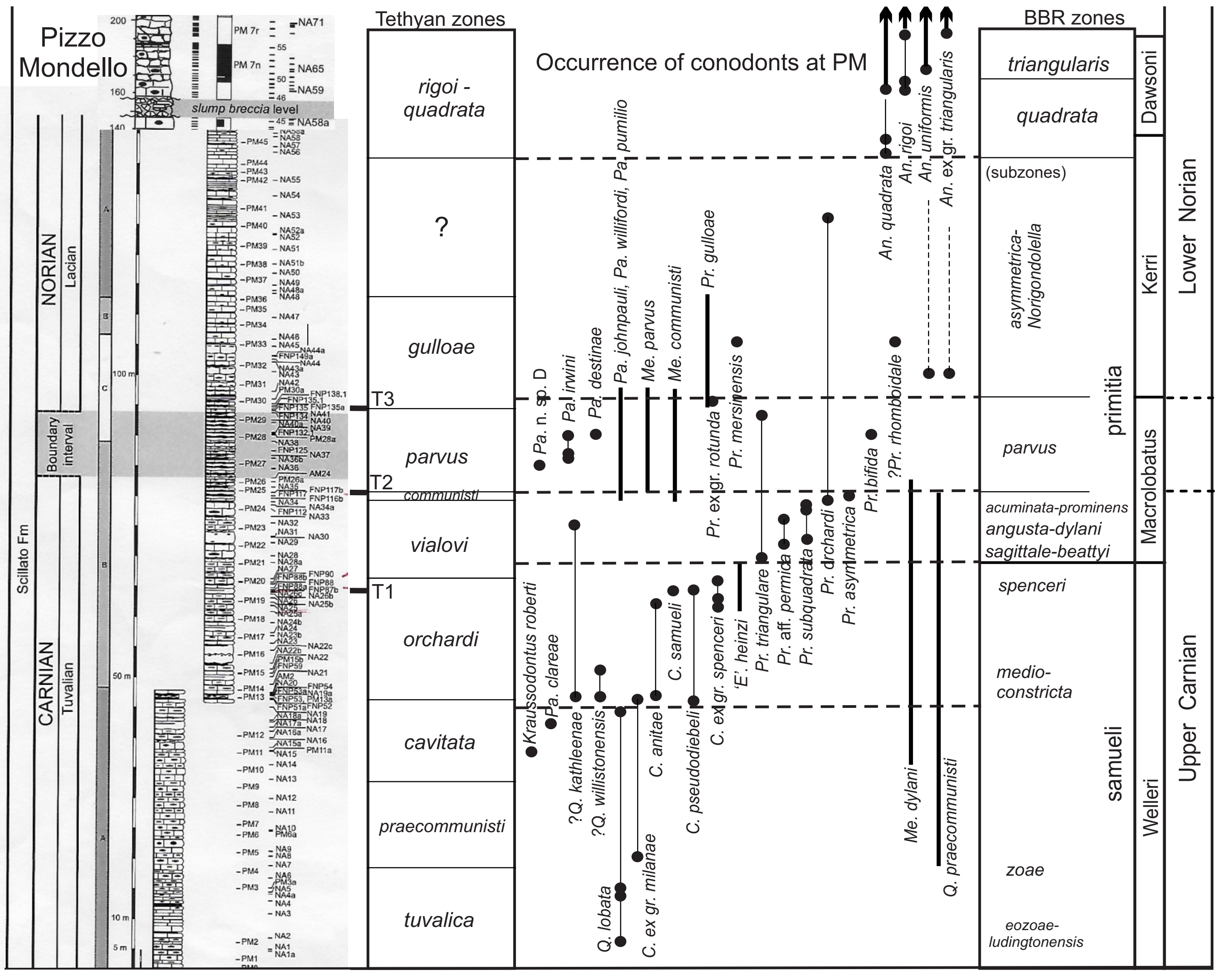

Figure 3 – The Pizzo Mondello section, Sicily showing sample numbers (after Mazza et al., 2012b) and the Tethyan conodont zonation and faunal turnovers T1-T3 (after Rigo et al., 2018) on left; on the right, the conodont and ammonoid zonations at Black Bear Ridge, British Columbia with suggested equivalence, including correlation of top *C. samueli* Zone, and base and top of *Me. parvus* Subzone. Revised conodont occurrences at PM (dots) based on published illustrations (see taxonomy text for details). Abbreviations as in Fig. 2, plus *An.* = *Ancyrogondolella* and '*E*' = '*Epigondolella*'. Thin vertical bars connect multiple new records; thick vertical bars are ranges of selected taxa at PM (from Rigo et al., 2018; Mazza at al., 2018); broken lines connect early records of *An. uniformis* and *An. triangularis* that appear out-of-place based on Canadian data.

equivalent at PM. None of these are known from BBR prior to the *Pr. primitia* Zone. On the contrary, the distribution of *Q. lobata* (see taxonomy) at PM correlates well with BBR occurrences, where it ranges midway through the *C. samueli* Zone.

Younger representatives assigned to *Carnepigondolella* at PM, i.e., *C. pseudoechinata* and *C.? gulloae*, are herein re-assigned to *Primatella*, so *Carnepigondolella* sensu Orchard (2014) does indeed disappear within the "*E.*" *vialovi* Zone. This reconciles the apparently different successions at BBR and PM and counters the suggestion (Mazza et al., 2018, p. 88) that the "proliferation of the endemic North American genera ….. absent in the Tethys, allowed the epigondolellids to proliferate earlier in the Tethys." In fact, the same late stage *Carnepigondolella* evolutionary trends and appearance of "*Epigondolella*" occur in both regions.

The *Carnepigondolella* fauna is replaced at BBR by species of *Acuminatella*, *Primatella*, and *Parapetella*, none of which are explicitly recorded at PM. However, rather than being endemic, species of *Primatella* do occur in the younger parts of the "*E.*" *vialovi* Zone, and sporadic examples of *Parapetella* occur (Fig. 3). A reinterpretation of illustrated specimens of long-ranging "*Epigondolella*" *vialovi* from PM identifies within it examples of upper Carnian *C. samueli*, CNB *Primatella* aff. *permica*, and lower Norian *Ancyrogondolella uniformis* (Mazza et al., 2010, 2012b) (see taxonomy). The holotype of *E. vialovi* actually resembles *An. uniformis*, and *An*. aff. *vialovi* has been interpreted as a lower Norian species by Orchard (2014).

In the higher part of the "*E.*" *vialovi* Zone, several additional species assigned to *Epigondolella* are reported by Rigo et al. (2018), namely *E. triangularis*, *E. uniformis*, *E. rigoi*, and *E. quadrata*. These species were all established in the lower Norian and are now assigned to *Ancyrogondolella* (Orchard, 2018). Their presence in the upper Carnian and basal Norian is doubtful based on available illustrations, for example: *E. quadrata* from PM (Nicora et al., 2007; Balini et al., 2010) have either been previously re-assigned to '*Epigondolella*' *miettoi* (Balini et al., 2010), or are here re-assigned to *Primatella* species; *Me. mersinensis* from the upper Carnian (Mazza et al., 2012b) resembles *Pr. subquadrata*; *E. rigoi* from the upper Carnian (Nicora et al., 2007) resembles the ornate *Pr. permica*; *E. rigoi* from the *Me. parvus* Zone (Nicora et al., 2007; Mazza et al., 2010) is close to *Pr. triangulare*; and a Norian specimen of *E. uniformis* illustrated by Mazza et al. (2012b) resembles *Pr. rhomboidale* (see Fig. 3) None of these are to be confused with younger, lower Norian occurrences of *Ancyrogondolella quadrata* (Mazza et al., 2012b; Mazza & Martinez-Perez, 2015) and *An. rigoi* (Nicora et al., 2007; Mazza et al., 2010; Mazza et al., 2012b; Mazza & Martinez-Perez, 2015).

Concerning illustrated specimens of *Ancyrogondolella triangularis* and *An. uniformis* from PM, none of the alleged upper Carnian occurrences of those species have been illustrated. In North America, examples of these posteriorly ornate *Ancyrogondolella* species, often determined as *An*. ex gr. *triangularis*, typically occur in the younger lower Norian *M. dawsoni* and *Juvavites magnus* ammonoid zones and their appearance within the "*C.?*" *gulloae* Zone at PM (sample NA43, in Mazza & Martinez-Perez, 2015, pl. 5), equivalent to the *Pr. asymmetrica - Norigondolella* Subzone and prior to the *An. quadrata* Zone at BBR, is problematic: these records need verification.

In summary, the conodont successions at both BBR and PM are interpreted to consist of a diverse *Carnepigondolella* clade that disappears in the upper Carnian and is superseded by faunas that include *Metapolygnathus*, *Quadralella* and the first *Primatella*.

The Carnian-Norian boundary turnover

A second major conodont turnover at BBR involving the disappearance of several Carnian genera begins in the *Acuminatella acuminata – Parapetella prominens* Subzone of the *Pr. primitia* Zone (Fig. 2). This interval represents both a period of evolutionary innovation, and the initial die-off of long-ranging Carnian taxa, which reaches its peak midway through the overlying *Me. parvus* Subzone. At BBR, species with anteriorly shifted pits (*Metapolygnathus* sensu Mazza et al., 2018) are common at this level and therefore probably equate with the original faunal turnover T2 at PM (Mazza et al., 2010, p. 131), which is within the *Me. communisti* Zone of Rigo et al. (2018), where *Metapolygnathus* becomes dominant over "*Epigondolella*".

Faunal turnover PM-T2 has recently been updated to equate with sample NA35 and to approximate the base of the *Metapolygnathus parvus* Zone (Mazza et al., p. 83, tab.1; Rigo et al., 2018). That revision lowers the base of the *Me. parvus* Zone (=boundary interval of Mazza et al., 2012b, fig. 2) and reduces the *Me. communisti* Zone of Rigo et al. (2018) to a single sample (Mazza et al., 2018, tab.1, FNP117). Reassessment of published illustrations from both the *Me. communisti* and *Me. parvus* zones at PM confirms that, as at BBR, a mixture of *Metapolygnathus*, *Parapetella*, *Primatella*, and *Quadralella* species dominate the interval (Fig. 3). Besides *Me. communisti*, *Me. dylani*, and *Me. parvus*, these additional BBR species are recognized (see taxonomy for details): *Pa. destinae* (Mazza et al., 2012b), *Pa. irwini* (Mazza et al., 2012b); ?*Pa*. n. sp. D of Orchard, 2014 (Mazza et al., 2018); *Pr. asymmetrica* (Mazza & Martinez-Perez, 2015), *Pr. bifida* (Mazza et al., 2012b); and *Pr. triangulare* (Nicora et al., 2007; Mazza et al., 2010). The diminutive *Pa. johnpauli*, *Pa. pumilio*, and *Pa. willifordi* are also stated to occur at PM as "Tethyan morphotypes of the *Me. communisti* fauna" (Mazza et al., 2018), but none of these diminutive species have been illustrated, or their range documented. *Quadralella multinodosus* and similarly ornate ?*Me. dylani* also occur at PM but are not found at BBR (see taxonomy).

As recently discussed by Mazza et al. (2018), the FAD of *Metapolygnathus parvus,* which defines the base of the *Me. parvus* (Sub-)Zone, is a datum recognized at both BBR and PM. However, the concept of *Me. parvus* currently embraces several morphotypes (Orchard, 2014; Mazza et al., 2018) with variable platform shape and ornament. The subrectangular-oval alpha morphotype, close to the holotype of the species, appears to be the more stable concept and occurs in both sections. The elongate beta morphotype, which lacks strong nodes or denticles, was erroneously called *Me. echinatus* by Orchard (2007b), a determination that was followed by Mazza et al. (2012b, 2018) both for elements that lacked pronounced ornament (=*Me. parvus* beta morphotype of Orchard, 2014) and others that had a distinctive pair of anterior nodes or denticles, which were assigned to *Pa. destinae* by Orchard (2014). Finally, the gamma morphotype of *Me. parvus* described by Orchard (2014) has a much longer posterior process than that illustrated by Mazza et al. (2018) and is not clearly the same taxon.

The successive first occurrences of the alpha, beta, and gamma morphotypes of *Metapolygnathus parvus* occur in that order at BBR. According to Mazza et al. (2018, fig. 4), a comparable succession of the BBR morphotypes occurs at PM, but the revisions above imply a somewhat different succession involving *Parapetella destinae* and *Me. parvus* new morphotype. Notably, *Pa. destinae* first appears in the *Ac. acuminata – Pa. prominens* Subzone at BBR, prior to the *Me. parvus* Subzone (Fig. 2; Orchard, 2014, fig. 28), so it is important to specify the scope of the chosen index species.

The substantial and rapid faunal turnover in the Canadian section begins below the base of the *Me. parvus* Subzone and continues through the entire span of the subzone, which is further subdivided into three divisions. The lowest 40 cm of the *Me. parvus* Subzone contains the FAD of *Me. parvus* and of five *Primatella* species, including *Pr. asymmetrica*; the next 40 cm of the *Me. parvus* Subzone contains the first appearance of several more diminutive *Parapetella* species. Most larger Carnian species other than *Acuminatella* and *Primatella* disappeared within this middle division of the *Me. parvus* Subzone at BBR and the greater part of the *Me. parvus* Subzone is assigned to its upper division (~2+ m at BBR), which is characterized by a bloom of diminutive elements (Fig. 2; Orchard, 2014, Fig. 6). No such division or succession is currently identified at PM.

Norian stasis

At BBR, the top of the *Metapolygnathus parvus* Subzone is defined by the disappearance of the name-giver and its associated diminutive taxa (Fig. 2). Above the *Me. parvus* Zone, faunas are dominated by relatively stable populations of *Acuminatella* and *Primatella* +/- *Norigondolella* species. There are very few first occurrences about the top of the *Me. parvus* Zone through the remainder of the *Pr. primitia* Zone at BBR, the rare occurrence of *Acuminatella curvata* being an exception. Hence, recognition of the *Pr. asymmetrica – Norigondolella* Subzone of the *Pr. primitia* Zone is generally based on *Primatella* dominated faunas lacking *Me. parvus* Subzone indicators, or by the common association of *Norigondolella*.

The end of the extinction of typical Carnian taxa at BBR approximates PM-T3, which corresponds to the base of the *Carnepigondolella*? *gulloae* Zone of Rigo et al. (2018, fig. 2). The top of the range of *Me. parvus* at PM is above the base of the "*C.*?" *gulloae* Zone, so the upper boundary of the *Me. parvus* Subzone sensu Orchard (2014) correlates to that higher level (Fig. 3). Illustrated examples of the *Carnepigondolella*? *gulloae* from PM (Mazza et al., 2012b) are variable and show affinity with several species of *Primatella*, including *Pr. subquadrata*, *Pr. triangulare*, and *Pr. rotunda*. These similarities emphasize the re-assignment here of the PM index species to *Primatella*, and again suggests there was less endemism than previously assumed. Each of these similar *Primatella* species range through the boundary interval at BBR, which suggests that *Pr. gulloae* and its predecessors might be located at BBR. However, the species lacks clear ancestry and is too poorly known to be a suitable index.

The "*C.*?" *gulloae* Zone post-T3 turnover at PM also corresponds to the occurrence of "abundant epigondolellids" (Mazza et al., 2018, p. 83), but in view of the previous observations these may be species of *Primatella* rather than '*Epigondolella*' (=*Ancyrogondolella*). The presumably correlative *Pr. asymmetrica – Norigondolella* Subzone strata of the *Pr. primitia* Zone at BBR appears to have been a relatively stable time without notable evolutionary developments. Then, the wholesale replacement of *Primatella* by *Ancyrogondolella* occurred near the top of the *S. kerri* ammonoid Zone, which is at the base of the "type" *An. quadrata* Zone. Similar platform shapes occur in populations of both *Primatella* and early *Ancyrogondolella* but the anterior denticles of the latter are higher and sharper, which is also reflected in their differing platform microreticulation (Orchard, 1983, figs. 3, 9). This late *S. kerri* Zone event may correlate with the appearance of "advanced forms of *E. quadrata*" at PM (Mazza et al., 2012b, fig. 2). The earlier occurrence of *An.* ex gr. *triangularis* low in the PM succession (sample NA43) remains an anomaly because strongly sculptured posterior platforms like those illustrated from PM (see taxonomy) are only known to occur above the *An. quadrata* Zone in western Canada. Notable endemism in the *Pr. primitia* Zone and equivalent strata are shown by some *Norigondolella* species, with *N. trinacriae* occurring at PM, and *N. norica* at BBR.

CONODONT TAXONOMY & NOMENCLATURE

In this section, the conodont taxonomy developed in North America is explained and compared with that adopted at PM. Although there are faunal differences that can be attributed to endemism, there is far more commonality than hitherto documented.

Generic differentiation of the Upper Triassic platform conodonts is based primarily on the nature of the anterior platform margins (Figure 4; Orchard, 1991a, pl. 3). Ornament is absent or consists of rudimentary to poorly differentiated, low or incised nodes in *Quadralella* (Fig. 4 a-c), *Kraussodontus*, and *Metapolygnathus*; elevated anterior buttresses occur in *Parapetella* (Fig. 4 k, l); well differentiated nodes becoming relatively short and sharp denticles characterize *Acuminatella* and *Carnepigondolella* (Fig. 4 g-j); discrete and high, often apically rounded and microreticulated nodes occur in *Primatella* (Fig. 4 d-f); and very high and sharp denticles occur in *Ancyrogondolella* (*Epigondolella* sensu Orchard, 1991a, 2014; Fig. 4 m-o). Younger, largely middle to upper Norian *Mockina*, *Orchardella*, and *Epigondolella* (Fig. 4 p) also have very high and sharp denticles (see Orchard, 2018) that reach a peak development in *Mockina englandi* (Fig. 4 q).

Within each of the CNB genera, the pit migrates anteriorly through time producing a longer posterior keel. At PM, many species with medial to anteriorly shifted pits were combined as *Metapolygnathus* (Mazza et al., 2012b), which results in the combination of species of several BBR genera. The BBR taxonomy works well in formerly distant Panthalassan terranes

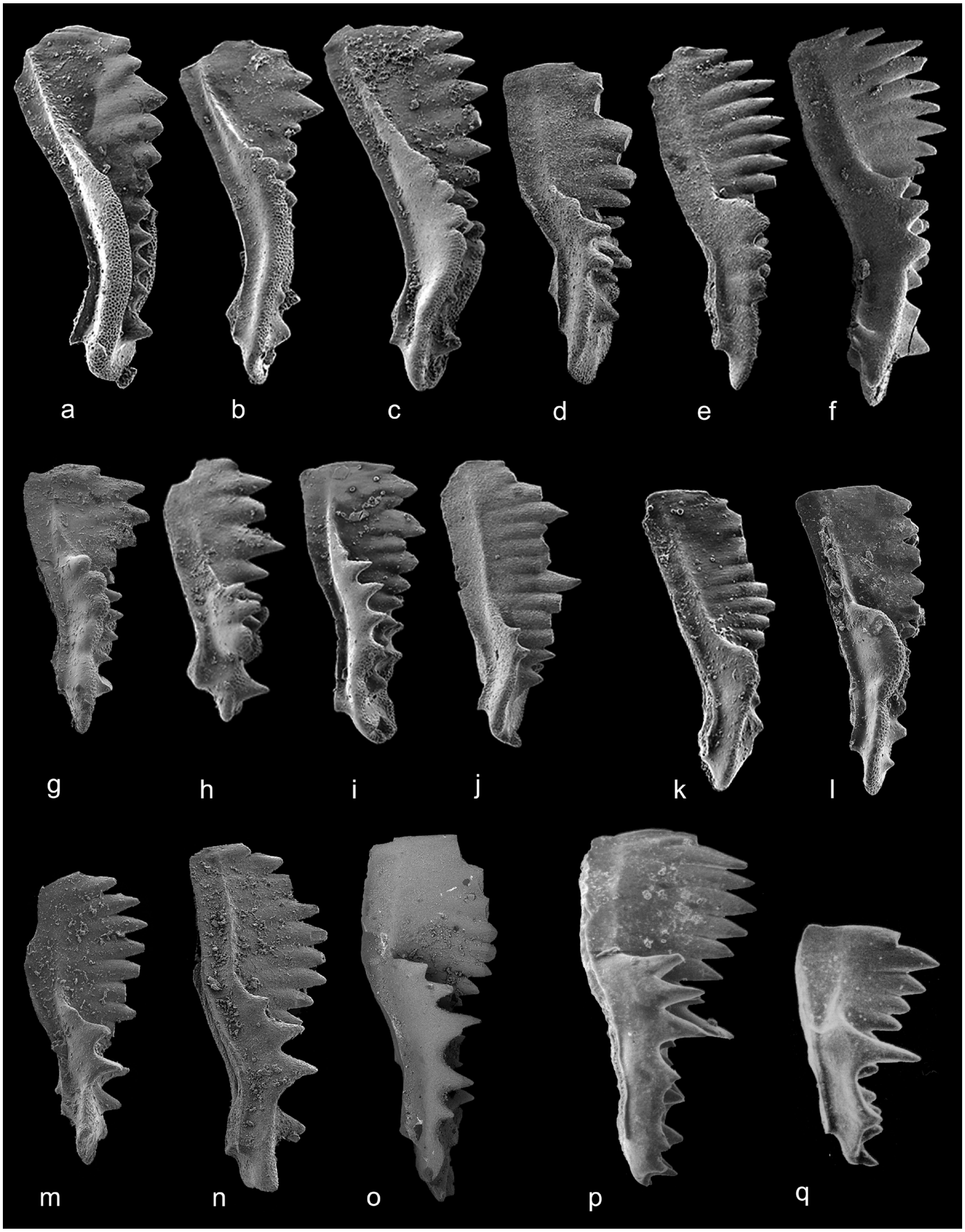

Figure 4 – Lateral profiles of some Upper Triassic genera: a-c, *Quadralella*; d-f, *Primatella*; g-l, *Carnepigondolella*; k-l, *Parapetella*; m-o, *Ancyrogondolella*; p, *Epigondolella*; q, *Mockina*. Specifically, a (flipped) = *Q. carpathica* (Mock), GSC 131354, sample C; b = *Q. carpathica* (Mock), GSC 131248, sample 0; c = *Q. tuvalica* (Mazza and Rigo), GSC 132604, sample 7; d (flipped) = *Pr. asymmetrica* Orchard, GSC 132947, sample PHE-24, Pardonet Hill east; e (flipped) = *Pr. stanleyi* Orchard, beta morphotype, GSC 132591, sample PHE-23, Pardonet Hill east; f = *Pr. vanlierae* Orchard, GSC 131340, sample PHE-23. Pardonet Hill east; g = *C. zoae* (Orchard), GSC 95203, Peril Formation, Huston Inlet, Haida Gwaii; h (flipped) = *C. anitae* Orchard, GSC 132681, sample 1a; i (flipped) = *C. samueli* (Orchard), GSC 132718, sample C; j (flipped) = *C. spenceri* Orchard, GSC 132714, sample 4; k = *Pa. beattyi* Orchard, GSC 132832, sample 5; l = *Pa. prominens*, GSC 132920, sample 18e; m (flipped) = *An.* aff. *vialovi* (Buryi), GSC 132741, sample 10/06; n = *An. quadrata* (Orchard), GSC 95265, sample PH-213b, Juvavites Cove; o = *An. equalis* (Orchard), GSC 131624, sample 00/B2, Pink Mt.; p = *E. tozeri* Orchard, GSC 95287, sample C-98518, Pardonet Hill; q (flipped) = *Mockina englandi* (Orchard), GSC 95290, sample C-87005, Lewes River Group, Laberge. Samples are from the Pardonet Formation of Black Bear Ridge unless stated otherwise. Flipped images have been re-orientated 180° horizontally for uniform views.

such as Wrangellia (e.g., Orchard & Carter, 2013), and more southerly, low paleolatitude regions such as Nevada in the USA (Balini et al., 2014), where species of *Acuminatella*, *Parapetella*, *Primatella* and *Quadralella* are recorded. Further afield, this nomenclature has been adopted in Japan (Zhang et al., 2018; Yamashita et al., 2016, 2018), South China (Sun et al., 2016; Zhang et al., 2017, 2018; Jiang et al., 2019), and Turkey (Chen & Lukeneder, 2017). These examples suggest that the BBR taxonomic framework is widely, if not globally, applicable. The following review is arranged alphabetically.

Genus: *Acuminatella* Orchard, 2013

Type species: *Acuminatella acuminata* Orchard, 2013

Acuminatella species differ from most contemporaneous taxa in the strongly reduced and tapered posterior platform and well developed posterior carina. Species bear well differentiated anterior platform nodes or small, apically rounded denticles that become more pronounced through the BBR section, hence their use as subzonal indices (*Ac. sagittale*, *Ac. acuminata*) in the lower *Pr. primitia* Zone. The genus is allied with *Primatella* and, like that genus, appears near the base of the *Pr. primitia* Zone and extends through the entire zone, including the *Me. parvus* Zone extinctions.

Kozur (2003) introduced *Orchardella* for similar but more denticulate middle-late Norian species, formerly referred to *Epigondolella*, that he regarded as North American endemics (Moix et al., 2007, p. 294); he selected *Epigondolella multidentata* as the type species. Kozur (2003) also suggested that CNB species was ancerstral to the younger species, but because there is no stratigraphic continuity between the two, the older homeomorph were referred to the new genus *Acuminatella* (Orchard, 2013). The genus has been described from Haida Gwaii (Carter & Orchard, 2013) and Nevada (Balini et al., 2014), but not outside North America.

Genus: *Ancyrogondolella* Budurov, 1972

Type species: *Ancyrogondolella triangularis* Budurov, 1972

This genus is now used for mostly lower Norian species that were previously assigned to *Epigondolella* by Orchard (1991b; 2014), plus others introduced in a recent revision (Orchard, 2018). The genus accommodates platform elements with high and sharp anterior denticles and a bifid basal keel, features of the first representatives in the '*E.*' *quadrata* fauna (Orchard, 2014, figs. 40, 41). A bifid keel may be developed in other broad-platform Late Triassic genera, but the anterior platform ornament is never as pronounced as in *Ancyrogondolella*. Sharp denticles in *Carnepigondolella* are shorter, while those of *Primatella* are typically high nodes or apically rounded denticles (Fig. 4). At PM, only the "advanced Epigondolellae species" identified by Mazza et al. (2012b) in the lower Norian are included in *Ancyrogondolella*.

Keel bifurcation generally arises during growth close to the subcentral pit, with the secondary keels being widely divergent in older representatives and much less so in the youngest species. *Ancyrogondolella* is believed to have evolved from *Primatella* in the early Norian, as documented in many Canadian sections where the former replaces the latter near the top of the *S. kerri* Zone (Orchard, 1991b, 2001a, b, 2014). Populations of *Ancyrogondolella* and *Primatella* have convergent platform shapes, but differing anterior ornamentation. *Ancyrogondolella* is regarded as ancestral to middle Norian *Epigondolella* sensu stricto, *Mockina*, and *Orchardella* (Orchard, 2018), all of which differ in their carina development and lack of a primary bifid keel.

Several species of *Ancyrogondolella* are common to BBR and PM, including Norian *An. quadrata*, *An. triangularis* sensu lato, and *An. uniformis*. Other species differentiated within the *An. quadrata* Zone at BBR (Orchard, 2014) have not been recorded at PM, while *An. rigoi* is not yet found at BBR. New species of *Ancyrogondolella* are anticipated in abundant undescribed faunas of *An*. ex gr. *triangularis* from the *M. dawsoni* and *J. magnus* ammonoid zones in B.C. The following revisions are proposed for illustrated PM material (sample numbers in bold):

An. rigoi (= *E. rigoi* in Mazza et al., 2012b, pl. 6, figs. 1-7. **NA59**, **NA61**; Mazza & Martinez-Perez, 2015, pl. 4). **NA68**

An. quadrata (= *E. quadrata* in Mazza et al., 2012b, pl. 5, figs. 2-10. **NA60**, **NA58**, **NA56**; Mazza & Martinez-Perez, 2015, pl. 3). **NA56**, **NA60**

An. ex gr. *triangularis* (= *E. triangularis* in Nicora et al., 2007, pl. 4, fig. 10; =Mazza et al., 2010, pl. III, fig. 9). **NA68**

An. ex gr. *triangularis* (= *E. triangularis* in Mazza & Martinez-Perez, 2015, pl. 5, figs. 1-12). **NA43**

An. uniformis (= *E. triangularis* in Nicora et al., 2007, pl. 4, figs. 8, 9). **NA43**.

An. uniformis (= *E. vialovi* in Mazza et al., 2012b, pl. 7.3). **NA66**

An. uniformis (=*E. uniformis* in Mazza & Martinez-Perez, 2015, pl. 5, figs. 24, 25 only). **NA43**

Genus: *Carnepigondolella* Kozur, 2003

Type species: *Metapolygnathus zoae* Orchard, 1991a

This genus includes upper Carnian platform conodonts with characteristic short, sharp denticles on anterior platform margins, and sometimes on the posterior margins too. The type species, *C. zoae*, is atypical in having very well-defined, rounded nodes, but its ancestral relationship to the denticulate species is evident in *C. anitae*, in which both ornament styles are present as anterior denticles and posterior nodes. The origin of the genus lies in older strata than is preserved at BBR (*C. gibsoni* is already present near the base), and there may be more than one lineage represented (Orchard, 2014, figs. 17, 18).

At BBR, a succession of *Carnepigondolella* species ends with the *C. spenceri* Subzone of the *C. samueli* Zone, which is characterized by relatively small species with reduced platforms, long blades, and anteriorly shifted pits. The same evolutionary development occurs at PM within the "*E.*" *vialovi* Zone where Mazza et al. (2012b; Martinez Perez, 2016) have characterized these taxa as the beginning of the *Epigondolella* clade. Hence, as discussed above, realignment of the top *C. samueli* Zone at BBR with a position within the "*E.*" *vialovi* Zone at PM is suggested.

Several PM species that were formerly assigned to *Carnepigondolella* by Mazza et al (2012b) are here assigned to

Quadralella (e.g., *Q. carpathica*, *Q. tuvalica*) or *Primatella* (*Pr. pseudoechinata*, *Pr. gulloae*). The elements described as *C. orchardi* by Mazza et al. (2012b) are examples of the genus but not the species, which was interpreted as a *Primatella* species by Orchard (2014)(see below).

The succession of *Carnepigondolella* species in the Ludington and basal Pardonet formations at BBR (Orchard, 2014) includes several species identical or allied to those recognized at PM, some of which were assigned to *Epigondolella* (see above). Although informal morphotype designations have also been assigned to variants of *C. zoae*, *C. pseudodiebeli*, and *C. samueli*, all occurrences fall within the *C. samueli* Zone.

C. anitae (= *C. zoae* B in Mazza et al., 2010, pl. I, fig. 8. **FNP53a**

C. anitae (= *C. zoae* in Nicora et al., 2007, pl. 3, figs. 6a-c.). **PM19**

C. ex gr. *milanae* (= *C. zoae* morphs in Mazza et al., 2012b, pl.4, figs. 1-3). **PM19**, **NA8**

C. pseudodiebeli (= *Me. mersinensis* in Mazza et al., 2012b, pl. 4, fig. 10). **NA32**

C. pseudodiebeli (= *C. orchardi* in Mazza, 2009, pl. I, fig. 11; 2012b, pl. 2, figs. 1, 2). **FNP53**, **FNP88a**

C. samueli (= *E. vialovi* in Mazza et al., 2012b, pl. 7.2). **FNP88a**

C. miettoi holotype (= *E. quadrata* in Nicora et al., 2007, pl. 3, fig. 8). **FNP88a**

C. miettoi paratype (= *E. quadrata* in Balini et al., 2010, pl. 3, fig. 5). **FNP88a**

C. ex gr. *spenceri* (= *E. heinzi* in Mazza, Cau & Rigo, 2012a, fig. 9. C-E). **NA25**, **NA27**

C. spenceri (= *C. pseudoechinata* in Mazza et al., 2012, pl. 2, fig. 5). **NA25**

Genus: *Epigondolella* Mosher, 1968

Type species: *Polygnathus abneptis* Huckriede, 1958

As discussed previously by several authors (e.g., Kozur, 2003), the holotype of *Epigondolella abneptis* is of Middle Norian, Alaunian age and differs from similar lower Norian elements. Orchard (2018) has argued that *Epigondolella* is best used for middle Norian species that, in common with the holotype, are broad and lack both a primary bifid keel and a strong posterior carina. These attributes separate the genus from contemporary *Mockina* and *Orchardella*, and the lower Norian *Ancyrogondolella* (see above).

Species from the upper Carnian of PM were also assigned to *Epigondolella* by Mazza et al. (2012a, b; 2018) but, as discussed above, these were included in *Carnepigondolella* by Orchard (2014). These species are considered here as end-members of that clade, but if a separate genus was to be used, it should not be *Epigondolella* because neither that genus nor its lower Norian replacement, *Ancyrogondolella*, are directly related.

As discussed above, at least some records of *Epigondolella* from high Carnian and low Norian strata at PM can be re-assigned to *Primatella* (q.v.; Fig. 3). These specimens provided Mazza et al. (2012b) the basis for proposing continuity between *Carnepigondolella* and *Epigondolella*, which is disputed here. Rather, Orchard (2014) proposed a lineage from *Quadralella* to *Primatella* to *Ancyrogondolella* (formerly *Epigondolella*).

Genus: *Kraussodontus* Orchard, 2013

Type species: *Kraussodontus peteri* Orchard, 2013

Platform elements of this genus are characterized by largely subparallel lateral margins of generally uniform height, and a relatively rounded posterior margin that is never broader than the anterior platform. The anterior margins are smooth to weakly ornate. Both relative blade length and pit position varies. Species of *Kraussodontus* are most similar to some *Quadralella* but differ in their rounded, unexpanded posterior platforms.

Kraussodontus has not been widely differentiated in the past, but has now been recognized in the late Carnian of Okinawa-jima, Japan (Yamashita et al., 2016), and from the Taurus Mts., Turkey (Chen & Lukeneder, 2017). Some elements similar to *K. roberti* were included in *Metapolygnathus praecommunisti* by Mazza et al. (2011, fig. 3, D).

Genus: *Metapolygnathus* Hayashi, 1968

Type species: *Metapolygnathus communisti* Hayashi, 1968

The taxonomic scope of *Metapolygnathus* has changed in recent decades. Orchard (1991a, b) assigned almost all platform conodonts of Carnian age to the genus, although he recognised revision was necessary. Many of these species were later assigned to the new genus *Carnepigondolella*, or to those introduced more recently by Orchard (2013). A more restricted scope for *Metapolygnathus* limits it to the late Carnian clade around the type species, *Metapolygnathus communisti*, and its cohorts with mostly inornate platforms and an anteriorly shifted pit (Orchard, 2014). The origins of *Me. dylani* and *Me. parvus* lie in the diverse but uncommon older elements identified as morphotypes of *Me.* ex gr. *communisti* by Orchard (2014, see front-piece), and not within the more ornate *Quadralella praecommunisti*.

Noyan & Kozur (2007, p. 176) included four species in *Metapolygnathus*: *Me. communisti* with two subspecies (*Me. c. communisti* and *Me. c. parvus* – now elevated to species), *Me. linguiformis*, *Me. angustus*, and *Me. multinodosus*. The last of these was exceptional in bearing common anterior nodes. Later Mazza et al. (2012b, p. 112) restricted the genus to include only elements with an ".. absence of ornamentation or, at most, the presence of tiny nodes at geniculation points", a diagnosis followed by Orchard (2014). However, more recently Mazza & Martinez-Perez (2015, pl. 6) have divided the *Me. communisti* group into three morphotypes: A bears 1-2 anterior nodes; B corresponds to *Me. multinodosus*, and C has no nodes. At BBR, morphotypes A and B are included in *Me.* ex gr. *communisti* by Orchard (2014), whereas morphotype C, or *Quadralella multinodosus*, does not occur.

Other species previously assigned to *Metapolygnathus* that bear larger, more developed anterior nodes, i.e. *Me. mersinensis* and *Me. primitia*, are now referred to *Primatella* (see below). This includes *Me. mazzai*, the growth series of which (Mazza & Martínez-Pérez, 2015) includes *Pr. asymmetrica*. Notably, these authors also illustrated growth series of *Me. communisti* morphotypes that included elements close to *Pr. asymmetrica* (as morphotype B) and of *Parapetella irwini* (as morphotype C). This diversity appears to be a consequence of a focus on the anteriorly shifted pits of these elements, a feature that is seen also in species of *Parapetella*, *Primatella*, and *Quadralella*.

Metapolygnathus communisti is rare at BBR, where Orchard (2014, fig. 46) differentiated five uncommon morphotypes of *Me*. ex gr. *communisti*, all of which either lack anterior nodes or have one or two poorly developed; they differ from one another in their anterior profile and platform outline. Morphotypes 1–4 appear well below the CNB at BBR, before the common occurrence of the *Quadralella praecommunisti*. The inclusion of Morphotypes 1–4 into *Me. praecommunisti* by Mazza et al. (2018) broadens the scope of that species even more than its already substantial variability (Mazza et al., 2011), and obscures a more complex phylogeny. Two lineages may be represented - one with ornate *Quadralella* species (including *Q. praecommunisti*, *Q. multinodosus*), and a second with inornate *Metapolygnathus* species - both showing anterior pit migration, and ultimately reduction of the platform. The types of *Me. dylani* from BBR are mostly inornate like those of *Me*. ex gr. *communisti*, whereas most of those illustrated from PM are ornate. The final expression in these two lineages may be the diminutive and smooth *Me. parvus*, and some diminutive and noded specimens called *Me. echinatus* by Mazza et al. (2018, pl. 5).

Regarding *Metapolygnathus parvus*, Orchard (2014) differentiated three morphotypes (alpha, beta, and gamma) at BBR, each showing progressive reduction of the already small platform, ending in the platform-less gamma morphotype. As discussed above, the alpha morphotype corresponds broadly to the holotype of *Me. parvus*, but the beta and gamma morphotype of Mazza et al. (2018) differ. The beta morphotype of Orchard (2014) does not correspond to *Gladigondolella echinata* Hayashi, whose short platform has a distinctive anterior node on each margin. The identification of *Me. echinatus* in Orchard (2007c, pl. 2, figs 10-12, 22-24) was incorrect because those specimens, which were subsequently re-assigned to the *Me. parvus* beta morphotype (Orchard, 2014), are smooth or have only a few low nodes. Rather, strongly noded specimens like those referred to *Me. echinatus* by Mazza et al. (2018) are examples of *Parapetella destinae*, and one is closer to *Pa*. n. sp. D of Orchard, 2014 (Mazza et al., 2018).

Regarding the holotype of *Gondolella echinata*, the age of which is uncertain, Carter & Orchard (2013, p. 72, fig. 3. 10-12) discussed and illustrated a specimen from the top of the *C. samueli* Zone in Haida Gwaii that strongly resembles the holotype: they assigned it to *Carnepigondolella* and regarded it an end-member of that clade. Therefore, use of the specific name *echinatus* for *Me. parvus* Subzone CNB indices is discouraged.

Genus: *Paragondolella* Mosher, 1968

Type species: *Paragondolella excelsa* Mosher, 1968

Mazza et al. (2009) emphasized the lower side morphology as diagnostic for this genus, namely a posteriorly situated pit and no bifurcation of the keel, as well as a lack of any platform nodes on the upper surface. Also regarded as important features of the type species, *P. excelsa*, are the high anterior carina, and the absence of anterior geniculation points. The latter distinguishes it from all *Quadralella* species. Typical Ladinian *Paragondolella* species often have a broad, relatively flat platform, above which the carina is conspicuous in lateral view. Although platform ornament is generally absent, some species, e.g., P. *inclinata*, occasionally exhibit some weak anterior nodes (e.g., Orchard, 2007a, fig. 3. 1-3). Furthermore, according to Orchard (2005), the genus has a distinctive multielement apparatus.

Paragondolella certainly ranges into the lower Carnian, but probably no higher. Most of the species assigned to the genus by Mazza et al. (2009) should be assigned to *Quadralella*. This includes elements from PM assigned to *P. praelindae* that, unlike the holotype, display a geniculation point and free blade. These PM elements (Mazza et al., 2012b; Rigo et al., 2018) are probable examples of *Q. lobata*, characteristic of the *C. samueli* Zone at BBR.

Genus: *Parapetella* Orchard, 2013.

Type species: *Parapetella prominens* Orchard, 2013.

The genus *Parapetella* was introduced for conodont elements from BBR with mostly smooth anterior margins that become increasingly elevated into prominent buttresses. This genus has an uncertain origin but appears widespread in the upper Carnian (e.g., Carter & Orchard, 2013; Orchard, 2014), and apparently occurs in the lower Carnian of South China (Jiang, 2016). In common with several contemporaneous genera, species exhibit anterior pit migration and progressive diminution in the *Me. parvus* Subzone.

Parapetella was not explicitly differentiated at PM (Rigo et al., 2018; Mazza et al., 2018) although, as discussed above, *Pa. destinae* is one species that does occur there (identified as *Metapolygnathus echinatus*). Mazza et al. (2018, p. 88) also stated that *Parapetella pumilio*, *Pa. irwini*, *Pa. johnpauli,* and *Pa. willifordi* occurred at PM as "Tethyan morphotypes of the *Me. communisti* fauna", although only *Pa. irwini* was illustrated (i.e. Mazza et al., 2012b, see list below). Similarly, Mazza et al. (2018) synonymized *Metapolygnathus* n. sp. Y of Orchard, 2007c, as one of many morphotypes combined in an equally broad *Metapolygnathus praecommunisti*; they did not figure a specimen of the species, which was subsequently described by Orchard (2014) as *Parapetella broatchi*. Hence, up to eight species of *Parapetella* differentiated at BBR may also occur at PM:

?*Pa. broatchi* (= *Me*. n. sp. Y Orchard, 2007c = in synonymy with *Me. praecommunisti* in Mazza et al., 2018, p. 90.

Pa. clareae (= *Me. praecommunisti* in Mazza et al., 2011, pl. 2E only). **NA18**

Pa. destinae (= *Me. echinatus* in Mazza et al., 2012b, pl. 8, figs. 7, 8; =Mazza et al., 2010, pl. II, fig. 12; =Mazza et al., 2018, fig. 5.4 only). **NA39**

Pa. irwini (= *Me. communisti* in Mazza et al., 2012b, pl. 8, fig. 6 only). **NA37**

Pa. aff. *irwini* (= *Me. communisti* morphotype C, in Mazza & Martinez-Perez, 2015, pl. 6, fig. 25). **NA36–NA39**

Pa. johnpauli, *Pa. willifordi*, *Pa. pumilio* (= recorded but not figured as "Tethyan morphotypes of the *Me. communisti* fauna" in Mazza et al., 2018, p. 88).

?*Pa*. n. sp. D of Orchard, 2014 (=*Me. echinatus* in Mazza et al., 2018, fig. 5.2). **PM27**

Genus: *Primatella* Orchard, 2013

Type species: *Epigondolella primitia* **Mosher, 1970**

Primatella is characterized by larger and higher nodes or denticles than those of *Carnepigondolella*, and much more differentiated than those of *Quadralella*; those of *Ancyrogondolella* are much higher and sharper than in *Primatella* (Fig. 4). The genus appears rarely at the end of the *C. samueli* Zone at BBR and thereafter becomes more common until it dominates the lower Norian fauna above the *Me. parvus* Subzone in BBR. *Primatella* bridges the gap between the disappearance of *Carnepigondolella* (top *C. samueli* Zone) and the appearance of the *Ancyrogondolella* late in the *S. kerri* ammonoid Zone. *Primatella* is regarded as the precursor to *Ancyrogondolella*, but not as a derivative of *Carnepigondolella* but rather evolving from ornate *Quadralella* species (Orchard, 2014, figs. 20, 23). *Pr. primitia* itself is rather rare but it is retained as the zonal name-giver for sake of consistency.

Several ornate species previously assigned to *Metapolygnathus* - namely *Epigondolella primitia, Me. mersinensis*, and *Me. mazzai* - are assigned to *Primatella*. Also, a variety of elements from PM assigned to *Carnepigondolella* and *Epigondolella* are regarded as examples of *Primatella*. As discussed by Orchard (2014, p. 97), the holotype of *Me. mazzai* (in Mazza et al., 2012b) from PM (chosen by Karádi et al., 2013) appears to be fall within the range of *Me. mersinensis*. Those elements included in *Me. mersinensis* and illustrated by Mazza et al. (2012b) are regarded as a variety of *Primatella* and *Quadralella* species (see synonymy in Orchard, 2014, p. 94), including *Pr*. aff. *asymmetrica* and *Pr. subquadrata*. The *Me. mazzai* growth series of elements illustrated by Mazza & Martínez-Pérez (2015, pl. 7, fig. 15) also includes *Pr. asymmetrica*, whereas those illustrated by Karádi et al. (2013) have much larger anterior denticles than in *Primatella* and are regarded as closer to *Ancyrogondolella quadrata*.

In addition to the *Primatella* species discussed above, two other species have been misinterpreted at PM but are clearly useful for trans-Panthalassan correlation, namely *P. bifida* and *Pr. triangulare*. Orchard (2014, p. 89-90) included *Metapolygnathus linguiformis* sensu Mazza et al. (2012b) in synonymy with *P. bifida* but he did not regard the holotype of *Me. linguiformis* as conspecific as claimed by Mazza et al. (2018, p. 88). In contrast to *P. bifida* (and *Me. linguiformis* sensu Mazza et al.), Hayashi's species differs in having no anterior nodes, as previously discussed by Noyan & Kozur (2007, p. 172).

A second example concerns *Ancyrogondolella rigoi*. Mazza et al. (2018, p. 88) synonymized *Primatella triangulare* with *Epigondolella rigoi* but, as described by Orchard (2014, p. 105), *Pr. triangulare* differs in its posterior platform, lower anterior denticles, longer carina, and less pronounced keel bifurcation. Younger specimens of typical *An. rigoi*, which Noyan & Kozur (2007) regarded as diagnostic of a zone occurring above that of *An. quadrata*, are well illustrated by Mazza et al. (2012b). The long range attributed to *An. rigoi* by Rigo et al. (2018) apparently combines both that species and *Pr. triangulare*.

Other species assigned to *Primatella* at BBR include *Epigondolella orchardi*, and *E. pseudoechinata*, both of which have been included in *Carnepigondolella* at PM (Rigo et al., 2018). The type species of *E. orchardi* is from the lower Norian *E. orchardi* – *N. navicula* Zone of Slovakia (Kozur, 2003), the same age as attributed to *Primatella orchardi* at BBR. Specimens of *C. orchardi* illustrated by Mazza (2009, 2012b) are older and close to *C. pseudodiebeli* beta morphotype at BBR, whereas those illustrated by Nicora et al. (2007) and Balini et al. (2010) are probably true *Pr. orchardi*. As interpreted by Orchard (2014), *Pr*. ex gr. *pseudoechinata* embraces broad variation, but the only example of "*Carnepigondolella*" *pseudoechinata* illustrated from PM (Mazza et al., 2012b) is re-interpreted here as *C. spenceri* (see above).

The youngest species assigned by Mazza et al. (2018) with question to *Carnepigondolella*, *C*.? *gulloae*, is also interpreted here as a *Primatella* species with affinity with, and a possible origin in, *Pr. rotunda*. The appearance of the species at PM is sudden and without clear ancestry, so its FAD (T3 of Rigo et al., 2018) lacks context.

Pr. aff. *asymmetrica* (= *Me. communisti* morphotype B in Mazza & Martínez-Pérez, 2015, pl. 6, fig. 15). **NA36–NA39**

Pr. asymmetrica (= *Me. mazzai* in Mazza & Martinez-Perez, 2015, pl. 7, fig.15 only). **FNP117**

Pr. bifida (= *Me. linguiformis* in Mazza et al., 2012b, pl. 8, fig. 11; = Balini et al., 2010, pl. 4, fig. 1). **NA39**

Pr. mersinensis (= *Me. communisti* B in Mazza et al., 2010, pl. III, fig. 4). **NA46**

Pr. orchardi (= *C. orchardi* in Nicora et al. 2007, pl. 3, fig. 11). **NA33**

Pr. orchardi (= *C. orchardi* in Balini et al., 2010, pl. 3, fig. 30. **NA53**

Pr. aff. *permica* (= *E. rigoi* in Nicora et al., 2007, pl. 3, fig. 12). **NA33**

Pr. aff. *permica* (= *E. vialovi* in Mazza et al., 2010, pl. II, fig. 4). **NA29**

?*Pr. rhomboidale* (= *E. uniformis* in Mazza et al., 2012b, pl. 7, fig. 1). **NA46**.

Pr. ex gr. *rotunda* (= *C*.? *gulloae* in Mazza et al., 2012b, pl. 1, figs. 4, 6-9). **FNP134**, **PM30a**

Pr. subquadrata (= *Me. mersinensis* in Mazza et al., 2012b, pl. 4, fig. 7, 9). **NA30**, **NA34**

Pr. subquadrata–*Pr. permica* (=*E. quadrata* in Nicora et al., 2007, pl. 3, fig. 9. **NA30**; in Mazza et al., 2010, pl. II, fig. 3). **FNP112**

Pr. triangulare (= *E. rigoi* in Nicora et al., 2007, pl. 4, fig. 6 = Mazza et al., 2010, pl. II, fig. 5). **NA28**

Pr. aff. *triangulare* (= *C*.? *gulloae* in Mazza et al., 2012b, pl. 1, fig. 5 only). **FNP134**

Genus: *Quadralella* Orchard, 2013

Type species: ***Quadralella lobata*** **Orchard, 2013**

The oldest upper Carnian species at BBR are assigned to *Quadralella*, a genus introduced by Orchard (2013) with a type species, *Q. lobata*. The genus is characterized by anterior geniculation points and anterior ornament that varies from absent to low, weakly differentiated, and irregular nodes. In lateral view, these nodes are often defined by incisions into the anterior platform margins whereby the nodes do not rise above the posterior platform margins as they do in *Primatella* (Fig. 4). *Paragondolella* lacks geniculation points, and both *Carnepigondolella* and *Ancyrogondolella* have more organized and sharper anterior denticulation.

Although focussed on upper Carnian taxa, Orchard (2013, p. 456) thought it probable that older taxa should be referred to *Quadralella*, including *Gondolella polygnathiformis* and *Metapolygnathus nodosus*. This comment seems to have been overlooked by Kiliç et al. (2015), who subsequently introduced a new genus, *Hayashiella*, with the unfortunate choice of *Me. nodosus* as the type species. The holotype of that species is of uncertain age and unknown morphological range because it originated in a poorly preserved and stratigraphically mixed fauna extracted from chert in Japan (Hayashi, 1968). In fact, the holotype of *Me. nodosus* has been favourably compared to '*Epigondolella*' *carnica* (see discussion in Noyan and Kozur, 2007, p. 173), which was chosen as the type species of a second new genus *Mazzaella* Kiliç et al. Notwithstanding those uncertainties, the scope of *Hayashiella* Kiliç et al. is embraced by *Quadralella*. Besides, the name *Hayashiella* is preoccupied for a beetle (Vives & Ohbayashi, 2001). Hence, *Hayashiella* is both a junior synonym and a junior homonym.

Mazza et al. (2018) have recently argued for the suppression of *Quadralella* because the lower Carnian *Metapolygnathus lobatus* was erroneously mislabelled "*Quadralella lobatus*" (sic) in a review paper on Middle to Upper Triassic conodonts (Chen at al., 2015, fig. 4). This apparent homonymy arose due to an uncritical re-assignment of all lower Carnian species formerly referred to *Metapolygnathus* by Orchard (2007a) to *Quadralella* subsequent to the former genus being more narrowly defined in the upper Carnian (Orchard, 2014). The lower Carnian *Me. lobatus* is not a *Quadralella* but an example of *Paragondolella*, probably derived from *P. inclinata*. *Quadralella lobata* Orchard, 2013 remains the type species of the genus *Quadralella*.

The species *Quadralella praecommunisti*, which first appears in the *Ac. angusta – Me. dylani* Subzone of the *Pr. primitia* Zone at BBR, is regarded as an advanced *Quadralella* with a forward shifted pit, and not a precursor to the inornate *Metapolygnathus communisti*. Elements of the latter group, which are rare at BBR, occur much earlier at BBR and are thought to be unrelated to *Q. praecommunisti*, which is common in the latest Carnian there. At PM, *Q. praecommunisti* appears earlier but is much broader in scope (Mazza et al., 2011), including some elements similar to *Parapetella* and *Kraussodontus*. There appears to be no examples at BBR of more advanced species with a more anteriorly shifted pit, as in *Q. multinodosus*, or with reduced platforms, as in some ornate elements referred to *Me. dylani* by Mazza et al. (2018).

More ornate species of *Quadralella*, such as *Q. kathleenae* and *Q. willistonensis*, may also occur at PM although it is difficult to evaluate isolated specimens. They too occur in the *C. samueli* Zone, earlier than at BBR. The two species mentioned above are characterized by posterior pits, unlike the similar *Q. praecommunisti* and *Q. mcrobertsi*, which are also noded species but with more medial pits (see below). The following species assigned to *Quadralella* explicitly occur at both BBR and PM (from Mazza et al., 2012b; Rigo et al., 2018, with their former generic assignment):

Q. angulata (previously *Carnepigondolella*)
Q. carpathica (previously *Carnepigondolella*, then *Hayashiella*)
Q. noah (previously *Paragondolella*)
Q. oertlii (previously *Paragondolella*)
Q. praecommunisti (previously *Metapolygnathus*)
Q. tuvalica (previously *Carnepigondolella*, then *Hayashiella*)

Additional species of *Quadralella* interpreted from the literature may include:

?*Q. kathleenae* (= *C. pseudodiebeli* Morphotype A in Mazza et al., 2012b, pl. 2, fig. 8). **FNP53a**
Q. lobata (= *P. praelindae* in Mazza et al., 2012b, pl. 7, fig. 13; Rigo et al., 2018, fig. 6.6d). **NA4a**
Q. lobata (= *P. noah* in Mazza & Martinez-Perez, 2015, pl. 1, figs.1-5 only). **NA2**, **PM3a**
Q. praecommunisti (= *Me. praecommunisti* in Mazza et al., 2011, fig. 2C, fig. 3C, F, G, H).
?*Q. willistonensis* (= *Me. mersinensis* in Mazza et al., 2012b, pl. 4, figs., 5, 8). **FNP53**, **NA22**

PLACEMENT OF THE CARNIAN-NORIAN BOUNDARY

Event horizons recognized at BBR and suggested primary options for definition of the CNB cluster around the range of *Metapolygnathus parvus*: the base (T2 at PM), top (~T3 at PM), or a datum within *Me. parvus* Subzone. The earlier end-*Carnepigondolella* event (top *C. samueli* Zone) is also a primary biostratigraphic marker but it clearly lies within the upper Carnian even though the position of PM-T1 is disputed.

The highest suggested position for the CNB is at the base of the *Carnepigondolella*? *gulloae* Zone at PM, or the top of the *Me. parvus* Subzone at BBR, which are close but not coincident. The event is marked at BBR by the disappearance of all the diminutive conodont species that dominate the upper division of the *Me. parvus* Subzone. This might be viewed as a natural Norian base after disappearance of Carnian stocks, but the datum does not clearly correspond to the appearance of any common conodont taxon. At PM, the first appearance datum (FAD) of *Primatella gulloae* is suggested to be an approximation of this level, although *Metapolygnathus parvus* ranges higher there (Fig. 3). However, as discussed above, *Pr. gulloae* is regarded as a member of the *Pr. rotunda* group, which appears at BBR below the *Me. parvus* Subzone and may contain a precursor for *Pr. gulloae*. At the moment, in the absence of a known ancestry, the choice of *Pr. gulloae* as a CNB index is problematic.

In support of defining the CNB at the top of the *Me. parvus* Subzone is the totality of ammonoid data from British Columbia. Ammonoid fauna of the traditionally latest Carnian *Klamathites macrolobatus* Zone (see Tozer, 1994) is known from many western Canadian localities and many of them have also yielded conodonts. Figure 5 shows the subzonal assignment

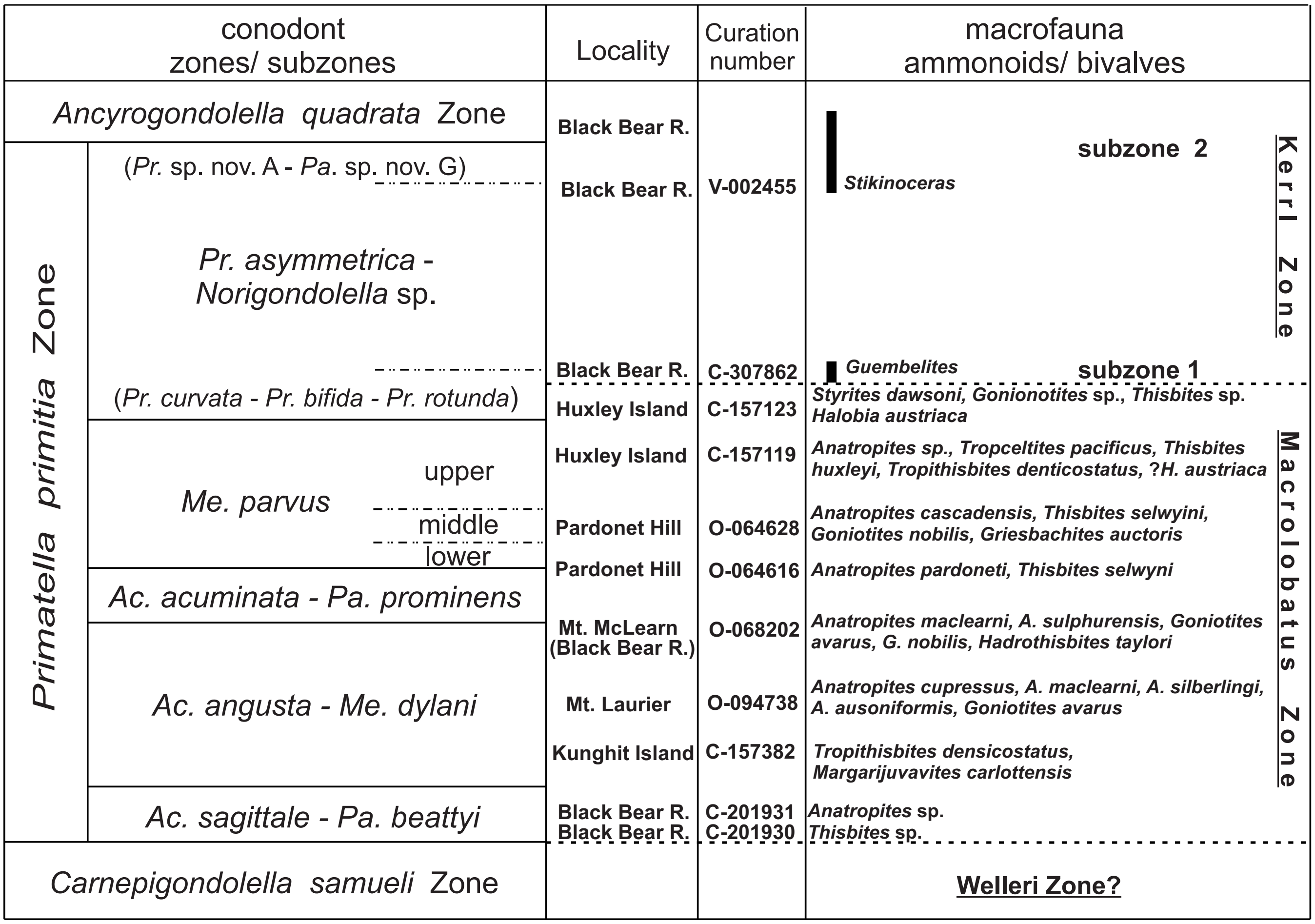

Figure 5 – Composition of *Klamathites macrolobatus* Zone ammonoid faunas (partly after Tozer, 1994), accompanying halobiids, and their assignment to conodont subzones of the *Pr. primitia* Zone. The oldest collections are in section at Black Bear Ridge, two are archive from Pardonet Hill (see Orchard, 2014, fig. 30), two are archive from elsewhere in northeastern B.C. (Mount Laurier, Mount McLearn), and three are from Kunghit and Huxley islands, Haida Gwaii (Wrangell Terrane). These collectively demonstrate that the stratigraphic scope of the *K. macrolobatus* Zone embraces the *Pr. primitia* Zone up to and including the *Me. parvus* Subzone at Black Bear Ridge, including the ~5 m CNB interval that lacks ammonoid zonal indices. The occurrences of the lower and upper *S. kerri* Zone indices (vertical bars) at BBR are also shown. (Modified from Orchard, 2014, fig. 31).

of nine conodont collections, which are from a variety of *K. macrolobatus Zone* faunas and localities, most of them characterized by the diagnostic ammonoid *Anatropites*. At BBR it has been demonstrated that this ammonoid zone corresponds to the *Acuminatella sagittale - Parapetella beattyi* and *Ac. angusta - Metapolygnathus dylani* subzones of the lower *Pr. primitia* Zone, while other localities support that calibration and extend it upward through the *Me. parvus* Subzone and just beyond. A single *K. macrolobatus* Zone collection (lacking *Anatropites*) from Huxley Island, Haida Gwaii contains only *Primatella* conodonts and is regarded as younger than the *Me. parvus* Subzone. Both this latter collection and a second from nearby on Huxley Island may also contain *Halobia austriaca*, which is consistent with the FAD of that species in the *Me. parvus* Subzone of BBR.

Hence, it appears that the totality of the *Me. parvus* Subzone, as well as the entire lower *Pr. primitia* Zone, is embraced by the traditionally uppermost Carnian *K. macrolobatus* Zone. This also conforms to the lowest occurrence of the lower Norian *S. kerri* Zone species *Guembelites clavatus* immediately above the *Me. parvus* Subzone at BBR, low in the *Pr. asymmetrica - Norigondolella* sp. Subzone. A consequence of a position at the base of the *Me. parvus* Zone for the CNB places the upper part of the "Carnian" *K. macrolobatus* ammonoid Zone in the Norian.

The choice of the base *Me. parvus* Subzone/ Zone as the definitive CNB datum, as advocated by Mazza et al. (2018), has many advantages in spite of the realignment of the ammonoid zones. These are summarized in Figure 6. As has been noted previously, the major faunal turnover occurs around the *Me. parvus* Subzone where most long-ranging Carnian genera and numerous species disappear over several metres of strata. Prior to this, there is a rise in the abundance of small conodont elements, the forebears of which are known in the preceding beds (Orchard, 2014, figs. 13, 15, 16), and then they too disappear (Fig. 6, A). Two genera, *Acuminatella* and *Primatella*, continue on and in higher strata are joined by *Norigondolella*. This turnover is complete by the end of the *Me. parvus* Subzone, whereas its lower division is marked by most of the extinctions and by first appearances of key macrofaunal elements, including *Halobia* *austriaca* and *Pterosirenites* (Fig. 2); these latter taxa have been regarded as Norian indicators.

Geochemical data from BBR point to underlying causes for the biological events. Williford et al. (2007; Fig. 6, B) identified a small but significant negative excursion of the carbon isotope of total organic carbon with a minimum precisely between the lower and middle divisions of the *Me. parvus* Subzone. This suggests the presence of low oxygen conditions that were conducive to efficient burial of organic matter (Williford et al., 2007). Later, Onoue et al. (2015) presented further geochemical data that they interpreted as recording a period of deep-water anoxic deposition (indicated by the V/(V + Ni) and V/Cr indices), and reflecting a transition from dysoxic conditions in the *Ac. acuminata–Pa. prominens* Subzone to anoxic conditions in the *Me. parvus* Subzone; $\delta^{13}C_{carb}$ values increased through these zones and then decreased in the *Pr. asymmetrica–Norigondolella* sp. Subzone (Fig. 6, C). Onoue et al. (2015) linked the conodont faunal turnover event with a widespread oceanic anoxic event, but noted $^{87}Sr/^{86}Sr$ and $\delta^{13}C_{carb}$ isotopic data largely exclude the possibility that the event was triggered by dissociation of methane hydrates and degassing related to large-scale volcanic activity.

Very recent work has looked at the oxygen isotopes preserved in conodont apatite (Sun et al., 2019; in press; Fig. 6, D). These indicate temperature increase of several degrees into the *Me. parvus* Subzone followed by lower temperatures in the *Pr. asymmetrica – Norigondolella* Subzone. Sun et al. (2019) also determined that *Quadralella* and *Norigondolella* were cooler/deeper water genera. The first of these conodonts disappears as both deep water anoxia and elevated temperatures are indicated, whereas *Norigondolella* appears and becomes common during the cooling trend in the earliest Norian. All these events provide boundary proxies for definition of the CNB. The FAD of

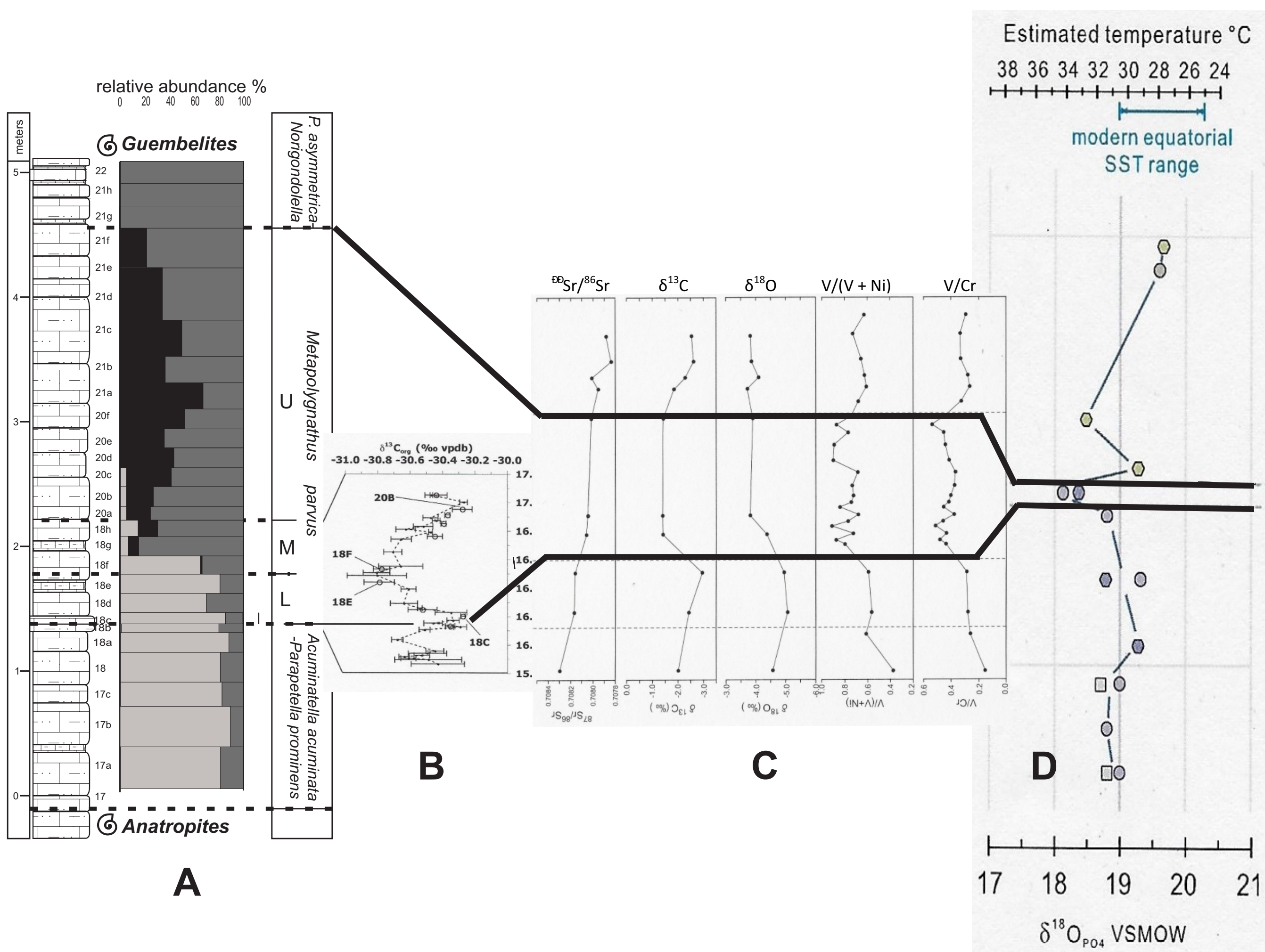

Figure 6 – Conodont fauna and zonation through a 5 m boundary interval in the Pardonet Formation between the highest *K. macrolobatus* (*Anatropites*) Zone and lowest *S. kerri* (*Guembelites*) Zone ammonoid indicators. A. Shows replacement of typical Carnian conodonts (pale gray bars) by *Primatella* and *Acuminatella* (medium gray bars) with an intervening bloom of diminutive derivatives (black bars) during the *Me. parvus* Subzone (after Orchard, 2014, fig. 6). B. Peak negative organic carbon isotope excursion at the lower-middle division boundary of the *Me. parvus* Subzone (after Williford et al., 2007). C. Isotope geochemistry showing excursions at the base and top of the *Me. parvus* Subzone (after Onoue et al., 2016). D. Paleotemperatures derived from conodont apatite $\delta^{18}O_{PO4}$ showing an increase in temperature in the *Me. parvus* Subzone and subsequent drop. Data are calibrated to NBS 120c with an analytical uncertainty of ±0.14 ‰ (1 σ). Genus-specific depth corrections are applied; circle, hexagon and square stand for data measured on *Quadralella*, *Primatella* and *Carnepigondolella*, respectively (after Sun et al., 2019; in press).

Metapolygnathus parvus alpha morphotype at the base of the *Me. parvus* Subzone/ Zone may serve that purpose. However, the scope of this index fossil and its ancestry need to be well defined. Notably, *Primatella asymmetrica* and *Pr. rhomboidale* also appear at the base of the *Me. parvus* Zone at BBR and are known to occur at PM. Similarly, the FAD of *Parapetella johnpauli* and *Pa. willifordi* mark the base of the middle division of the *Me. parvus* Subzone at BBR, and these too are noted to occur at PM. None of these species have been well documented at PM so their full utility remains unknown.

SUMMARY

The conodont taxonomy about the Carnian-Norian boundary (CNB) interval at the GSSP candidate at Black Bear Ridge (BBR), British Columbia is reviewed and compared with that used at Pizzo Mondello (PM), Sicily. Correlation of these sections has been impeded to some extent by fossil endemism but it is concluded that differing taxonomic approaches have obscured similarities. Both the North American (BBR) and Tethyan (PM) conodont successions contain species of the platform genera *Carnepigondolella*, *Ancyrogondolella*, ?*Kraussodontus*, *Metapolygnathus*, *Norigondolella*, *Parapetella*, *Primatella*, and *Quadralella*; only *Acuminatella* and some non-platform genera appear to be endemic, although there may be endemic species. Further nomenclatural and taxonomic revisions revise the use of several generic names at PM: *Quadralella* is valid and a senior synonym of *Hayashiella*; *Paragondolella* is an inappropriate name for upper Carnian species; "*Epigondolella*" species at PM are revised as *Carnepigondolella* in the upper Carnian, as *Primatella* around the CNB, and as *Ancyrogondolella* in the lower Norian. The evolutionary trend of anterior pit migration is recognized in all 6 genera that exist in the lower part of the *Pr. primitia* Zone at BBR (Orchard, 2014) so the practise of combining in a single genus all specimens with an anterior pit (as in *Metapolygnathus*) obscures relationships.

These revisions suggest that faunal turnover intervals at PM-T1 and -T3 were not endemic events (Mazza et al., 2018, pp. 83, 88, 90) but can be recognized at BBR by reference to evolutionary events in, respectively, *Carnepigondolella* and *Primatella*. At PM, these are cast as, respectively, a transition from *Carnepigondolella* to *Epigondolella* (T1), and as a sudden appearance of *C*.? *gulloae* (T3). At BBR, the transitional species near the top of the *C. samueli* Zone are all included in *Carnepigondolella*, whereas the *C*.? *gulloae* fauna is allied to, and is now assigned to, the *Primatella* fauna that dominates above the *Me. parvus* Subzone.

Hence, it is concluded that: the top of the *C. samueli* Zone at BBR is equivalent to a position within the "*E.*" *vialovi* Zone at PM; the overlying zone containing *Primatella* species crosses the CNB in both sections, including *Pr. asymmetrica*, *Pr. bifida*, *Pr*. aff. *permica*, ?*Pr. rhomboidale*, *Pr. subquadrata*, and *Pr. triangulare*; correlation of the *Me. parvus* Subzone within the *Pr. primitia* Zone is strengthened by these and other revised conodont occurrences, including *Parapetella destinae*, *Pa. johnpauli*, *Pa. willifordi*, *Pa. pumilio*, and *Pa. irwin*i; and the well-known lower Norian succession of *Ancyrogondolella quadrata* followed by *An. triangularis* in western Canada appears corrupted at PM (sample NA43).

As previously concluded, the *Me. parvus* Sub-/ Zone can be correlated between both sections based on the FAD of the nominal conodont (PM-T2) as well as the demise of many typical Carnian taxa, and is a suitable datum for definition of the CNB. However, the morphological scope of the index species and its morphotypes needs agreement, as does its evolutionary cline. Orchard (2014, front piece) illustrated the progression from *Metapolygnathus* ex gr. *communisti* to *Me. dylani* to *Me. parvus,* but these did not include ornate elements like those shown by Mazza et al. (2018), for which reason *Quadralella praecommunisti* and *Q. multinodosus* are excluded from that genus.

It is demonstrated that, based on both BBR and other British Columbian locations from where diagnostic ammonoid faunas are known in association with conodonts, a CNB defined at the base of the *Me. parvus* Subzone has the effect of placing the upper part of the traditional Carnian *K. macrolobatus* ammonoid Zone in the Norian. On the plus side, additional fossil (e.g., *Halobia austriaca*, *Pterosirenites* sp.) and geochemical proxies coincide with the *Me. parvus* Subzone.

At BBR, the highly resolved taxonomy provides numerous morphospecies as guide fossils. It also provides documentation of a progressive diminution of surviving clades around the CNB, particularly in *Metapolygnathus* and *Parapetella*. These observations have not been explicitly recorded at PM where the *Me. parvus* Zone (~12 m thick) is undifferentiated, although the presence of diminutive taxa is indicated. This biological event appears related to geochemical observations at BBR that imply paleoecological stress in terms of both anoxia and temperature. Considering generic preferences, the disappearance of *Quadralella* and the later appearance of common *Norigondolella* may reflect the direct impact of these changes.

ACKNOWLEDGEMENTS

I thank Martyn Golding, Leo Krystyn, Chris McRoberts for their reviewer comments. In so much as this work draws on data reported in a previous publication (Orchard, 2014), I acknowledge the support of the Geological Survey of Canada and the collaboration of those cited in that work.

REFERENCES

Balini, M., Bertinelli, A., Di Stefano, P., Guaiumi, C., Levera, M., Mazza, M., Muttoni, G., Nicora, A., Preto, N. & Rigo, M. 2010. The Late Carnian-Rhaetian succession at Pizzo Mondello (Sicani Mountains). Albertiana, 39: 36–61.

Balini, M., Krystyn, L., Levera, M. & Tripodo, A. 2012. Late Carnian-Early Norian ammonoids from the GSSP candidate section Pizzo Mondello (Sicani Mountains, Sicily): Rivista Italiana di Paleontologia e Stratigrafia, 118: 47–84.

Balini, Me., Jenks, J.F., Martin, R., McRoberts, C.A., Orchard, M.J. & Silberling, N.J. 2014. A new Carnian/Norian boundary section from Berlin-Ichthyosaur State Park (Upper Triassic, central Nevada, USA). Palaontologische Zeitschrift. DOI 10.1007/s12542-014-0244-2

Carter, E.S. & Orchard, M.J. 2013. Intercalibration of conodont and radiolarian faunas from the Carnian-Norian Boundary Interval in Haida Gwaii, British Columbia, Canada. *In*, Tanner, L.H., Spielman, and Lucas, S.G. (eds.), The Triassic System. New Mexico Museum of Natural History and Science, Bulletin 61: 67–92.

Chen, Y., Krystyn, L., Orchard, M.J., Lai, X, & Richoz, S. 2015. A review of the evolution, biostratigraphy, provincialism, and diversity of Middle and Early Late Triassic conodonts. Papers in Palaeontology, 2: 235–263.

Chen, Y. & Lukeneder, A. 2017. Late Triassic (Julian) conodont biostratigraphy of a transition from reefal limestones to deep-water environments on the Cimmerian Terranes (Taurus Mountains, S. Turkey). Palaeontology, 3(3): 441–460.

Hayashi, S., 1968a. The Permian conodonts in chert of the Adoyama Formation, Ashio Mountains, central Japan. Journal Earth Science Japan, 22(2): 63–77.

Hayashi, S., 1968b, Redescription of new forms proposed in "The Permian conodonts in chert of the Adoyama Formation, Ashio Mountains, central Japan," 1968, by Shingo Hayashi. Journal Earth Science Japan, 22(6): p. 11.

Jiang, H., Yuan, J., Chen, Y., Ogg, J.G. & Yan, J. 2019. Synchronous onset of the Mid-Carnian Pluvial Episode in the East and West Tethys: Conodont evidence from Hanwang, Sichuan, South China. Palaeogeography, Palaeoclimatology, Palaeoecology, 520: 173–180.

Johns, M.J., Barnes, C.R. & Orchard, M.J., 1997. Taxonomy and biostratigraphy of Middle and Late Triassic elasmobranch ichthyoliths from northeastern British Columbia. Geological Survey Canada, Bulletin 502: 1–235.

Karádi, V., Kozur, H.W. & Gorog, A. 2013. Stratigraphically important Lower Norian conodonts from the Csövar Borehole (CSV-1), Hungary - comparison with the conodont succession of the Norian GSSP candidate Pizzo Mondello (Sicily, Italy). *In*, Tanner, L.H., Spielman, J.A., and Lucas, S.G. (eds.), The Triassic System: New Mexico Museum of Natural History and Science Bulletin 61: 445–457.

Kiliç, A. M., Plasencia, P., Ishida, K. & Hirsch, F. 2015. The Case of the Carnian (Triassic) Conodont Genus *Metapolygnathus* Hayashi. Journal of Earth Science, 26(2): 219–223. doi:10.1007/s12583-015-0534-y

Kozur, H.W. 2003. Integrated ammonoid, conodont and radiolarian zonation of the Triassic. Hallesches Jahrbuch für Geowissenschaften, 25: 49–79.

Mazza, M., Furin, S., Spotl, C. & Rigo, M. 2010. Generic turnovers of Carnian/Norian conodonts: Climatic control or competition? Palaeogeography, Palaeoclimatology, Palaeoecology, 290: 120–137. doi: 10.1016/j.palaeo.2009.07.006

Mazza M., Cau A., and Rigo M. 2012a, Application of numerical cladistic analyses to the Carnian-Norian conodonts: a new approach for phylogenetic interpretations: Journal of Systematic Palaeontology, 10(3): 401–422.

Mazza, M., Rigo, M. & Gullo, M. 2012b. Taxonomy and biostratigraphic record of the Upper Triassic conodonts of the Pizzo Mondello section (western Sicily, Italy), GSSP candidate for the base of the Norian. Rivista Italiana di Paleontologia e Stratigrafia, 118: 85–130.

Mazza, M. & Martínez-Pérez, C. 2015. Unravelling conodont (Conodonta) ontogenetic processes in the Late Triassic through growth series reconstructions and X-ray microtomography Bollettino della Società Paleontologica Italiana, 54 (3): 161-186. doi:10.4435/BSPI.2015.10

Mazza, M. & Martínez-Pérez, C. 2016. Evolutionary convergence in conodonts revealed by Synchrotron-based Tomographic Microscopy. Palaeontologia Electronica 19.3.52A: 1–11 palaeo-electronica.org/content/2016/1710-conodont-x-ray-tomographies

Mazza, M., Nicora, A. & Rigo, M. 2018. *Metapolygnathus parvus* Kozur, 1972 (Conodonta): a potential primary marker for the Norian GSSP (Upper Triassic). Bollettino della Società Paleontologica Italiana, 57 (2): 81–101. doi:10.4435/BSPI.2018.06

McGowan, C., 1995. A remarkable small ichthyosaur from the Upper Triassic of British Columbia, representing a new genus and species. Canadian Journal of Earth Sciences, 32(3): 292–303.

McGowan, C., 1996. A new and typically Jurassic ichthyosaur from the Upper Triassic of British Columbia. Canadian Journal of Earth Sciences, 33(1): 24–32.

McRoberts, C.A. 2011, Late Triassic Bivalvia (chiefly Halobiidae and Monotidae) from the Pardonet Formation, Williston Lake area, northeastern British Columbia, Canada. Journal of Paleontology, 85(4): 613–664.

McRoberts, C.A. & Krystyn, L. 2011. The FOD of *Halobia austriaca* at Black Bear Ridge (northeastern British Columbia) as the base-Norian GSSP: 21st Canadian Paleontology Conference, UBC, August 19–21, Proceedings 9: 38–9.

Moix, P., Kozur, H.W., Stampfli, G.M. & Mostler, H. 2007. New paleontological, biostratigraphic and paleogeographic results from the Triassic of the Mersin Mélange, SE Turkey. *In*, Lucas, S.G., and Spielmann, J.A. (eds.), The Global Triassic: New Mexico Museum of Natural History and Science Bulletin 41: 282–311.

Mosher, L.C., 1968a. Triassic conodonts from western North America and Europe and their correlation. Journal of Paleontology, 42(4): 895–946.

Mosher, L.C., 1968b. Evolution of Triassic platform conodonts. Journal of Paleontology, 42(4): 947–954.

Muttoni, G., Kent, D.V. & Orchard, M.J. 2001. Paleomagnetic reconnaissance of early Mesozoic carbonates from Williston Lake, northeastern British Columbia, Canada: evidence for late Mesozoic remagnetization. Canadian Journal of Earth Science 38: 1157–1168.

Nicora, A., Balini, M., Bellanca, A., Bertinelli, A., Bowring, S.A., Di Stefano, P., Dumitrica, P., Guaiumi, C., Gullo, M., Hungerbuehler, A., Levera, M., Mazza, M., McRoberts, C.A., Muttoni, G., Preto, N. & Rigo, M. 2007. The Carnian/Norian boundary interval at Pizzo Mondello (Sicani Mountains, Sicily) and its bearing for the definition of the GSSP of the Norian Stage. Albertiana 36: 102–129.

Noyan, Ö. F. & Kozur, H.W. 2007. Revision of the Late Carnian-Early Norian conodonts from the Stefanion section (Argolis, Greece) and their palaeobiogeographic implications: Neues Jahrbuch für Geologie und Paläontologie, Abhandlungen, 245(2): 159–178.

Onoue, T., Zonneveld, J-P, Orchard, M. J., Yamashita, M., Yamashita, K., Sato, H. & Kusaka, S. 2016. Paleoenvironmental changes across the Carnian/Norian boundary in the Black Bear Ridge section, British Columbia, Canada. Palaeogeography, Palaeoclimatology, Palaeoecology, 441: 721–733.

Orchard, M. J., 1983. *Epigondolella* populations and their phylogeny and zonation in the Norian (Upper Triassic). Fossils and Strata, 15: 177–192.

Orchard, M. J., 1991a. Late Triassic conodont biochronology and biostratigraphy of the Kunga Group, Queen Charlotte Islands, British Columbia. *In*, Woodsworth, G.W. (ed.), Evolution and Hydrocarbon Potential of the Queen Charlotte Basin, British Columbia. Geological Survey of Canada Paper 1990-10: 173–193.

Orchard, M.J., 1991b. Upper Triassic conodont biochronology and new index species from the Canadian Cordillera. *In*, Orchard, M.J. and McCracken, A.D. (eds.), Ordovician to Triassic Conodont Paleontology of the Canadian Cordillera. Geological Survey of Canada Bulletin 417: 299–335.

Orchard, M.J. 2005. Multielement conodont apparatuses of Triassic Gondolelloidea. Special Papers in Palaeontology, 73: 73–101.

Orchard, M.J. 2007a. New conodonts and zonation, Ladinian-Carnian boundary beds, British Columbia, Canada. New Mexico Museum of Natural History and Science, Bulletin 41: 321–330.

Orchard, M.J. 2007b. Conodont lineages from the Carnian-Norian boundary at Black Bear Ridge, northeast British Columbia: New Mexico Museum of Natural History and Science, Bulletin 41: 331–332.

Orchard, M.J. 2007c. A proposed Carnian-Norian boundary GSSP at Black Bear Ridge, northeast British Columbia, and a new conodont framework for the boundary interval. Albertiana, 36: 130–141.

Orchard, M.J. 2010. Triassic conodonts and their role in stage boundary definition, in Lucas, S. G., ed., The Triassic Timescale. Geological Society, London, Special Publications, 334: 139–161.

Orchard, M.J. 2013. Five new genera of conodonts from the Carnian-Norian Boundary beds, northeast British Columbia, Canada. *In*, Tanner, L.H., Spielman, and Lucas, S.G. (eds.), The Triassic System: New Mexico Museum of Natural History and Science, Bulletin 61: 445–457.

Orchard, M.J. 2018. The Lower-Middle Norian (Upper Triassic) Boundary: new conodont taxa and a refined zonation. Conodont Studies Dedicated to the Careers and Contributions of Anita Harris, Glenn Merrill, Carl Rexroad, Walter Sweet, and Bruce Wardlaw. *In*, Over, D.J. & Henderson, C.M. (eds.), Bulletins of American Paleontology, 395–396: 165–193. doi: 10.32857/bap.2018.395.12

Orchard, M.J., McRoberts, C.A., Tozer, E.T., Johns, M.J., Sandy, M.R. & Shaner, J.S. 2001a. An intercalibrated biostratigraphy of the Upper Triassic of Black Bear Ridge, Williston Lake, northeast British Columbia. Geological Survey of Canada Current Research 2001-A6: 1–10.

Orchard, M.J., Zonneveld, J-P., Johns, M.J., McRoberts, C.A., Sandy, M.R., Tozer, E.T. & Carrelli, G.G. 2001b. Fossil succession and sequence stratigraphy of the Upper Triassic and Black Bear Ridge, northeast B.C., and a GSSP prospect for the Carnian-Norian boundary. Albertiana, 25: 10–22.

Rigo, M., Mazza, M., Karádi, V. & Nicora, A. 2018. New Upper Triassic conodont biozonation of the Tethyan Realm. *In*, Tanner, L. (ed.), The Late Triassic World, Topics in Geobiology, 46: 189–235.

Sun, Y.D., Wignall, P.B., Joachimski, M.M., Bond, D.P.G., Grasby, S.E., Lai, X.L., Wang, L.N., Zhang, Z.T. and Sun, S., 2016. Climate warming, euxinia and carbon isotope perturbations during the Carnian (Triassic) Crisis in South China. Earth and Planetary Science Letters, 444: 88–100.

Sun, Y.D., Orchard, M.J. & Joachimski, M.M. 2019. Palaeotemperature evolution in the Carnian-Norian transition (Late Triassic): conodont oxygen isotope evidence from the Canadian Cordillera. EGU General Assembly, Vienna, EGU2019–8232.

Sweet, W.C. 1988. The Conodonta. Morphology, Taxonomy, Paleoecology, and Evolutionary History of a Long-Extinct Animal Phylum. Clarendon Press, Oxford, 218 p.

Tozer, E.T., 1994. Canadian Triassic ammonoid faunas. Geological Survey of Canada, Bulletin 467: 663 p.

Vives, E. & Ohbayashi, N. 2001. A new lepturine, *Hayashiella malayana* gen. et sp. nov. from Sabah, Malaysia (Coleoptera, Cerambycidae). Japanese Journal of Systematic Entomology, 7(1): 29–33.

Williford, K.H., Orchard, M.J., Zonneveld, J.P., McRoberts, C.R. & Beatty, T.W. 2007. A record of stable organic carbon isotopes from the Carnian-Norian boundary section at Black Bear Ridge, Williston Lake, British Columbia, Canada. Albertiana, 36: 146–148.

Yamashita, D., Yasuda, C., Ishibashi, T., Martini, R. & Onoue, T. 2016. Stratigraphy and conodont and ammonoid ages of Upper Triassic Nakijin Formation in Hedomisaki area, Okinawa-jima, Japan. Journal of the Geological Society of Japan, 122 (9): 477–493.

Yamashita, H., Kato, H., Onoue, T. & Suzuki, N. 2018. Integrated Upper Triassic conodont and radiolarian biostratigraphies of the Panthalassa Ocean. Paleontological Research, 22 (2): 167–197.

Zhang, Z.T., Sun, Y.D., Joachimski, M.M. & Wignall, P. 2017. Early Carnian conodont fauna at Yongyue, Zhenfeng area and its implication for Ladinian-Carnian subdivision in Guizhou, South China. Palaeogeography, Palaeoclimatology, Palaeoecology, 486: 142–157.

Zhang, Z.T., Sun, Y.D., Wignall, P.B., Fu, J.L., Li, H.X., Wang M.Y. & Lai, X.L. 2018. Conodont size reduction and diversity losses during the Carnian (Late Triassic) Humid Episode in SW China. Journal of Geological Society, 175: 1027–1031.

Zonneveld, J-P., Beatty, T.W., Williford, K.H., Orchard, M.J. & McRoberts, C.A. 2010. Stratigraphy and sedimentology of the lower Black Bear Ridge section, British Columbia: candidate for the base-Norian GSSP. Stratigraphy, 7: 61–82.

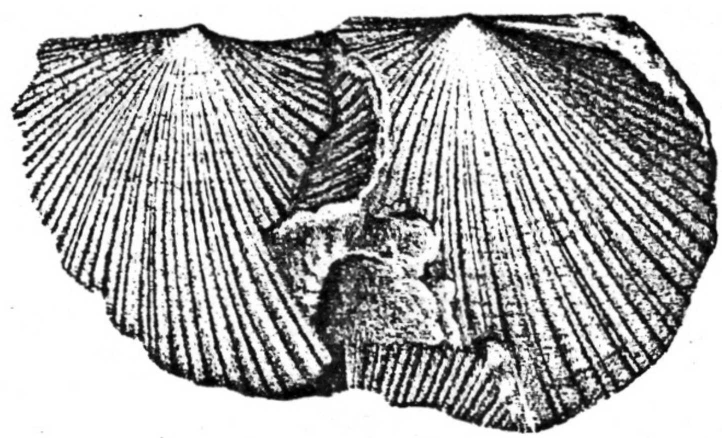

FROM THE SECRETARY

VOTING RESULTS FOR NEW SUBCOMMISSION ON TRIASSIC STRATIGRAPHY EXECUTIVE, OCTOBER 30, 2019

Following IUGS and ICS statutes, a new slate for the 2020-2024 STS Executive is required by the close of 2019. The slate of candidates were nominated by the current executive. Ballots were sent by e-mail to all 24 voting members of the STS. Twenty-two completed ballots were returned by the specified time for a return rate of 92% and the results are tabulated below:

	Yes	No	Abstain	% Affirmative
For Chair: Zhong-Qiang Chen	21	1	0	87.5
For Vice Chair: Wolfram Kürschner	20	1	1	83.3

Both Zhong-Qiang Chen (Wuhan, China) for Chair and Wolfram Kürschner (Oslo, Norway) for Vice Chair were dully elected for a four-year term. Chair elect Zhong-Qiang Chen has appointed Yadong Sun (Erlangen, Germany) to serve as the new secretary of the Triassic Subcommission. The newly elected executive will begin their terms to coincide with the start of the 36th International Geological Congress (Delhi, March 2020) at which time Mark Hounslow will assume the position of Past Chair.

Duly submitted,

Christopher McRoberts
STS Secretary

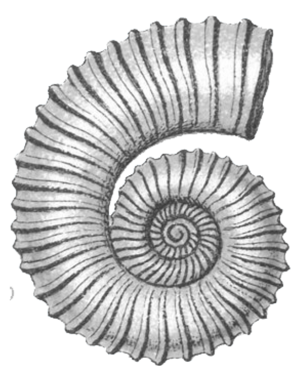

Publication Announcement

Early-Middle Triassic boundary interval: Integrated chemo-bio-magneto-stratigraphy of potential GSSPs for the base of the Anisian Stage in South China. By Yan Chen, Haishui Jiang, James G. Ogg, Yang Zhang, Yifan Gong, & Chunbo Yan, 2019. Earth and Planetary Science Letters, [access on-line 23 Oct 2019]. https://doi.org/10.1016/j.epsl.2019.115863 [Includes an additional 29-page PDF supplement, plus an Excel supplement of 7 worksheets including full demagnetization data for all samples, stable isotopes, TSCreator visualization datapacks, etc.]

Highlights

The Wantou section (Guangxi province) S. China) had been previously studied for ammonoid, conodont and carbon-isotope stratigraphy (Galfetti et al., 2007, 2008) and the main events and trends are bracketed by a succession of a dozen volcanic ashes that have yielded ID-TIMS U-Pb ages (Ovtcharova et al., 2006, 2015). This new study added a detailed magnetostratigraphy and enhanced the conodont and stable isotope stratigraphy for high-resolution global correlation, plus replicated the main magneto-biostratigraphic events in an additional section at Youping. The combined results indicate that the Wantou section is an ideal candidate for the Early-Middle Triassic boundary stratotype. The preferred level for the Anisian GSSP is a horizon that records the first *Chiosella timorensis* s.str. conodont near the brief polarity chron MT1n.

Abstract—The Wantou and Youping sections of Guangxi, South China provide a detailed high-resolution integrated calibration of the Early-Middle Triassic boundary succession for lithostratigraphy, volcanic episodes, conodont first occurrences (FOs), ammonoid biostratigraphy, geomagnetic polarity, inorganic carbon isotopes, sea-surface temperatures derived from conodont-apatite oxygen-isotopes, and ID-TIMS U-Pb radiometric dating. The upper Spathian (late Early Triassic) magnetostratigraphy is characterized by normal polarity (magnetozone LT9n) that encompasses the FOs of the typical Spathian conodonts *Triassospathodus homeri* and *Gladigondolella carinata*, the late Spathian *Neopopanoceras haugi* ammonoid zone and the beginning of a progressive positive shift in inorganic carbon isotopes. The overlying reversed polarity interval (LT9r) contains two brief normal-polarity subzones (MT1n and MT2n) that can be recognized in several other marine and terrestrial sections. The FO of conodont *Chiosella timorensis* sensu stricto, a proposed base-Anisian global marker, is near MT1n and near the end of the positive $\delta^{13}C_{carb}$ excursion. Sea-surface temperatures were reported to have cooled by 4°C during this rise in $\delta^{13}C_{carb}$, suggesting a sequestration of carbon dioxide. The lowermost Anisian at Wantou and Youping is dominated by normal polarity (MT3n, with the presence of one major reversed-polarity subzone MT3n.1r), contains the FO of typical Anisian conodonts (*Gladigondolella tethydis*/*Magnigondolella alexanderi*), and has the onset of a plateau in inorganic carbon isotopes values (stabilizing around +4‰). The combination of the FO of conodont *Chiosella timorensis* s.str., the brief normal polarity zone (MT1n) and the last portion of the rising carbon-isotope trend are suitable for primary proxies for global correlation of the Early-Middle Triassic boundary (base of Anisian) to other marine and non-marine settings. Radiometric dates at the Wantou and at the Guandao sections, coupled with a composite cyclostratigraphy for Early Triassic through Anisian, indicate that the FO of the conodont *Chiosella timorensis* s.str. is at approximately 246.7 Ma.

Additional details and figures

The Wantou section (24.5915°N, 106.8625°E) at Jinya, Fengshan County, Guangxi province, South China, and the Youping section (24.9583°N, 206.5391°E), about 52 km northwest of the Wantou section (Fig. 1), have a similar lithological conformable succession of thick-bedded limestone with abundant bioclasts (Unit V of the Luolou Fm), transition beds of thin-bedded, siliceous mudstone containing calcareous nodules and the basal Baifeng Fm with laminated shale (Figs. 2 and 3). This succession is punctuated by a series of fine- and coarse- grained volcanic ash layers, of which the thickest are known informally as the "Green Bean Rock", that have yielded precise radiometric ages.

The conodont biostratigraphy at Wantou in this study embraced the Early-Middle Triassic boundary conodont faunal turnover from previous studies, which is the complete replacement of late Spathian assemblages of *Triassospathodus*, *Spathicuspus* and *Novispathodus* by basal Anisian fauna of *Gladigondolella*, *Chiosella* and *Neogondolella* (*Magnigondolella*). There are five conodont appearance events identified as expedient in constraining the boundary interval in the Wantou and on a global scale. They are, in ascending order: FO of *Tr. homeri*/*Tr.* ex gr. *homeri*; FO of *Gl. carinata*; FO of *Ch. timorensis* s.str.; FO of *Gl. tethydis*; and FO of *Magnigondolella alexanderi*/*Ng.* ex gr. *regalis* (Fig. 2).

The Wantou section is dominated by normal polarity, with one significant reversed-polarity zone spanning the EMTB interval and another at the top (WT2r). The overall generalized polarity pattern is consistent with the cycle-tuned geomagnetic polarity time scale (GPTS) for the Early-Middle Triassic (Hounslow and Muttoni, 2010; Li et al., 2016, 2018; Ogg et al., 2016). Based on the conodont distribution and inorganic carbon isotope trends, polarity zone WT1n is equivalent to LT9n of Hounslow and Muttoni (2010), subzone WT1r.4n as MT1n, WT1r.7n as MT2n, and WT2n as MT3n (Fig. 2). The WT1r (EMTB interval) contains multiple normal-polarity subzones, of which two (WT1r.4n, WT1r.7n) are documented by multiple paleomagnetic samples and are considered coeval with MT1n and MT2n of Hounslow and Muttoni (2010) with global correlation potential (Fig. 2).

Published online: December 9, 2019

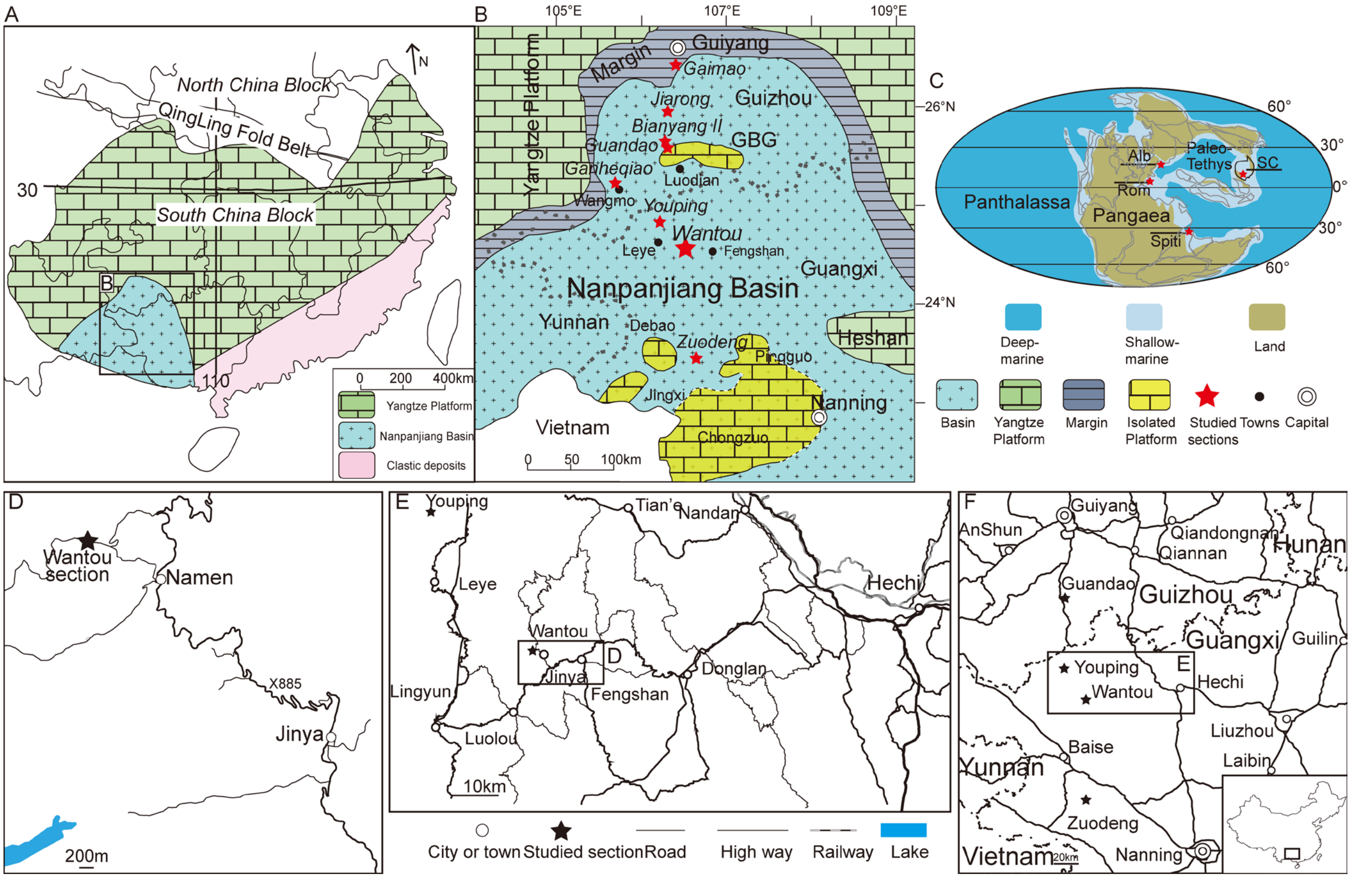

Figure 1 – Paleogeographic context and location of Wantou section. ***A***,***B***, Early-Middle Triassic paleogeography map of Yangtze Block (***A***) and Nanpanjiang Basin (***B***) (modified from Lehrmann et al. (2015), indicating previous studies (red stars) across the EMTB, including Wantou. ***C***, Early-Middle Triassic paleogeography (modified from http://www.scotese.com). Red dots show paleo-positions of research areas: SC= South China; Rom= Romania; Alb= Albania; Spiti= North India. ***D***,***E***,***F***, Locations of Wantou section. ***D***, Jinya town to Wantou section, which is an enlarged portion of map (***E***) of Fengshan Country to Jinya town and Wantou section. ***F***, Locations relative to the Nanning province capital and Hechi city. (Base maps modified from https://map.baidu.com)

The late Spathian positive carbon isotope shift followed by an early Anisian plateau has been documented at Losar, North India (Galfetti et al., 2007), Deşli Caira, Romania (Grădinaru et al., 2007), Guandao, South China (Lehrmann et al., 2015) and at Wantou (Ovtcharova et al., 2015; and this study). The beginning of the $\delta^{13}C_{carb}$ plateau is near the base of polarity zone WT2n (= chron MT3n of Hounslow and Muttoni, 2010) (Fig. 2) and slightly above the FO of *Ch. timorensis* s.str. at Guandao, Wantou and Deşli Caria.

The combination of potential global isochronous markers includes magnetic polarity chrons, conodont occurrences (the FO of *Ch. timorensis* s.str., the preferred potential proxy in this study for the Anisian GSSP level, is at about 20% up within the reversed-polarity subchron MT1r between the brief MT1n and MT2n), typical ammonoid occurrences (the FO of *Ch. timorensis* s.str. level is 1.3 m above the last occurrence of *Neopopanoceras haugi*), carbon isotopes (the FO of *Ch. timorensis* s.str. level is 0.74 m below the peak of a significant positive excursion) (Fig. 2), and an age model from the combination of U-Pb dates with regional cyclostratigraphy (the FO of *Ch. timorensis* s.str. is projected to be at approximately 246.7 Ma).

This combination implies that the Wantou outcrops of Guangxi, South China, have great potential as the GSSP reference section for the Early-Middle Triassic boundary and can enable precise global correlation into different facies.

A formal GSSP proposal is being prepared by this group in coordination with the other teams that have studied this section, and a potential Anisian working-group field meeting is being planned for May-June of 2020 in association with a Geobiology Congress in Wuhan, China.

References

Galfetti, T., Bucher, H., Brayard, A., Hochuli, P.A., Weissert, H., Kuang, G.D., Atudorei, V., & Guex, J., 2007a. Late Early Triassic climate change: Insights from carbonate carbon isotopes, sedimentary evolution and ammonoid paleobiogeography. Palaeogeography Palaeoclimatology Palaeoecology, 243(3-4): 394-411. https://doi.org/10.1016/j.palaeo.2006.08.014

Galfetti, T., Bucher, H., Martini, R., Hochuli, P.A., Weissert, H., Crasquin-Soleau, S., Brayard, A., Goudemand, N., Bruehwiler, T., & Kuang, G.D., 2008. Evolution of Early Triassic outer platform paleoenvironments in the Nanpanjiang Basin (South China) and their significance for

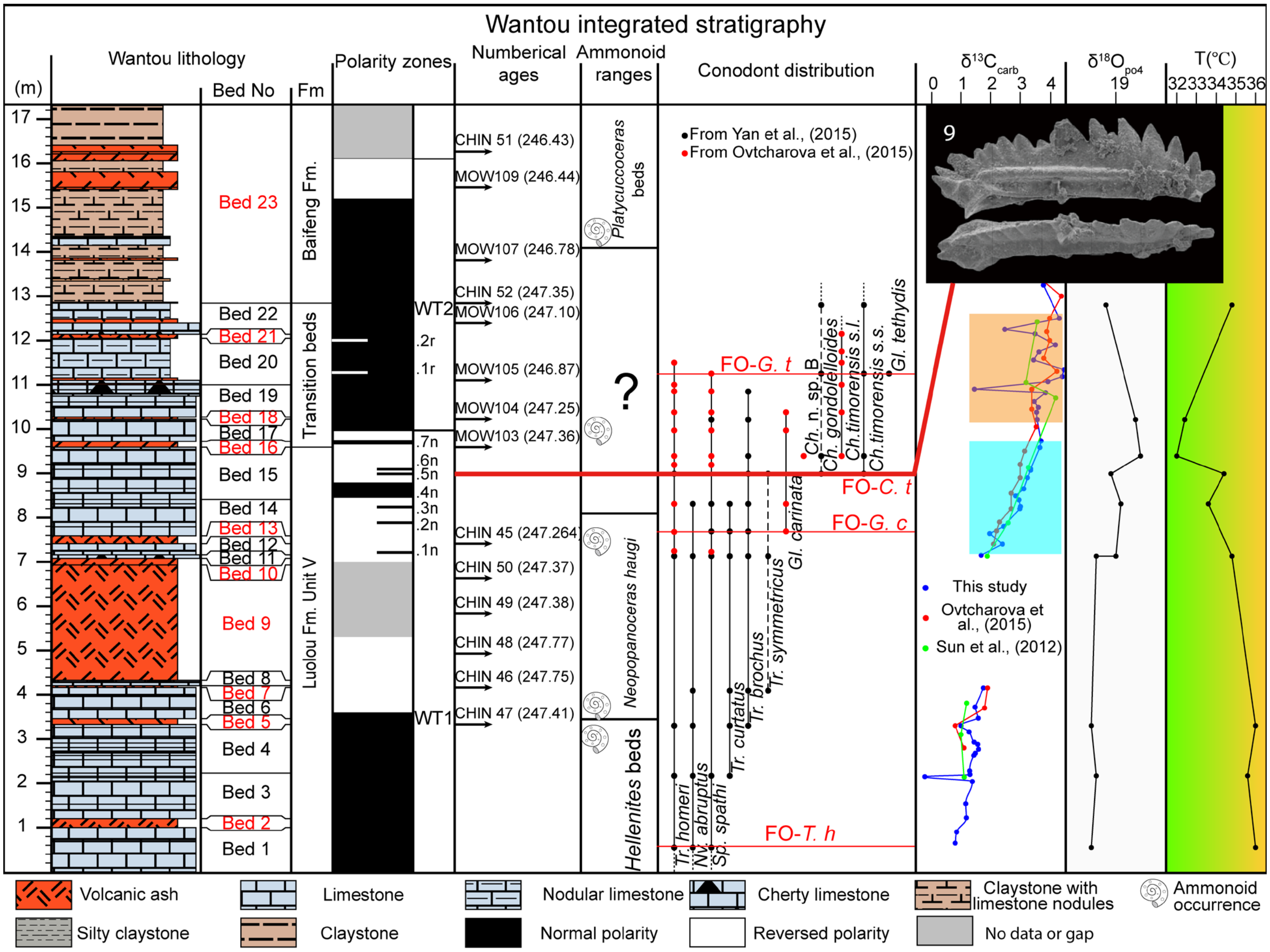

Figure 2 – Integrated stratigraphy of the Wantou section with magnetic polarity zones (this study; black is normal polarity, white is reversed), U-Pb dates from zircons (Ovtcharova et al., 2015), ammonoid zones (Galfetti et al., 2008), conodont ranges and datums (Ovtcharova et al., 2015; Yan et al., 2015), $\delta^{13}C_{carb}$ curve (Ovtcharova et al., 2015; Sun et al., 2012, and this study), and $\delta^{18}O$ and interpreted sea-surface temperatures from conodont apatite (Sun et al., 2012). Beds of volcanic ash in the lithology column have their names in red. Positive shift in $\delta^{13}C_{carb}$ is highlighted by blue, and the plateau is marked by orange. Conodont abbreviations: FO-*T. h* = first occurrence (FO) of *Tr. homeri*; FO-*G. c* = First occurrence of *Gl. carinata*; FO-*C. t* = First occurrence of *Ch. timorensis* sensu stricto; FO-*G. t* = First occurrence of *Gl. tethydis*; FO-*M. a* = First occurrence of *M. alexander*, *Ch.* = *Chiosella*, *Tr.* = *Triassospathodus*, *Nv.* = *Novispathodus*, *Gl.* = *Gladigondolella*, *M.* = *Magnigondolella*, *Sp.* = *Spathicuspus*. The photo of conodont *Ch. timorensis*. s.str. is from Yan et al. (2015).

the biotic recovery. Sedimentary Geology, 204(1-2): 36-60. https://doi.org/10.1016/j.sedgeo.2007.12.008

Grădinaru, E., Kozur, H., Nicora, A., & Orchard, M.J, 2006. The *Chiosella timorensis* lineage and correlation of the ammonoids and conodonts around the base of the Anisian in the GSSP candidate at Desli Caira (North Dobrogea, Romania). Albertiana, 34: 34-39.

Hounslow, M.W., and Muttoni, G., 2010. The geomagnetic polarity timescale for the Triassic: linkage to stage boundary definitions. Geological Society, London, Special Publications, 334(1): 61-102. https://doi.org/10.1144/sp334.4

Lehrmann, D.J., Stepchinski, L., Altiner, D., Orchard, M.J., Montgomery, P., Enos, P., Ellwood, B.B., Bowring, S.A., Ramezani, J., Wang, H.M., Wei, J.Y., Yu, M.Y., Griffiths, J.D., Minzoni, M., Schaal, E.K., Li, X.W., Meyer, K.M., & Payne, J.L., 2015. An integrated biostratigraphy (conodonts and foraminifers) and chronostratigraphy (paleomagnetic reversals, magnetic susceptibility, elemental chemistry, carbon isotopes and geochronology) for the Permian-Upper Triassic strata of Guandao section, Nanpanjiang Basin, South China. Journal of Asian Earth Sciences, 108: 117-135. https://doi.org/10.1016/j.jseaes.2015.04.030

Li, M.S., Huang, C.J., Hinnov, L.A., Chen, W.Z., Ogg, J.G., & Tian, W., 2018. Astrochronology of the Anisian stage (Middle Triassic) at the Guandao reference section, South China. Earth and Planetary Science Letters, 482: 591-606. https://doi.org/10.1016/j.epsl.2017.11.042

Li, M.S., Ogg, J.G., Zhang, Y., Huang, C.J., Hinnov, L.A., Chen, Z.Q., & Zou, Z.Y., 2016. Astronomical tuning of the end-Permian extinction and the Early Triassic Epoch of South China and Germany. Earth and Planetary

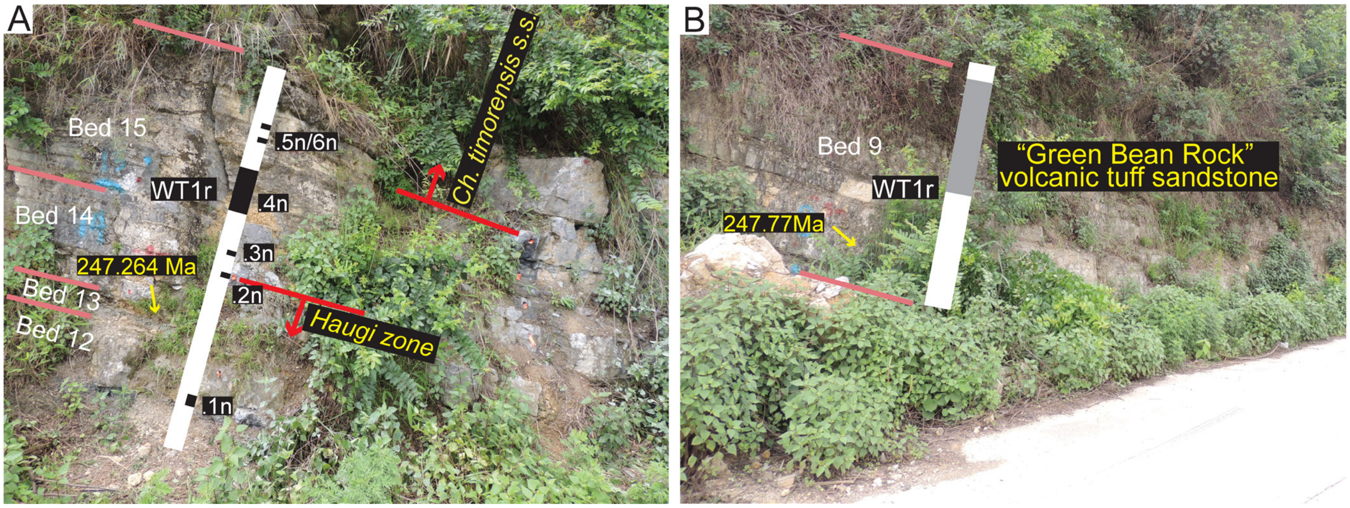

Figure 3 – Field photographs focusing on the Early-Middle Triassic Boundary interval in the Wantou (***A***,***B***), with bed numbers (white font and pink lines), occurrence of thick bed of volcaniclastic sandstone (Green-bean Rock; B; Bed 9), U-Pb dated levels (yellow numbers in ***A*** and ***B***), FOs of conodont (red upward arrows with yellow labels), and highest occurrence of the ammonoid *Neopopanoceras haugi* (red downward arrow with yellow label in ***A***), Conodont abbreviations: *Ch. timorensis* s.s.= *Ch. timorensis* sensu stricto. Polarity zone WT1r.4n is equivalent to chron MT1n of Hounslow and Muttoni (2010). See Fig. 2 for meter scale of the beds.

Science Letters, 441: 10-25. https://doi.org/10.1016/j.epsl.2016.02.017

Ogg, J.G., Ogg, G.M., and Gradstein, F.M., 2016. A Concise Geological Timescale 2016: Elsevier, 234 pp. ISBN 9780444637710.

Ovtcharova, M., Bucher, H., Schaltegger, U., Galfetti, T., Brayard, A., & Guex, J., 2006. New Early to Middle Triassic U–Pb ages from South China: calibration with ammonoid biochronozones and implications for the timing of the Triassic biotic recovery. Earth and Planetary Science Letters, 243(3-4): 463-475. https://doi.org/10.1016/j.epsl.2006.01.042

Ovtcharova, M., Goudemand, N., Hammer, Ø., Kuang, G.D., Cordey, F., Galfetti, T., Schaltegger, U., & Bucher, H., 2015. Developing a strategy for accurate definition of a geological boundary through radio-isotopic and biochronological dating: The Early-Middle Triassic boundary (South China). Earth-Science Reviews, 146: 65-76. https://doi.org/10.1016/j.earscirev.2015.03.006

Sun, Y.D., Joachimski, M.M., Wignall, P.B., Yan, C.B., Chen, Y.L., Jiang, H.S., Wang, L.N., & Lai, X.L., 2012. Lethally hot temperatures during the Early Triassic greenhouse. Science, 338(6105): 366-70. https://doi.org/10.1126/science.1224126

Yan, C.B., Jiang, H.S., Lai, X.L., Sun, Y.D., Yang, B., and Wang, L.N., 2015. The Relationship between the "Green-bean Rock" layers and conodont *Chiosella timorensis* and implications on defining the Early-Middle Triassic boundary in the Nanpanjiang Basin, South China. Journal of Earth Science, 26(2): 236-245. https://doi.org/10.1007/s12583-015-0535-x